

UNIVERSITI TEKNOLOGI MALAYSIA

**BORANG PENGESAHAN
LAPORAN AKHIR PENYELIDIKAN**

TAJUK PROJEK : UTILISATION OF NOISE SUPPRESSION TECHNIQUES
IN THE DEVELOPMENT OF TWO-STROKE, STRATIFIED-CHARGE,
LEAN-BURN GASOLINE ENGINES.

Saya PM. DR. ROSLIAN ABD RAHMAN
(HURUF BESAR)

Mengaku membenarkan **Laporan Akhir Penyelidikan** ini disimpan di Perpustakaan Universiti Teknologi Malaysia dengan syarat-syarat kegunaan seperti berikut :

1. Laporan Akhir Penyelidikan ini adalah hakmilik Universiti Teknologi Malaysia.
2. Perpustakaan Universiti Teknologi Malaysia dibenarkan membuat salinan untuk tujuan rujukan sahaja.
3. Perpustakaan dibenarkan membuat penjualan salinan Laporan Akhir Penyelidikan ini bagi kategori TIDAK TERHAD.
4. * Sila tandakan (/)

☐

SULIT

(Mengandungi maklumat yang berdarjah keselamatan atau Kepentingan Malaysia seperti yang termaktub di dalam AKTA RAHSIA RASMI 1972).

☐

TERHAD

(Mengandungi maklumat TERHAD yang telah ditentukan oleh Organisasi/badan di mana penyelidikan dijalankan).

☐

TIDAK
/ TERHAD

TANDATANGAN KETUA PENYELIDIK

Nama & Cop Ketua Penyelidik

Tarikh : _____

CATATAN : * Jika Laporan Akhir Penyelidikan ini SULIT atau TERHAD, sila lampirkan surat daripada pihak berkuasa/ organisasi berkenaan dengan menyatakan sekali sebab dan tempoh laporan ini perlu dikelaskan sebagai SULIT dan TERHAD.

**UTILISATION OF NOISE SUPPRESSION TECHNIQUES
IN THE DEVELOPMENT OF TWO-STROKE, STRATIFIED-
CHARGE, LEAN-BURN GASOLINE ENGINES**

ROSLAN ABD RAHMAN

**RESEARCH VOTE NO:
74520**

**Fakulti Kejuruteraan Mekanikal
Universiti Teknologi Malaysia**

2005

ABSTRACT

UTILISATION OF NOISE SUPPRESSION TECHNIQUES IN THE DEVELOPMENT OF TWO-STROKE, STRATIFIED-CHARGE, LEAN-BURN GASOLINE ENGINES

(Keywords: Noise and vibration, finite element method, structural dynamics, two-stroke engine)

New two-stroke gasoline engines were to be developed by Universiti Teknologi Malaysia. This project is intended to fulfill the noise and vibration requirements in the development of two-stroke engines. The objective is to adopt current state-of-art technologies in noise, weight and vibration reduction without compromising the criteria for high power-to-weight ratio, low emission, low fuel consumption and multiple platform applications.

Overall vibration on existing engines was carried to identify the dominant frequency range and vibration level. Vibration simulation using FEM was done on the proposed new engine and some modifications were proposed. Noise radiation simulation was also carried out on the proposed and modified engine models to ensure uniform distribution of noise. Balancing calculations on three types of engines were analyzed as well. The effect of back-pressure in exhaust system, the usage of catalytic converter and new materials on engine components, the calculation of heat loss from engine surface were also included.

Exhaust and intake for the new engine were designed to complete the system. Parameter analysis was also carried out for both intake and exhaust. The prototype engine was finally tested for noise radiation by using sound intensity technique to identify possible dominant noise radiation sources. It was concluded that the prototype engine produced acceptable amount of noise radiation at no load condition.

Researchers:

Assoc. Prof. Dr Roslan Abd. Rahman (Head)
Dr. Nazri Kamsah
Mr. Zulkarnain bin Abd. Latif

E-mail : roslan@fkm.utm.my
Tel. No. : 07-5534670
Vote No. : 74520

ABSTRAK

PENGUNAAN TEKNIK PENGURANGAN KEBISINGAN DALAM PEMBANGUNAN ENJIN PETROL DUA LEJANG BERCAJ BERTINGKAT DAN PEMBAKARAN LENGKAP

*(Katakunci: kebisingan dan getaran, kaedah unsur terhingga,
dinamik struktur, enjin dua lejang)*

Sebuah enjin gasolin baru dua-lejang telah dihasilkan oleh Universiti Teknologi Malaysia. Projek ini bertujuan untuk memenuhi keperluan getaran dan kebisingan dalam membangunkan enjin dua-lejang. Objektif projek adalah untuk menggunakan teknologi terkini dalam mengurangkan kebisingan, berat dan getaran tanpa tolakansur kriteria untuk nisbah kuasa-berat yang tinggi, emisi yang rendah, penggunaan bahanapi yang rendah dan aplikasi keatas beberapa platform.

Pengukuran getaran keseluruhan ke atas enjin sedia ada dibuat untuk mengenalpasti julat frekuensi yang dominan serta tahap getaran. Simulasi getaran menggunakan FEM dibuat ke atas enjin baru dan beberapa tambahbaik dicadangkan. Simulasi radiasi kebisingan juga dilakukan ke atas enjin baru dan enjin yang ditambahbaik bagi memastikan pengagihan kebisingan yang seragam. Penggiraan imbalan ke atas tiga jenis enjin juga dikaji. Kesan tekanan balikan dalam sistem ekzos, penggunaan *catalytic converter* dan bahan baru bagi komponen enjin, dan penggiraan kehilangan haba dari permukaan enjin juga dikaji.

Ekzos dan masukan bagi enjin baru juga direka untuk melengkapkan sistem enjin. Analisis parameter juga dilakukan dan enjin prototype diuji bagi radiasi kebisingan dengan mengguna teknik keamatan bunyi. Ini adalah untuk mengenalpasti punca radiasi kebisingan yang dominan. Kesimpulan projek ini adalah enjin prototype ini menghasilkan radiasi kebisingan yang boleh diterima pada keadaan tanpa beban.

Penyelidik:

Assoc. Prof. Dr Roslan Abd. Rahman (Head)

Mr. Zulkarnain bin Abd. Latif

Dr. Nazri Kamsah

E-mail : roslan@fkm.utm.my

Tel. No. : 07-5534670

Vote No. : 74520

ACKNOWLEDGEMENT

The authors would like to express their sincere gratitude to MOSTE for granting the project to the group via project no. 03-02-06-0055 PR0005/03-03. The authors also wish to express their thanks and appreciation to Research Management Centre (RMC), Universiti Teknologi Malaysia for every assistance in ensuring the smooth running of the project.

The groups would like to express their sincere gratitude and appreciation to the Head of Program, Prof. Dr. Azhar bin Dato' Abdul Aziz for offering this project. The Head of Project also wish to express his thanks and appreciation to his group members for their invaluable assistance, cooperation and helpful discussion throughout the research. Also to all the Research Officers, Mr. Norsham Amin, Mr. Mazlan Zubair, Mr. Faizul Akmar Abdul Kadir, and Mr. Rumaizi Salim for their hardwork and assistance.

Last but not least appreciation to all staff of Faculty of Mechanical Engineering, Universiti Teknologi Malaysia for their support and encouragement.

TABLE OF CONTENTS

CHAPTER	TITLE	PAGE
1	INTRODUCTION	1
2	LITERATURE REVIEW	3
2.1	Source of Noise	
2.2	Noise Suppression of Engine	4
2.3	Discussion	7
2.4	References	9
3	OVERALL VIBRATION ANALYSIS OF ENGINES	11
3.1	Introduction	11
3.2	Engine Specification	11
3.3	Test Instrumentation, Set-Up and Procedure	12
3.4	Experimental Results	14
3.5	Discussion	17
3.6	Conclusion	26
4	VIBRATION MEASUREMENT ON EXISTING ENGINE COMPONENTS	27
4.1	Introduction	27
4.2	Engine Description and Test set-up	27
4.3	Test Results	29
4.4	Discussion	34
4.5	Conclusion	34
4.6	Reference	34

5	NUMERICAL SIMULATION OF THE DYNAMIC BEHAVIOR OF NEW 2-STROKE SINGLE CYLINDER GASOLINE ENGINE	35
5.1	Introduction	35
5.2	Finite Element Model	36
5.3	Finite Element Analysis on Engine Components	38
5.4	Sensitivity Analysis	43
5.4.1	Sensitivity Analysis on Cylinder Head	43
5.4.2	Sensitivity Analysis on Cylinder Block	47
5.4.3	Sensitivity Analysis on Crankcase	49
5.4.4	Sensitivity Analysis on Crankcase Cover	52
5.4.5	Sensitivity Analysis on Magneto Cover	54
5.5	References	56
6	NOISE RADIATION PREDICTION OF SINGLE CYLINDER ENGINE	57
6.1	Introduction	57
6.2	Determination of Excitation Force	58
6.2.1	Introduction	58
6.2.2	CAD Model in SOLIDWORKS	58
6.2.3	Cylinder Pressure	60
6.3	Simulation Model	61
6.4	Force Calculation Results	62
6.5	Noise Radiation Prediction	63
6.5.1	Force Response Analysis	65
6.5.2	Radiated Sound Power	69
6.6	Conclusion	72
6.7	References	73
7	BALANCING OF 2-STROKE GASOLINE ENGINE	74
7.1	Balancing Of Single Cylinder 2-Stroke Engine	74
7.1.1	Introduction	74
7.1.2	Scope of Work	74
7.1.3	Objective	75

7.1.4	CAD model of engine	75
7.1.5	Motion Simulation Process	77
7.1.6	Constraint Setup	77
7.1.7	Force Computation Results	78
7.1.8	Findings and Discussion	83
7.2	Balancing Of Crankshaft for V-4 Compound Piston 2-Stroke Engine	83
7.2.1	Scope of Works	83
7.2.2	Methodology	84
7.2.3	Flow of Study	84
7.2.4	Engine Parts Arrangement and Component Properties	85
7.2.5	Isometric View of Simulated Model	85
7.2.6	Motion Simulation	87
7.2.7	Balancing Study	89
7.2.8	Discussion	95
7.2.9	Suggestions	95
7.2.10	Conclusion	96
7.3	Dynamic Balancing Of Scotch Yoke 2-Stroke Gasoline Engine	98
7.3.1	Objective	98
7.3.2	Methodology and Approach	99
7.3.3	Results	102
7.3.4	Discussion	108
7.3.5	Conclusion	113
8	BACK PRESSURE, CATALYTIC CONVERTER, MATERIALS AND HEAT LOSSES	114
8.1	Back Pressure	114
8.1.1	Back Pressure Test	114
8.2	Catalytic Converter	115
8.3	Materials For Two-Stroke Engine	119
8.3.1	Conclusion	123

8.4	Heat Transfer Analysis On Engine Fins	123
8.4.1	Objective	123
8.4.2	Scope of Work	123
8.4.3	Problems And Solutions	124
8.4.4	Fins Geometry	124
8.4.5	Finite Element Model	126
8.4.6	Results	128
8.4.7	Conclusion	131
9	DESIGN OF EXHAUST SYSTEM	138
9.1	Single Cylinder Exhaust System	138
9.1.1	Introduction	138
9.1.2	Literature Review	138
9.1.3	Theory of Silencer Design	141
9.1.4	Study on the Existing Silencer (Suzuki TXR Gamma 150cc)	145
9.1.5	New Muffler Design	153
9.1.6	Flow Analysis	165
9.1.7	Conclusion	166
9.1.8	References	167
9.2	Multi Cylinder Exhaust System	169
9.2.1	Background of the engine	169
9.2.2	Design characteristics	169
9.2.3	Materials	173
9.2.4	References	173
10	PARAMETRIC STUDY ON NOISE ATTENUATION OF MUFFLER	174
10.1	Diffusing Silencer Element	174
10.2	Side-Resonant Silencer Element	180
10.3	References	186

11	DESIGN OF 2-STROKE INTAKE SYSTEM	187
11.1	Introduction	187
11.2	Literature Review	187
11.3	Theory of Intake Silencer	189
11.3.1	Transmission loss and its relationship with intake silencer (Physical properties)	191
11.3.2	Simulation Process	192
11.4	Development of Intake System	193
11.5	Conclusion	197
11.6	References	198
12	SOUND INTENSITY MEASUREMENT	200
12.1	Introduction	200
12.2	Background Theory	201
12.3	Sound Intensity Mapping	203
12.4	Sound Intensity Equipment Testing	204
12.5	Test Set-up and Procedure	205
12.6	Test Results	206
13	OVERALL VIBRATION AND NOISE MEASUREMENTS ON NEW 2-STROKE SINGLE CYLINDER GASOLINE ENGINE	
13.1	Engine Specification	211
13.2	Test Instrumentation, Set-up and Procedure	212
13.3	Experimental Results	214
13.4	Discussion	218
13.5	Overall Noise Measurements	224
13.6	Conclusion	225
14	DISCUSSION, CONCLUSION AND RECOMMENDATION	
14.1	Introduction	226
14.2	Overall Discussion	226
14.3	Problem	228
14.4	Conclusion	229
15.5	Recommendation	229
	Appendix	230

UNIVERSITI TEKNOLOGI MALAYSIA

**BORANG PENGESAHAN
LAPORAN AKHIR PENYELIDIKAN**

TAJUK PROJEK : UTILISATION OF NOISE SUPPRESSION TECHNIQUES
IN THE DEVELOPMENT OF TWO-STROKE, STRATIFIED-CHARGE,
LEAN-BURN GASOLINE ENGINES.

Saya PM. DR. ROSLIAN ABD RAHMAN
(HURUF BESAR)

Mengaku membenarkan **Laporan Akhir Penyelidikan** ini disimpan di Perpustakaan Universiti Teknologi Malaysia dengan syarat-syarat kegunaan seperti berikut :

1. Laporan Akhir Penyelidikan ini adalah hakmilik Universiti Teknologi Malaysia.
2. Perpustakaan Universiti Teknologi Malaysia dibenarkan membuat salinan untuk tujuan rujukan sahaja.
3. Perpustakaan dibenarkan membuat penjualan salinan Laporan Akhir Penyelidikan ini bagi kategori TIDAK TERHAD.
4. * Sila tandakan (/)

☐

SULIT

(Mengandungi maklumat yang berdarjah keselamatan atau Kepentingan Malaysia seperti yang termaktub di dalam AKTA RAHSIA RASMI 1972).

☐

TERHAD

(Mengandungi maklumat TERHAD yang telah ditentukan oleh Organisasi/badan di mana penyelidikan dijalankan).

☐

TIDAK
TERHAD

TANDATANGAN KETUA PENYELIDIK

Nama & Cop Ketua Penyelidik

Tarikh : _____

CATATAN : * Jika Laporan Akhir Penyelidikan ini SULIT atau TERHAD, sila lampirkan surat daripada pihak berkuasa/organisasi berkenaan dengan menyatakan sekali sebab dan tempoh laporan ini perlu dikelaskan sebagai SULIT dan TERHAD.

**UTILISATION OF NOISE SUPPRESSION TECHNIQUES
IN THE DEVELOPMENT OF TWO-STROKE, STRATIFIED-
CHARGE, LEAN-BURN GASOLINE ENGINES**

ROSLAN ABD RAHMAN

**RESEARCH VOTE NO:
74520**

**Fakulti Kejuruteraan Mekanikal
Universiti Teknologi Malaysia**

2005

ABSTRACT

UTILISATION OF NOISE SUPPRESSION TECHNIQUES IN THE DEVELOPMENT OF TWO-STROKE, STRATIFIED-CHARGE, LEAN-BURN GASOLINE ENGINES

(Keywords: Noise and vibration, finite element method, structural dynamics, two-stroke engine)

New two-stroke gasoline engines were to be developed by Universiti Teknologi Malaysia. This project is intended to fulfill the noise and vibration requirements in the development of two-stroke engines. The objective is to adopt current state-of-art technologies in noise, weight and vibration reduction without compromising the criteria for high power-to-weight ratio, low emission, low fuel consumption and multiple platform applications.

Overall vibration on existing engines was carried to identify the dominant frequency range and vibration level. Vibration simulation using FEM was done on the proposed new engine and some modifications were proposed. Noise radiation simulation was also carried out on the proposed and modified engine models to ensure uniform distribution of noise. Balancing calculations on three types of engines were analyzed as well. The effect of back-pressure in exhaust system, the usage of catalytic converter and new materials on engine components, the calculation of heat loss from engine surface were also included.

Exhaust and intake for the new engine were designed to complete the system. Parameter analysis was also carried out for both intake and exhaust. The prototype engine was finally tested for noise radiation by using sound intensity technique to identify possible dominant noise radiation sources. It was concluded that the prototype engine produced acceptable amount of noise radiation at no load condition.

Researchers:

Assoc. Prof. Dr Roslan Abd. Rahman (Head)
Dr. Nazri Kamsah
Mr. Zulkarnain bin Abd. Latif

E-mail : roslan@fkm.utm.my
Tel. No. : 07-5534670
Vote No. : 74520

ABSTRAK

PENGUNAAN TEKNIK PENGURANGAN KEBISINGAN DALAM PEMBANGUNAN ENJIN PETROL DUA LEJANG BERCAJ BERTINGKAT DAN PEMBAKARAN LENGKAP

*(Katakunci: kebisingan dan getaran, kaedah unsur terhingga,
dinamik struktur, enjin dua lejang)*

Sebuah enjin gasolin baru dua-lejang telah dihasilkan oleh Universiti Teknologi Malaysia. Projek ini bertujuan untuk memenuhi keperluan getaran dan kebisingan dalam membangunkan enjin dua-lejang. Objektif projek adalah untuk menggunakan teknologi terkini dalam mengurangkan kebisingan, berat dan getaran tanpa tolakansur kriteria untuk nisbah kuasa-berat yang tinggi, emisi yang rendah, penggunaan bahanapi yang rendah dan aplikasi keatas beberapa platform.

Pengukuran getaran keseluruhan ke atas enjin sedia ada dibuat untuk mengenalpasti julat frekuensi yang dominan serta tahap getaran. Simulasi getaran menggunakan FEM dibuat ke atas enjin baru dan beberapa tambahbaik dicadangkan. Simulasi radiasi kebisingan juga dilakukan ke atas enjin baru dan enjin yang ditambahbaik bagi memastikan pengagihan kebisingan yang seragam. Penggiraan imbalan ke atas tiga jenis enjin juga dikaji. Kesan tekanan balikan dalam sistem ekzos, penggunaan *catalytic converter* dan bahan baru bagi komponen enjin, dan penggiraan kehilangan haba dari permukaan enjin juga dikaji.

Ekzos dan masukan bagi enjin baru juga direka untuk melengkapkan sistem enjin. Analisis parameter juga dilakukan dan enjin prototype diuji bagi radiasi kebisingan dengan mengguna teknik keamatan bunyi. Ini adalah untuk mengenalpasti punca radiasi kebisingan yang dominan. Kesimpulan projek ini adalah enjin prototype ini menghasilkan radiasi kebisingan yang boleh diterima pada keadaan tanpa beban.

Penyelidik:

Assoc. Prof. Dr Roslan Abd. Rahman (Head)

Mr. Zulkarnain bin Abd. Latif

Dr. Nazri Kamsah

E-mail : roslan@fkm.utm.my

Tel. No. : 07-5534670

Vote No. : 74520

ACKNOWLEDGEMENT

The authors would like to express their sincere gratitude to MOSTE for granting the project to the group via project no. 03-02-06-0055 PR0005/03-03. The authors also wish to express their thanks and appreciation to Research Management Centre (RMC), Universiti Teknologi Malaysia for every assistance in ensuring the smooth running of the project.

The groups would like to express their sincere gratitude and appreciation to the Head of Program, Prof. Dr. Azhar bin Dato' Abdul Aziz for offering this project. The Head of Project also wish to express his thanks and appreciation to his group members for their invaluable assistance, cooperation and helpful discussion throughout the research. Also to all the Research Officers, Mr. Norsham Amin, Mr. Mazlan Zubair, Mr. Faizul Akmar Abdul Kadir, and Mr. Rumaizi Salim for their hardwork and assistance.

Last but not least appreciation to all staff of Faculty of Mechanical Engineering, Universiti Teknologi Malaysia for their support and encouragement.

TABLE OF CONTENTS

CHAPTER	TITLE	PAGE
1	INTRODUCTION	1
2	LITERATURE REVIEW	3
	2.1 Source of Noise	
	2.2 Noise Suppression of Engine	4
	2.3 Discussion	7
	2.4 References	9
3	OVERALL VIBRATION ANALYSIS OF ENGINES	11
	3.1 Introduction	11
	3.2 Engine Specification	11
	3.3 Test Instrumentation, Set-Up and Procedure	12
	3.4 Experimental Results	14
	3.5 Discussion	17
	3.6 Conclusion	26
4	VIBRATION MEASUREMENT ON EXISTING ENGINE COMPONENTS	27
	4.1 Introduction	27
	4.2 Engine Description and Test set-up	27
	4.3 Test Results	29
	4.4 Discussion	34
	4.5 Conclusion	34
	4.6 Reference	34

5	NUMERICAL SIMULATION OF THE DYNAMIC BEHAVIOR OF NEW 2-STROKE SINGLE CYLINDER GASOLINE ENGINE	35
5.1	Introduction	35
5.2	Finite Element Model	36
5.3	Finite Element Analysis on Engine Components	38
5.4	Sensitivity Analysis	43
5.4.1	Sensitivity Analysis on Cylinder Head	43
5.4.2	Sensitivity Analysis on Cylinder Block	47
5.4.3	Sensitivity Analysis on Crankcase	49
5.4.4	Sensitivity Analysis on Crankcase Cover	52
5.4.5	Sensitivity Analysis on Magneto Cover	54
5.5	References	56
6	NOISE RADIATION PREDICTION OF SINGLE CYLINDER ENGINE	57
6.1	Introduction	57
6.2	Determination of Excitation Force	58
6.2.1	Introduction	58
6.2.2	CAD Model in SOLIDWORKS	58
6.2.3	Cylinder Pressure	60
6.3	Simulation Model	61
6.4	Force Calculation Results	62
6.5	Noise Radiation Prediction	63
6.5.1	Force Response Analysis	65
6.5.2	Radiated Sound Power	69
6.6	Conclusion	72
6.7	References	73
7	BALANCING OF 2-STROKE GASOLINE ENGINE	74
7.1	Balancing Of Single Cylinder 2-Stroke Engine	74
7.1.1	Introduction	74
7.1.2	Scope of Work	74
7.1.3	Objective	75

7.1.4	CAD model of engine	75
7.1.5	Motion Simulation Process	77
7.1.6	Constraint Setup	77
7.1.7	Force Computation Results	78
7.1.8	Findings and Discussion	83
7.2	Balancing Of Crankshaft for V-4 Compound Piston 2-Stroke Engine	83
7.2.1	Scope of Works	83
7.2.2	Methodology	84
7.2.3	Flow of Study	84
7.2.4	Engine Parts Arrangement and Component Properties	85
7.2.5	Isometric View of Simulated Model	85
7.2.6	Motion Simulation	87
7.2.7	Balancing Study	89
7.2.8	Discussion	95
7.2.9	Suggestions	95
7.2.10	Conclusion	96
7.3	Dynamic Balancing Of Scotch Yoke 2-Stroke Gasoline Engine	98
7.3.1	Objective	98
7.3.2	Methodology and Approach	99
7.3.3	Results	102
7.3.4	Discussion	108
7.3.5	Conclusion	113
8	BACK PRESSURE, CATALYTIC CONVERTER, MATERIALS AND HEAT LOSSES	114
8.1	Back Pressure	114
8.1.1	Back Pressure Test	114
8.2	Catalytic Converter	115
8.3	Materials For Two-Stroke Engine	119
8.3.1	Conclusion	123

8.4	Heat Transfer Analysis On Engine Fins	123
8.4.1	Objective	123
8.4.2	Scope of Work	123
8.4.3	Problems And Solutions	124
8.4.4	Fins Geometry	124
8.4.5	Finite Element Model	126
8.4.6	Results	128
8.4.7	Conclusion	131
9	DESIGN OF EXHAUST SYSTEM	138
9.1	Single Cylinder Exhaust System	138
9.1.1	Introduction	138
9.1.2	Literature Review	138
9.1.3	Theory of Silencer Design	141
9.1.4	Study on the Existing Silencer (Suzuki TXR Gamma 150cc)	145
9.1.5	New Muffler Design	153
9.1.6	Flow Analysis	165
9.1.7	Conclusion	166
9.1.8	References	167
9.2	Multi Cylinder Exhaust System	169
9.2.1	Background of the engine	169
9.2.2	Design characteristics	169
9.2.3	Materials	173
9.2.4	References	173
10	PARAMETRIC STUDY ON NOISE ATTENUATION OF MUFFLER	174
10.1	Diffusing Silencer Element	174
10.2	Side-Resonant Silencer Element	180
10.3	References	186

11	DESIGN OF 2-STROKE INTAKE SYSTEM	187
11.1	Introduction	187
11.2	Literature Review	187
11.3	Theory of Intake Silencer	189
11.3.1	Transmission loss and its relationship with intake silencer (Physical properties)	191
11.3.2	Simulation Process	192
11.4	Development of Intake System	193
11.5	Conclusion	197
11.6	References	198
12	SOUND INTENSITY MEASUREMENT	200
12.1	Introduction	200
12.2	Background Theory	201
12.3	Sound Intensity Mapping	203
12.4	Sound Intensity Equipment Testing	204
12.5	Test Set-up and Procedure	205
12.6	Test Results	206
13	OVERALL VIBRATION AND NOISE MEASUREMENTS ON NEW 2-STROKE SINGLE CYLINDER GASOLINE ENGINE	
13.1	Engine Specification	211
13.2	Test Instrumentation, Set-up and Procedure	212
13.3	Experimental Results	214
13.4	Discussion	218
13.5	Overall Noise Measurements	224
13.6	Conclusion	225
14	DISCUSSION, CONCLUSION AND RECOMMENDATION	
14.1	Introduction	226
14.2	Overall Discussion	226
14.3	Problem	228
14.4	Conclusion	229
15.5	Recommendation	229
	Appendix	230

CHAPTER I

INTRODUCTION

Global activities in the advancement of two-stroke engine technologies accelerate at rapid rate most notably in Europe, Japan, Taiwan and India. Engine/auto makers such as Orbital Corp.(Australia), Piaggio (Italy), Ford (Europe) and Subaru (Japan) are actively engaging in the development of two-stroke engines, particularly from the aspect of noise reduction. Many two-stroke engines are used where low bulk and weight features are required, thereby reducing the space available for muffling and potentially giving the engine type an undeserved reputation for being naturally noisy. However, many research works have shown that if they are tuned (the exhaust pipe) they will produce high specific engine outputs. Low compression ratio will reduce the maximum value of air intake velocity thus will lower the higher-frequency content of the sound produced and lower peak combustion pressure will reduce the noise spectrum generated from the combustion process.

The low combustion efficiency of today's two-stroke engine design can be improved through various means, making it possible to compliment the four-stroke version. The latter is a more complicated engine configuration having more weight-to-power ratio characteristic than the two-stroke version. During the last decade, there have been many improvement made to the two-stroke engine design. A few have found commercial ventures while many are still at the prototype level or even on the drawing board.

Two-stroke petrol engines can be applied to a wide range of platforms ranging from the marine, inland (highway and off-highway) and small aerial vehicles. IN Malaysia the two-stroke engines are virtually imported. Some of the brands are Yanmar

and Kubota (Japan), Lombardi (Italy), Robbin and Perkin (UK), Briggs & Stratton and John Deere (US). They have been making in-roads for more than 40 years meeting the needs of builders, farmers and numerous utility users. They range in price from as little as RM 900.00 to RM 5,000.00 depending on the make, configuration, capacity and application.

The simplistic nature of the design, with relatively simple machining processes (Than the four-stroke version), will provide improved weight-to power ratio (kg/kW) and specific displacement (m^3/kW). Development of new two-stroke engines must address fundamental problems i.e. piston scuffing, ring wear, oil consumption, starting, idling and scavenging. Where engine cost, fuel efficiency and the exhaust emissions are stressed, the development of new fuelling system is envisaged. The potential to include the new features will not only help to raise performance but also fuel consumption and exhaust emissions respectively.

The future of two-stroke engines with improved scavenging ports will be assisted by the development of an all new lubrication system, especially in engine management system architecture is making inroads in two-stroke engine performance improvements to achieve lean-burn combustion. To further improve fuel atomization, the development or the use of miniature (air-assisted) fuel injector is crucial.

To offset the weight factor due to the addition of more components, the use of new materials and aluminium die-casting and plastic moulding (minimizing part count and assembly line) are envisaged, making this mobile powerhouse extremely compact and light. This calls for the comprehensive investigations on the dynamic structural behavior and improvement in the noise radiation problem. In addition, the technology breakthrough in post-treatment of exhaust can make the two-stroke configuration much more efficient and environment-friendly, leading the way for their application becoming more robust and widespread.

Hence, in this research the objective is to adopt current state-of-art technologies (attenuation and material engineering) in noise, weight and vibration reduction (emitted by the prototype engines due to combustion, flow and mechanical means) without compromising the criteria for high power-to-weight ratio, low emission, low fuel consumption and multiple platform applications.

CHAPTER II

LITERATURE REVIEW

In some country, machinery that is quiet gets tax advantages under the law. Quietness is one of the main concerns of both manufactures and users. Engines must be improved in order to expand the demand in the near future by solving the major problems such as vibration, noise, air pollution, performance of engines. The forces which include cylinder pressure, bearing and gear impacts, piston slap, valve and overhead clearances, etc. are applied inside the engine and drive the structure to vibrate. The structure in turn causes the radiating surfaces to vibrate and radiate noise. Noise generation and its reduction study are now a well establish field. A number of specialized techniques have been developed and many of these are brought into use when dealing with engine noise.

The objective of this chapter is to review the noise suppression technique used in reducing the radiated noise from the engine surface of a 2-stroke cycle engine. It is required to know the frequency range that we are working with so that suitable and reliable software could be identified and acquired to assist in the project. It is also important to identify typical source of noise and suitable noise reduction techniques.

For the purpose of effective noise reduction, it is very important to understand the entire system of noise generation. The noise generation system can be separated into three main phases (1). The first phase is the noise source, such as combustion, piston slap, or gear. The next phase is the transfer path of an exciting force; the piston, the connecting rod, the crank shaft, the cylinder head, etc. The last phase is the radiation surface, such as the cylinder block, the oil pan, the gear case, or the flywheel.

2.1 Source of Noise

The engine noise consists of number of different components such as exhaust and intake noise, noise emitted by engine surface, noise of the accessories and that emitted by parts connected with the engine.

The main noise sources of a diesel engine are the exhaust and air intake (2). Diesel engine noise can also originate from several mechanical sources such as piston slap, timing gear rattle, etc, as well as from the sharp rise in cylinder pressure which attends combustion. If reduction of noise at source is contemplated, it is necessary to diagnose which of these sources are primarily responsible for the noise. In gasoline engines, engine noise is created in the area of the main bearings by vibration of the crankshaft (3).

Askhedkar et.al (4) identified the vibration characteristics of engine structures and the cranktrain structure as important parameters contributing to the engine surface noise. Honda et. Al (5) found that the combustion noise is the major source of the engine noise within lower engine speed range (2500 rpm), and the mechanical noise is the major source in higher engine speed range.

Ågren et al.(6) shows that the radiation of noise is dominated by the low end of the engine sides and by the engine front. In the engine front, the noise radiation is shown to have contributions from the timing casing, the oil-sump front and the crankshaft torsion vibration damper.

2.2 Noise Suppression of Engine

Noise suppression has become one of the primary goals of new engine development and an increasing amount of time and money is being spent to achieve this goal. In working towards a quieter vehicle, it is usually the engine that is most difficult to quieten in an acceptable fashion. In order that effective measures may be taken, the characteristics of any particular engine must be understood (7). This require formulating

a model to determine engine noise from surface vibration characteristics. This required determination of engine model characteristics, engine spectral force levels and finally the combination of all these into a model to predict engine surface response and hence radiated sound pressure levels.

Honda et.al. (8) reduced the vibration and noise of the cylinder blocks by investigating the characteristics of the natural frequencies, relationship between natural frequencies and vibration modes, the effect of the rigidity on the natural frequency, the effect of the material on the rigidity and weight. The main emphasizes was to increase the rigidity and also to decrease the weight of the engine. Aluminum and cast iron (FC200) were used to simulate on the material effect on the characteristics of the crank case vibration. The rigidity was varied by increasing or decreasing the thickness of crank case and crankshaft bush. It was clarified that the rigidity of the cylinder block has the dominant effects on the natural frequencies in the high frequency ranges, the weight has the great effect on those in the low frequency range. Thus vibration stress of the cylinder block can be reduced by higher rigidities and more lightening weights of the crankcase and crank journals in the measured frequency range.

The noise from engine surface can be reduced by treatment of individual components or by modifying radiating surfaces (9). Remove or eliminate noise character by modifying the fins in such a away that the resonant frequency should be eliminate. Harmonic analysis using FEM model and experimental modal analysis were carried out on the modified head. Noise reduction of crankcase assembly by fine tune the structure so that noise related frequencies are eliminated.

H.Kanda (1) carried out a detailed analysis of the entire system of noise generation which comprise of noise source analysis, transfer path analysis and radiation surface analysis. The radiation surface contribution was measured using acoustic intensity method with two microphones. Results showed that the largest force transfer path from sources to radiation surfaces is through the connecting rod to the crank shaft to the main bearing to the cylinder block. Modification of the connecting rod or crank shaft is not easy because their inherent stiffness imposes severe limitations. Thus the main effort is directed towards modification of the main bearing structures.

C.V.Beidi et.al. (10) describes phases required for the development of low noise engines. These phases are the concept and design phase, the combustion and mechanical development phase and the NVH development and refinement phase. Noise behavior of an engine structure can be optimized early in the conceptual design stage through vibration simulation. This approach ensures that first generation engine hardware is already structurally optimized for noise. FEM were utilized for simulation of structural vibrations. Natural frequencies and mode shape may serve for verification purposes. The focus, however, is on forced vibrations of the engine structure with loads and boundary conditions as realistic as possible. In layout design stage, the complete engine is modeled. The target of the simulation is to finally arrive at a structure showing evenly distributed vibration levels over the outer surface.

In the Development Stage typical noise development work consists of four phases: analysis, testing and development of modifications, procurement of modified hardware, final testing and refinement. It was concluded that two-stage simulation process was required. The first stage focus on trend prediction; the second stage during the design phase means simulation with the consideration of all significant noise excitation mechanisms.

Ågren, Anders (6) studied various constructions to control the noise are tested. Two stiffeners are designed and tested to reduce vibrations in the engine low end, one ladder frame introducing stiffness at the crankcase flange and one bearing beam introducing stiffness at the main bearing caps. The stiffeners have been evaluated by sound intensity measurements and mobility measurements. The ladder frame gave good noise reductions but the bearing beam merely caused frequency shifts of the bearing modes. A decoupling of the oil sump resulted in significant noise and vibration reductions. The timing cover is modified by increasing the damping and by decrease the radiation efficiency. Various interior panels are tested, like plexiglass and aluminium panels of different thicknesses, a rubber damping layer and a combined rubber/steel-sheet damping layer. A thin plastic sheet has low radiation efficiency and may thereby lower the noise emission. A slightly improved model for calculation of radiation efficiency of small irregularly shaped plates was suggested.

Study on diesel engine noise by Russel (2) suggested the following noise control treatments on existing engines which could have cumulative benefits:

- a. Reduce noise at source by smoother cylinder pressure development, smaller piston to bore clearance or cushioning device incorporated into piston.
- b. Reduce vibration of thin external surface of engine structure by stiffening and divide cast crankcase and water jacket panels, isolate noise-radiating areas of stiff covers from vibration of crankcase and cylinder block casting.

Shigehoro (11) decreased the reciprocating inertial mass of an in-line 4-cylinder engine by 33 % which resulted in the reduction of engine vibration by 4 dB. Ryan (12) looks into the reduction of engine noise due to piston secondary motion and piston slap by varying the engine operating and design parameter. Advanced timing, increase in liner temperature, increase in speed, increase in ring tension and increase in piston skirt waviness caused increased in piston slap intensity.

Much of the noise reduction effort on diesel engines has focused on the structure and radiating surfaces of the engine (13). The combustion forcing function has received considerable attention over the years, resulting in features such as two spring injectors and pilot injection. Piston slap and overhead clearances have also been a subject of noise reduction efforts. Fuel system torsional dampers, crank gear isolators, and rear gear trains can reduce gear impact noise.

2.3 Discussion

Based on the literature review presented, other than the intake and exhaust noise, the source of noise for gasoline engines are identified as in the area of the main bearings due to vibration of the crankshaft. The combustion noise is the major source of the engine noise within lower engine speed range (about 45 Hz), and the mechanical noise is the major source in higher engine speed range.

Several methods of noise suppression have been put forward. The main target is to ensure the engine to have high rigidity and low weight. In summary, these methods can be described as in Figure 1.

In determining the dynamic response of the engine by simulation and experimental, it is important to note the frequency range of the engine structures as this will guide in identifying suitable software for simulation and transducers specification for experimental work. It was noted from this literature review that the frequency range is from low to 2kHz. Such frequency range is suitable for Finite Element Method. However, to ensure this frequency range, test shall be carried out on several existing engines in the market.

2.4 References

1. H.Kanda,M.Okubo,T.Yonezawa; “*Analysis of Noise Sources and their Transfer Paths in Diesel Engines*” SAE 900014.
2. M.F.Russell, “*Automotive Diesel Engine Noise and its Control*”, SAE Paper 730243
3. H.H.Priebsh, J. Affenzeller, G. Kulpers, “*Structure-borne Noise Prediction Techniques*”, SAE 900019.
4. A.R.Askhedkar, R.R. Askhedkar and P.R. Sajanpawar, “*Application of Computer Simulation Using FEM and Experimental Techniques for the Reduction of Noise in Air Cooled Engine and Crankcase Cover of Motorcycle*”, SAE paper 1999-01-1800.
5. Y. Honda, K. Wakabayashi, T. Kodama, R. Kihara , “*A Basic Study on Reduction of Cylinder Block Vibrations for Small Diesel Cars*” SAE Technical Paper Series No. 2000-01-0527
6. Ågren, Anders “*On measurement, assessment and control of diesel engine noise*“, Phd Thesis, Lulea Tekniska Universitet, 1994.
7. M.G.Hawkins and R. Southall, “*Analysis and Prediction of Engine Structure Vibration*” SAE 750832
8. Y. Honda, K. Wakabayashi, T. Kodama, R. Kihara , “*A Basic Study on Reduction of Cylinder Block Vibrations for Small Diesel Cars*” SAE Technical Paper Series No. 2000-01-0527
9. A.R.Askhedkar, R.R. Askhedkar and P.R. Sajanpawar, “*Application of Computer Simulation Using FEM and Experimental Techniques for the Reduction of Noise in Air Cooled Engine and Crankcase Cover of Motorcycle*”, SAE paper 1999-01-1800.
10. C.V.Beidi, A. Rust and M. Rasser, “*Key steps and methods in the Development of Low Noise Engines*”, Sound and Vibration, April 2001.
11. Shigehiro Usuda, Takao Suzuki, Tatsua Uno, and Tooru Ichimiya, “*Interior Noise Reduction by Decreasing the Reciprocating Inertial Mass of Engine*”, Ninth International Pacific Conf. On Automotive Engineering, Bali. Nov. 16-21, 1997.

12. James P Ryan, Victoe W.Wong, Richard H.Lyon, David P. Hoult, “ *Engine Experiments on the Effects of Design and Operational Parameters on Piston Secondary Motion and Piston slap*”, SAE Technical Paper Series 940695
13. Helin Zhao and Thomas E Reinhart,”The influence of Diesel Architecture on Noise Levels”, SAE 1999-01-1747.

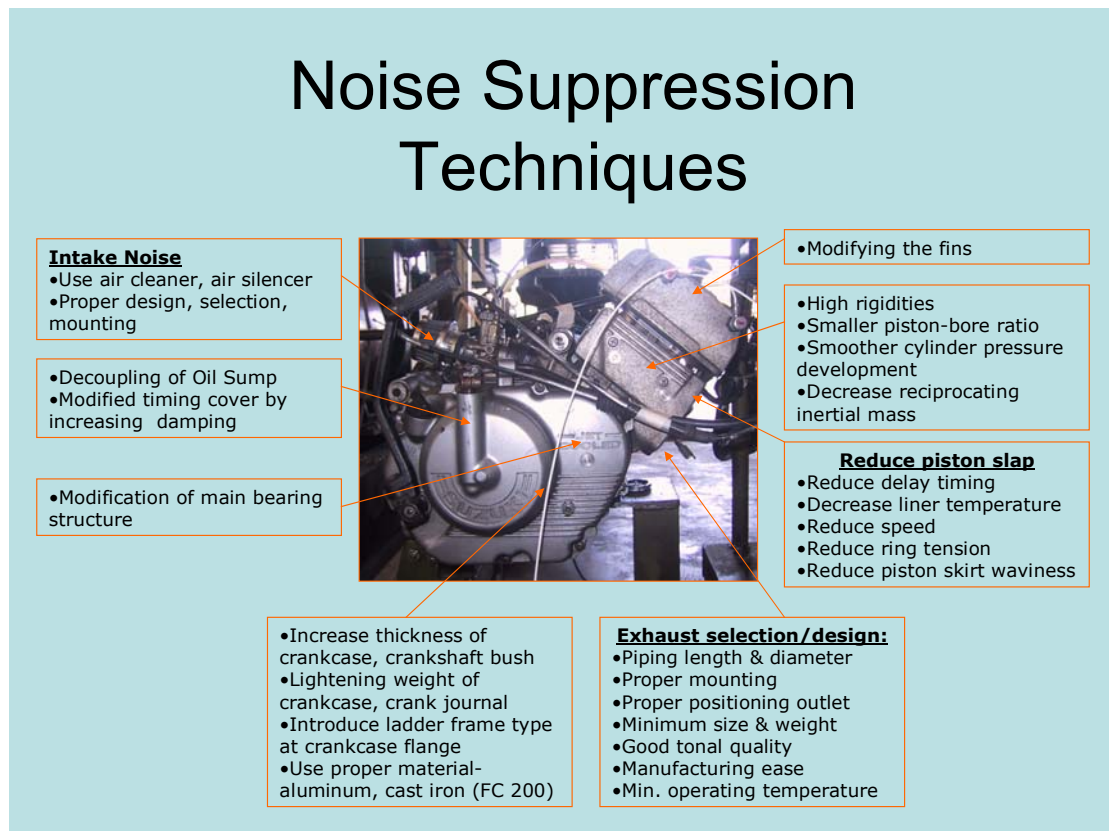


Figure1

CHAPTER III

OVERALL VIBRATION ANALYSIS OF ENGINES

3.1 Introduction

In the development of a new 2-stroke engine, as far as noise and vibration are concerned, the overall vibration of existing engines during operation need to be measured and analyzed. This is important as we need to know the frequency range of the operating engines, the frequency range for sources of vibration such as combustion noise, mechanical motion, etc. Such frequency range will enable to identify suitable numerical method to use and focus the analysis within such frequency range.

The objective of the chapter is to highlight the results of overall vibration measurement of several existing engines and to identify the dominant frequency range for the running engines. A paper of such work was presented at the ASIA-PACIFIC Vibration Conference on Nov. 2003 at Gold Coast, Australia and is attached at Appendix

3.2. Engine Specification

Overall vibration test was carried out on three (3) types of engine at Automotive Development Center Universiti Teknologi Malaysia from November 2002 until May 2003. The test undertaken intends to gather vibration data and identifying dominating frequency range. Table 3.1 lists the types of engines under test that are close to the capacity of the new engine.

Table 3.1: Engine Specifications

Engine	Type
Engine A	150CC single cylinder, gasoline two-stroke, carburetor, air-cooled
Engine B	110CC single cylinder, gasoline two-stroke, carburetor, air-cooled
Engine C	125CC single cylinder, gasoline four-stroke, carburetor, air-cooled

These engines were installed on a test bed mounted on the floor and isolated with rubber mounting pad to reduce the transfer of vibration force to the test bed. Figure 3.1 shows the test bed used on Engine A.



Fig.3.1: Two- Stroke 150cc Gasoline Engine (Engine A)

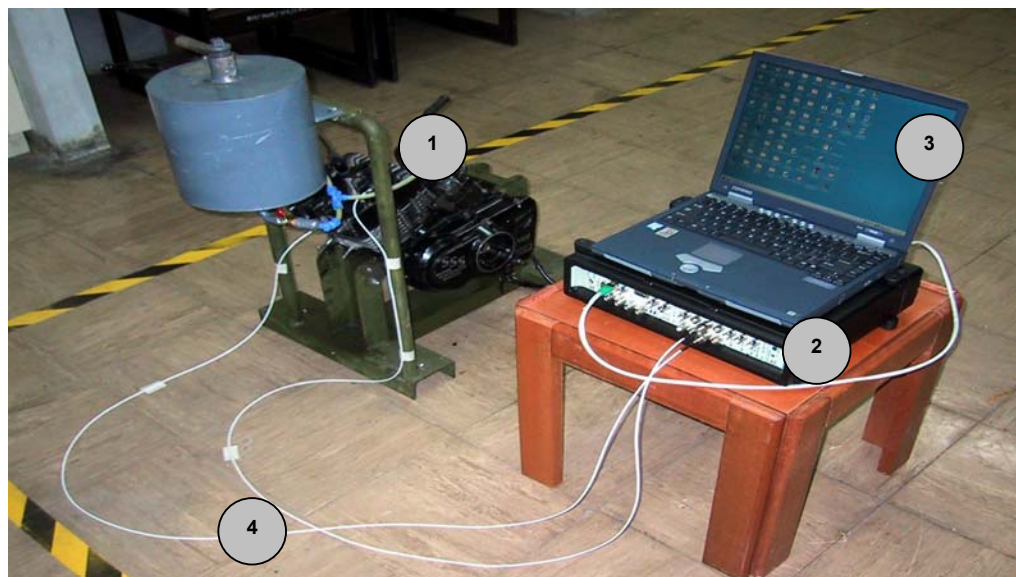
3.3 Test Instrumentation, Set-Up and Procedure

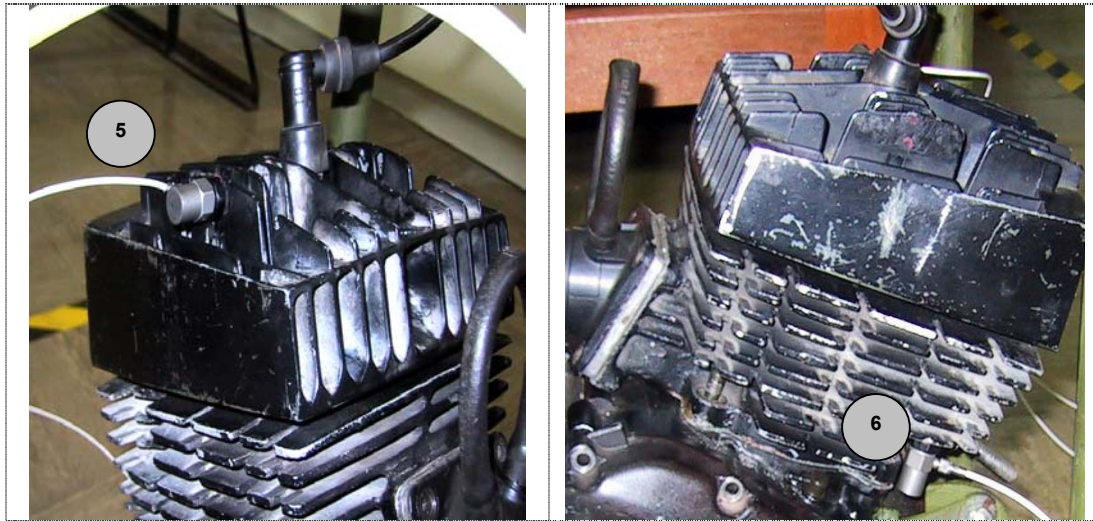
The instruments used consist of a multi analyzer, accelerometers and a tachometer. Overall vibration data completely analyze via FFT Analyzer within B&K Pulse 6.0 environment. Table 3.2 shows the specifications of the instruments used for

the test. The instrumentation set-up is illustrated in Figure 3.2. Accelerometers were attached at measurement points (glued with cement stud) at cylinder head, engine block, crankcase and crankcase covers.

Table 3.2: Instrumentation

Instruments	Type
Multi Analyzer Unit	Bruel & Kjaer Pulse Multi-Analyzer Type 3560C
Computer Laptop	Compaq Evo N160 Installed with B&K Pulse Type 7700 Noise And Vibration Software
Accelerometer	Kistler High Temperature Accelerometer Type 8702B500M8
Tachometer	Portable Tachometer Type DT-2236 Lutron





Equipments Description

1	Motorcycle Engine
2	Bruel & Kjaer Pulse Multi Analyzer Type 3560 C
3	Laptop with Software Pulse Labshop Version 6.0
4	BNC connecting cable between accelerometers and input channel
5 & 6	Kistler high temperature accelerometer

Figure 3.2

The engines were ran at idling speed under no load condition and vibration spectrums at several points on the engines were then recorded. The procedures were repeated for several constant engine speeds. The engine speed were measured by using a stroboscope.

3.4 Experimental Results

Below are the results from Overall Vibration test on Engine A at 1000 rpm. (Figure 3.3), Engine B at 1280 rpm and 3000 rpm (Figure 3.4 and 3.5), and Engine C at 1800 rpm and 2400 rpm (Figure 3.6 and 3.7).

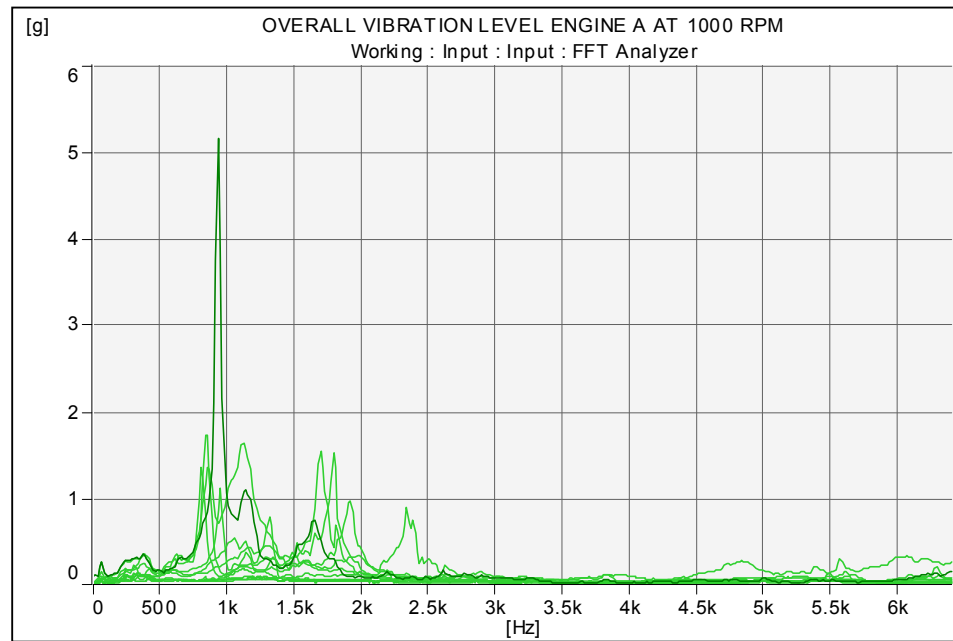


Figure 3.3: Superimpose of Overall Vibration Spectras Engine A at 1000 rpm for all measurement points

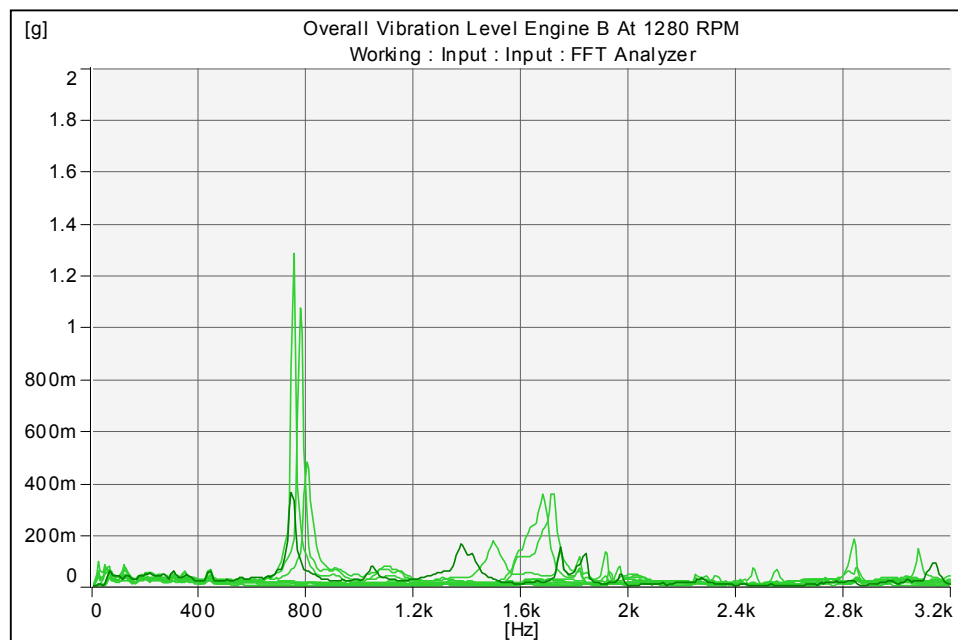


Figure 3.4: Superimpose of Overall Vibration Spectras Engine B at 1280 rpm for all measurement points

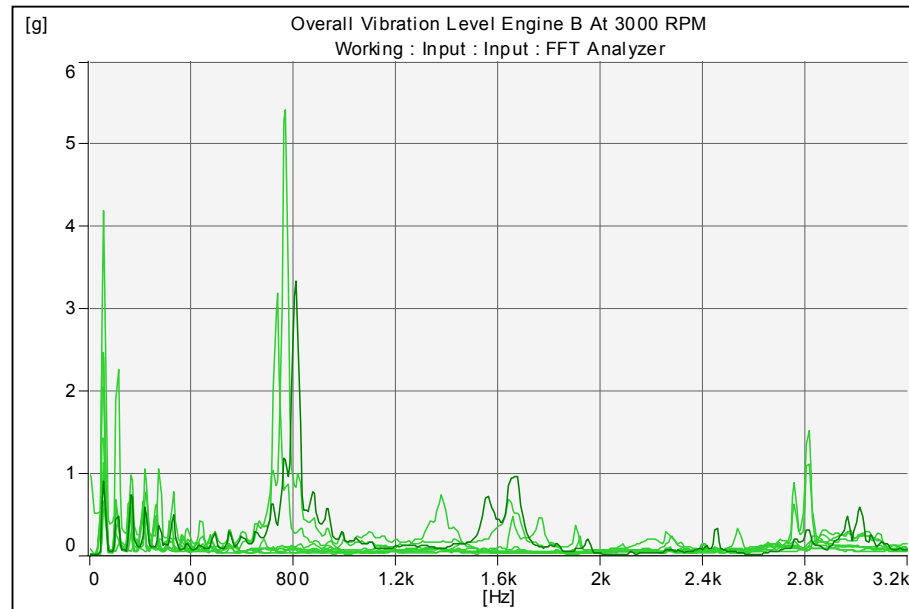


Figure 3.5: Superimpose of Overall Vibration Spectras Engine B at 3000 rpm for all measurement points

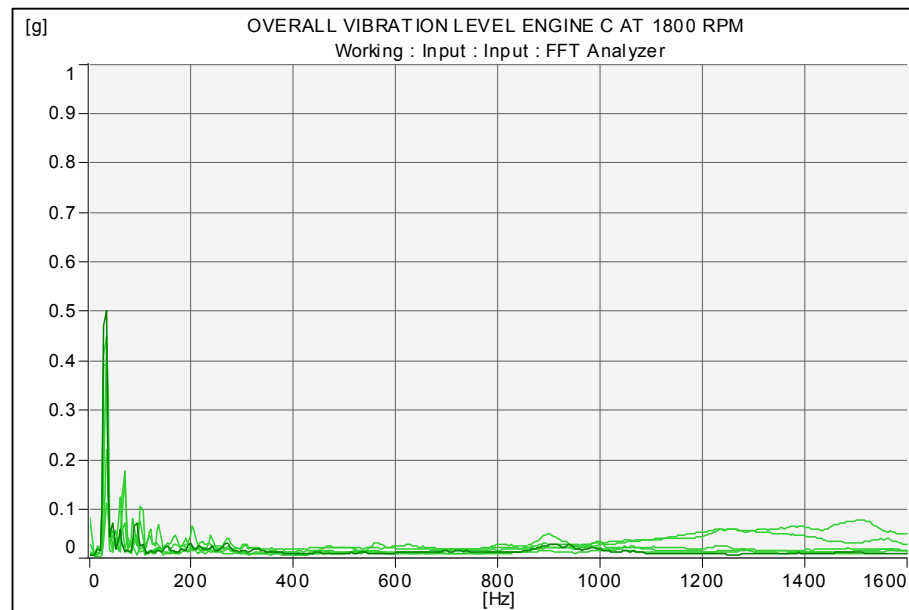


Figure 3.6: Superimpose of Overall Vibration Spectras Engine C at 1800 rpm for all measurement points

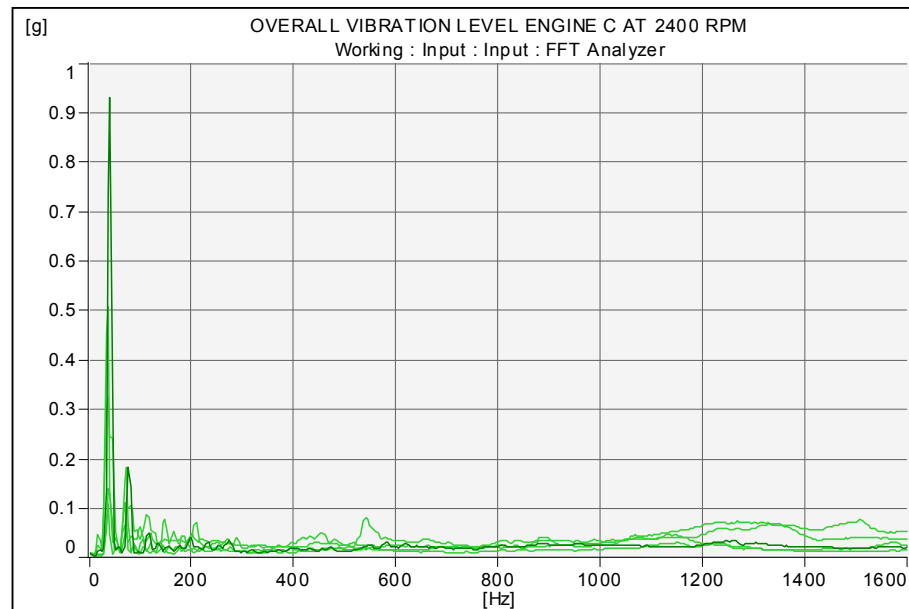


Figure 3.7: Superimpose of Overall Vibration Spectras Engine C at 2400 rpm for all measurement points

3.5.1 Discussion

Overall vibration level for the above engines has been studied and it was observed that the vibration occurred between 0-2500 Hz. Both Engine A and Engine B showed peak frequencies above 1g at cylinder head fin. While at other measurement points such as crankcase and crankcase cover, vibration levels were very low. For Engine C all measured points showed vibration peaks at the two speeds but the levels were below 1g.

Below are detail discussions on vibration at various point on Engine A.

a). Cylinder Head Overall Vibrations Response Level

Measurement points on cylinder head were set at 3 locations; fin at right side, fin at left side and stiffener at top-rear side (Fig.3.8).

It is observed that the vibration amplitude is below 2G for rear-top side and fin at left side (Fig.3.8a and Fig.3.8c) except vibration amplitude for fin at right side which is very high and reaching 5G at 928 Hz (Fig.3.8b).

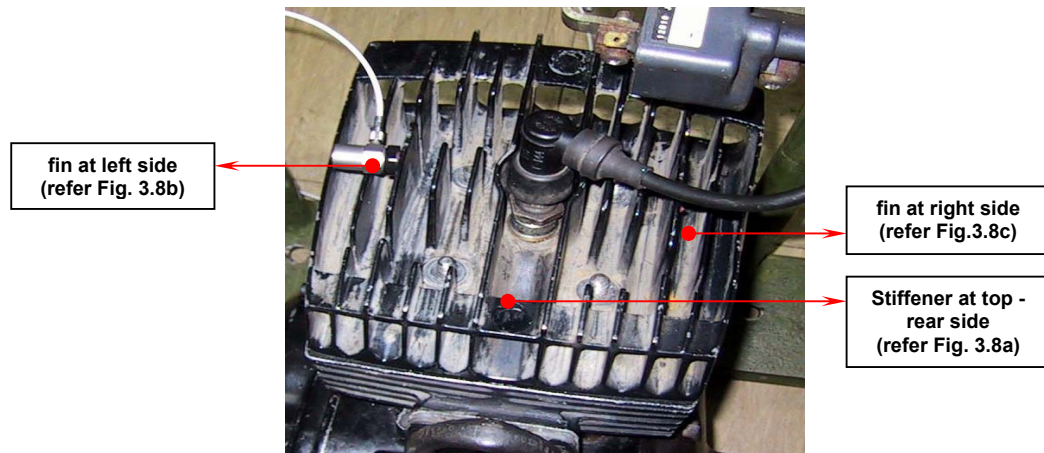


Fig. 3.8: Measurement points at Cylinder head

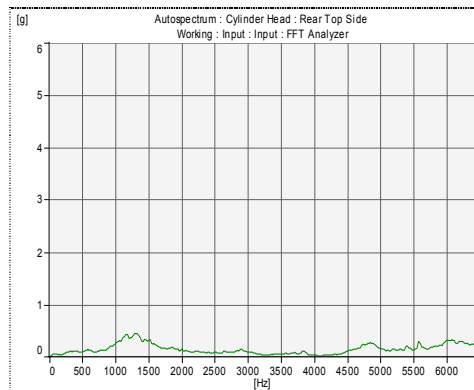


Figure 3.8 (a)

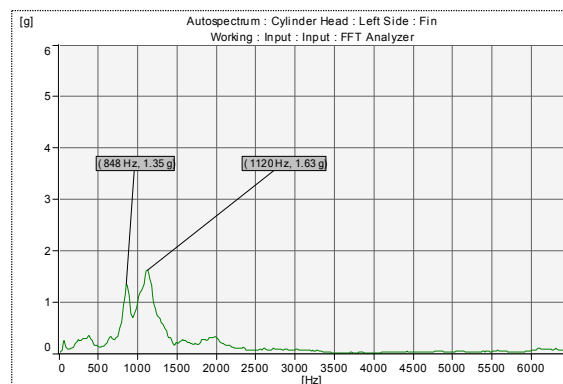


Figure 3.8 (b)

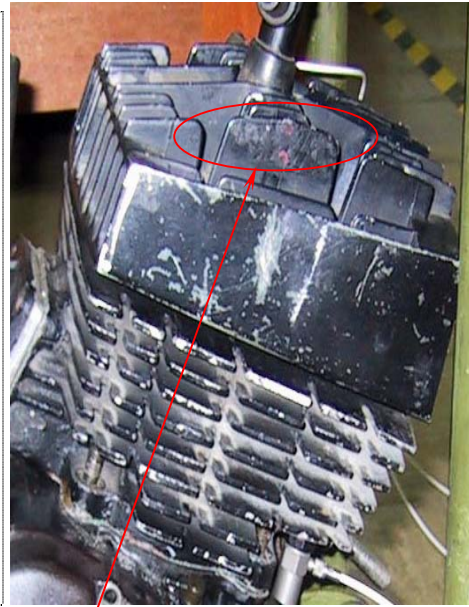
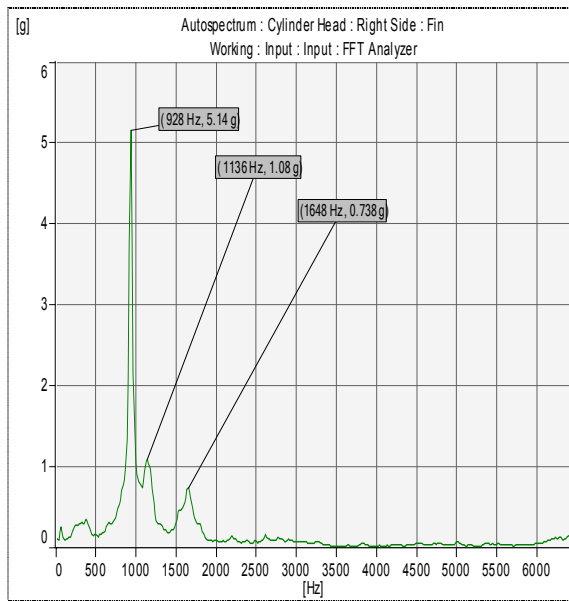


Figure 3.8 (c): Ride side fin

Highest vibration amplitude occurred at this right side fin

The high vibration on the right side fin occurred as it was not rigid enough and the vibration can be reduced by fitting a rubber cube in-between the fins.

(b). Engine Block Overall Vibrations Response Level

Measurement points on engine block were set at 4 locations, two of them is shown in Figure 3.9. Figure 3.10 (a) and (b) shows the vibration spectrums at these points. The results indicate that the amplitude of vibration is below 2G with two high peaks between 800 Hz to 2500 Hz.

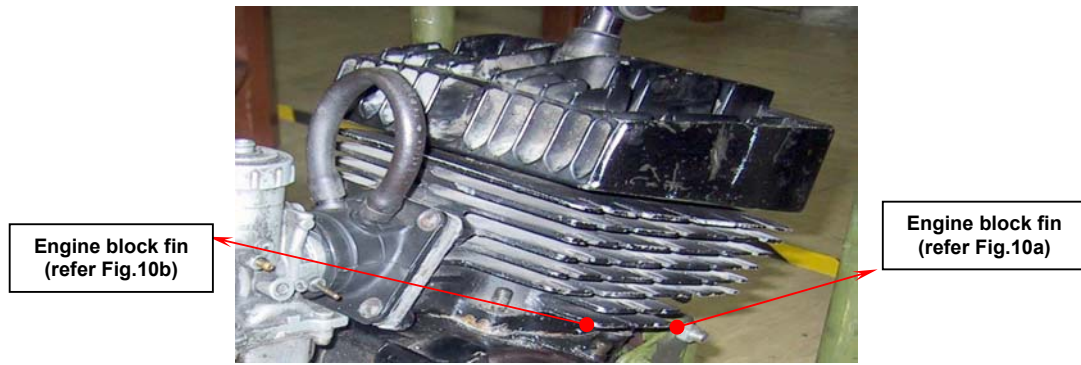


Figure 3.9: Measurement points at Engine Block Right Side

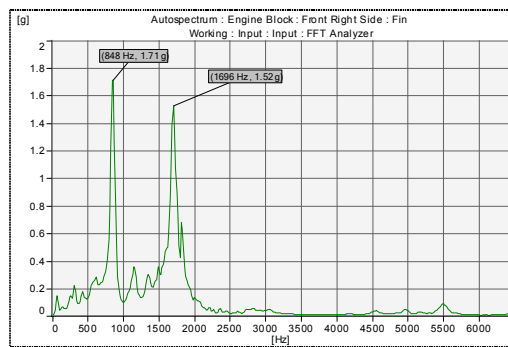


Figure 10 (a)

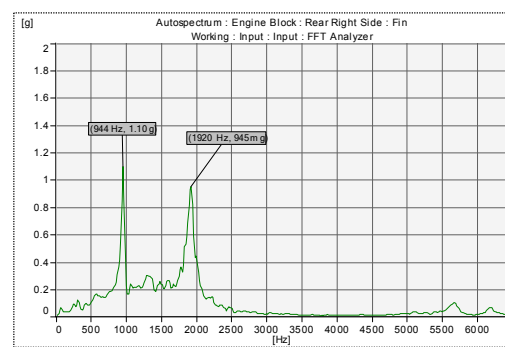


Figure 10(b)

(c). Crankcase Overall Vibrations Response Level

Measurement points on crankcase were set at 2 locations as shown in Fig. 11. The measured vibration spectra for the crankcase are shown in Fig.12(a) and Fig.12(b). The amplitude is below 0.2 G and no high peak was observed in the plots.

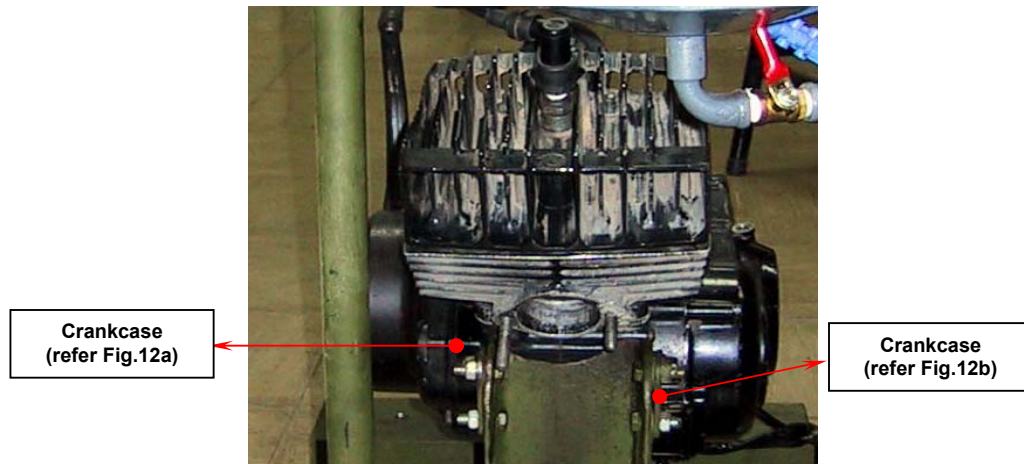


Fig.11: Measurement points at Crankcase

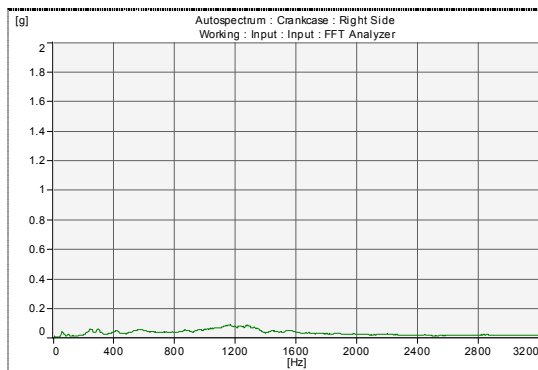


Figure 12(a)

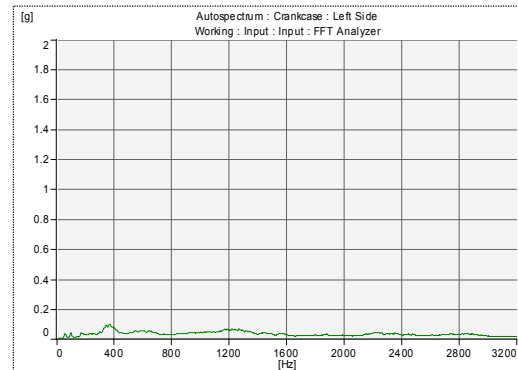


Figure 12 (b)

(d) Clutch Cover

Figure 13 shows the location of the measurement point on the clutch cover, with the measured vibration spectrum shown in Figure 14. The amplitude is also below 0.2 G and no peak was found in the plots. This is due to the stiffening of the clutch cover.

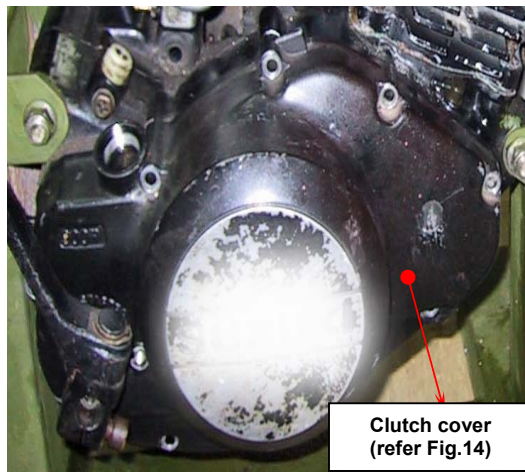


Fig.13: Measurement Point on Clutch Cover

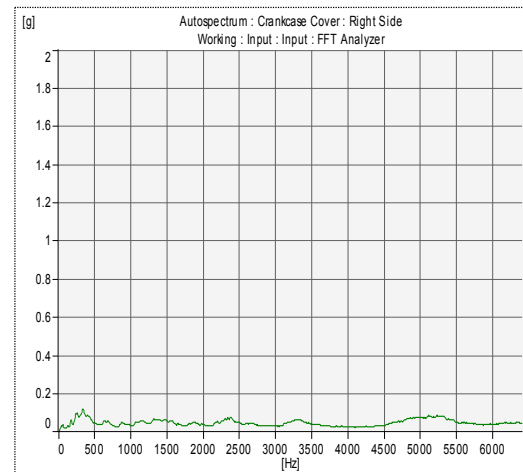


Figure 14

(e) Magneto Cover

Measurement point on magneto cover was set at a point shown in Fig. 15. with the measured spectra displayed in Fig. 16. The amplitude is also low, below 0.2 G which indicates effective stiffening of the cover.

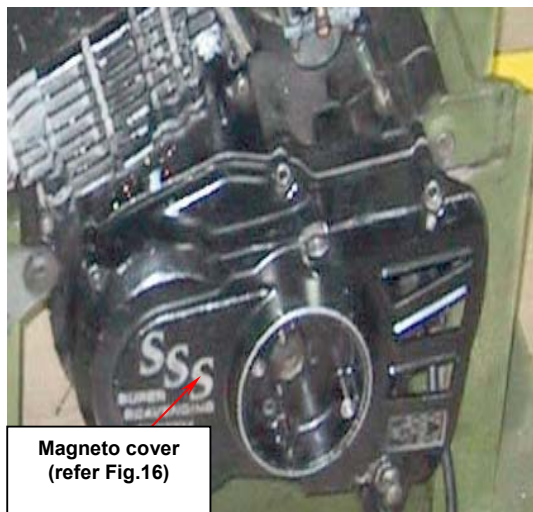


Fig.15: Measurement point at Magneto Cover

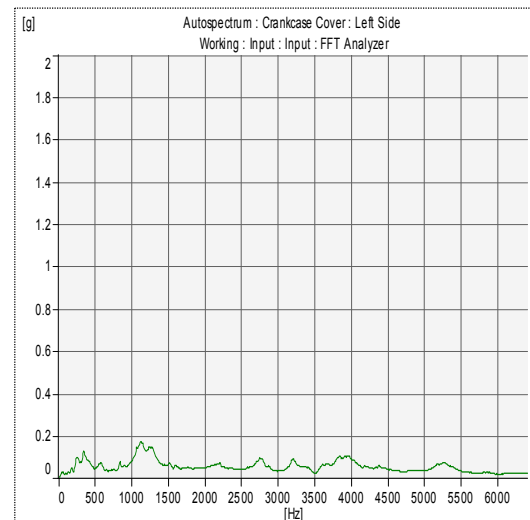


Figure 16

The overall vibration frequency for all the engines tested is summarized in Table 3.3 to 3.7. with respect to various components of the engine. Engine B and C show dominant frequency range below 200 Hz which is different from Engine A which shows peaks above 500 Hz. Thus it can be said that the dominant frequency range of the engines lies from 0 to 2.5 kHz.

Table 3.3: Summary of Overall Vibration for Engine A Operating at 1000 RPM

Part	Direction	Point	Peak Frequency				
			0-500 Hz	500-1000 Hz	1000-1500 Hz	1500-2000 Hz	2000-2500 Hz
Cylinder Head	Horizontal right	Fin	-	X	X	X	-
	Horizontal Left	Fin	-	X	X	-	-
	Vertical Up		-	-	-	-	-
Cylinder Block	Vertical Down	Fin Right Front	-	X	-	X	-
		Fin Right Rear	-	X	-	X	-
		Fin Left Front	-	X	-	X	
		Fin Left Rear	-	-	X	-	X
Crankcase	Horizontal Front	Right Side	-	-	-	-	-
		Left Side	-	-	-	-	-
Clutch Cover	Horizontal Right	Right Side	-	-	-	-	-
Magneto Cover	Horizontal Left	Left Side	-	-	-	-	-

Table 3.4: Summary of Overall Vibration for Engine B Operating at 1280 RPM

Part	Direction	Point	Peak Frequency				
			0-400 Hz	400-800Hz	800-1200 Hz	1200-1600 Hz	1600-2000 Hz
Cylinder Head	Horizontal right	Fin Right Front	-	X	-	-	-
		Fin Right Rear	-	X	-	-	-
	Horizontal Left	Fin Left Front	-	X	-	-	-
		Fin Left Rear	-	X	-	-	-
Cylinder Block	Horizontal Right	Front	-	-	-	-	-
		Rear	-	-	-	-	-
Crankcase	Horizontal Rear	Right	-	-	-	-	-
		Middle	-	-	-	-	-
		Left	-	-	-	-	-

Table 3.5: Summary of Overall Vibration for Engine B Operating at 3000 RPM

Part	Direction	Point	Peak Frequency				
			0-400 Hz	400-800Hz	800-1200 Hz	1200-1600 Hz	1600-2000 Hz
Cylinder Head	Horizontal right	Fin Right Rear	Harmonics	X	-	-	-
	Horizontal Left	Fin Left Front		X	-	-	-
		Fin Left Rear		X	-	-	-
Cylinder Block	Horizontal Right	Front		-	-	-	-
		Rear		-	-	-	-
Crankcase	Horizontal Rear	Right		-	-	-	-
		Middle		-	-	-	-
		Left		-	-	-	-

Table 3.6: Summary of Overall Vibration for Engine C Operating at 1800 RPM

Part	Direction And Point	Peak Frequencies							
		0-200 Hz	200-400 Hz	400-600 Hz	600-800 Hz	800-1000 Hz	1000-1200 Hz	1200-1400 Hz	1400-1600 Hz
Cylinder Head Cover	Horizontal Front (Aligned with stroke)	X	-	-	-	-	-	-	-
Cylinder Head	Vertical Up	X	-	-	-	-	-	-	-
Crankcase Cover	Horizontal Right	X	-	-	-	-	-	-	-
	Vertical Up	X	-	-	-	-	-	-	-
Crankcase	Vertical Up	X	-	-	-	-	-	-	-

Table 3.7: Summary of Overall Vibration for Engine C Operating at 2400 RPM

Part	Direction And Point	Peak Frequencies							
		0-200 Hz	200-400 Hz	400-600 Hz	600-800 Hz	800-1000 Hz	1000-1200 Hz	1200-1400 Hz	1400-1600 Hz
Cylinder Head Cover	Horizontal Front (Aligned with stroke)	X	-	-	-	-	-	-	-
Cylinder Head	Vertical Up	X	-	-	-	-	-	-	-
Crankcase Cover	Horizontal Right	X	-	-	-	-	-	-	-
	Vertical Up	X	-	-	-	-	-	-	-
Crankcase	Vertical Up	X	-	-	-	-	-	-	-

3.6 Conclusion

The overall vibration test on several existing engines at several constant speeds and no load condition indicate that the dominant frequency lies form 0 to 2.5 kHz. Such frequency range will assist us in identifying suitable numerical methods in determining the dynamic characteristics of the engine. Finite Element Method has been identified to be suitable for such frequency range and this technique will be used in the following study

CHAPTER IV

VIBRATION MEASUREMENT ON EXISTING ENGINE COMPONENTS

4.1 Introduction

This chapter reports on the measurement of vibration response on existing engine components to determine their natural frequencies individually. Such tests are required to gather data on the dynamic characteristics of the engine components and to be used for diagnose faults in engines. Several components of each engine were tested and in this report the measurements spectrum of only one of the engines is shown. The test results of all the engines are listed in the table. Three B.Eng. Thesis have been produced on this topic and is listed in reference (1) to (3) of this chapter.

4.2 Engine Description and Test set-up

Three existing engines were selected for the test and is describe in Table 4.1.

Table 4.1: Engine Description

No.	Engine	Type
1	Engine A	150 cc Two-stroke, air-cooled, carburetor
2	Engine B	110 cc Two-stroke, air-cooled, carburetor
3	Engine C	125 cc Two-stroke, air-cooled with fan, carburetor

The test samples were all suspended with light cables to simulate free-free condition and both impact and shaker types of excitations were executed to excite the structure and measure the response using a single accelerometer. Figure 4.1 shows the example of test set-up of the cylinder block.

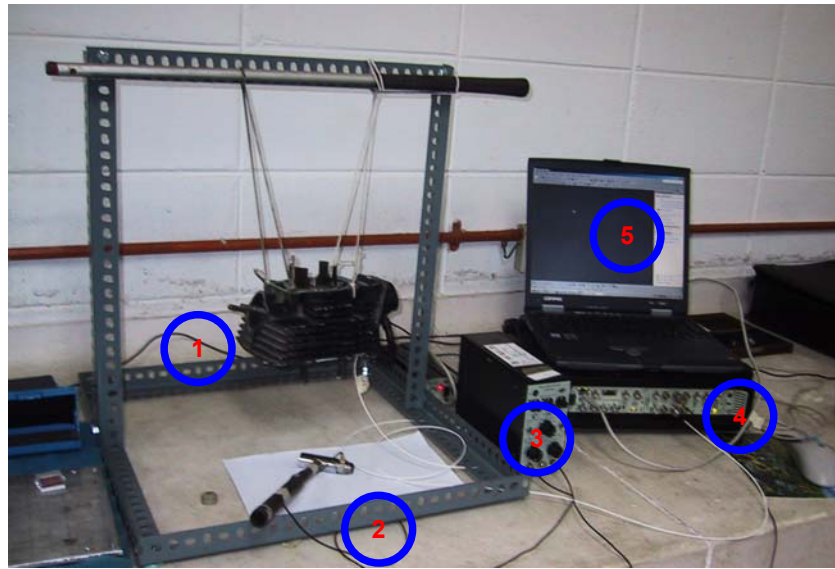


Figure 4.1

Table 4.2: Equipments description

Number	Equipment
1	Test Rig and Test Piece
2	Impact Hammer with Force Transducer B&K Type 8200
3	Charge Amplifier B&K Type 2635
4	B&K Pulse Multi Analyzer Type 3560C
5	Compac Evo Laptop with B&K Pulse Type 7700A Software

4.3 Test Results

The following are examples of test results of vibration measurements carried out on cylinder head, cylinder block, magneto cover and clutch cover (Fig.4.2-4.5) of engine B.

(a) Cylinder Head

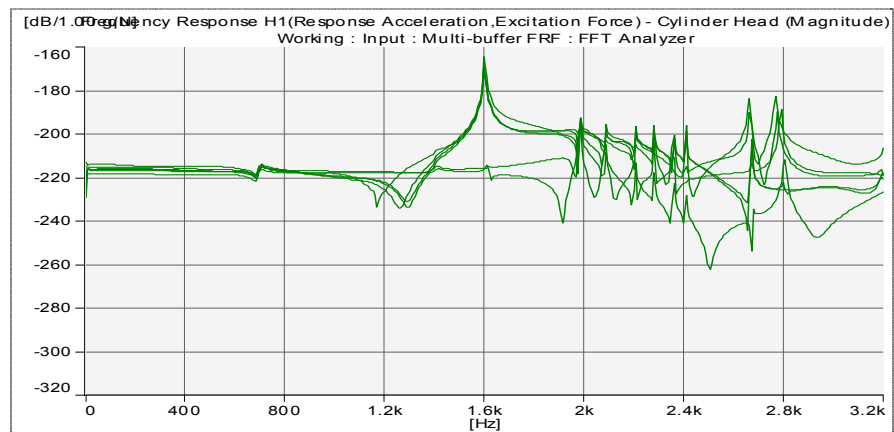
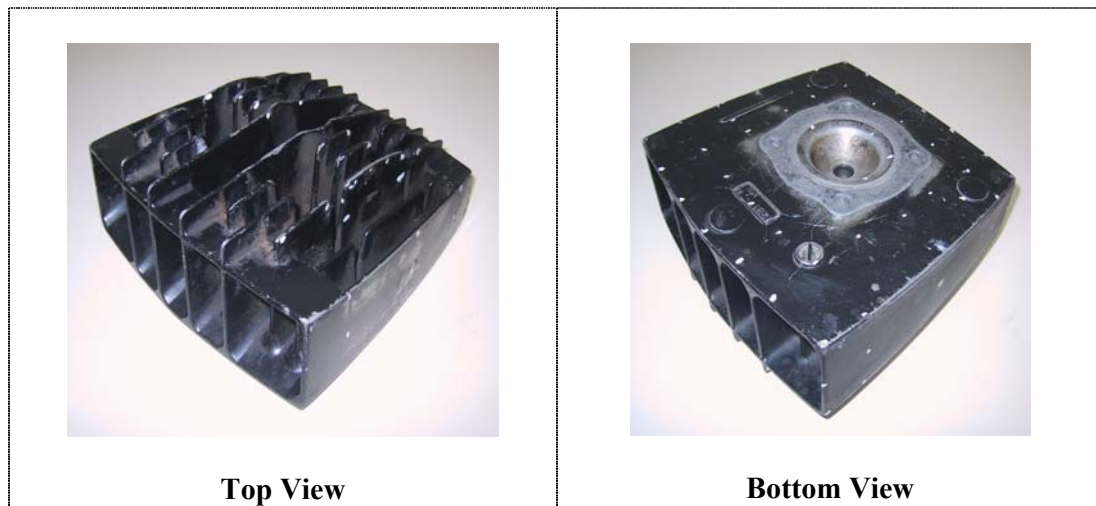


Figure 4.2: Measured frequency response functions (6 points)

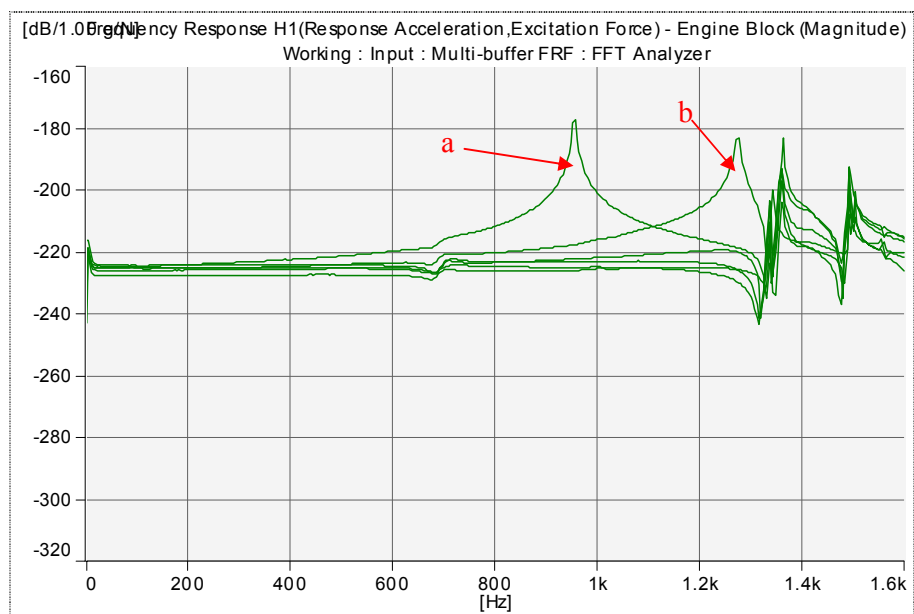
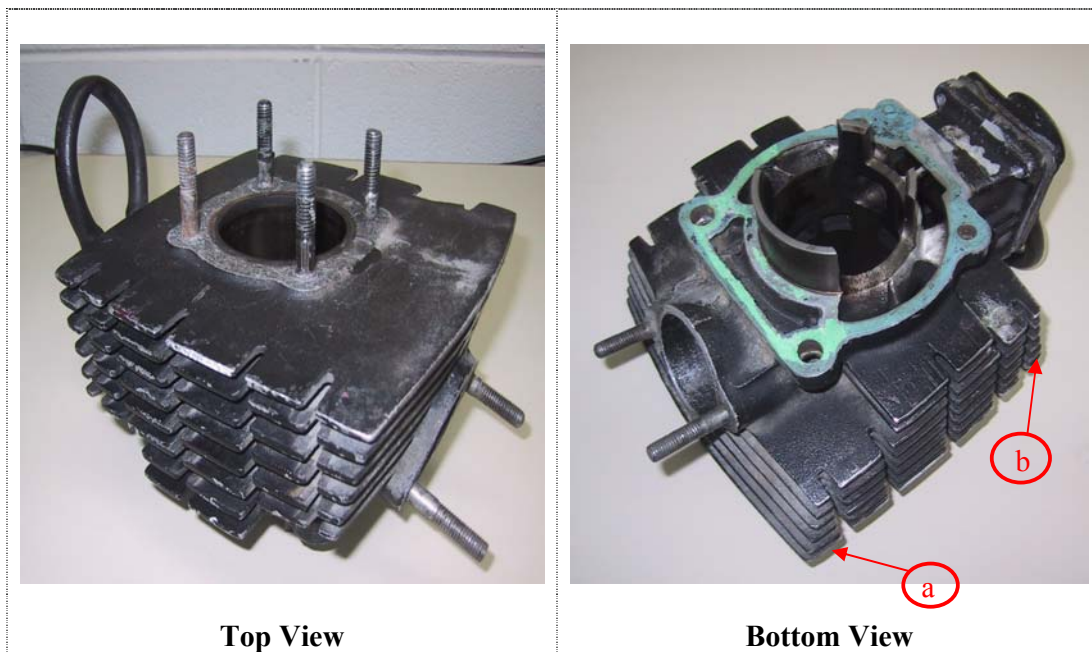
(b). Engine Block

Figure 4.3: Measured frequency response functions (6 points)

(c) Clutch Cover

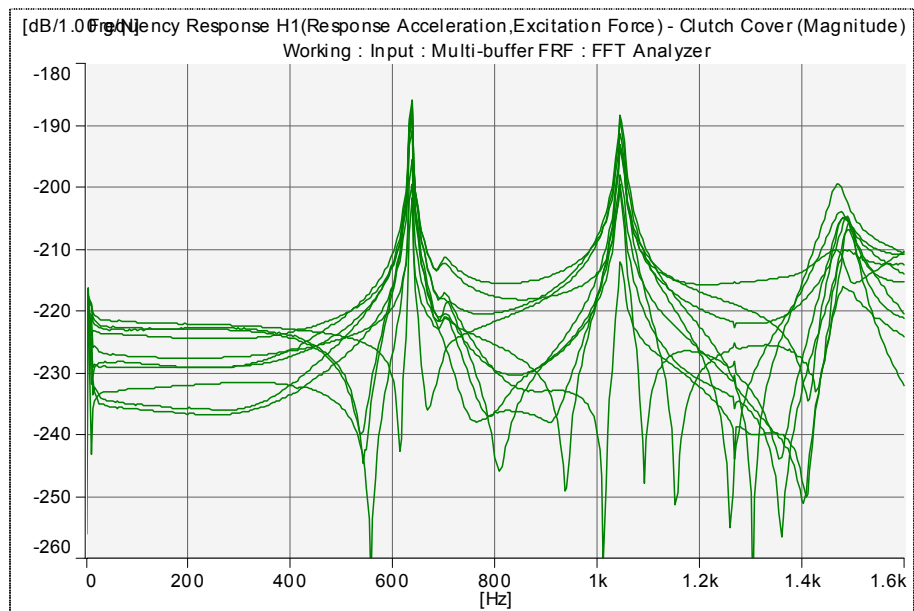


Figure 4.4: Measured frequency response functions (10 points)

(d) Magneto Cover

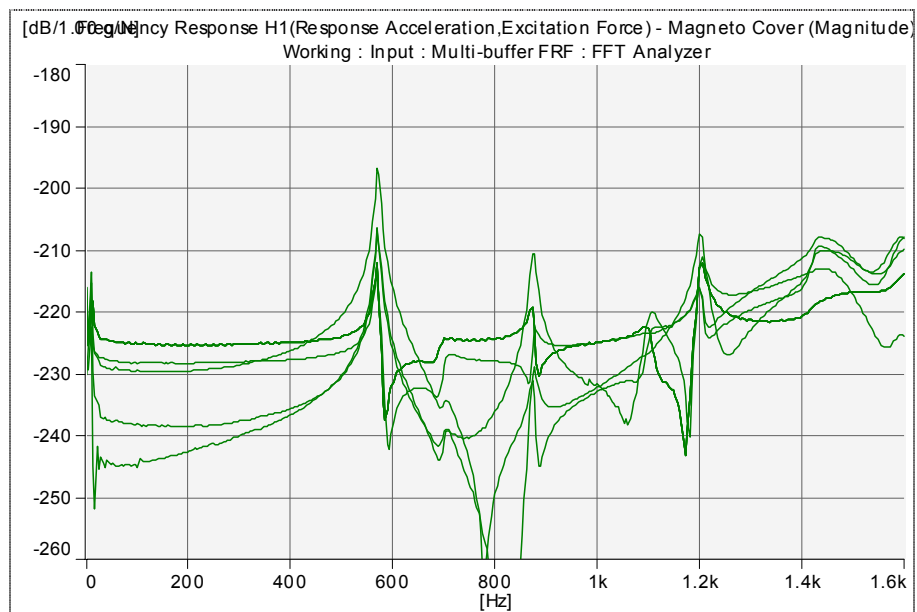


Figure 4.5: Measured frequency response functions (5 points)

Table 4.3 shows the components of each engines being tested and the natural frequencies are listed in Table 4.4.

Table 4.3: Components under Test as per engines

No.	Engine	Component Tested
1	B	Cylinder Head
		Engine Block
		Piston
		Connecting Rod
		Crankshaft
2	A	Cylinder Head
		Engine Block
		Magneto Cover
		Clutch Cover
3	C	Cylinder Head

Table 4.4: Natural Frequencies Data (First 4 Mode)

a) Engine B

Components	Natural Frequencies , Hz
Cylinder Head	776, 1050, 1130, 1530
Engine Block	952, 1160, 1240, 1350
Piston	3500, 3630, 3700, 5880
Connecting Rod	961, 2610, 3230, 6340
Crankshaft Left Side	1520, 2720, 3030, 4100
Crankshaft Right Side	130, 349, 550, 695

b) Engine A

Components	Natural Frequencies , Hz
Cylinder Head	704, 1600, 1984, 2088
Engine Block	956, 1272, 1344, 1504
Magneto Cover	568, 876, 1108, 1204
Clutch Cover	636, 704, 1044, 1472

c) Engine C

Components	Natural Frequencies , Hz
Cylinder Head	423, 434, 520, 535

4.4 Discussion

Almost all components of engines have natural frequencies between 400 Hz to 1.5 kHz except the small light components which include piston, crankshaft and connecting rod. These are the natural frequencies in free-free boundary condition, which gave us the dynamic characteristic of the structure. Such frequencies will not coincide with the exciting frequency of the running engines as the speeds of engines are low. However, it should be noted that these natural frequencies will shift to lower values when all the components are assembled. This is due to the increase in mass and reduction in the stiffness of the components. Since our target is to have high rigidity and low mass engine to achieve low noise engine, thus this means the engines structure will have high frequency which will be far away from the operating dominant frequency of the engines.

4.5 Conclusion

The natural frequencies of most of the engine components are within the range of 400 Hz to 1.5 kHz. The internal components such as the connecting rod, crankshaft and piston has a much higher natural frequencies which are then saved from the dominant frequency range of the operating engine.

4.6 Reference

1. Khong Khei Hon “ Vibration Characteristics of 2-Stroke Gasoline Engine”
B.Eng Thesis, 2003 UTM.
2. Jui Han Wen “ Kajian Getaran ke atas Omboh, Rod Penyambung dan Syaf
Engkol bagi Engin Gasoline Dua Lejang Secara Ujikaji”, B.Eng. Thesis 2003
UTM.
3. Fetea bin Yusha, “ Vibration Study on Engine Head Due to Combustion”,
B.Eng. Thesis 2004, UTM.

CHAPTER V

NUMERICAL SIMULATION OF THE DYNAMIC BEHAVIOR OF NEW 2-STROKE SINGLE CYLINDER GASOLINE ENGINE

5.1 Introduction

A new single cylinder, stepped-piston engine was conceptually developed by the engine design group and it was thus required to predict the dynamic behavior of the engine with respect to vibration and noise. The reduction of vibration and noise is a main engine development issue for the successful design on new engines. To overcome loss of time and high costs in building prototype at early stage of design, the simulation method has become the major tool of the engineer today.

In an engine, the main excitation force resulting from oscillating masses and the combustion process are introduced into the cylinder block and head through the main bearings of the crankshaft. The energy transferred to the engine surfaces results in surface vibrations which lead to noise radiation from these surfaces. The investigation of existing single cylinder engines in the previous chapter indicated that the frequency range of vibration is up to 2.5 kHz. This means that a finite element model of the engine and components should be able to describe the dynamic behavior of these components up to a frequency of 2.5 kHz. A B.Eng. Thesis on the vibration characteristics of 2-stroke gasoline engine using FE method was completed (1).

5.2 Finite Element Model

The FEM software used is MSC/NASTRAN and the finite element modeling of the engine components used Tet 10 element based on results of several types of elements found useful. It should be mentioned that the accuracy of a FEM calculation is basically dependent on the finite element representation of the considered structure.

The FE models of the cylinder head and block are shown in Figure 5.1.

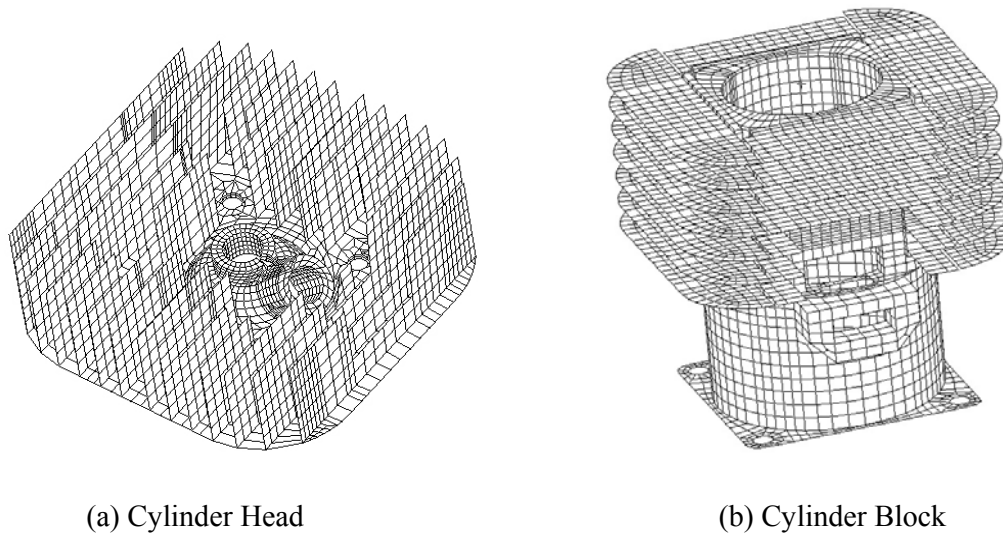
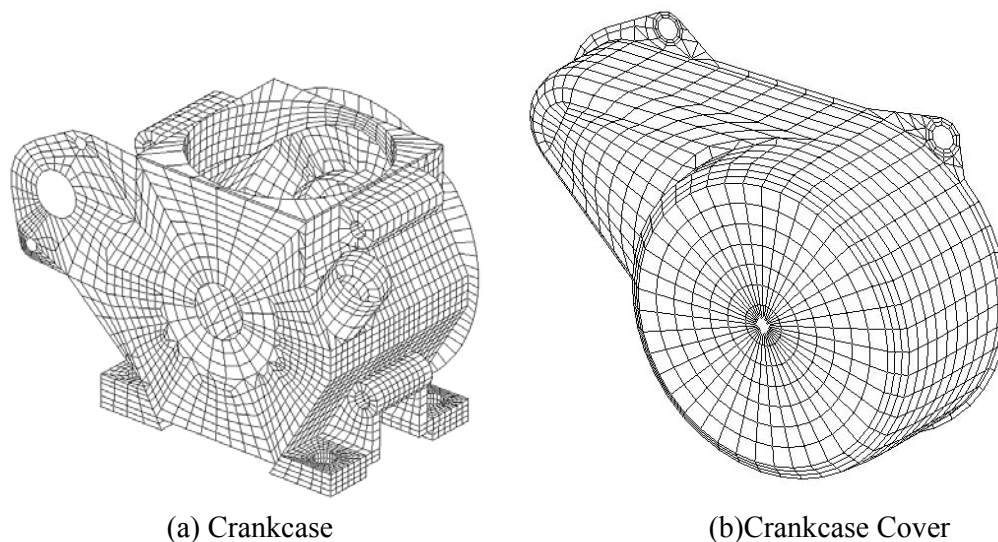
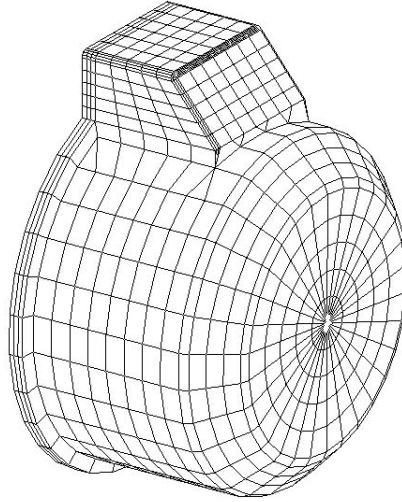


Figure 5.1: FE models

Figure 5.2 shows the FE models of crankcase, crankcase cover and magneto cover.





(c) Magneto Cover

Figure 5.2 FE models

Table 5.1 and 5.2 listed the materials, number of elements, nodes and material properties of all engine components.

Table 5.1: Materials, number of elements and nodes

Component	Material	No. of Elements	No. of Nodes
Cylinder Head	Aluminum Alloy	4453	5298
Cylinder Block	Aluminum Alloy	7790	10152
Crankcase	Aluminum Alloy	5644	7051
Crankcase Cover	Aluminum Alloy	1222	1241
Magneto Cover	Aluminum Alloy	968	994

Table 5.2: Material Property

Property	
Material type	Aluminum Alloy
Young's Modulus (GPa)	70
Poisson's Ratio	0.33
Density (kg/m^3)	2769

5.3 Finite Element Analysis on Engine Components

The natural modes for the components of the engines were calculated under free-fixed boundary condition with the fixed end bolted on a rigid body.

5.3 (a) Cylinder Head

Table 5.3 summarizes the results of the normal modes calculation and Figure 5.2 shows the corresponding mode shape for the cylinder head. The association of the eigenmodes to a subjective mode description is based on computer-animation of the eigenvectors. It is observed that the modes of cylinder head are dominated by the bending of the construction. Figure 5.2 shows the mode at each natural frequency of the cylinder block. The characteristics are dominated by the bending modes.

Table 5.3 Natural frequencies of Cylinder Head

No.	Frequency (Hz)	Mode
1	585.6	Global bending
2	671.7	Global bending
3	893.9	Fin bending

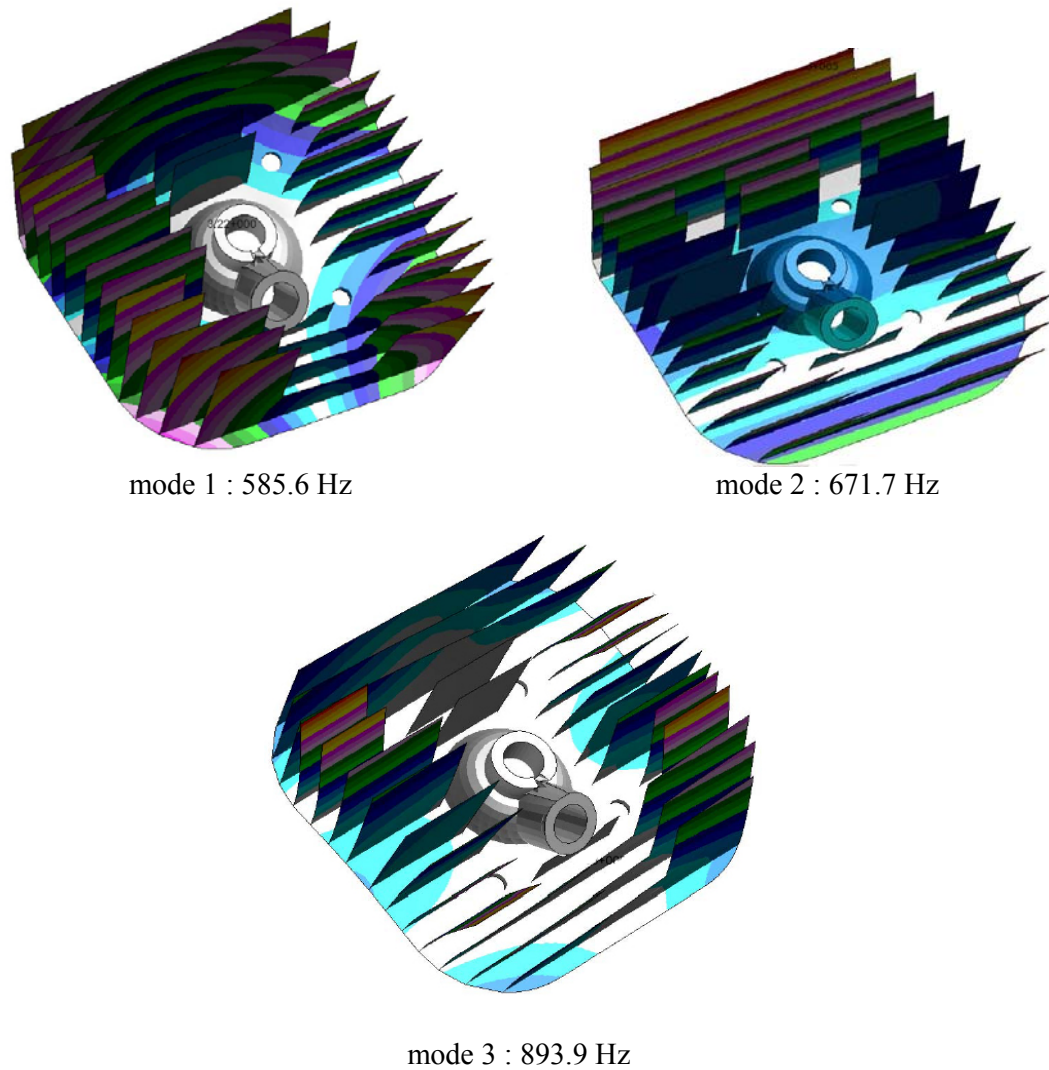


Figure 5.2: Mode shapes of cylinder head

5.3 (b) Cylinder Block

From the normal mode case in the Finite Element Analysis, 71 natural frequencies of the structure was found in the range of the operating frequency of the engine. All mode shapes are however, lie within this three dominant mode shape pattern and is shown in Figure 5.3 :

- 1- movement of the right and left hand side of the fin
- 2- movement of the intake fin
- 3- movement of the cylinder base

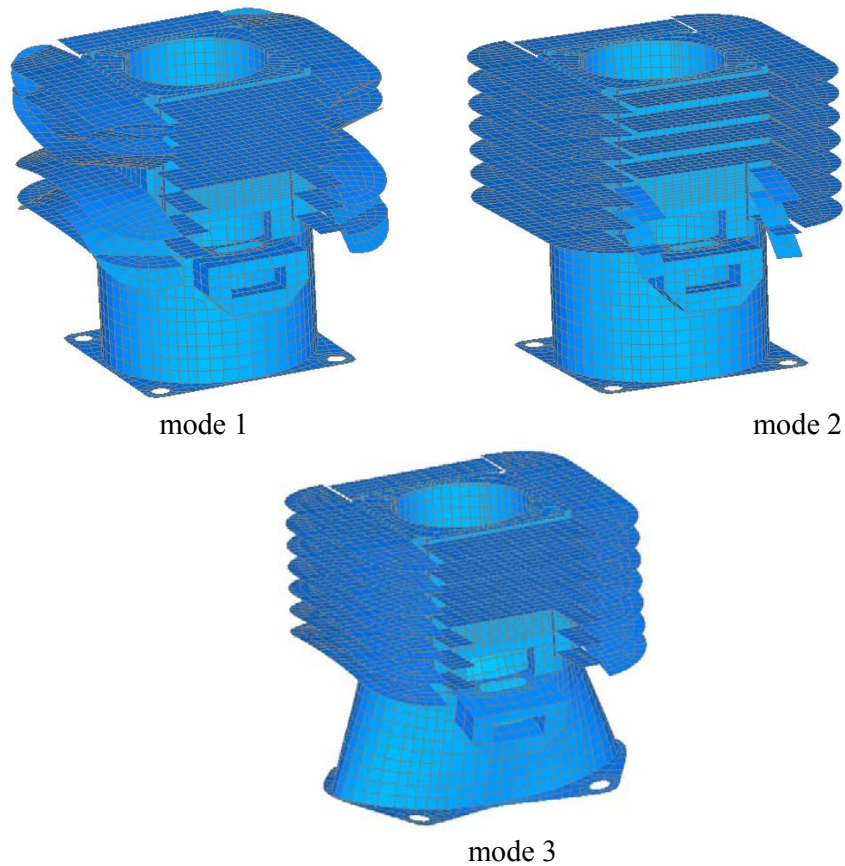


Figure 5.3 Mode shapes of cylinder block

5.3 (c) Crankcase

Only the first two natural frequencies were investigated since the desired frequency range is between 0 to 2500 Hz and is shown in Figure 5.4. This is due to the rigidity of the crankcase.



Figure 5.4 Mode shape of crankcase

5.3 (d) Crankcase Cover

Figure 5.5 shows the first six natural frequencies of crankcase since the desired frequency range is between 0 to 2500 Hz. The structure is fixed at all bolt location.

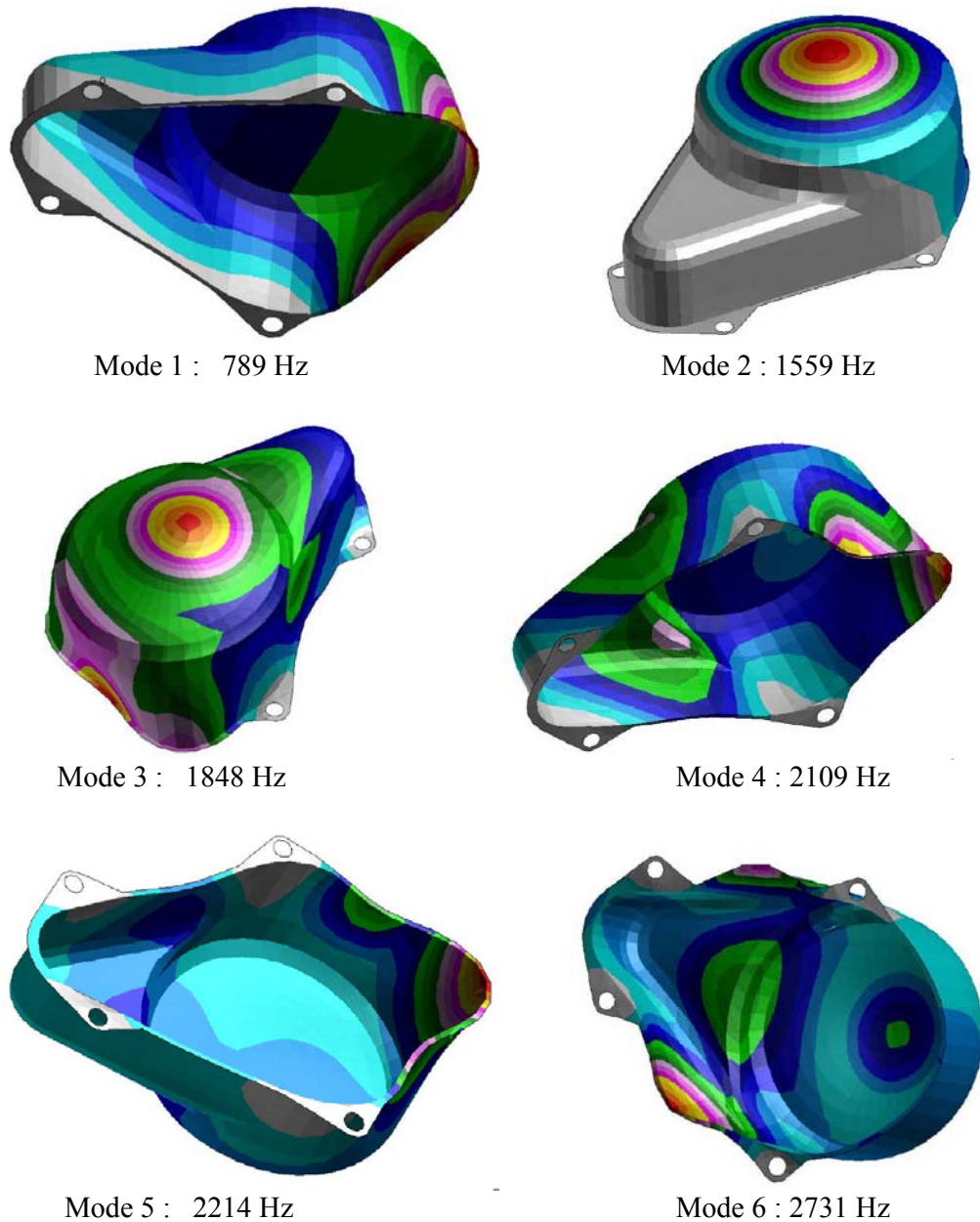
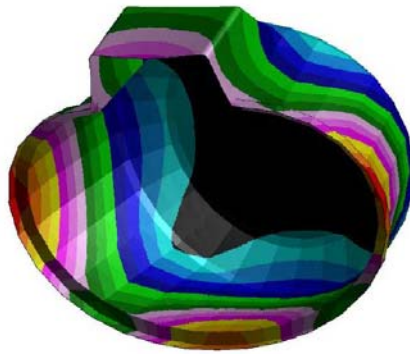


Figure 5.5: Mode shape of crankcase cover

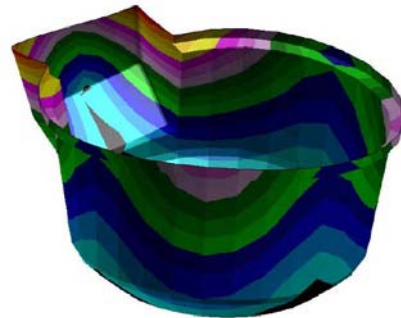
The mode shapes indicate that the first four modes are dominated by the response of the flat side cover of the crankcase cover which simulates a loud speaker modes. The fundamental natural frequency is high which indicates low rigidity of the cover.

5.3 (e) Magneto Cover

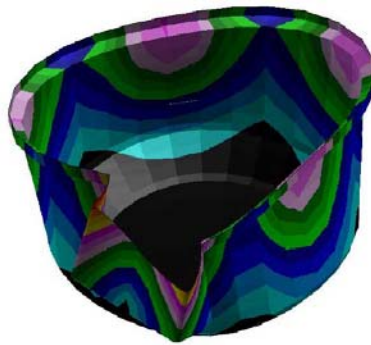
As for the magneto-cover, 6 mode shapes exist below frequency of around 2500 Hz and the loud speaker modes occurred at much higher frequencies at 4th and 5th modes.



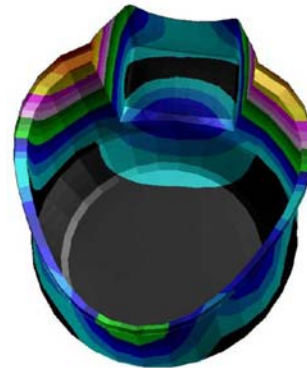
Mode 1: 737 Hz



Mode 2: 749 Hz



Mode 3: 1689 Hz



Mode 4: 1858 Hz



Mode 5: 2642 Hz



Mode 6: 2753 Hz

Figure 5.6 Mode shape of magneto cover

5.4 Sensitivity Analysis

Finite element analysis becomes worthless if the several assumption and simplifications unique to the method cannot be quantified. Assumptions often encountered in structural dynamics practice include : approximate values for nodal constraints, joint stiffness, lumped mass properties, etc. Since a FE model usually consists of numerous parameters, making an optimum selection that will be modified to obtain good response is a most difficult task. However, with the availability of FEMtools software (2), it will provide tools to assist in the selection of parameters.

Sensitivities indicate how a response value (e.g. resonance frequency) is influenced by a modification of a parameter value (3). These values are stored in a sensitivity matrix. Analyzing this matrix provides information on the sensitive and insensitive zones of the structure. Graphical tools allow the visualization of these different zones and a fast optimization of parameter selection. The resulting parameter changes are used to recalculate mass and stiffness matrices yielding new resonance frequencies and eigenvectors. An iterative process can then be continued until a convergence criterion is satisfied.

The FE models will be used in the sensitivity analysis to identify the appropriate part to be modified (stiffen) in order to reduce the vibration caused by resonance frequencies or, if possible, to shift the natural frequency of the structure away from the operating frequency. Modification is carried out on structure by adding thickness and ribs or using dampers without interfering with structure's main function and parameter

5.4.1. Sensitivity Analysis on Cylinder Head

Sensitivity analysis was carried out to find location where modification could be done to reduce vibration and stress due to natural frequencies of the structure. The weight and volume of the model is illustrated in Table 5.3.

Table 5.3: Properties of CAD and FE model

	CAD MODEL	FE MODEL
Material	ALUMINIUM ALLOY	ALUMINIUM ALLOY
Weight	0.65kg	0.62kg
Volume	$2.4\text{E-}4 \text{ m}^3$	$2.3\text{E-}4 \text{ m}^3$

Sensitivity analysis was carried out on the structure's thickness to get the modification location. The response was set as the natural frequencies and the parameter was set as thickness. The results are shown in Figure 5.7 to 5.8.

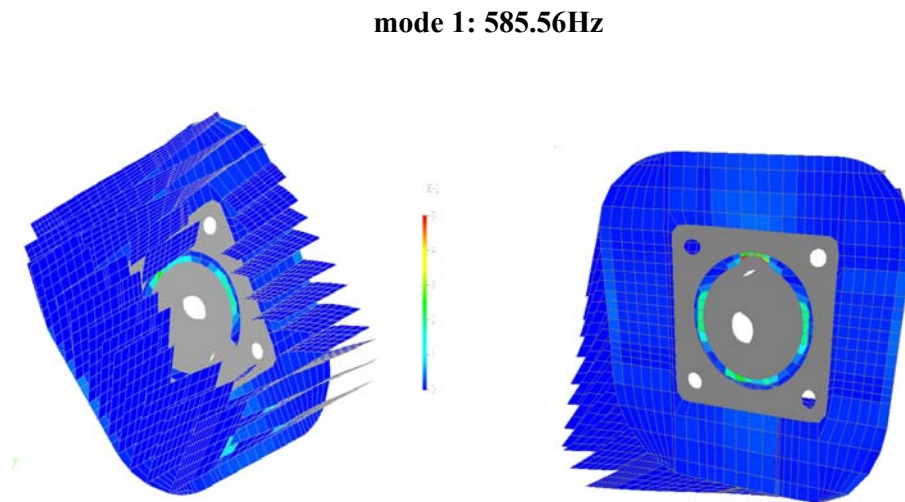


Figure 5.7: Location of thickness modification at first mode

It can be seen that this mode of vibration occurs at the base of the cylinder head. The free end of the fins has very high displacement while the other end has low displacement. It is suspected that stress distribution is high at the connection of the base and the fins.

The sensitivity analysis has also shown that the connection area has a highly significant effect on the first mode. Modifying these areas will cause the frequency to

shift and reduce the vibration amplitude. It can be concluded here that the connection area needs to be stiffened.

mode 2 : 671.69 Hz

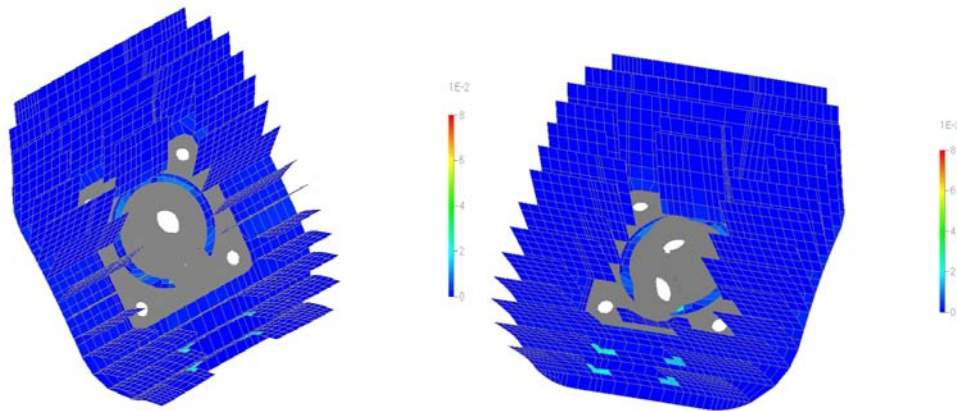


Figure 5.8 Location of thickness modification at second and third mode

mode 3 : 893.95 Hz

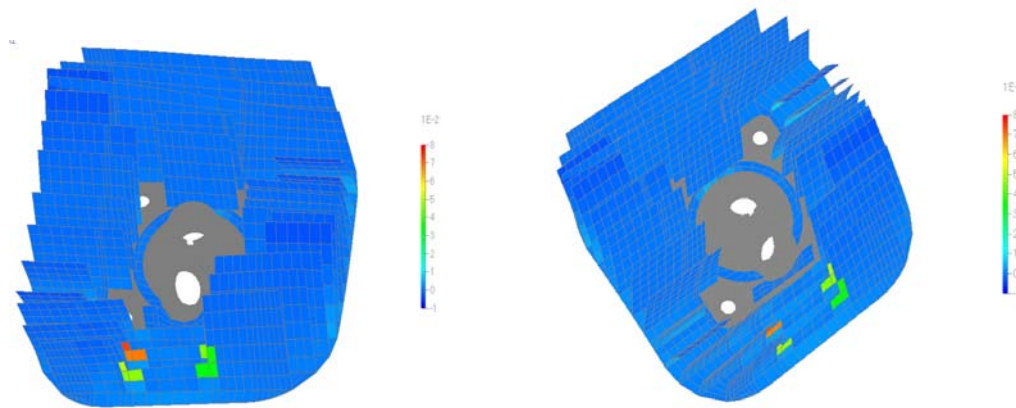


Figure 5.8 (continued): Location of thickness modification at second and third mode

These two modes are quite the same. The displacement plot shows that at the bottom of the fins has the high stress. The sensitivity analysis has shown the area that needs to be stiffened in order to reduce vibration amplitude as shown above.

In order to reduce the vibration of the cylinder head, there are some modifications needed to be applied. From the first three frequencies, it is observed that the vibration of the cylinder head will cause high stress at the base of the cylinder head

which it occurs at the connection between the base and the fins. In order to reduce this vibration, we need to add the thickness of the base as shown below. Red color in Figure 5.9 indicates the added mass to the base of the cylinder head. It should be noted that the base is fastened to the top of cylinder block

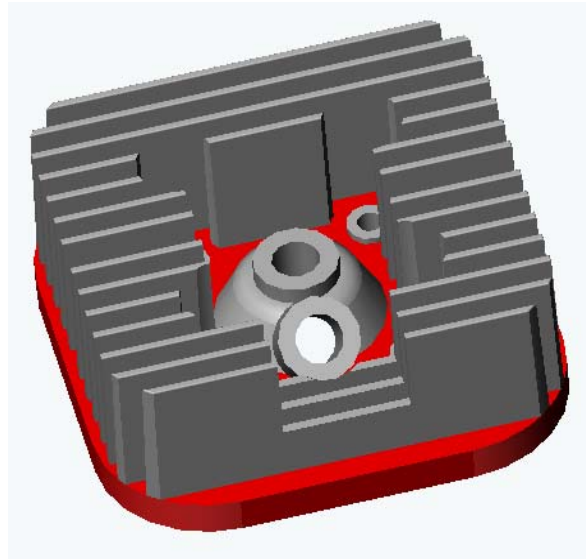


Figure 5.9: Added mass to the base of cylinder head

Another modification that can be done to increase the stiffness is by using rubber damper between the fins. The rubber damper can be inserted between the fins to reduce vibration as shown in Figure 5.10. Green color indicates rubber dampers being inserted between the fins.

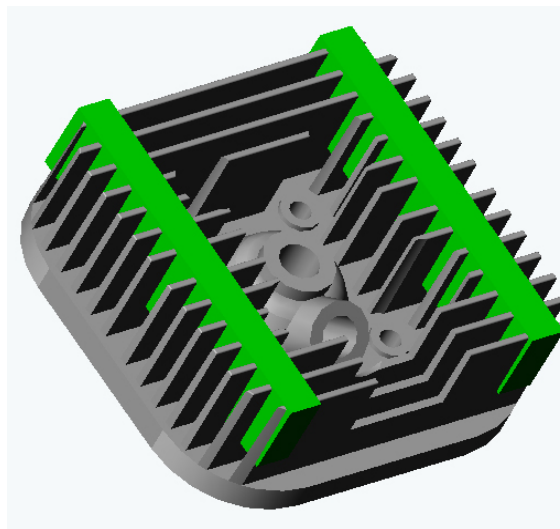


Figure 5.10: Rubber damper added to fin

5.4.2. Sensitivity Analysis on Cylinder Block

Modifying the structure based on three dominant mode shape can solve the vibration problem for the rest of the modes. Sensitivity analysis is carried out to find the appropriate part to be modified. Figure 5.11 shows the sensitivity analysis result for the models. Parts with color contour are the place where modification should be done.

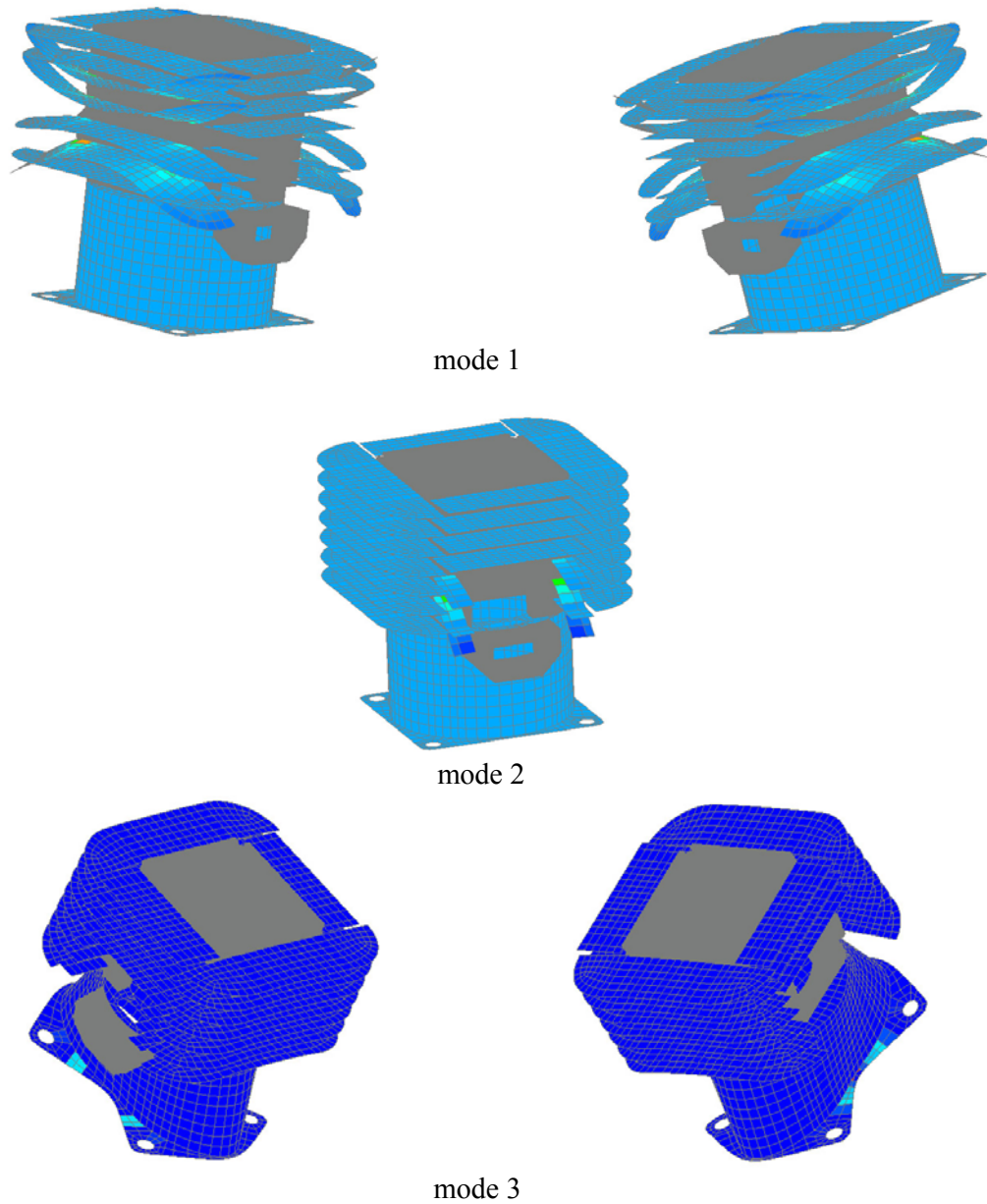


Figure 5.11 Location of adding thickness to cylinder block

The results obtained from the sensitivity analysis point out the place that needs to be stiffened. Additional mass is used to stiffen the structure and hence reduce the stress and amplitude caused by resonant. Additional mass on the structure is shown in Figure 5.12.

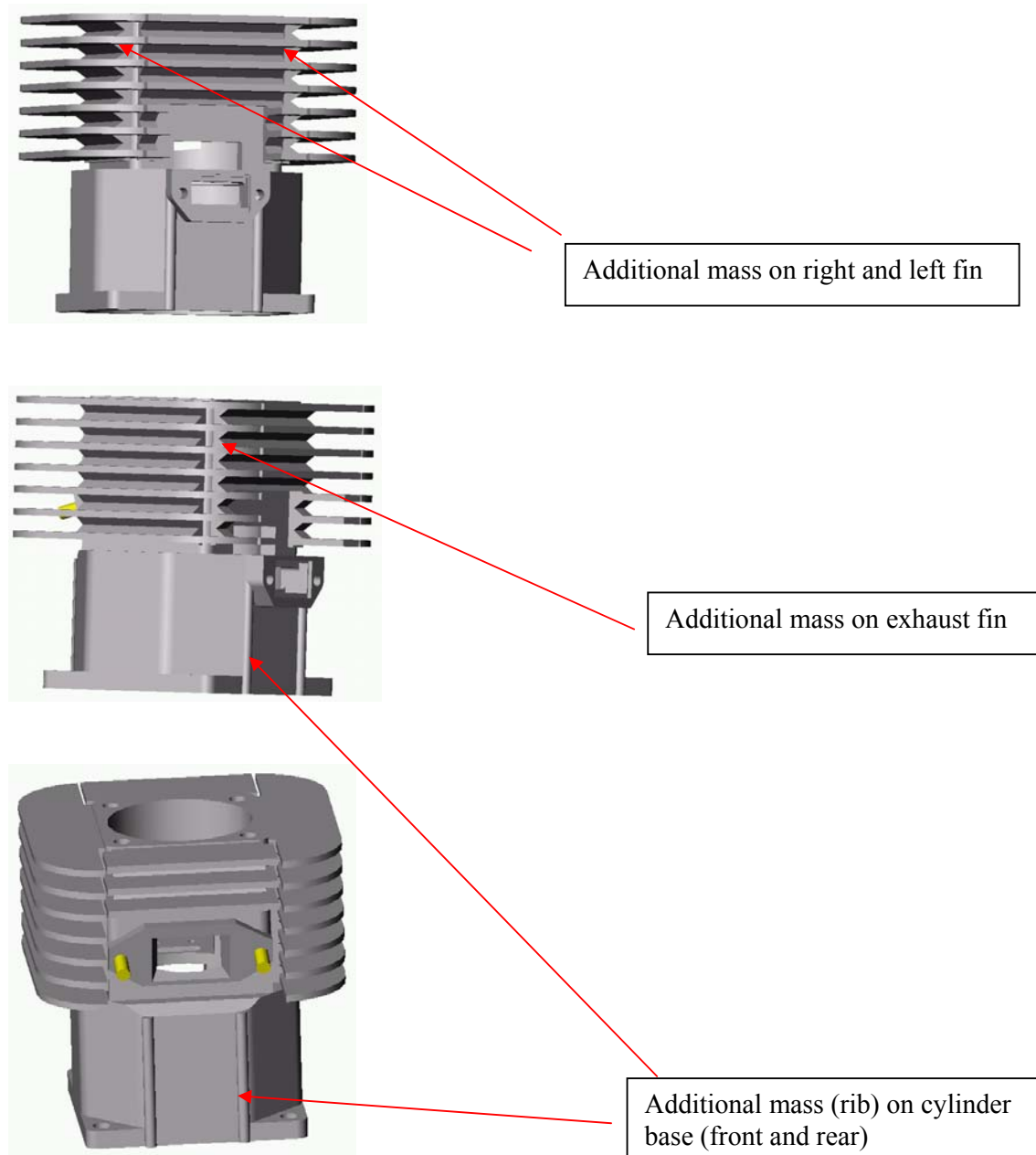


Figure 5.12: Location of additional mass on the cylinder block

The modified model is analyzed and the result is compared with the original structure as listed in Table 5.4

Table 5.4: Comparison after sensitivity analysis

	Original model	Modified model
Mass	1.33 kg	1.4 kg
Total mode shape	71	32

After modification, the total mode shape was reduced about half of the original model but the mass was increased by 5.26%. Most of the mode shapes (mode 1-25) are local, involving only left and right fin and the others are combination between fin and cylinder base and cylinder base itself. To further reduce the vibration level, it is suggested to insert rubber damper in between each fin and design a proper mounting for joining the base with crankcase.

5.4.3. Sensitivity Analysis on Crankcase

Sensitivity analysis was carried out on the structure's thickness to get the location to add stiffness. The response was set as the natural frequencies and the parameter was set as thickness. The results are shown in Figure 5.13 and 5.14.

Mode 1: 2536 Hz

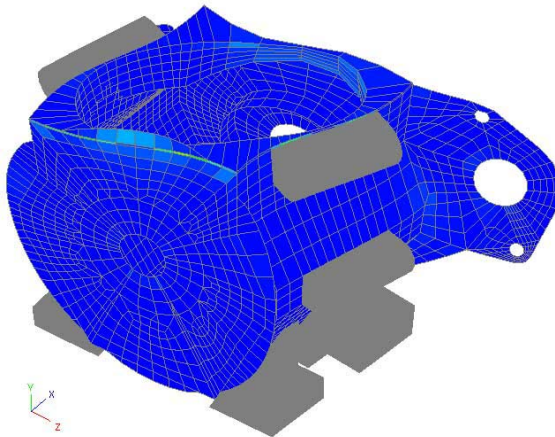


Figure 5.13

The first mode indicates a torsion type of vibration. It will cause high stress at the top section of the structure as indicated by the stress plot. The sensitivity analysis has shown that the area that needs to be stiffened in order to reduce vibration amplitude is as shown in Figure 5.13.

Mode 2 : 2972 Hz

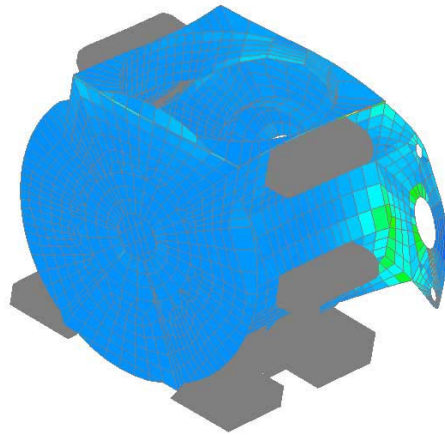


Figure 5.14

It can be seen in Figure 5.14 that this mode of vibration occurs at the flange. A cantilever effect can be clearly seen since the flange is quite long. The free end of the flange has very high displacement while the other end has low displacement. We can assume that stress is quite high at the connection of the body and flange.

The sensitivity analysis has also shown that the connection area has a highly significant effect on the first mode. Modifying the area will cause the frequency to shift and reduce the vibration amplitude. It can be concluded here that the connection area needs to be stiffened.

Modification is done, but bearing in mind that the objective is a lightweight and high rigidity crankcase. So, area with high sign of sensitivity should be stiffened while area with low sensitivity should be un-stiffened by reducing thickness or mass. The process of un-stiffening however should consider the fact that it will not create other problems such as stress failure, fatigue and etceteras.

In this case, modification can only be done based on mode 2 since it is located at an area where modification can be done without interfering with other major parts of the

engine. Figure 5.15 below shows the suggestion to increase stiffness by adding mass at the area of connection between the flange and the body. This will help to reduce the vibration cause by the cantilevered effect of mode 2.

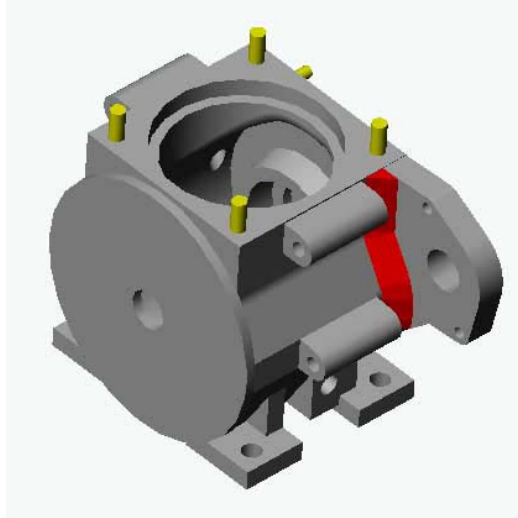


Figure 5.15: Suggested Modification on crankcase

The crankcase new weight is now 2.34 kg or an increase of 0.43 %. Modification has been done on the FE model and the results are illustrated in Table 5.5.

Table 5.5 Comparison of natural frequencies after modification

Mode No	Original Frequencies (Hz)	Modified Frequencies (Hz)	% Increase
1	2536	2556	0.8
2	2972	3174	6.8

From Table 5.5 it can be seen that there is significant increase for mode 2 rather than mode 1. This is because no modification is done based on mode 1 since the area for stiffening for mode 1 is unreachable and obstructed by other engine parts. However the area will be bolted to the cylinder block, therefore no modification is required since it will be stiffened by the engines assembly. The attempt to reduce weight of the crankcase cannot be done since the low sensitivity area is located at places where it is impossible to remove any mass due to the complexity of the crankcase.

5.4.4. Sensitivity Analysis on Crankcase Cover

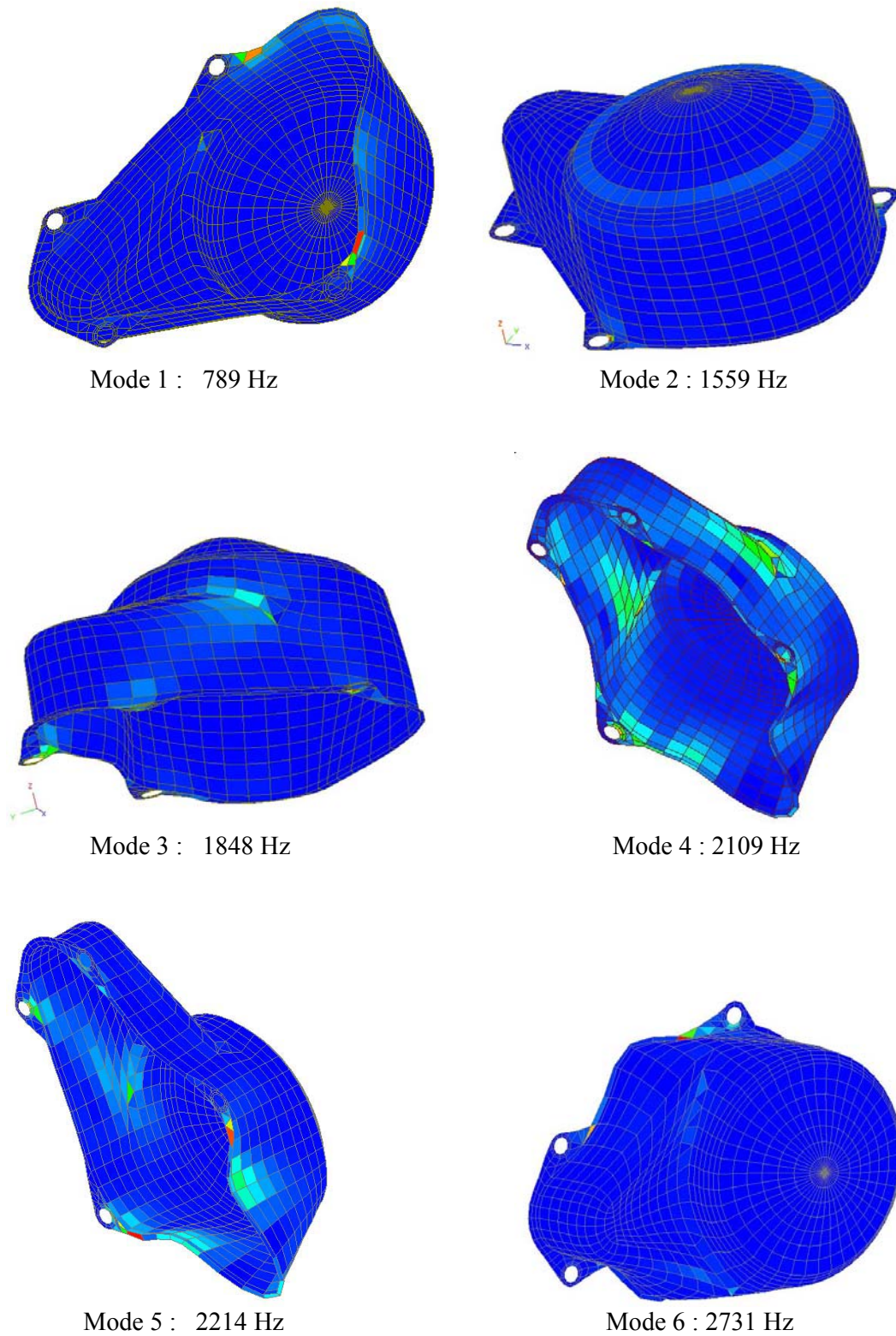


Figure 5.16: Location of additional thickness at each mode

Figure 5.16 shows results of sensitivity analysis on the crankcase cover indicating suggested location to be thickened. Figure 5.17 indicates areas that require stiffening and Figure 5.18 shows suggested modification that need to be considered.

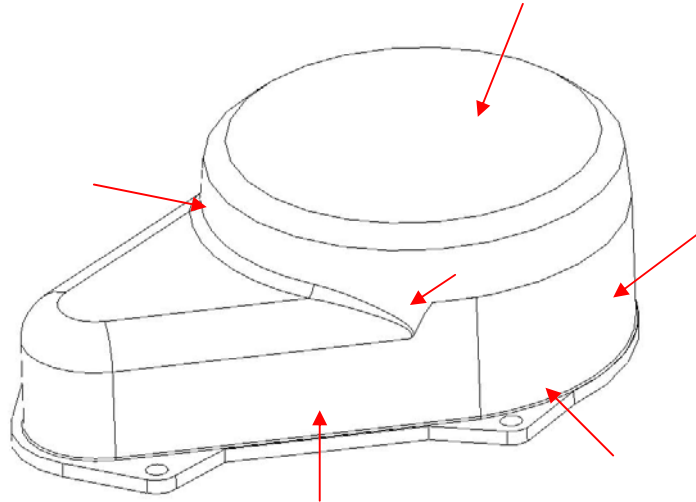


Figure 5.17: Area that requires stiffening

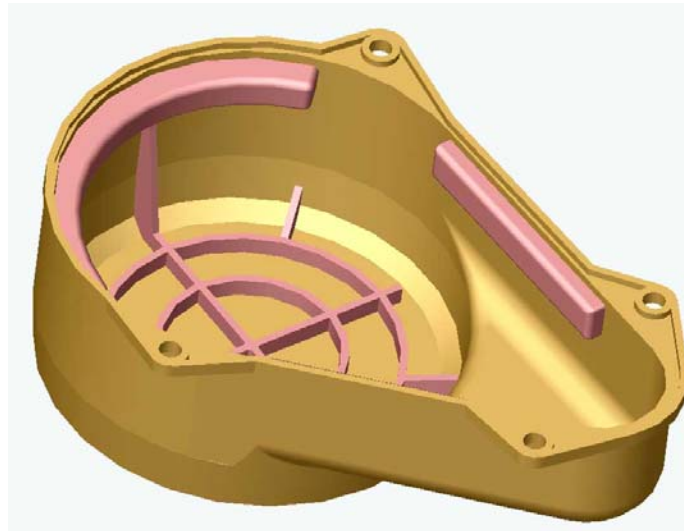


Figure 5.18: Crankcase cover with suggested modification

Modification of the structure resulted in the crankcase new weight to be 0.263 kg or an increase of 33% (65g) in weight. Modification has been done on the FE model and the results are listed in Table 5.6. This table has shown that the modification has shifted the first natural frequencies from 789 to 1490 Hz. The added stiffness has also reduced the natural frequencies within the range of 0-3500 Hz from 9 modes to only 5.

The attempt to reduce weight of the crankcase cover cannot be done since the low sensitivity area is located at places where it is impossible to remove any mass due to the complexity of the crankcase cover.

Table 5.6: Changes in Natural Frequencies after Modification

Mode No	Original Frequencies (Hz)	Modified Frequencies (Hz)
1	789	1490
2	1559	1877
3	1848	2264
4	2109	2561
5	2214	3238
6	2731	-

5.4.5. Sensitivity Analysis on Magneto Cover

Sensitivity analysis was carried out on the structure's thickness to get the location to add stiffness. The response was set as the natural frequencies and the parameter was set as thickness. From the normal modes results, it can be seen that the only mode shape that needs to be worried is mode no 6. This speaker like vibration occurs on the flat side of the magneto cover. The sensitivity analysis result for this mode is shown in Figure 5.19.

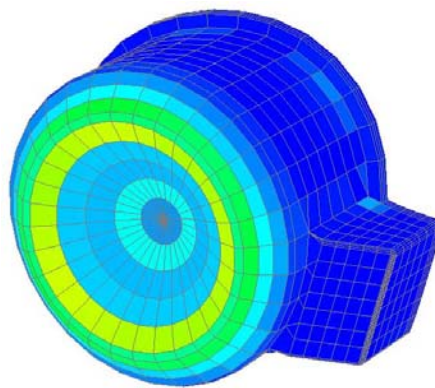


Figure 5.19: Sensitivity Analysis Results of Mode 6

Sensitivity analysis for other mode is as shown in Figure 5.20. Note that only two modes are shown as the results for mode 1, 2, 3, 4, 5, 7 and 8 are almost the same.

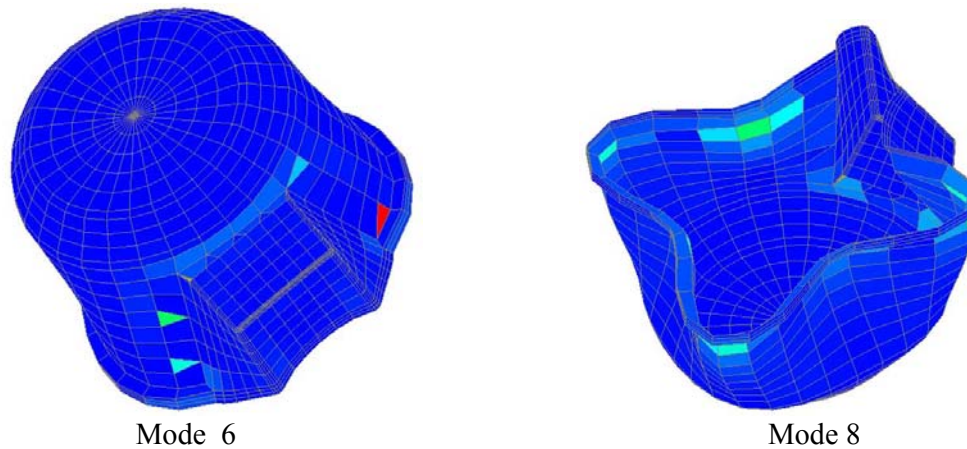


Figure 5.20: Sensitivity analysis results on mode 6 and 8

In this case, modification was done base on mode 6 only. This is because in all other mode, the edges of the magneto cover shall be fixed to the crankcase. Figure 5.21 suggested modification of the magneto cover.



Figure 5.21: Suggested Modification

The magneto cover new weight is 0.378 kg or an increase of 5.9% (29g) in weight. Modification has been done on the FE model and the results are listed in Table 5.7.

Table 5.7: Changes in Natural Frequencies after Modification

Mode No	Original Frequencies (Hz)	Modified Frequencies (Hz)
1	735	740
2	749	753
3	1689	1690
4	1858	1858
5	2642	2646
6	2753	3020

5.5 REFERENCES

1. Ong Choon Joo, B.Eng. Thesis “ Vibration Characteristics of a 2-Stroke Gasoline Engine (FE Method)”, UTM 2003.
2. FEMtools User’s Manual, www.femtols.com
3. P.Vanhonacker, “The use of modal parameters of mechanical structures in sensitivity analysis- System synthesis and identification methods”, Ph.D. Dissertation, Mechanical Eng. Department, K.U.Leuven, 1980.

CHAPTER VI

NOISE RADIATION PREDICTION OF SINGLE CYLINDER ENGINE

6.1 Introduction

It is an enormous challenge for the entire engineering team to design a new engine that fulfills several constraints, e.g. performance, low weight, durability, cost and acceptably low noise level during operation. The use of numerical modeling has become more and more important to help the engineer in the design process and to reduce the number of physical prototypes that will have to be built and tested. The availability of fast, simple and accurate modeling tools has thus become essential in automotive design.

Multi-body simulation provides a method for estimating the forces acting on an engine during operation, taking into account relevant effects such as combustion pressure and bearing loads. Together with a structural finite element model of the engine, they are used to evaluate the engine's structural response to operational conditions as a function of both RPM and frequency. The vibro-acoustic relationship between engine vibrations and the acoustic pressure field is then evaluated in order to calculate radiated engine noise. A new approach based on Acoustic Transfer Vector concept is used to evaluate the vibro-acoustic response of a radiating structure (1).

A B. Eng thesis entitle "Dynamic Analysis of 2-Stroke Gasoline Engine" (2) and a Master Thesis entitle " Prediction of Noise Radiation on Cylinder Head" were produced. A paper entitle "Utilization of numerical and experimental method in noise reduction of 2-stroke cycle engine" was presented in the Asia Pacific Vibration Conference 2004 in Australia (4).

The following is the report on the prediction of vibration response and noise radiation emitted from the surface of the modified engine structure.

6.2 Determination of Excitation Force

6.2.1 Introduction

The vibration of the cylinder block wall contributes greatly to engine noise and is mainly caused by cylinder pressure in each cylinder and the inertia forces of the piston and connecting rod. In this work, the calculated cylinder pressure of single cylinder two-stroke compound piston engine is transfer as input to simulation model built from Solidworks model. The simulation is carried out in Visual Nastran and the force at shaft where bearing is situated is presented here. The simulation is based on the model running at 5500 rpm with no external torque applied at the output shaft.

6.2.2 CAD Model in SOLIDWORKS

The CAD model used here is developed by the design team. Only rotating and reciprocating parts consist of piston, piston pin, connecting rod, crankshaft, crank pin and magneto are used in the simulation to include the effect of inertia forces produced by the parts. Figure 6.1 to 6.3 show the CAD model developed in SOLIDWORKS.

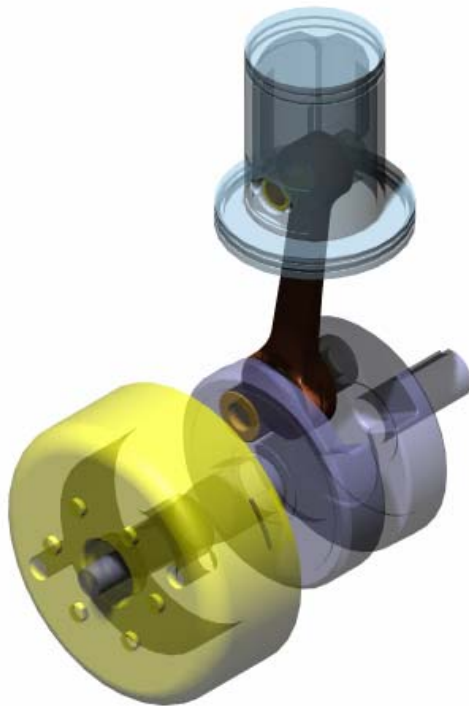


Figure 6.1: CAD Model (Isometric View)



Figure 6.2: CAD Model (Front View)

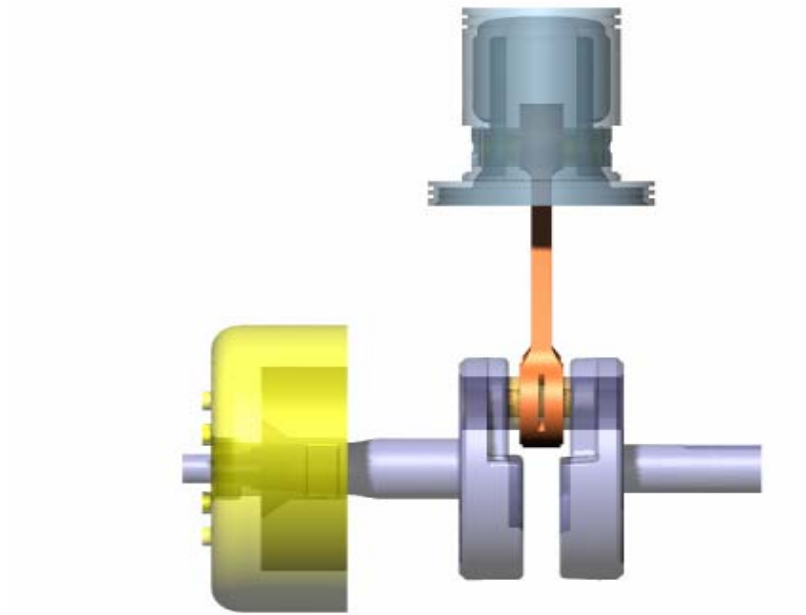


Figure 6.3: Cad Model (Side View)

6.2.3 Cylinder Pressure

The cylinder pressure is calculated by the design team. Cylinder pressure data in Figure 6.4 is transfer to Visual Nastran as input structural load. The pressure is applied to piston crown surface and it will push the piston and this will creates the crank slider mechanism motion.

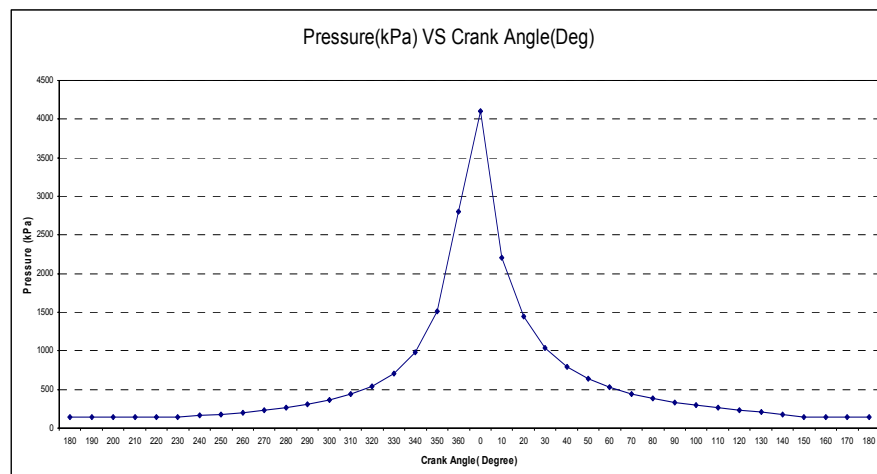


Figure 6.4: Cylinder Pressure Diagram

6.3 Simulation Model

Figure 6.5 shows the simulation model develops in Visual Nastran. The model consists of compound piston, piston pin, connecting rod, crank pin, crank shaft right and left part and magneto. Each part in the model is connected with different constraints provided in the constraints library in Visual Nastran. The constraints attachment purpose is to connect the body and to allow each part to be simulated in actual motion of the internal part in the engine. While for simulating the cylinder pressure, structural load is applied at piston surface (Constraint #1). Table 6.1 below describes the constraints numbered from 1 to 9 in Figure 6.5.

Table 6.1: Constraints Definition

Constraints Number	Constraint Type
1	Structural load (cylinder pressure)
2	Rigid joint on slot
3	Rigid joint
4	Revolute joint
5	Rigid joint
6	Revolute joint
7	Revolute joint
8	Revolute joint
9	Revolute joint

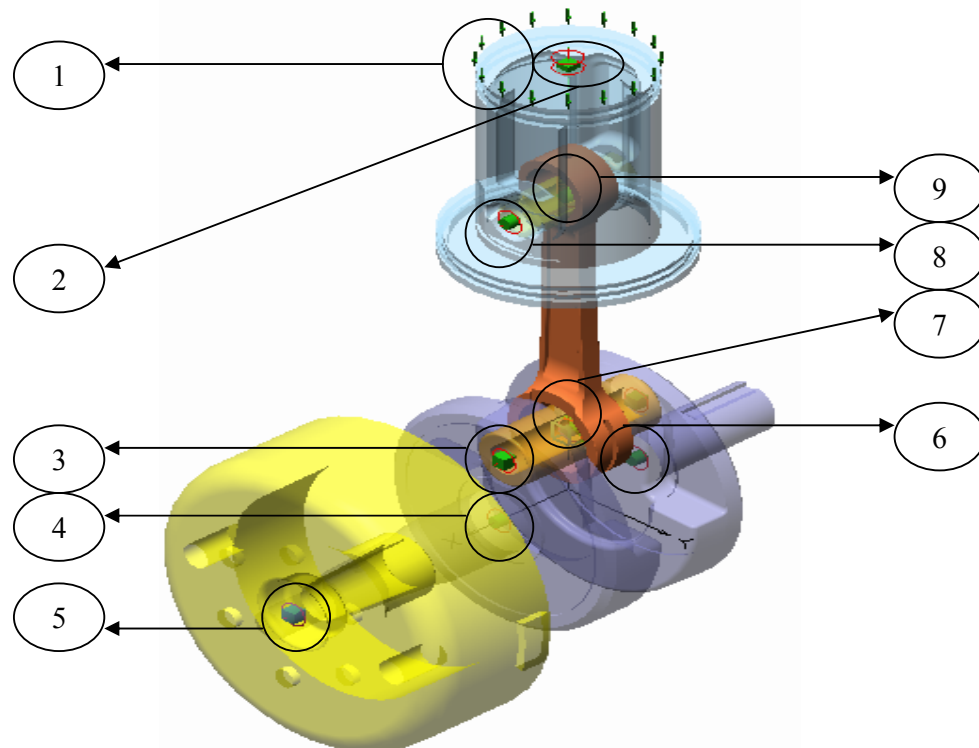


Figure 6.5: Simulation Model And The Constraints

6.4 Force Calculation Results

The model is simulated with cylinder pressure applied at the piston. The model succeeds to run at 5500 rpm under the applied cylinder pressure. Figure 6.6 shows the crankshaft speed in the simulation.

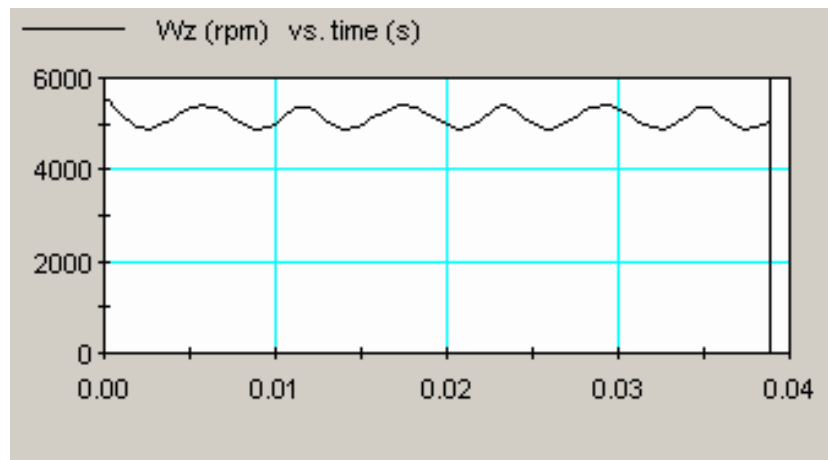


Figure 6.6: Crankshaft angular speed in the simulation

Figure 6.7 shows the load at Constraint (4) located at shaft based on Figure 6.5. This force will be transferred to Nastran for Forced Vibration simulation as the excitation load.

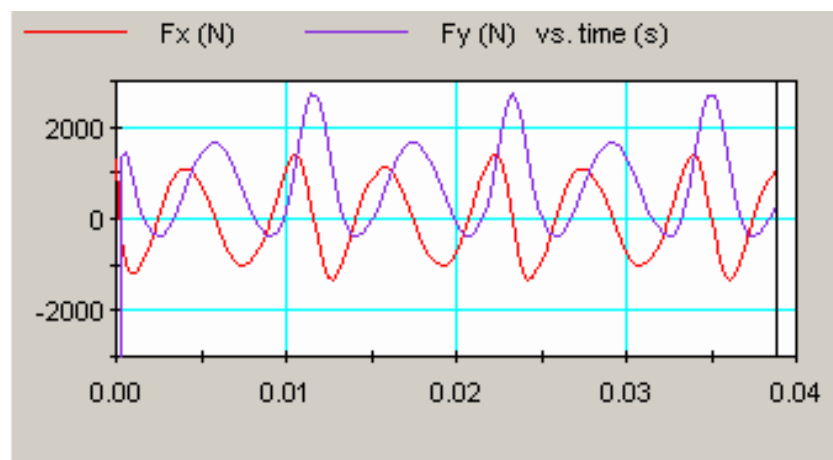


Figure 6.7: Force at Constraint (4)

6.5 Noise Radiation Prediction

Noise radiation prediction of engine structure is made possible nowadays with help from Finite Element (FE) and Boundary Element (BE) method. In order to get the end result, several steps are required which is described in Figure 6.8.

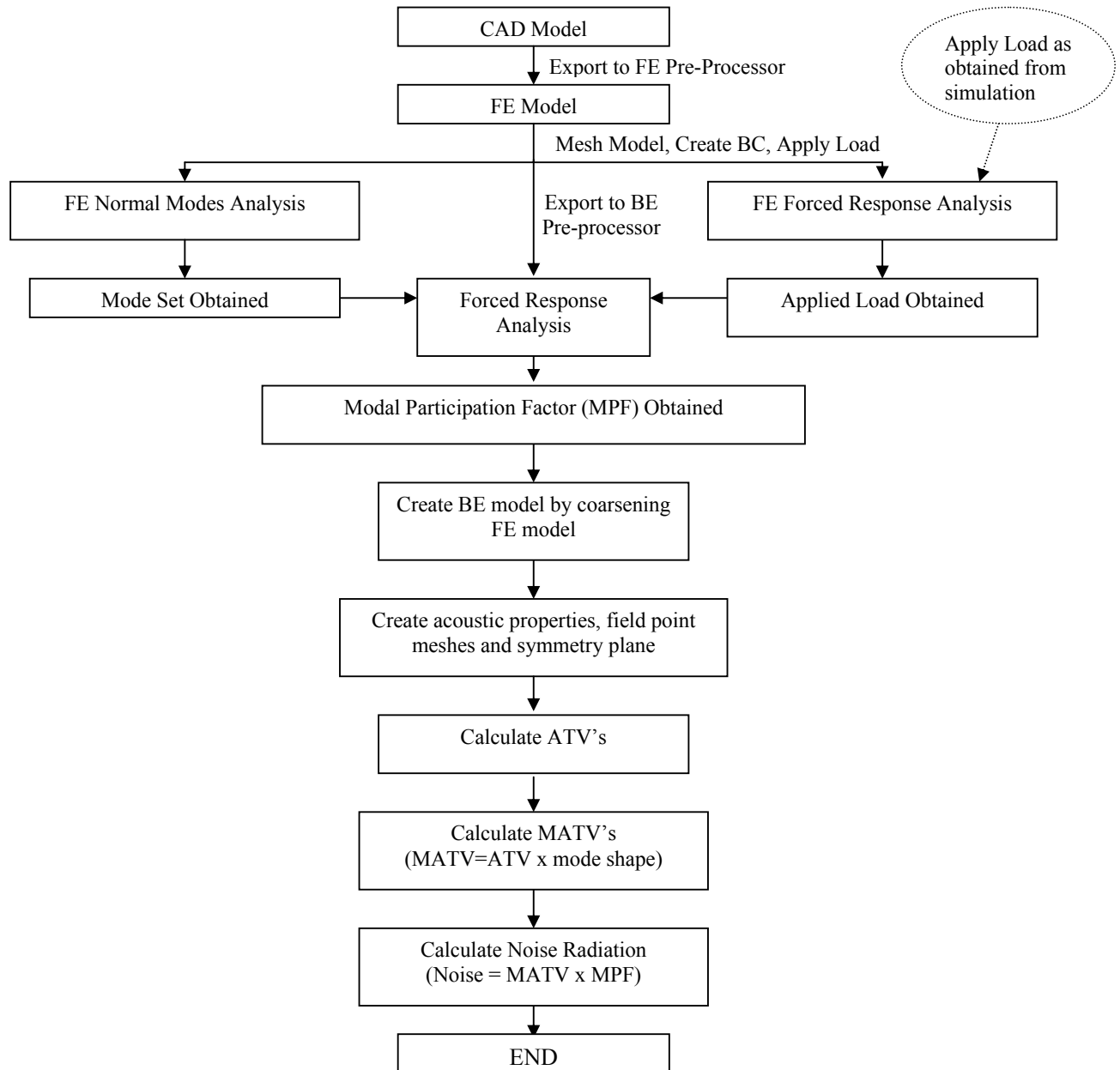


Figure 6.8: Noise Prediction Methodology

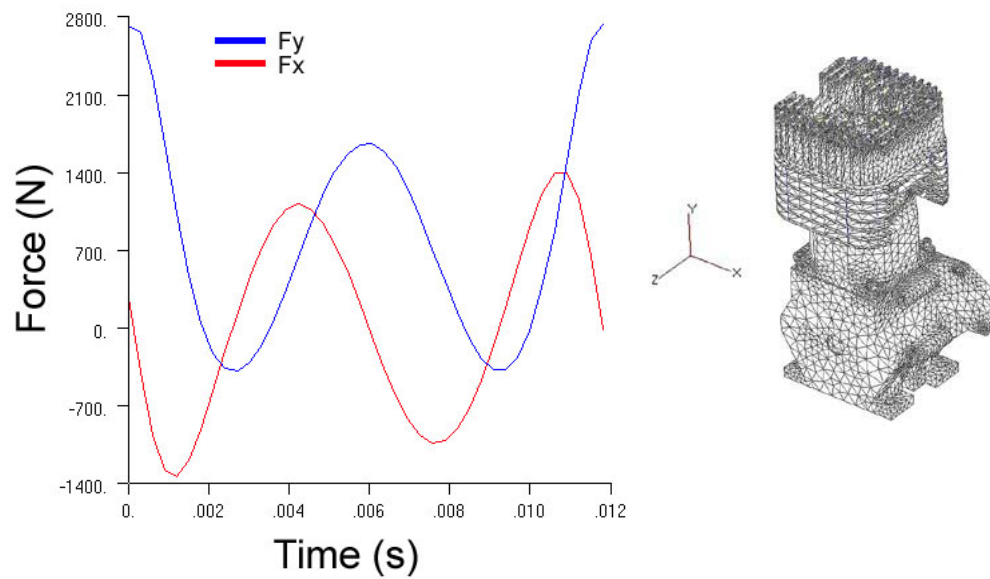


Figure 6.9: Components of Applied load in Time Domain as obtain from simulation

Figure 6.9 shows the components of applied load of crankshaft bearing in X and Y direction. This applied load in time domain is then transformed into frequency domain as illustrated in Figure 6.10. A constant resultant force of 2727 N is then applied on the FE model for Forced Response Analysis.

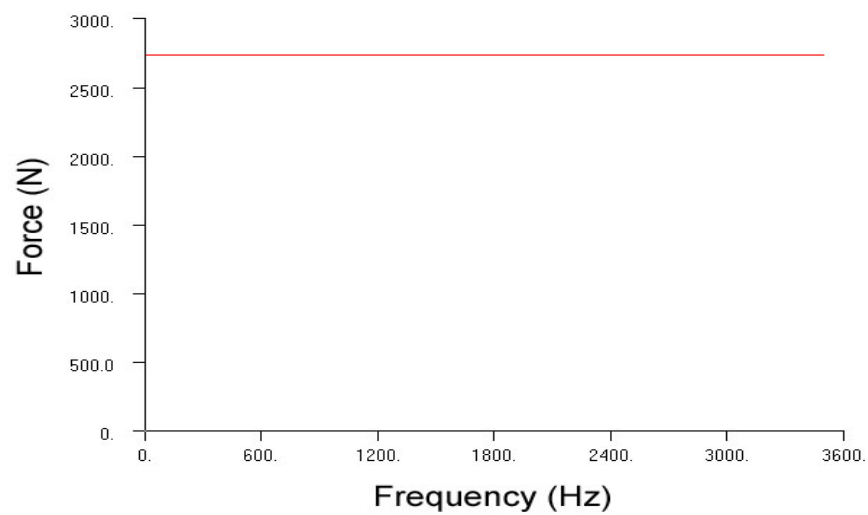


Figure 6.10: Resultant of Applied Load in Frequency Domain

Figure 6.11 and 6.12 show the FE and Boundary Element (BE) model of the structure. All modifications were done based on sensitivity analysis which has been presented in Chapter V.

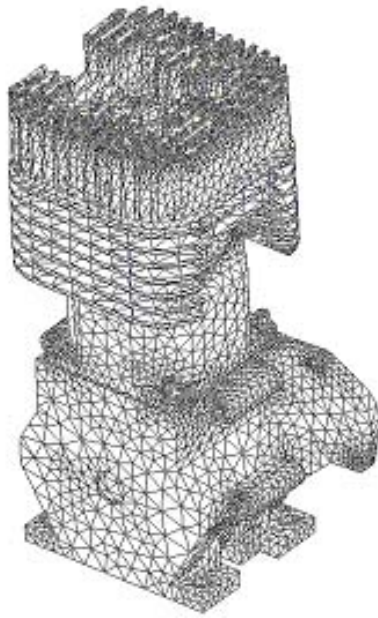


Figure 6.11: FE Model

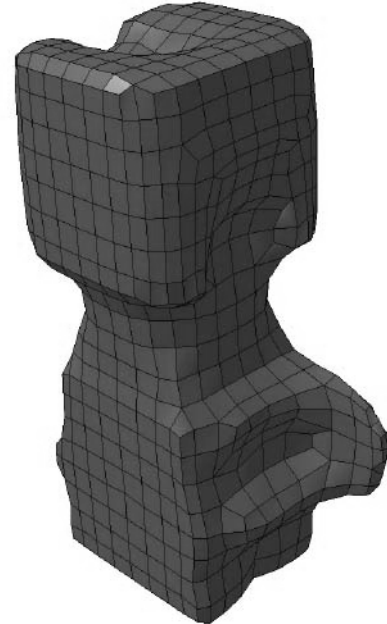


Figure 6.12: BE Model

6.5.1 Force Response Analysis

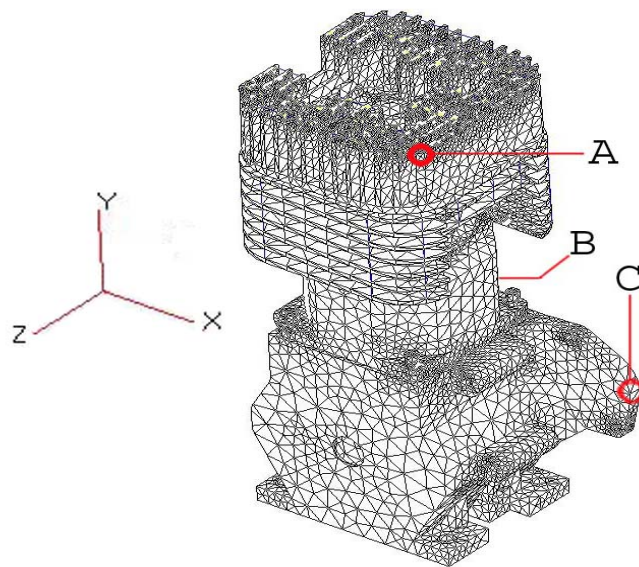


Figure 6.13: Measurement point of acceleration and displacement

The applied bearing load obtained in Figure 6.10 was applied into the FE model directly at crankshaft casing. No bearing was included as the stiffness of the bearing is not available. Thus the results shall be an extreme or critical case condition. Figure 6.13 shows the response point at cylinder head fin (Point A), cylinder block (Point B) and crankcase (Point C). Force Response analysis was carried out on the original and modified engine models and the results of response are displayed as acceleration and displacement. The responses at the 3 points are illustrated in Figure 6.14 to 6.19. Acceleration of around 0.6g occurred at around 450 Hz at the fin (Point A). Small acceleration and displacement occurred at Point B and C with peaks still occurred at around 450 Hz.

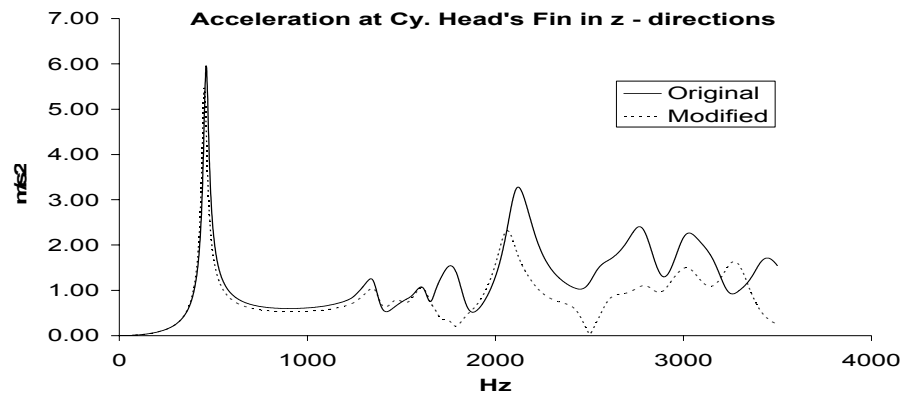


Figure 6.14: Acceleration at Cylinder Head's Fin (Point A) before and after Modification

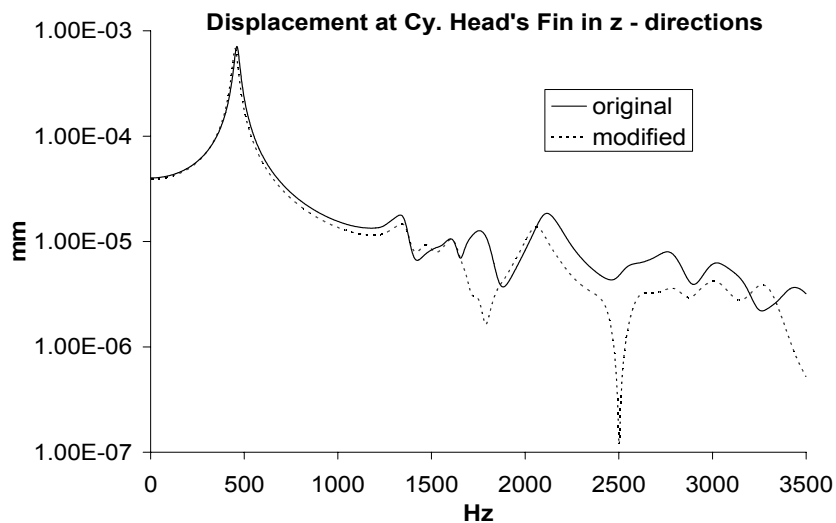


Figure 6.15: Displacement at Cylinder Head's Fin (Point A) before and after Modification.

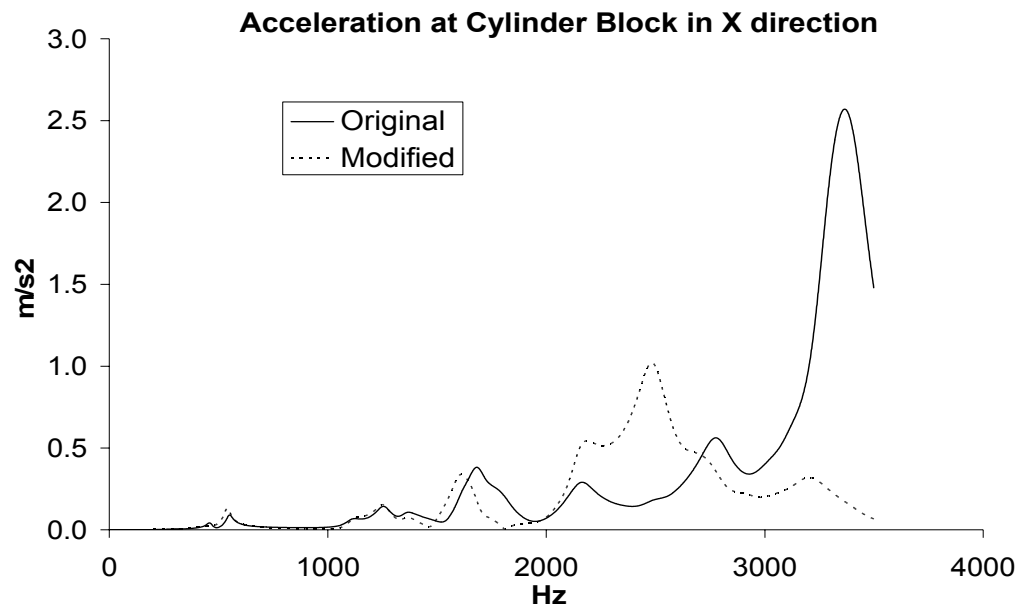


Fig.6.16: Acceleration at Cylinder Block Fin (Point B) Before and After Modification

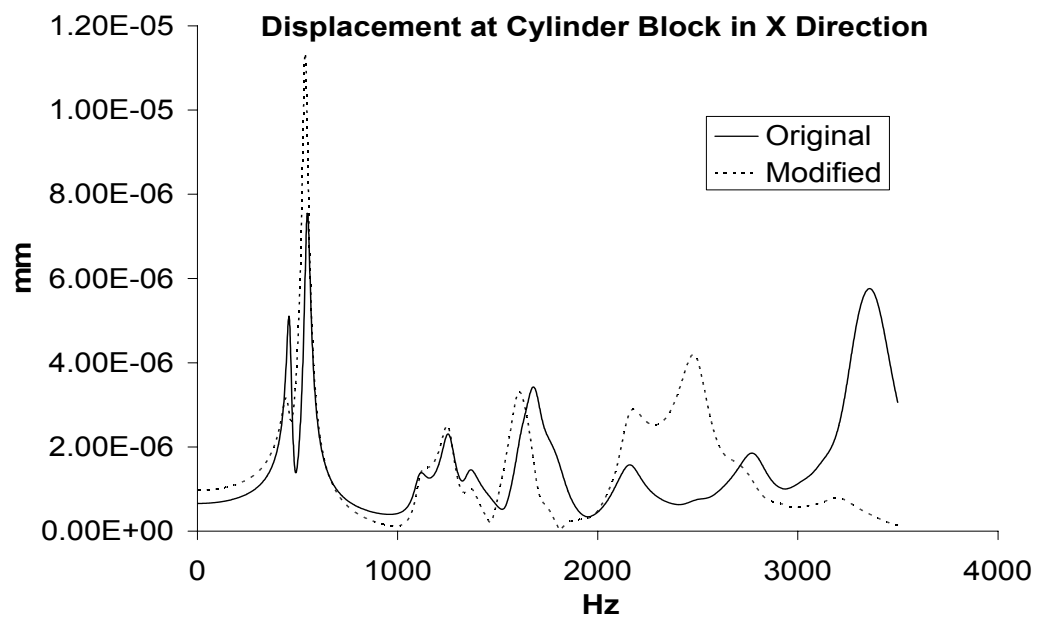


Figure 6.17: Displacement at Cylinder Block (Point B) Before and After Modification

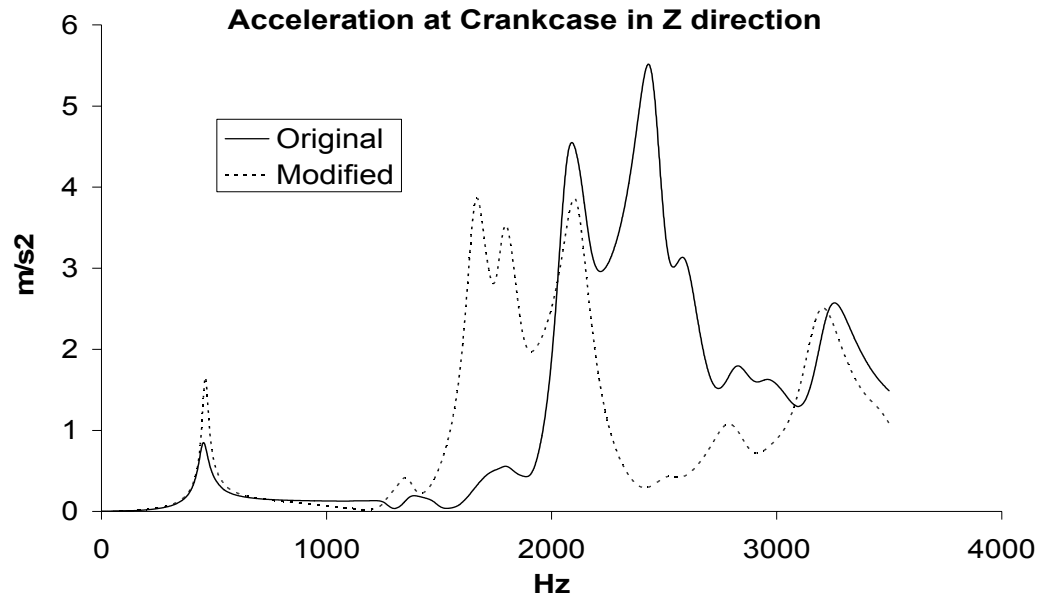


Figure6.18: Acceleration at Crankcase (Point C) Before and After Modification

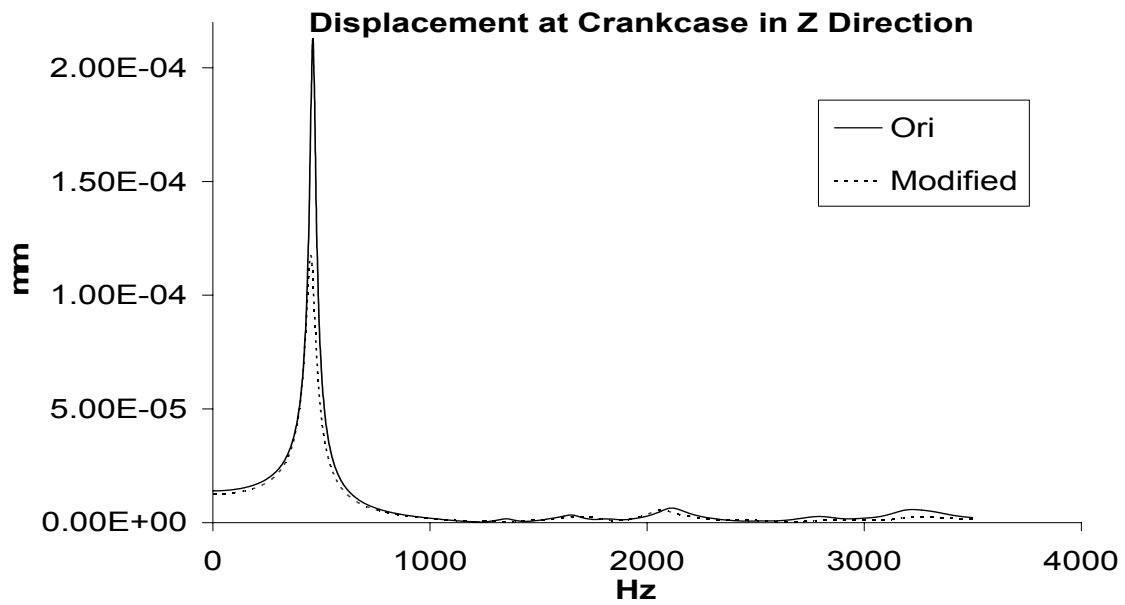


Figure 6.19: Displacement at Crankcase (Point C) Before and After Modification

6.5.2. Radiated Sound Power

The BE model was then used for the prediction of noise radiation by using LMS Virtual lab software (1). Figure 6.2 shows the sound power emitted from the engine surface due to the applied load acting on the surface of crankshaft bearing. It can be seen that there exist 2 significant peaks that indicate emission of noise which is at 451 Hz and 1682 Hz. Peak from other frequency seems to be small and is negligible.

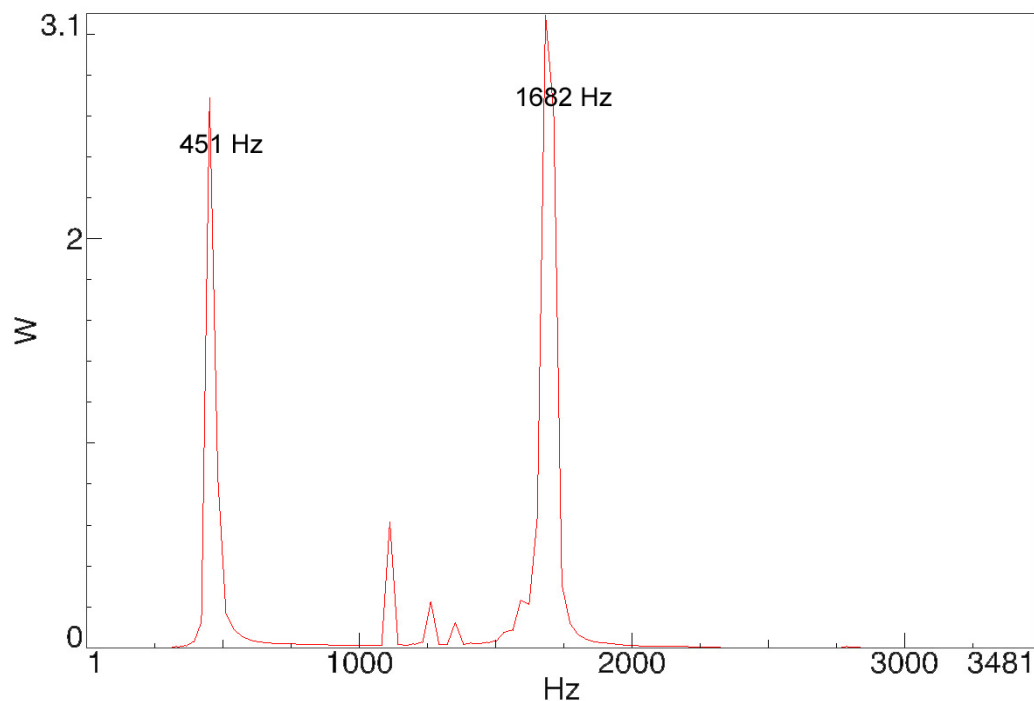


Figure 6.20: Graph of Sound Power (Watt) vs. Frequency

Figure 6.21 shows radiated sound pressure level 1 meter from the engine at 451 Hz. At this frequency, the sound pressure is the second highest within the range of 0 to 3500 Hz. This frequency also almost coincides with the engines first mode of vibration. The engine is applied with bearing load at 5500 RPM at one of the bearing. It can be seen that the maximum sound pressure level is at 125 dB occurring at areas in front of the crankcase where the bearing is located. The lowest sound pressure area is obviously located on top of the engine as no effect on combustion was considered. The main source of noise for this engine is the crankcase due to the exerted load from the rotating crankshaft. The energy from the combustion and high speed rotation is transferred from

internal components to the crankcase wall, thus turning the crankcase surface into a noise radiating surface.

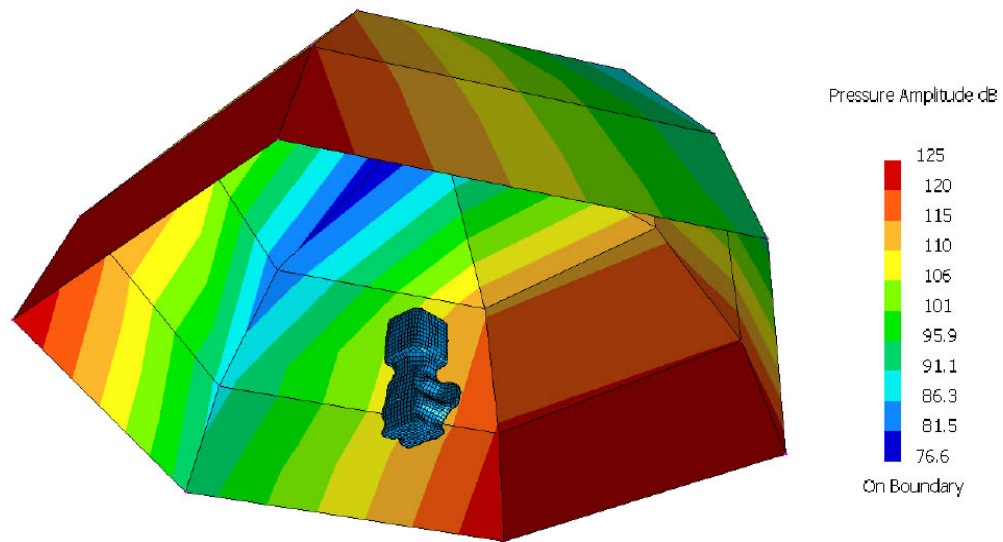


Figure 6.21: Sound Pressure Level at 451 Hz

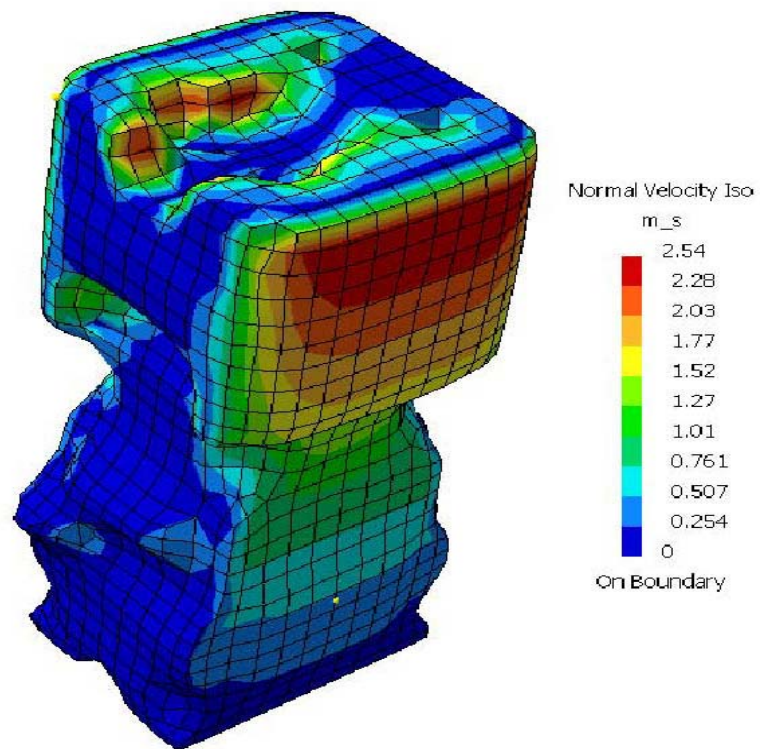


Figure 6.22: Normal velocity plot at 451 Hz

Figure 6.22 shows the normal velocity plot of the engine at 451 Hz. The high velocity area occurs at the top side of the engine. The engine is fixed at the bottom, thus give low velocity at area close to the bottom. The low velocity area is emitting high sound energy due to the constraints that prohibit it from vibrating. The upper side is free to vibrate thus emit less sound as indicated by Figure 6.21.

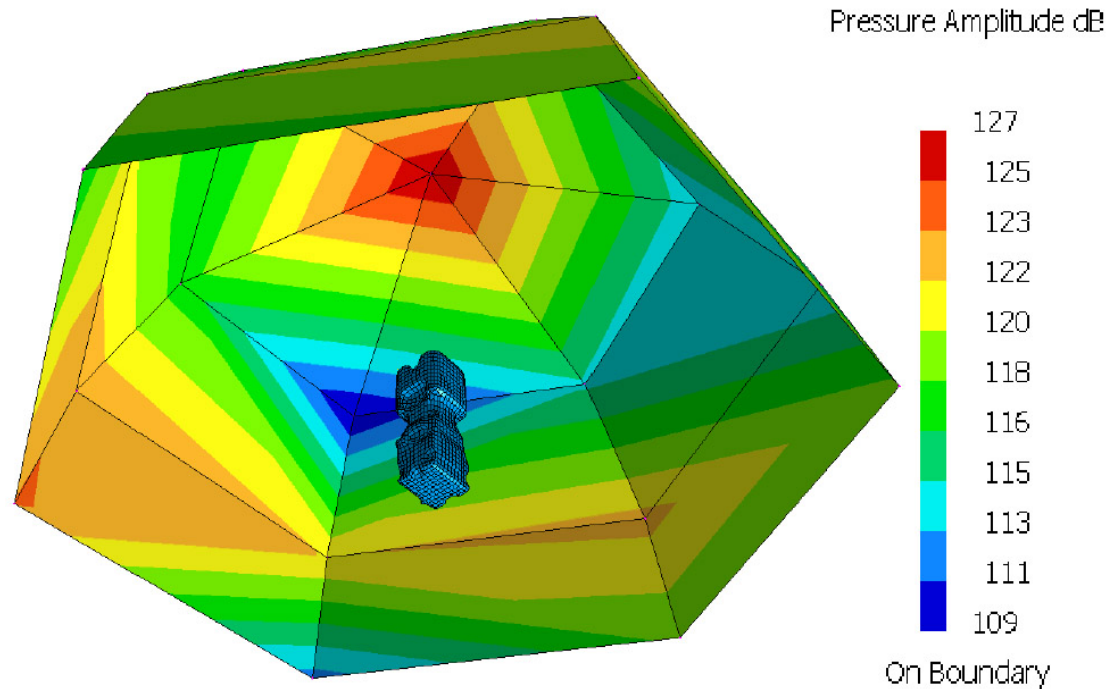


Figure 6.23: Sound Pressure Level at 1682 Hz

Figure 6.23 shows radiated sound pressure level 1 meter from the engine at 1682 Hz. At this frequency, the sound pressure is the highest within the range of 0 to 3500 Hz. This frequency also coincides with the engines 29th mode of vibration. The engine is applied with bearing load at 5500 RPM at one of the bearing. It can be seen that the maximum sound pressure level is at 127 dB occurring at areas on top of the cylinder head. This is caused by the vibration of the cylinder head's fins during high frequency.

Figure 6.24 shows the normal velocity plot of the engine at 1682 Hz. The normal velocity distribution is almost uniform indicating good distribution of vibration response at 1682 Hz which need not required to do improvement on the model.

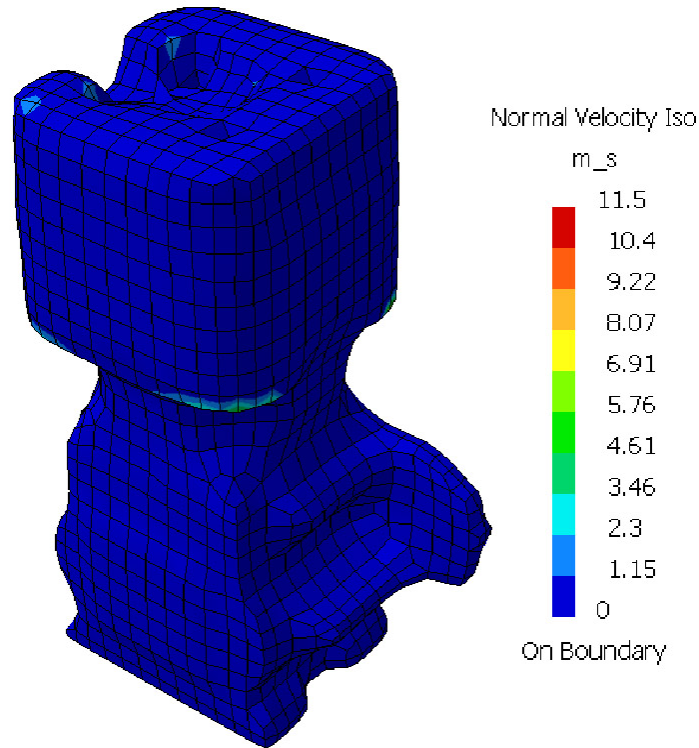


Figure 6.24: Normal velocity plot at 1682 Hz

6.6 Conclusion

The noise prediction results shows that the maximum sound pressure level at 127 and 125 dB is quite high. This however can be explained by the high value of simulated load. This load is simulated with the assumption that no bearing is in place. Therefore, the crankshaft is in direct contact with the crankcase. This assumption is due to the restriction of the simulation which requires the bearing's stiffness. In order to get better results, the stiffness of the bearing should be considered in the simulation. Other than that, an experimental load value would be better.

6.7 References

1. LMS VIRTUAL LAB, User Manual, “LMS International”.
2. Muhammad Al’Fauzul Azhim, “ Dinamik Engin Petrol 2-Lejang” B. Eng. Thesis, UTM, 2003.
3. Muhamad Khairudin bin Awang “ Prediction of Noise Radiation on Cylinder Head”, Master Thesis in Mechanical Eng., UTM 2004.
4. Rahman. R.A., Zubair ,M. and Amin,N., “Utilization of numerical and experimental method in noise reduction of 2-stroke cycle engine” 10th Asia Pacific Vibration Conference, 12-14 Nov. 2003, Australia.

CHAPTER VII

BALANCING OF 2-STROKE GASOLINE ENGINE

This chapter is divided into 3 sections to report on the balancing of three types of 2-stroke engines:

- a. Single-cylinder engine
- b. V-4 engine
- c. Scotch Yoke engine

7.1 Balancing Of Single Cylinder 2-Stroke Engine

7.1.1. Introduction

This report present the balancing analysis carried out on single cylinder compound piston engine. The balancing analysis has been carried out using Visual Nastran software in order to identify the unbalanced forces created due to crankshaft rotation.

7.1.2. Scope of Work

1. Cad model customization in Solidworks to be exported to Visual Nastran for motion simulation.
2. Motion simulation process: - model layout, constraint assignment, animation, force computation.
3. Identification of unbalanced inertial forces (magnitude and angle) due to crankshaft rotates at 1000 rpm simulated by revolute motor.

7.1.3. Objective

1. To simulate crankshaft, compound piston, connecting rod, piston pin, crank pin; assembly of single cylinder engine motion in Visual Nastran.
2. To identify unbalanced inertial forces created during crankshaft movement

7.1.4 CAD model of engine

The CAD model has been customized in order to include the relevant reciprocating parts and rotating parts which create unbalance dynamic forces. Figure 7.1 above shows the original assembly consists of magneto, starter gear, bearings and oil seals, crankshaft right and left side, crank pin, connecting rod, piston pin and piston. This model is then customized to only piston, piston pin, connecting rod, crank pin and crankshaft as shown in Figure 7.2. The customize CAD model from SOLIDWORK is used in the motion simulation process in Visual Nastran for balancing analysis. Table 7.1 shows the mass property of each component.

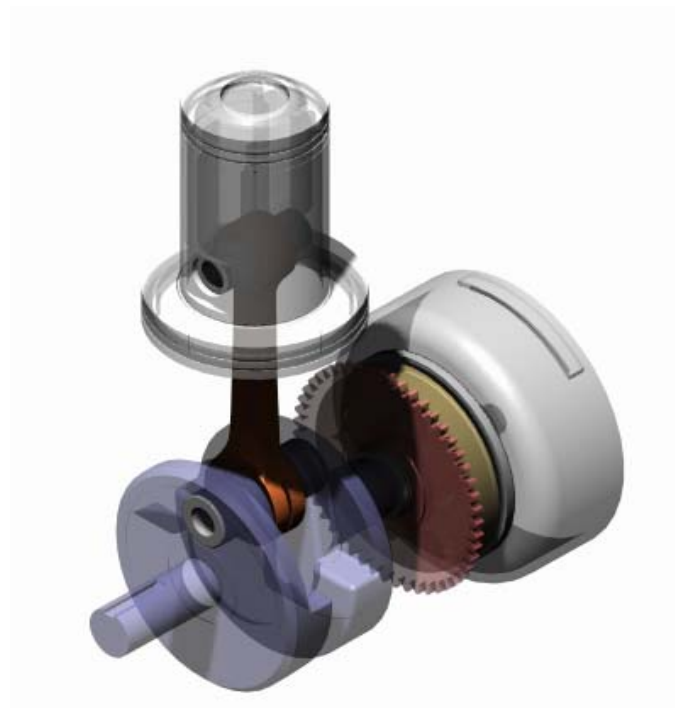


Figure 7.1: Original cad model of the engine in Solidworks

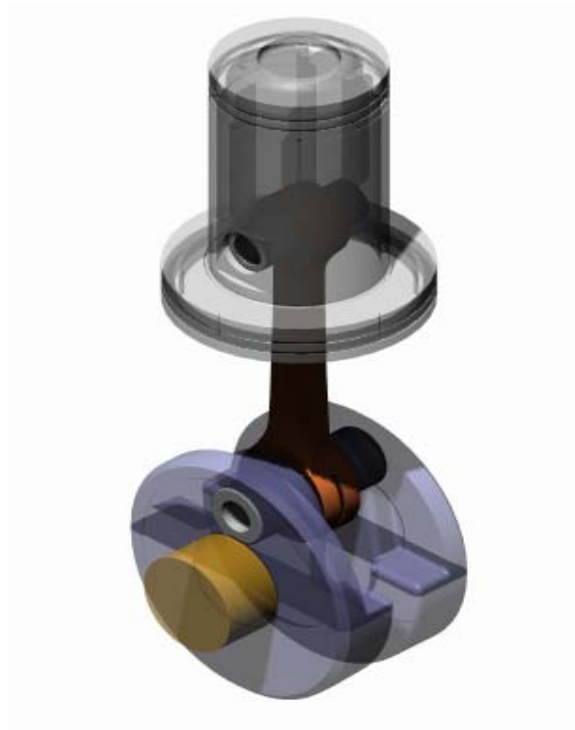


Figure 7.2: Customized cad model of the engine used in Visual Nastran

Table 7.1 Component Mass Property

Component	Mass property(kg)
Piston	0.233
Piston Pin	0.031
Connecting rod	0.130
Crank pin	0.107
Crankshaft(rear side)	0.317 (reciprocating section) 0.537 (counterweight section)
Crankshaft(front side)	0.309 (reciprocating section) 0.512 (counterweight section)

7.1.5. Motion Simulation Process

The model was exported to Visual Nastran for simulation process. Figure 7.3 shows briefly the flowchart of the process.

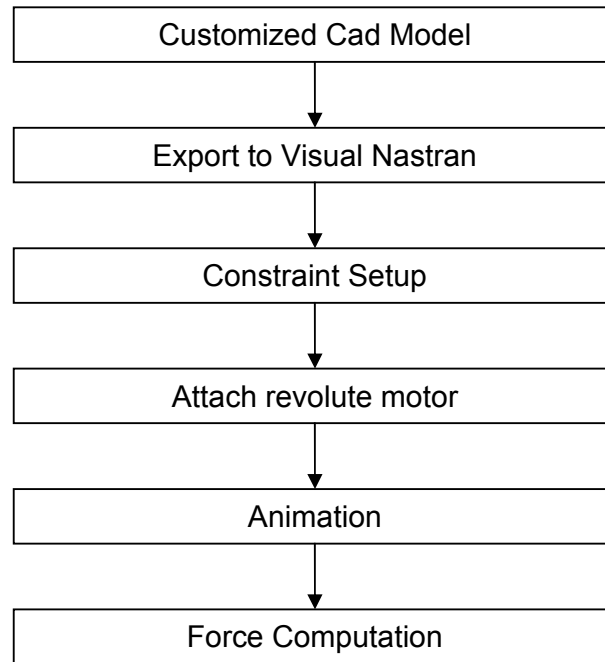


Figure 7.3: Motion Simulation Process flowcharts

7.1.6. Constraint Setup

At this stage, 4 types of constraints were used in the simulation. The constraints represent the degree of freedom for each joint to move as same as the actual model. Figure 7.4 shows the type of constraint applied in the simulation.

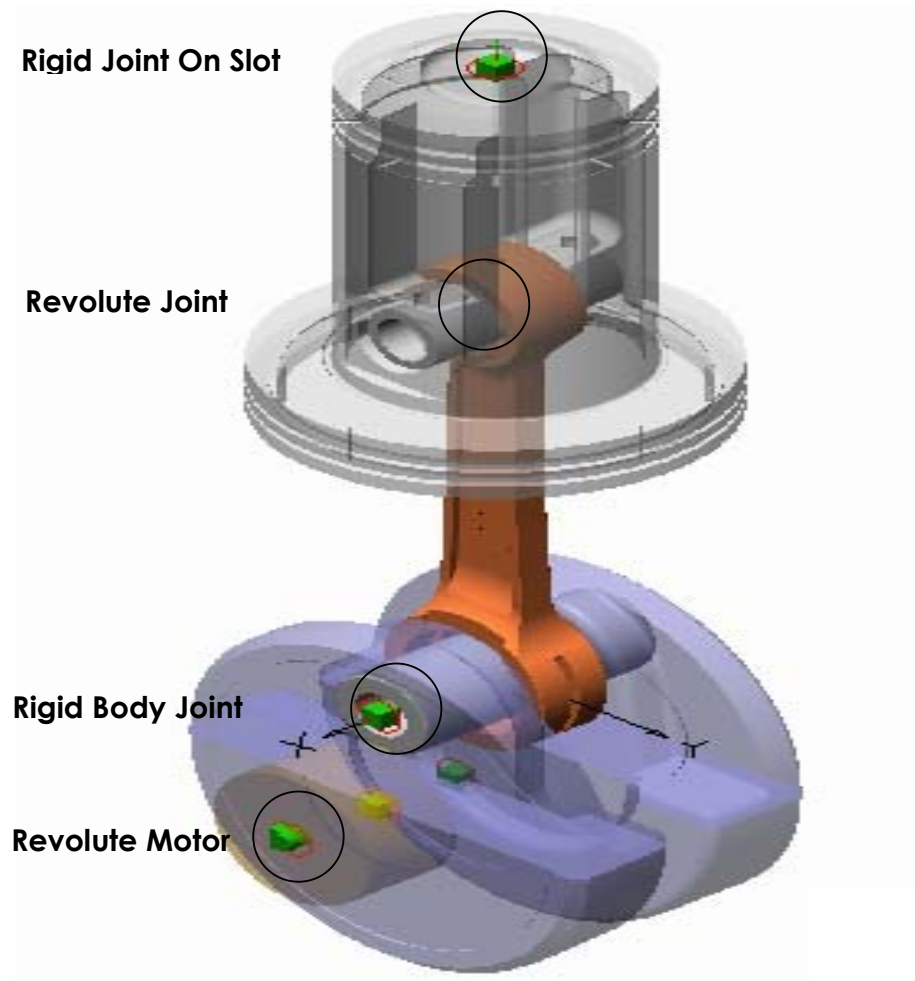


Figure 7.4: Types of Constraints

7.1.7. Force Computation Results

In calculating the forces created at the rotation axis, the analysis model was divided into two section, reciprocating section and counterweight section as illustrated in Figure 7.5. For the reciprocating section, the calculated forces are $F_y_Reciprocate$ to represent the force in horizontal direction and $F_z_Reciprocate$ to represent the force in vertical direction. For the counterweight section the forces are $F_y_Counterweight$ (horizontal direction) and $F_z_Counterweight$ (vertical direction). Figure 7.6 shows the calculated forces mentioned and are listed in Table 7.2, while Figure 7.7 shows the radar plot of the resultant forces for each section.

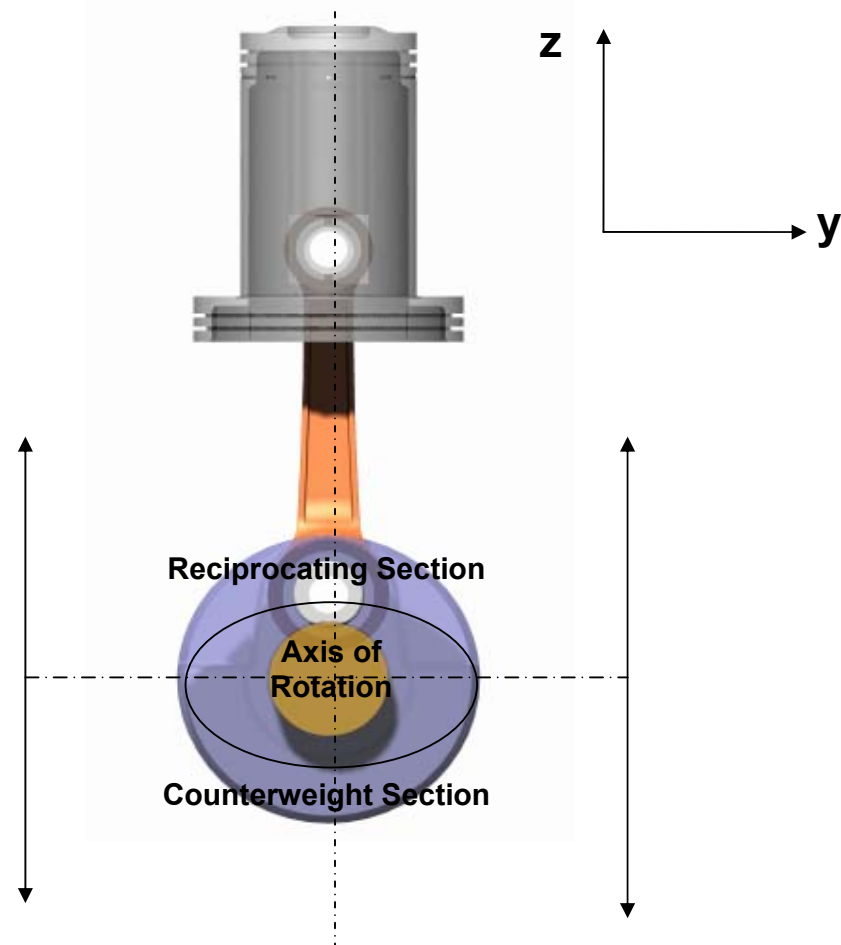


Figure 7.5: Analysis model divided into 2 sections for force calculation

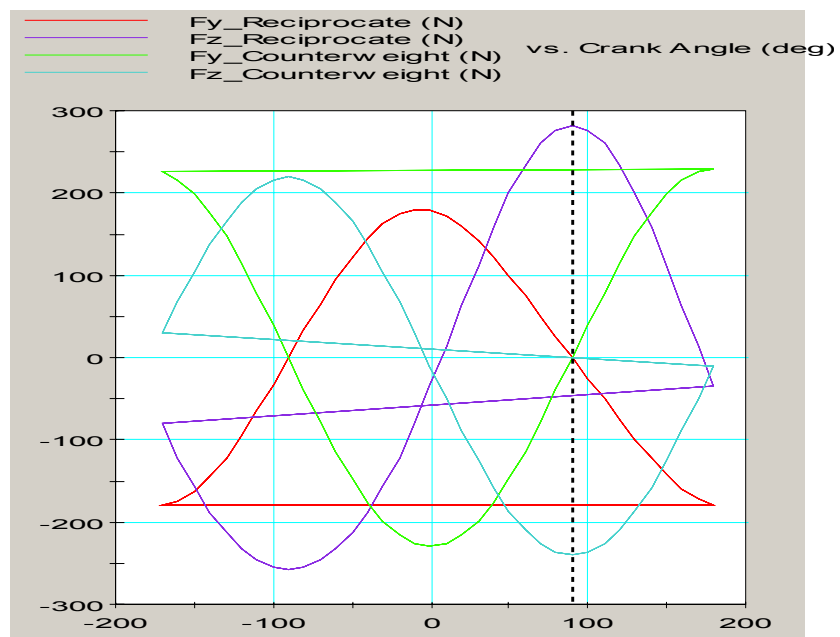


Figure 7.6: Calculated Forces vs Crank Angle At 1000 rpm

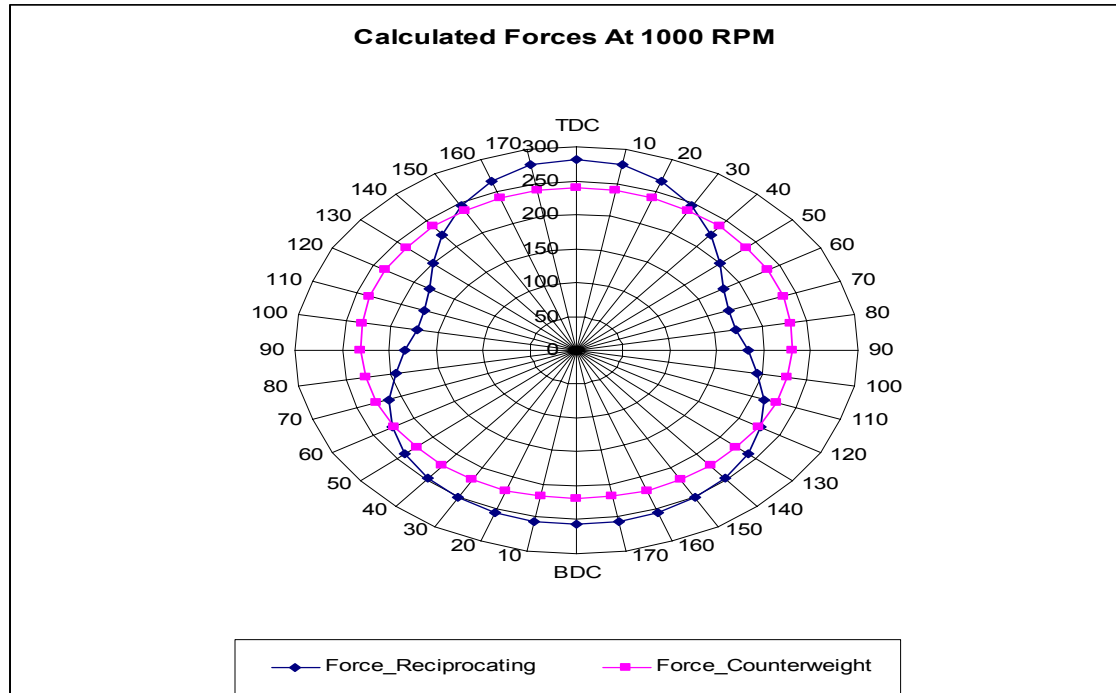


Figure 7.7: Radar plots of Resultant Forces

Table 7.2: Calculated forces Data

Crank Angle (deg)	Fy_Reciprocate (N)	Fz_Reciprocate (N)	Resultant Reciprocating Section	Fy_Counterweight (N)	Fz_Counterweight (N)	Resultant (Counterweight Section)
TDC	0.00	282.00	282.00	0.00	-239.93	239.93
(After TDC)10.00	25.14	276.34	277.48	-39.88	-236.44	239.78
20.00	50.18	260.27	265.07	-78.54	-226.08	239.34
30.00	74.91	234.36	246.04	-114.82	-209.17	238.61
40.00	98.92	199.86	223.00	-147.61	-186.21	237.62
50.00	121.58	158.42	199.70	-175.92	-157.90	236.39
60.00	142.00	112.06	180.89	-198.88	-125.11	234.96
70.00	159.12	62.93	171.11	-215.79	-88.83	233.36
80.00	171.78	13.22	172.29	-226.15	-50.17	231.65
90.00	178.98	-35.10	182.39	-229.64	-10.29	229.87
100.00	179.99	-80.39	197.13	-226.15	29.59	228.08
110.00	174.50	-121.45	212.60	-215.79	68.25	226.33
120.00	162.65	-157.49	226.40	-198.88	104.53	224.67
130.00	144.93	-188.10	237.46	-175.92	137.32	223.17
140.00	122.14	-213.11	245.64	-147.61	165.63	221.86
150.00	95.23	-232.51	251.25	-114.82	188.59	220.79
160.00	65.21	-246.32	254.80	-78.54	205.50	220.00
170.00	33.12	-254.58	256.73	-39.88	215.86	219.52

continue

BDC	0.00	-257.33	257.33	0.00	219.35	219.35
(After BDC)10.00	-33.12	-254.58	256.73	39.88	215.86	219.52
20.00	-65.21	-246.32	254.80	78.54	205.50	220.00
30.00	-95.23	-232.51	251.25	114.82	188.59	220.79
40.00	-122.15	-213.11	245.63	147.61	165.63	221.86
50.00	-144.93	-188.10	237.46	175.92	137.32	223.17
60.00	-162.65	-157.48	226.40	198.88	104.53	224.67
70.00	-174.50	-121.44	212.60	215.79	68.25	226.33
80.00	-179.99	-80.39	197.13	226.15	29.59	228.08
90.00	-178.98	-35.10	182.39	229.64	-10.29	229.87
100.00	-171.78	13.22	172.29	226.15	-50.17	231.65
110.00	-159.12	62.93	171.11	215.79	-88.83	233.36
120.00	-142.00	112.06	180.89	198.88	-125.11	234.96
130.00	-121.58	158.42	199.70	175.92	-157.90	236.39
140.00	-98.92	199.85	222.99	147.61	-186.21	237.62
150.00	-74.91	234.36	246.04	114.82	-209.17	238.61
160.00	-50.18	260.26	265.06	78.54	-226.08	239.34
170.00	-25.15	276.32	277.46	39.88	-236.44	239.78

7.1.8 Findings and Discussion

1. The simulation was implemented in Visual Nastran using the customized model in Solidworks.
2. The customized model was analyzed at speed of 1000 rpm with no external load applied. The scope of analysis only involved the inertia forces of the model.
3. The associated magnitude and direction of forces created by reciprocating section and counterweight section in vertical and horizontal direction was calculated.
4. Based on Figure 7.7 it was observed that the unbalance force is acceptable. The counterweight managed to counterbalance approximately 87% of the force created by reciprocating section.

(Note : It is a fact that it is quite impossible for a single cylinder engine to be 100% balanced. The best that can be done is a compromise)

7.2 Balancing Of Crankshaft for V-4 Compound Piston 2-Stroke Engine

The forces, moments and torques developed in engines are partly due to the acceleration of masses in the system. These forces should be reduced or eliminated from the engine as these give undesirable features which create noise and vibration.

7.2.1 Scope of Works

1. Engine Parts Arrangement And Component Properties Identification
2. Motion Simulation
3. Balancing Study

7.2.2 Methodology

1. Scope (1) is to arrange the rotating and reciprocating parts correctly according to the required V angle of 60° . The position of each part must be accurate to avoid misalignment and part collision which will affect the parts in contact. Each component mass (kg) in the simulation must be identified to countercheck the actual weight used.
2. Scope (2) is to assign the constraint at the connecting joint which represents the actual degree of freedom of the system.
3. Scope (3) is to calculate and identify the forces and moment produced by every part of the whole system. The balancing of primary forces and primary and secondary moment shall be concentrated in the study.

7.2.3 Flow of Study

Figure 7.8 shows the flow chart of the work process in balancing the V-4 engine.

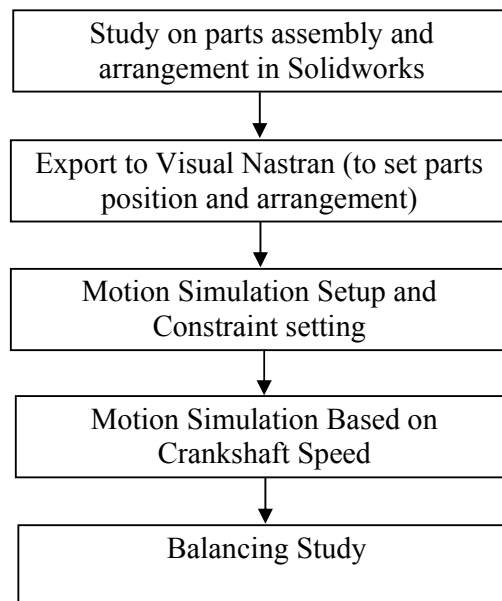


Figure 7.8: Flow of Study

7.2.4 Engine Parts Arrangement and Component Properties

The simulated model consists of the following components:-

- a. Piston assemblies (piston, gudgeon pin)
- b. Connecting rod
- c. Crankshaft

It was identified from SOLIDWORKS Assembly Drawing that the component properties are as presented in Table 7.3.

Table 7.3: Component Mass Properties

Component	Density(kg/m ³)	Weight (kg)
Piston + Gudgeon Pin	2700	0.20427
Connecting rod	7700	0.31105
Crankshaft	7300	6.400

Geometrical dimension : Length of connecting rod : 112 mm
 Radius of crank : 27 mm

7.2.5 Isometric View of Simulated Model

Figure 7.9 to 7.11 show the isometric view of the simulation model.

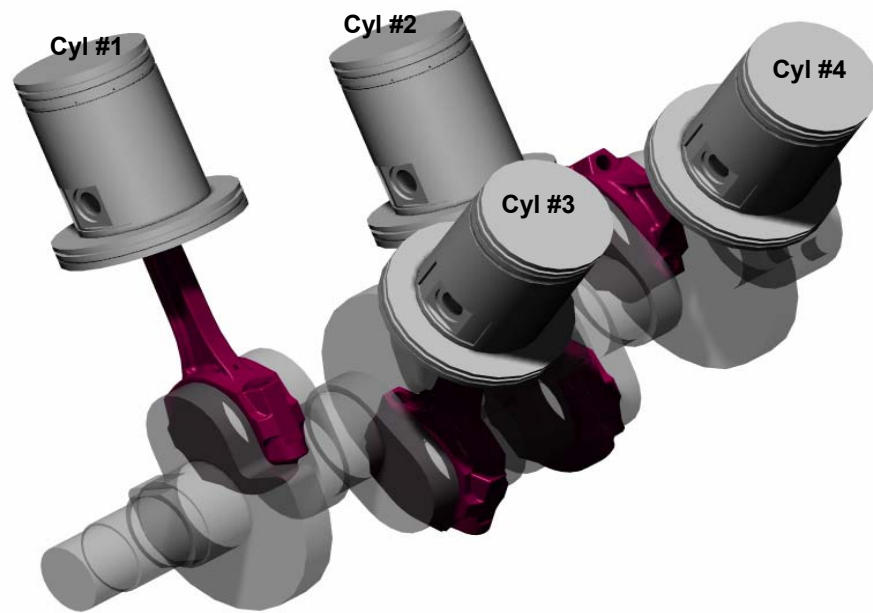


Figure 7.9: Isometric View of Simulated Model

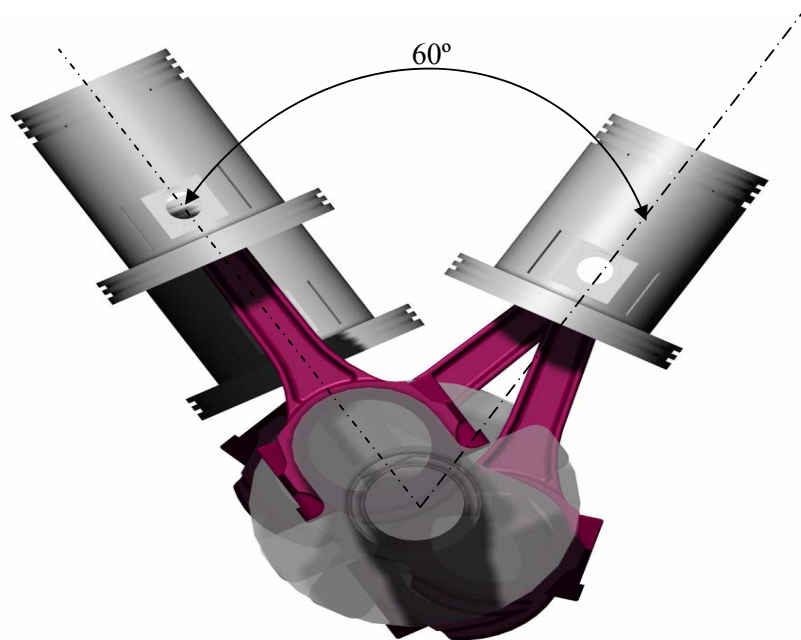


Figure 7.10: Front View of Simulated Model

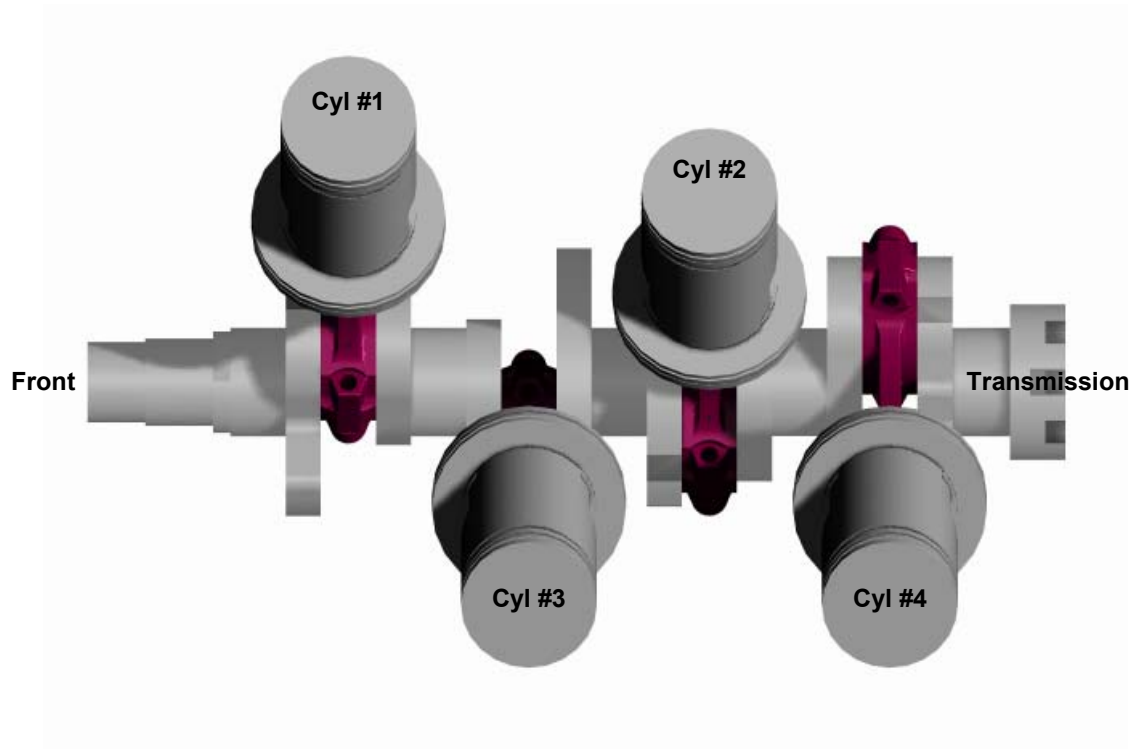


Figure 7.11: Top View of Simulated Model

7.2.6 Motion Simulation

a. Constraints Setting

The model in Solidworks was then exported to Visual Nastran for Constraint Assignment. Table 7.4 describes the type of constraint assigned to each connected bodies with the points shown in Figure 7.12.

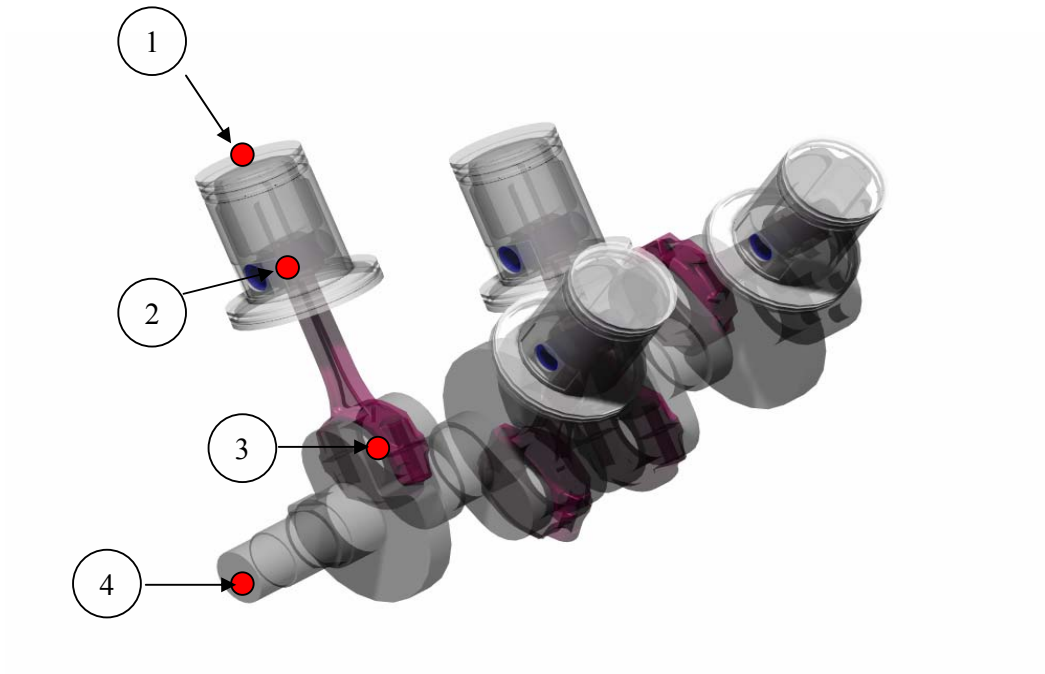


Figure 7.12: Constraint Points At Cylinder #1

Table 7.4: Description of Constraint Used

Number	Component → Component	Type of Constraint
1	Piston And Cylinder Head	Rigid Joint On Slot
2	Piston And Piston Pin	Revolute Joint
3	Connecting Rod And Crank throw	Revolute Joint
4	Crankshaft And Crankcase	Revolute Joint

b. Crankshaft Speed Control

Crankshaft was attached with revolute motor in the simulation to control the angular speed of the crankshaft. The motor have been set to rotate between 800 to 2000 rpm. The required speed can be set by the user using the Slider Control box.

7.2.7 Balancing Study

Balancing study was concentrated on the reciprocating inertia force and moment for both primary and secondary components. The rotating inertia effect contributes from the crank-throw is not considered as it is balanced by the counterweight already fixed on the opposite end of the crank.

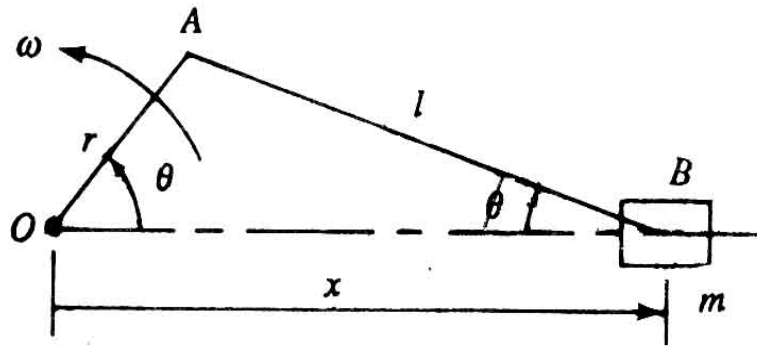


Figure 7.13: Reciprocating part rotates at ω

Figure 7.13 shows the reciprocating parts of an engine rotating at ω rad/s. The inertia force F_I is derived as,

$$F_I = (m\omega^2 r)\cos\theta + \left(m\omega^2 \frac{r}{n}\right)(\cos 2\theta)$$

$(m\omega^2 r)\cos\theta$ represent the primary inertia force,

$\left(m\omega^2 \frac{r}{n}\right)(\cos 2\theta)$ represent the secondary inertia force.

The shaking force, F_s , is the equal and opposite reaction force to the inertia force,

$$F_s = -F_I.$$

Figure 7.14 (a) shows the assembly model of Cylinder #1 at 0° position. Figure 7.14 (b) shows the equivalent system used in the calculation. The example of the calculation is shown in Appendix 7A.

The calculation of forces and moments are based on the crankshaft speed of 1000 rpm. Only the reciprocating parts (piston, piston pin and small end of connecting rod) are considered in the calculation. The value of the forces for each cylinder is shown in Table 7.5. The calculation example for Cylinder # 1 is shown in Appendix 7B.

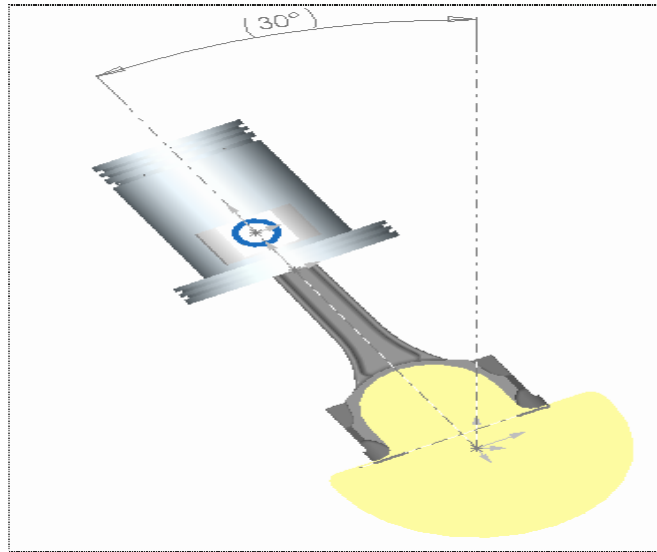


Figure 7.14 (a): Solidworks model of Cylinder #1

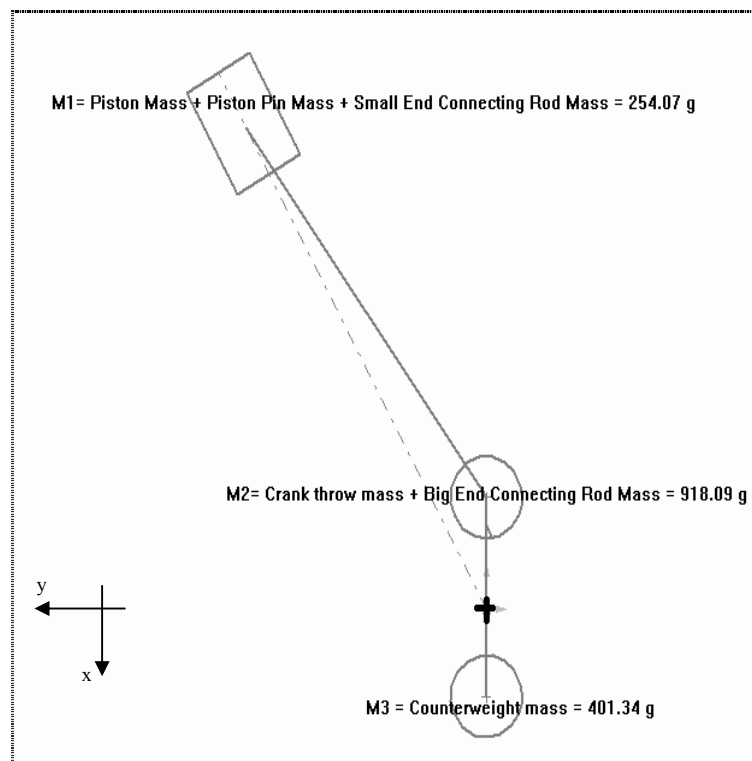


Figure 7.14 (b): Equivalent model of Cylinder #1

Table 7.5: Primary Force

Cylinder	Primary Force Magnitude
#1	(F1) =65.1486 N
#2	(F2) =65.1486 N
#3	(F3) =37.6136 N
#4	(F4) =37.6136 N

The primary force polygon is shown in Figure 7.15,

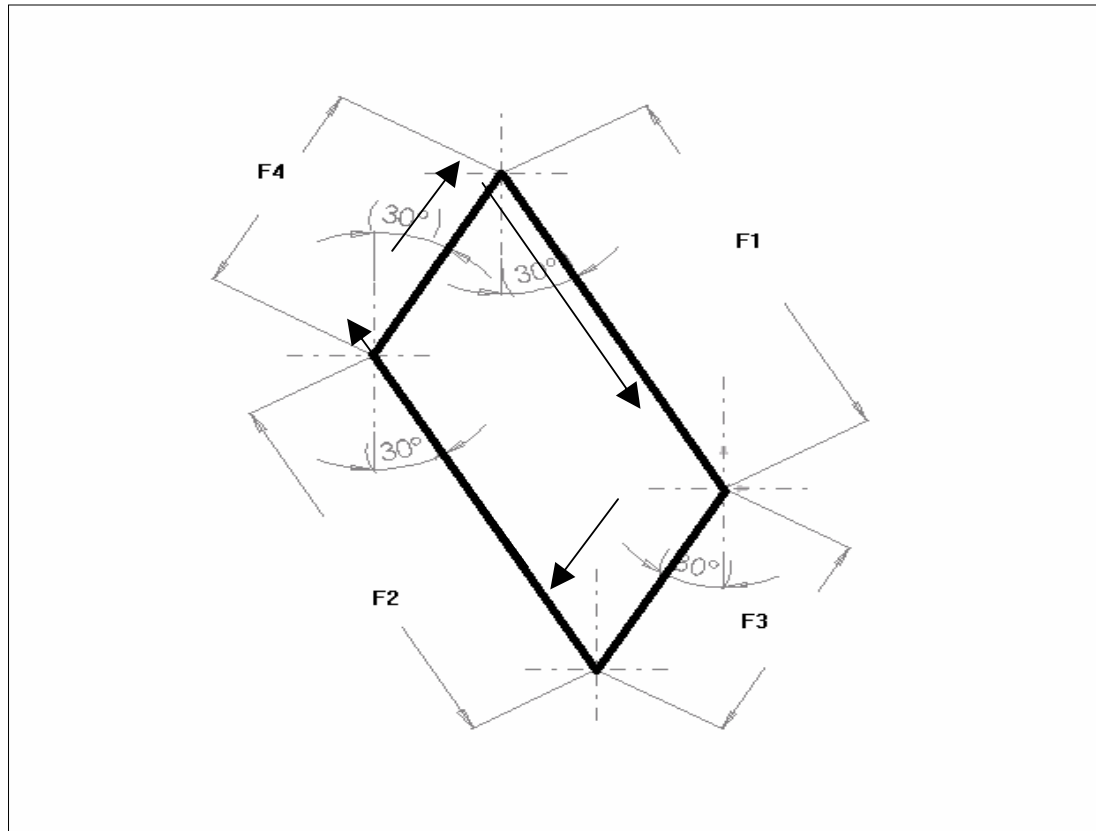


Figure 7.15: Primary Force Polygon

Figure 7.16 defines the distance between each cylinder and the center bearing. The forces for the calculation of primary moments are shown in Figure 7.17. The primary and secondary moment values are listed in Table 7.6 and Table 7.7 respectively.

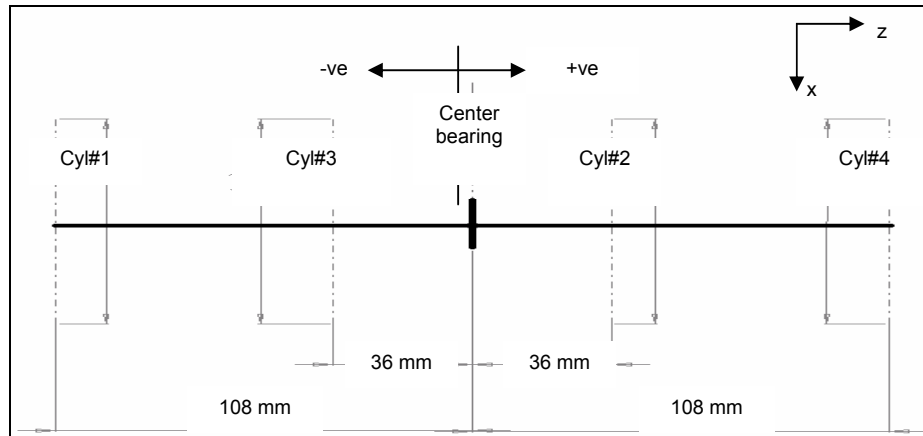
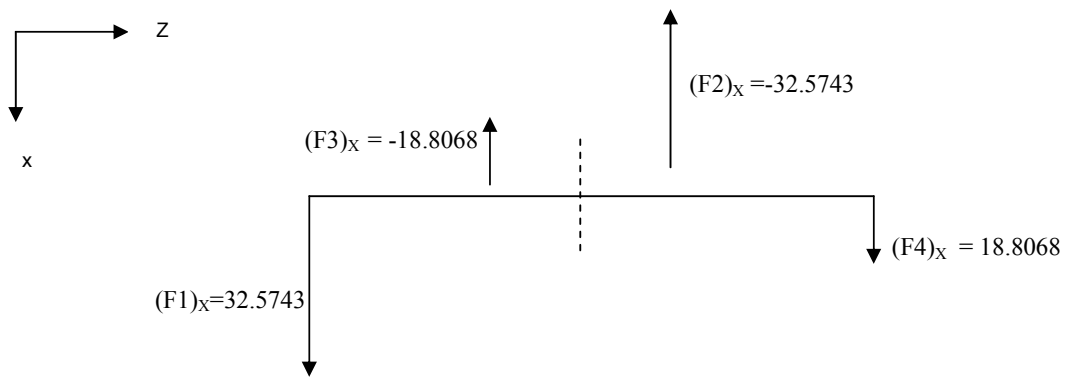


Figure 7.16: Distance between cylinders and center bearing

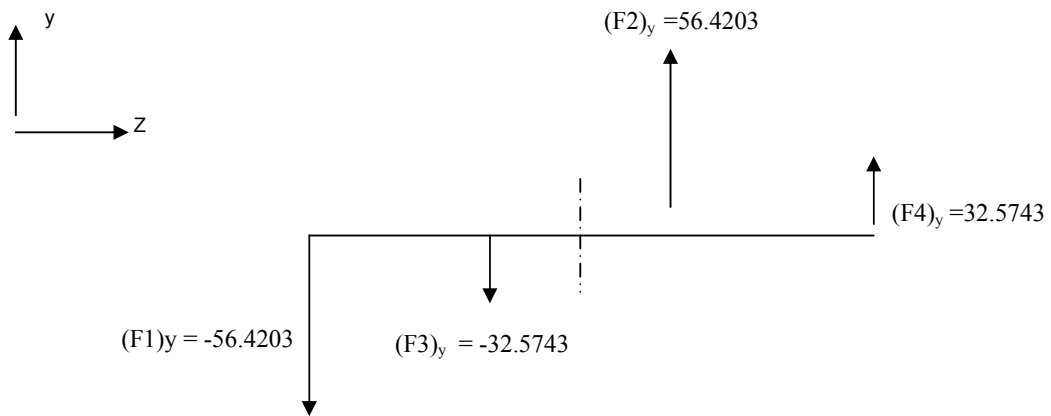
Table 7.6 Primary Moment

Cyl.	Primary Force (N)	F _x (N)	F _y (N)	Distance from Center bearing (L)(mm)	F _x .L(Nmm)	F _y .L(Nmm)
1	(F1) = 65.1486 N	32.5743	-56.4203	-108	- 3.1580X10 ³	6.9034X10 ³
2	(F2) = 65.1486 N	-32.5743	56.4203	+36	- 1.1726X10 ³	2.0311X10 ³
3	(F3) = 37.6136 N	-18.8068	-32.5743	-36	0.6770X10 ³	1.1727X10 ³
4	(F4) = 37.6136 N	18.8068	32.5743	+108	2.0311X10 ³	3.5180X10 ³
Σ Moment at Center Bearing					- 1.6225X10 ³ ↺	13.6252X10 ³ ↻

Primary Moment Diagram (x-z plane)



Primary Moment Diagram (y-z plane)



Primary Moment

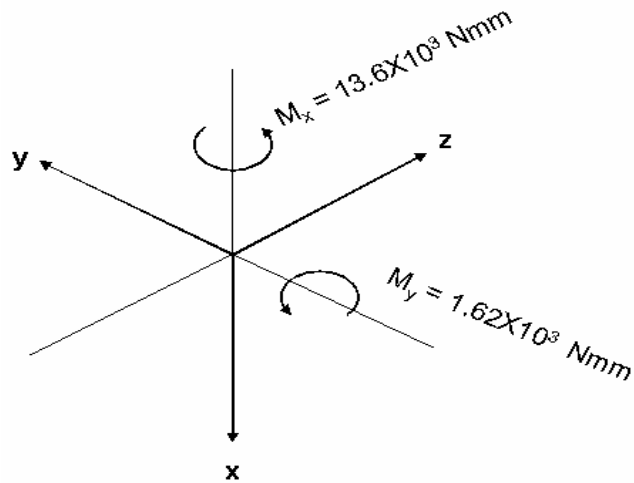


Figure 7.17 Primary moment Calculation

Table 7.7: Secondary Moment


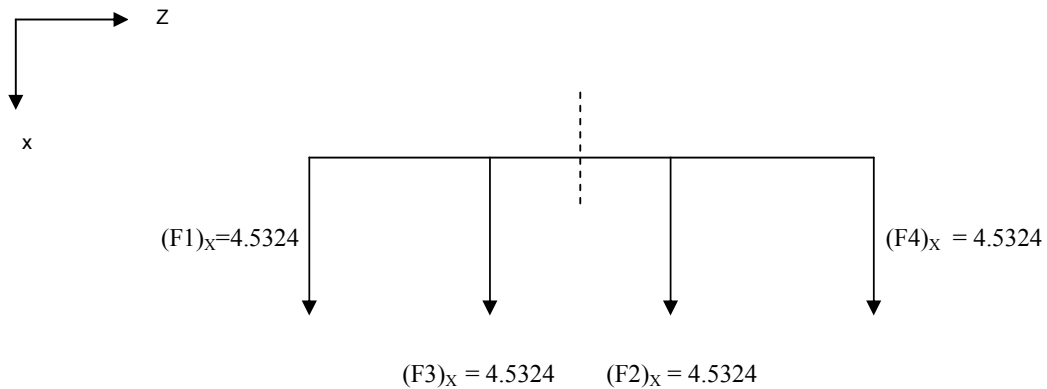
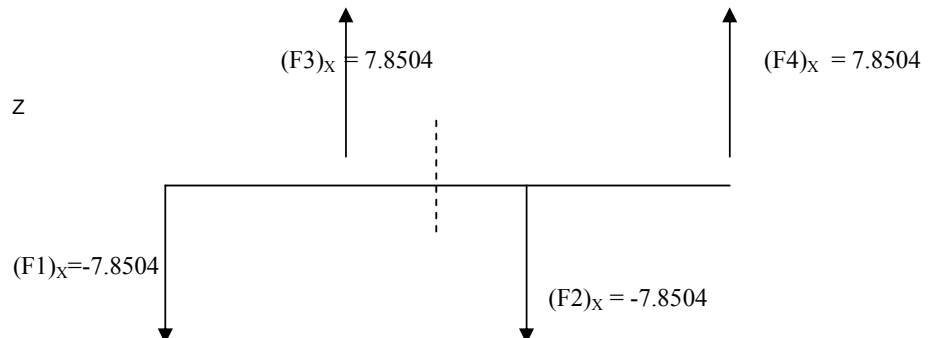
Cyl.	Secondary Force	F_x	F_y	Distance from Center bearing (L)(mm)	$F_x.L(\text{Nmm})$	$F_y.L(\text{Nmm})$
1	$(F1) = 9.064 \text{ N}$	4.5324	$\begin{matrix} - \\ 7.8504 \end{matrix}$	-108	$\begin{matrix} - \\ 0.4895 \times 10^3 \end{matrix}$	0.8788×10^3
2	$(F2) = 9.064 \text{ N}$	4.5324	$\begin{matrix} - \\ 7.8504 \end{matrix}$	+36	0.1632×10^3	-0.2826×10^3
3	$(F3) = 9.064 \text{ N}$	4.5324	7.8504	-36	$\begin{matrix} - \\ 0.1632 \times 10^3 \end{matrix}$	-0.2826×10^3
4	$(F4) = 9.064 \text{ N}$	4.5324	7.8504	+108	0.4895×10^3	0.8788×10^3
Σ Moment at Center Bearing					0	1.1924×10^3 

Figure 7.18 illustrated graphically the secondary forces and moments.

Secondary Moment Diagram (x-z plane)



Secondary Moment Diagram (y-z plane)



Secondary Moment

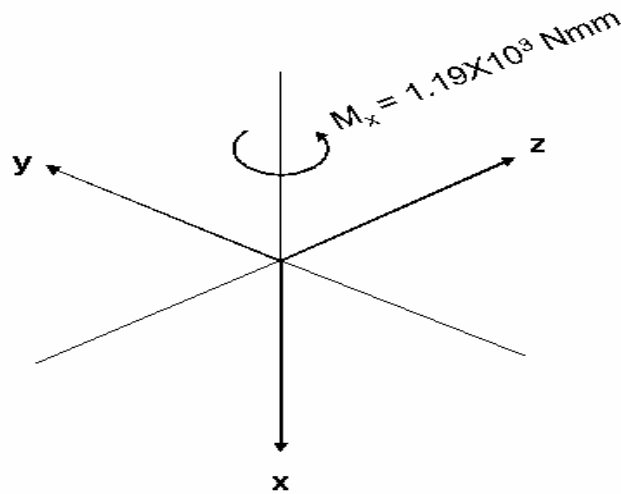


Figure 7.18: Secondary forces and moments

7.2.8 Discussion

1. Primary forces are balanced. The secondary forces are unbalanced and the value is relatively small.
2. Primary moments are unbalanced at both planes while secondary moments are balanced at x-z plane and unbalanced at y-z plane.
3. Even the primary forces are balanced; the force will increase with speed increment. These will cause the unbalanced primary moments to increase too.
4. The results indicate that pitching due to moment about vertical axis is much higher compared to about horizontal axis.

7.2.9 Suggestions

1. The unbalanced moment can be countered either with the addition of balance shafts or by changing the sequence of crank throw phase angles such that it is mirror symmetric.

7.2.10 Conclusion

1. Scope (1) is completed and the mass properties data have been correlated with actual materials used for fabrication. Accuracy of the model smooths the process in motion simulation.
2. Scope (2) is completed and the model succeeds to run within the speed given.
3. Scope (3) is completed; from the results, primary forces are balanced while primary moment and secondary moment are unbalanced.

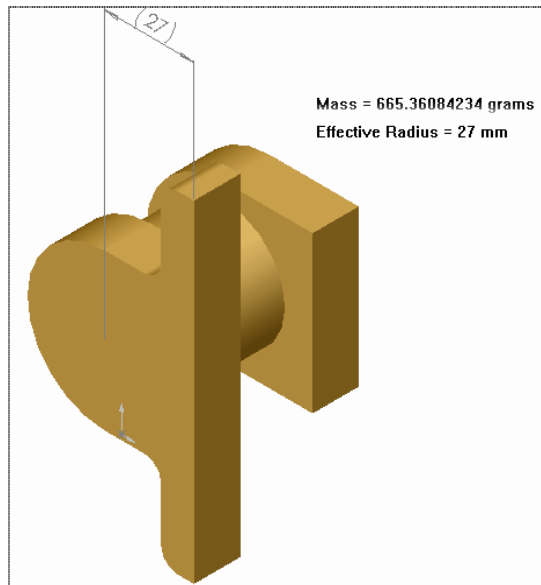
7.2.11 Appendix 7A

The calculation of each parts in the model is based on data calculated in Solidworks.

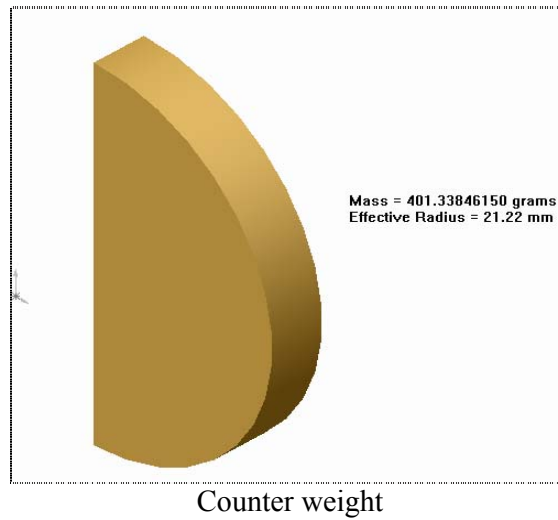
$$M1 = m_{\text{piston}} + m_{\text{crankpin}} + m_{\text{small end of connecting rod}} = 190.98g + 4.77g + 58.32g = 254.07g$$

$$M2 = m_{\text{crank throw}} + m_{\text{big end of connecting rod}} = 665.36g + 252.73g = 918.09g$$

$$M3 = m_{\text{counterweight}} = 401.34g$$



Crank throw



Appendix 7B

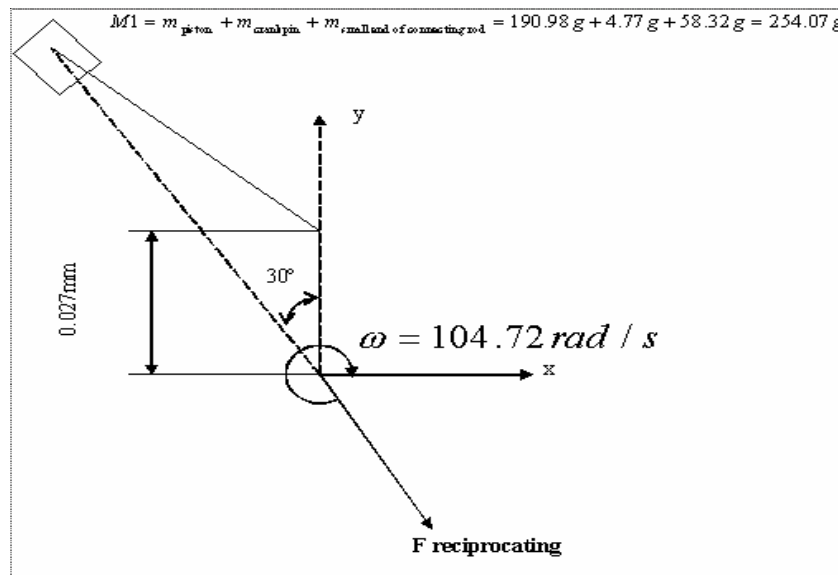
Calculation example for Primary force of Cylinder #1

$$F_{\text{reciprocating}} = [m_{\text{piston}} + m_{\text{crankpin}} + m_{\text{small end of connecting rod}}] \times \omega^2 \times r$$

$$M1 = m_{\text{piston}} + m_{\text{crankpin}} + m_{\text{small end of connecting rod}} = 190.98g + 4.77g + 58.32g = 254.07g$$

$$\omega = \frac{2\pi N}{60} (\text{rad} / s) = \frac{2\pi(1000)}{60} \text{rad} / s = 104.72 \text{ rad/s}$$

$$r = \text{crank radius} = 27\text{mm} = 0.027\text{m}$$



So,

$$\begin{aligned}
 F_{\text{reciprocating}} &= [m_{\text{piston}} + m_{\text{crankpin}} + m_{\text{small end of connecting rod}}] \times \omega^2 \times r \times \cos 30^\circ \\
 &= [0.25407] \times [104.72]^2 \times [0.027] \times 0.866 \text{ N} \\
 &= 65.1486 \text{ N}
 \end{aligned}$$

7.3 Dynamic Balancing Of Scotch Yoke 2-Stroke Gasoline Engine

A rotating member can be balanced either statically or dynamically. Static balance is a subset of dynamic balance. To achieve complete balance requires that dynamic balance be done.

In this report, the analysis of crankshaft assembly mechanism was carried out to estimate unbalanced inertia forces and moment for crankshaft rotates at 1000 revolution per minute (RPM).

The outcome of this practice will be the data on piston displacement, piston speed, piston acceleration, inertia forces and moment.

The analysis was managed to calculate the unbalance forces and moment and the sources of unbalanced was identified.

7.3.1 Objective

The list below states the objective of the analysis overall.

- a. To visualize crankshaft assembly mechanism
- b. By means of mechanism, displacement, speed and acceleration of various component such as piston and c-plate will be calculated
- c. To calculate and visualize inertia forces and moment
- d. To identify the sources of unbalanced forces and moment created by crankshaft rotation.

7.3.2 Methodology and Approach

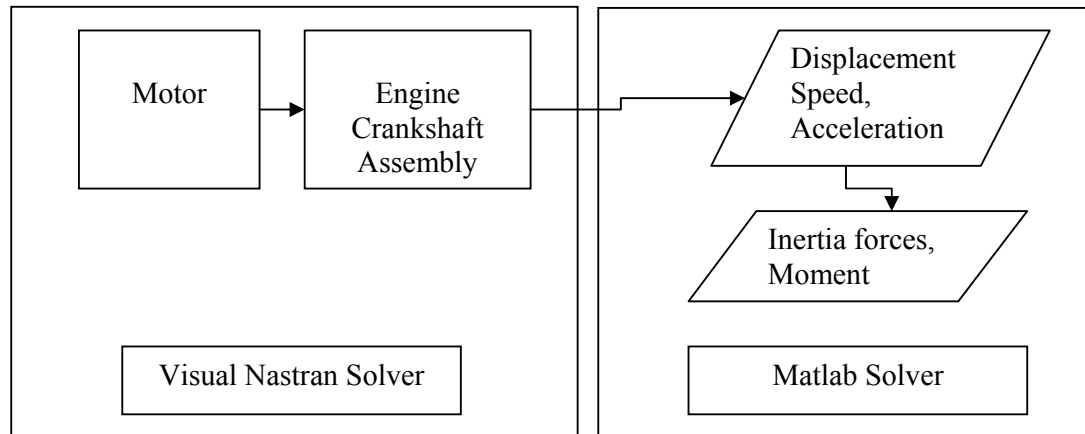


Figure 7.19: Block diagram of identification of inertia forces and moment

Figure 7.19 describes the flow in determining the inertia forces and moments on the crankshaft. The motor in the analysis was used to rotate the crankshaft assembly for various speed required in Visual Nastran . This is illustrated in Figure 7.20. For this practice, the simulation was run at the speed of 1000 to 8000 RPM. The crankshaft assembly consists of pistons, c-plates, crankshaft and sliders as depicted in Figure 7.21. By means of Visual Nastran motion simulation, the solver automatically calculates the piston displacement as shown in Figure 7.22.

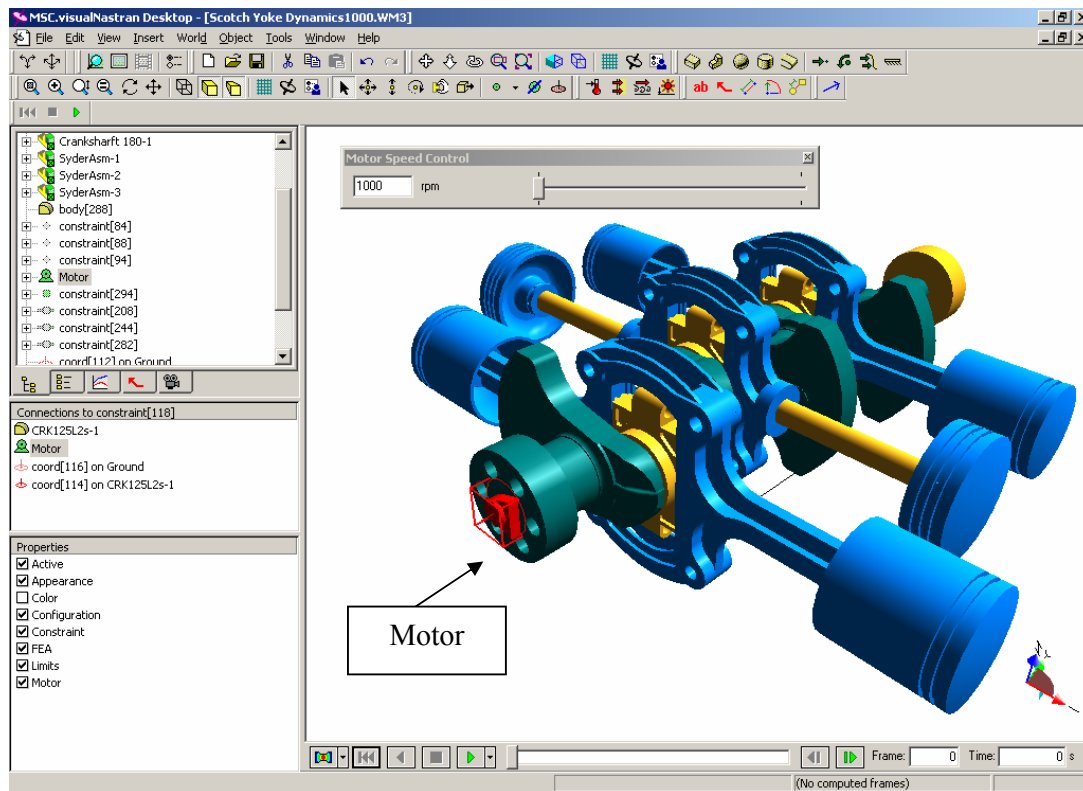


Figure 7.20: Motor colored in red attached at crankshaft

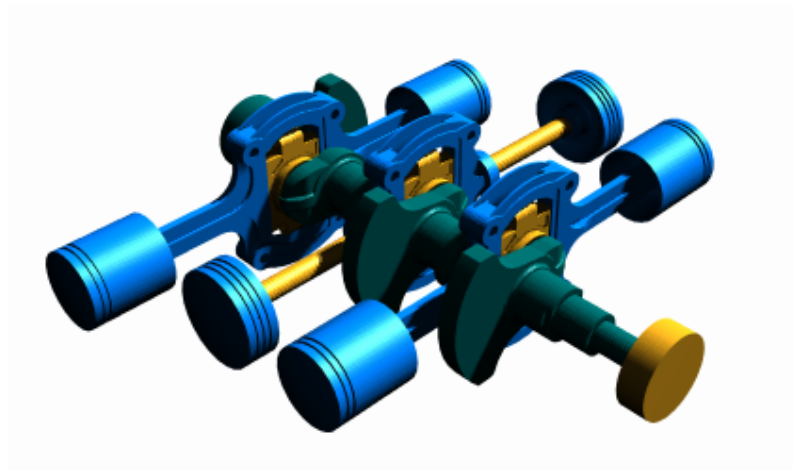


Figure 7.21: Crankshaft Assembly

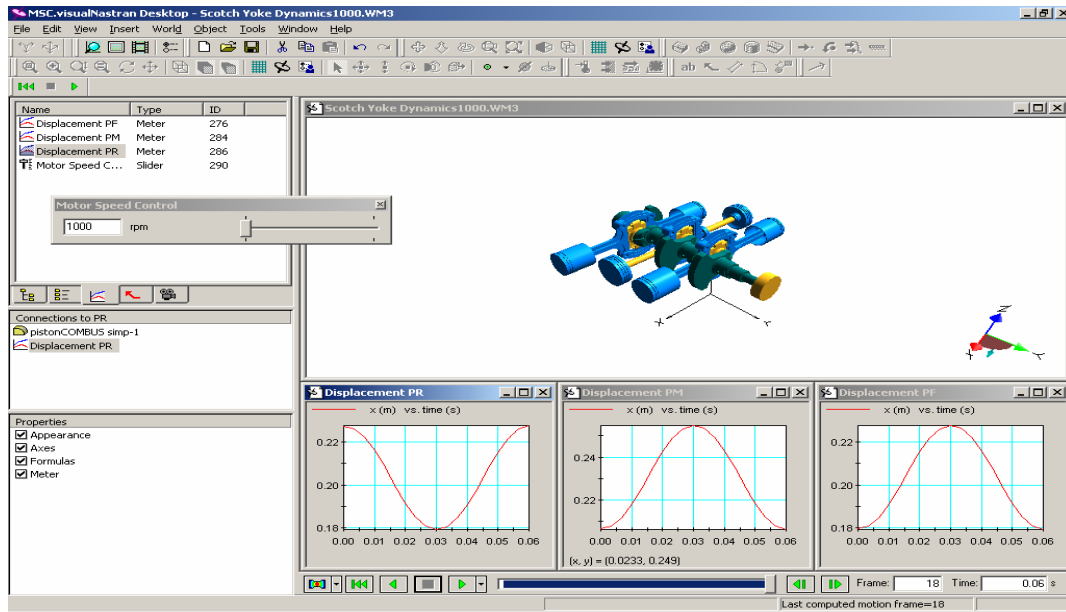


Figure 7.22: Motion Simulation In Visual Nastran to calculate piston displacement

The motion simulation plant was then embedded in Simulink Matlab to further the analysis for the calculation of piston speed and acceleration, inertia forces and moment as shown in Figure 7.22. The motion simulation results only for crankshaft speed at 1000 RPM is discussed in the next section.

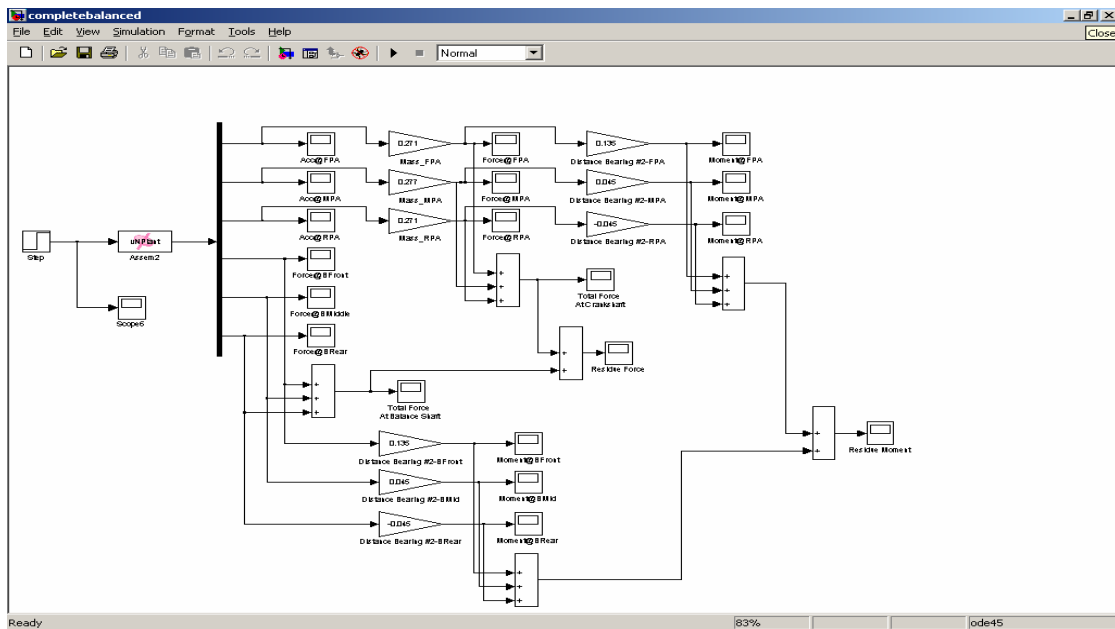


Figure 7.23: Calculation of piston speed, acceleration, inertia forces and moment in Matlab Simulink

7.3.3 Results

a. Piston Displacement, Speed and Acceleration at 1000 RPM

Figure 7.24 shows the top view of crankshaft piston assembly of the engine. The label of the component states the front piston, middle piston and rear piston. Figure 7.25 to 7.27 shows the displacement, velocity and acceleration of the pistons. Figure 7.28 to 7.30 shows the inertia forces on the pistons, moment of piston about bearings and the total unbalance forces and moments respectively.

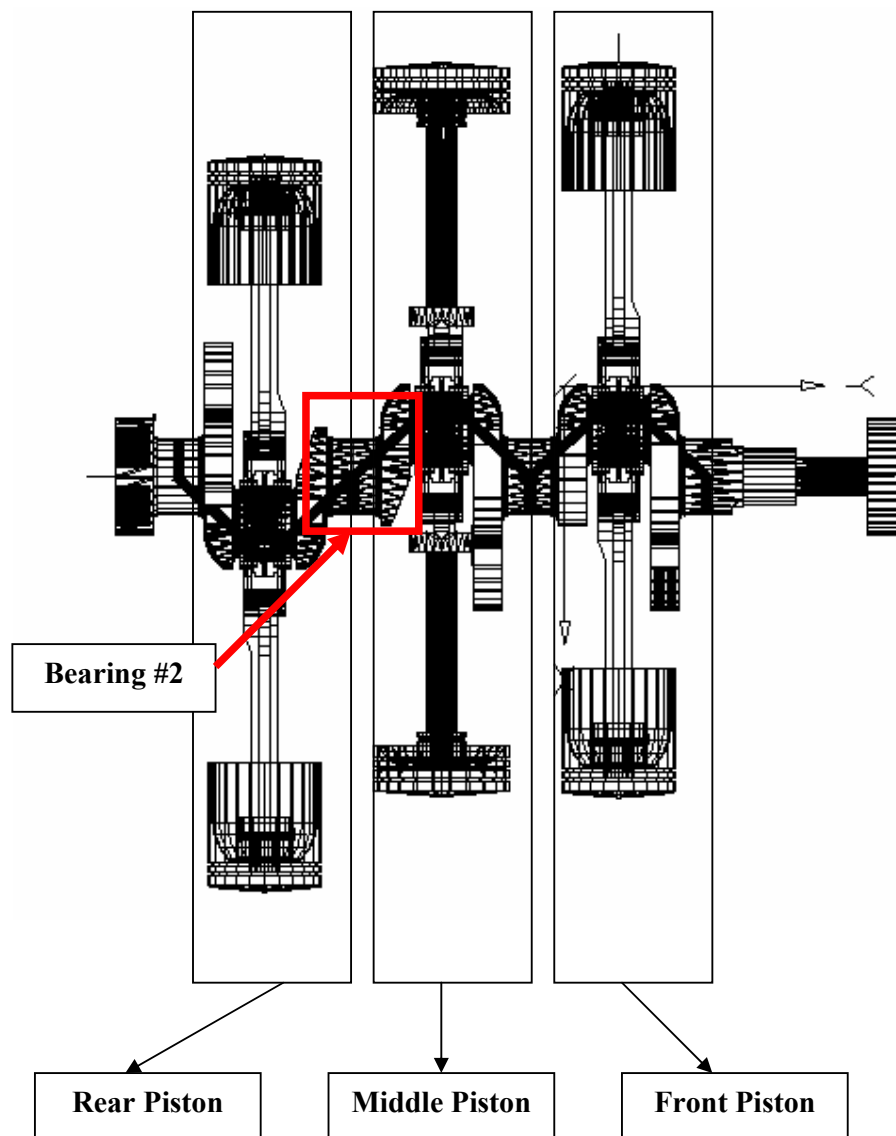


Figure 7.24: Engine Crankshaft Assembly Top View

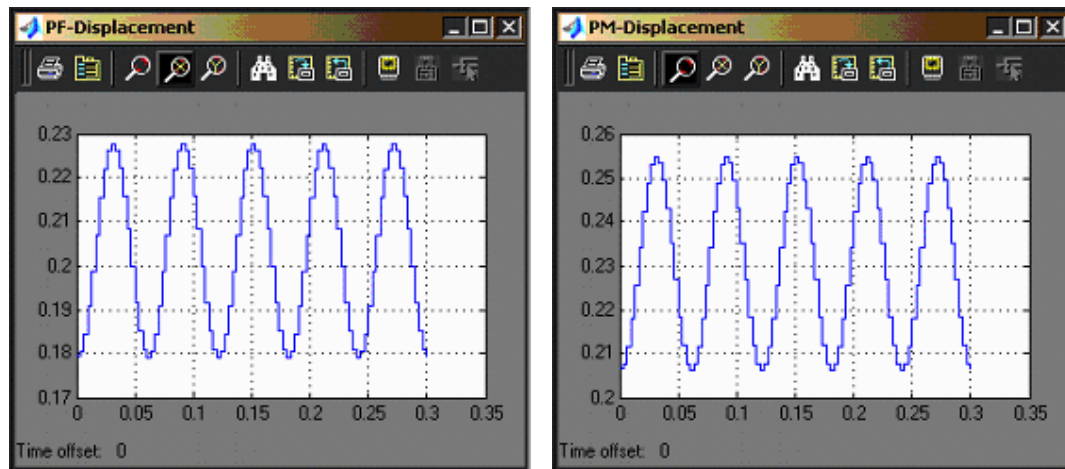
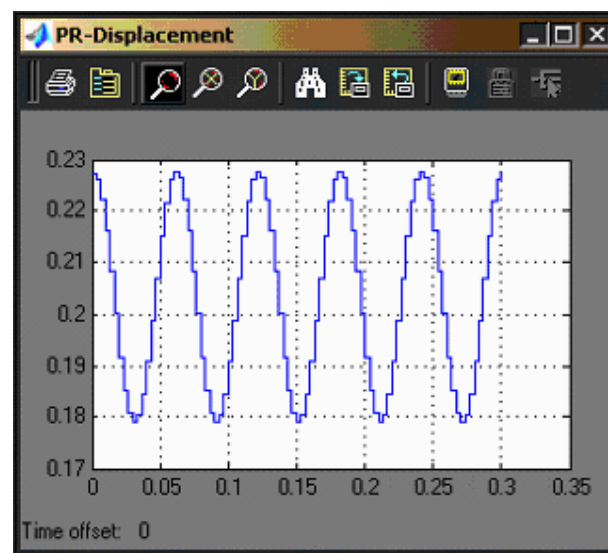
**Front Piston Displacement****Middle Piston Displacements****Rear Piston Displacements**

Figure 7.25: Pistons displacement motion

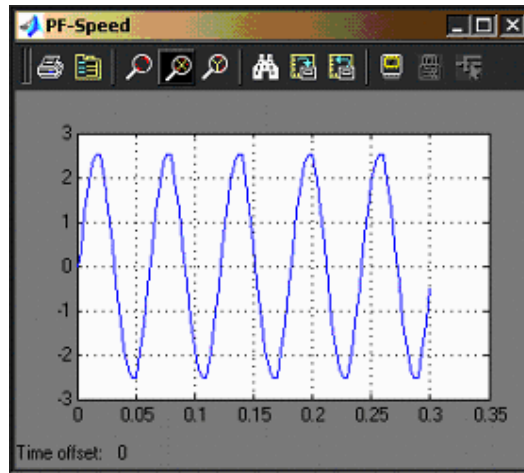
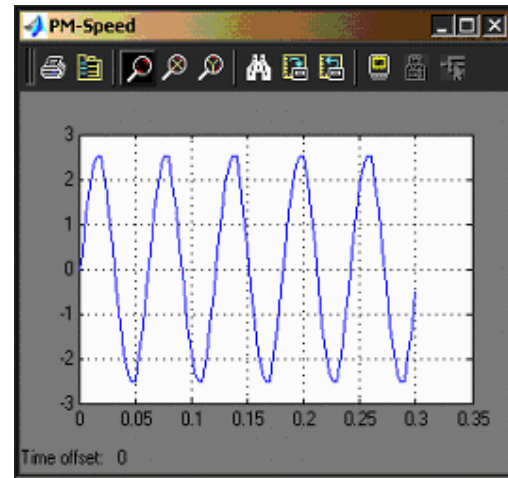
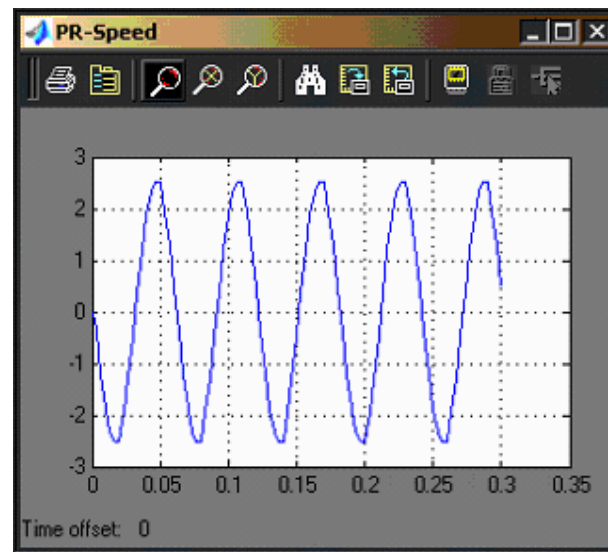
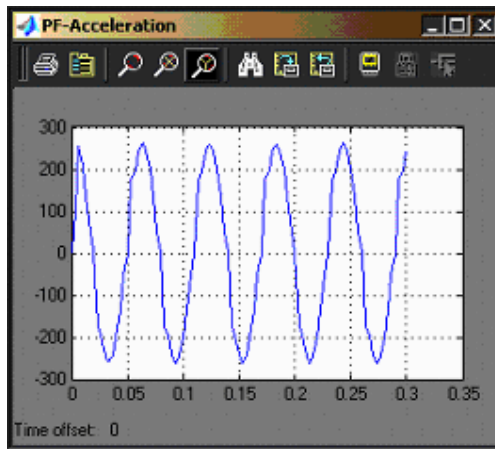
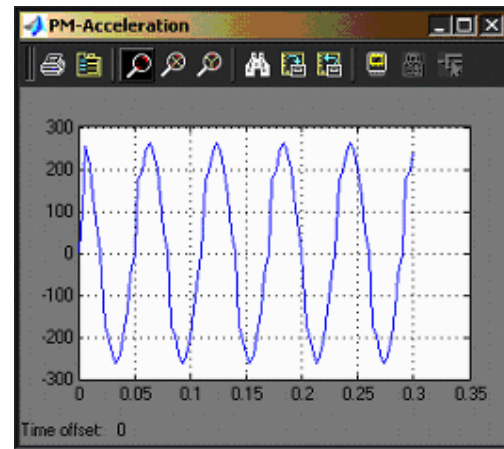
**Front Piston Speed****Middle Piston Speed****Rear Piston Speed**

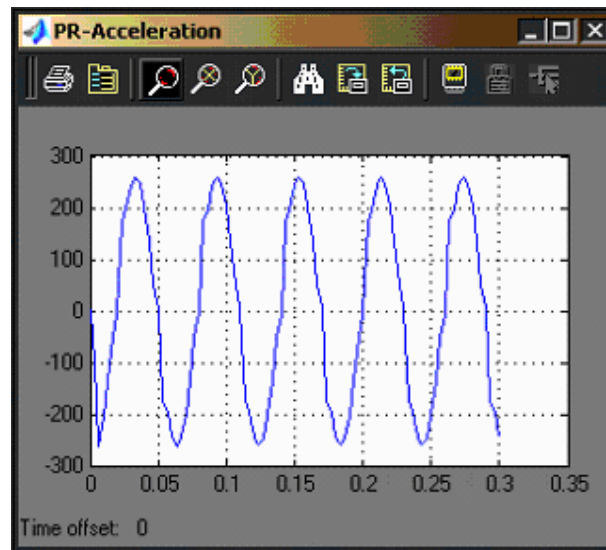
Figure 7.26: Pistons speed motion



Front Piston Acceleration

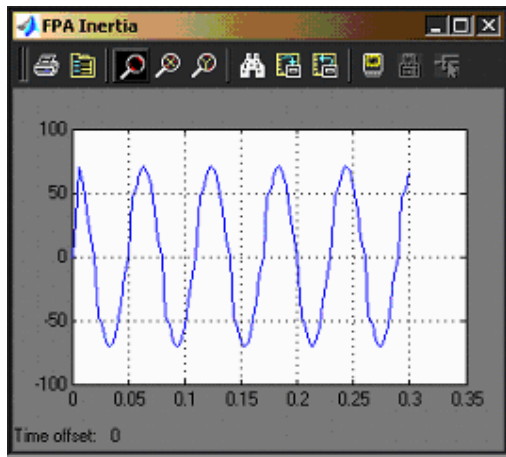


Middle Piston Acceleration

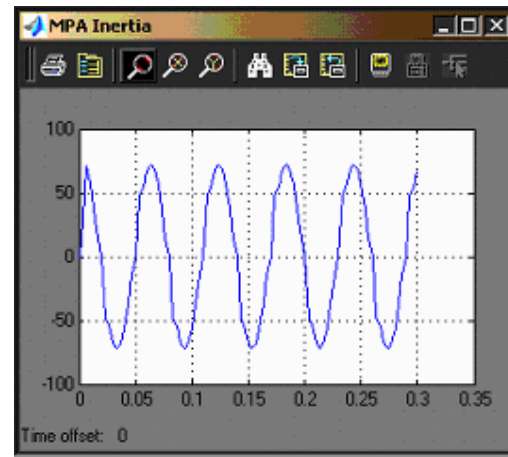


Rear Piston Acceleration

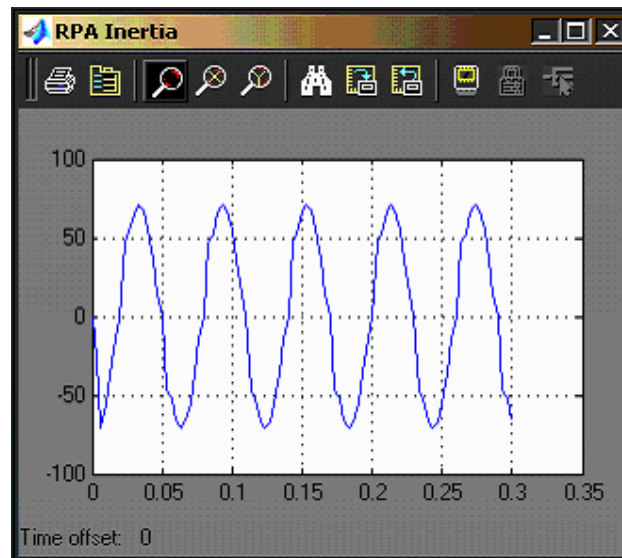
Figure 7.27: Acceleration of pistons



Inertia Force of Front Piston Assembly

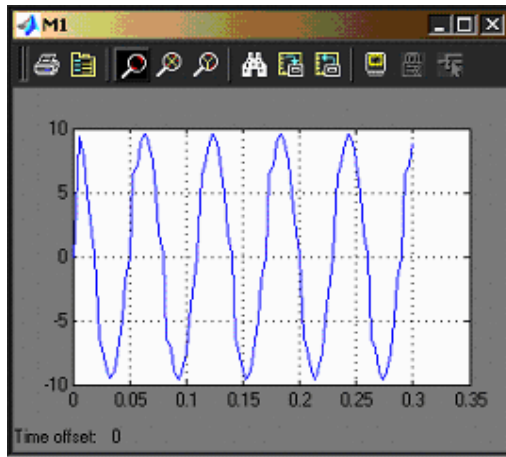


Inertia Force of Middle Piston Assembly

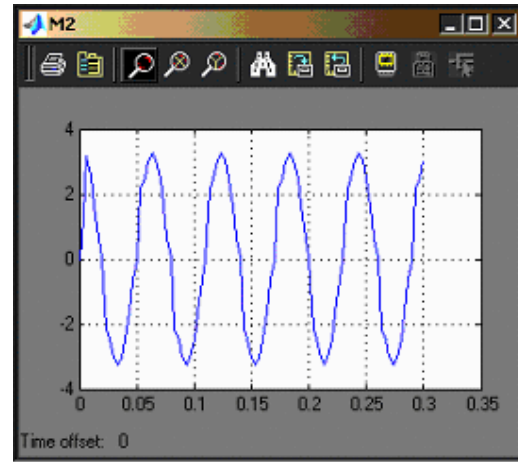


Inertia Force of Rear Piston Assembly

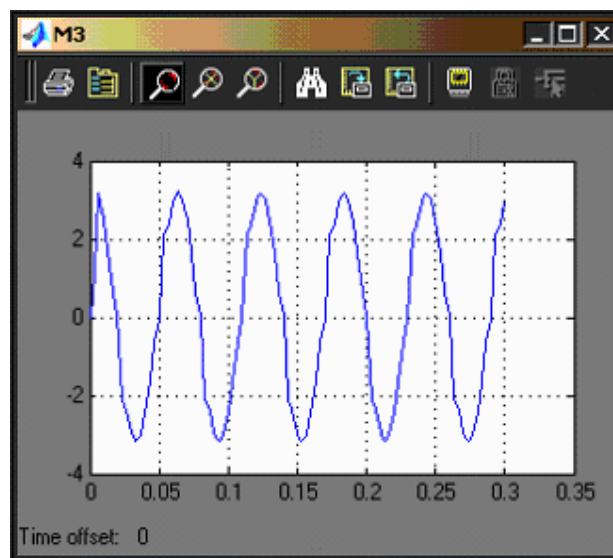
Figure 7.28: Inertia forces acting on the pistons



**Moment created by front piston
assembly acted at Bearing #2**

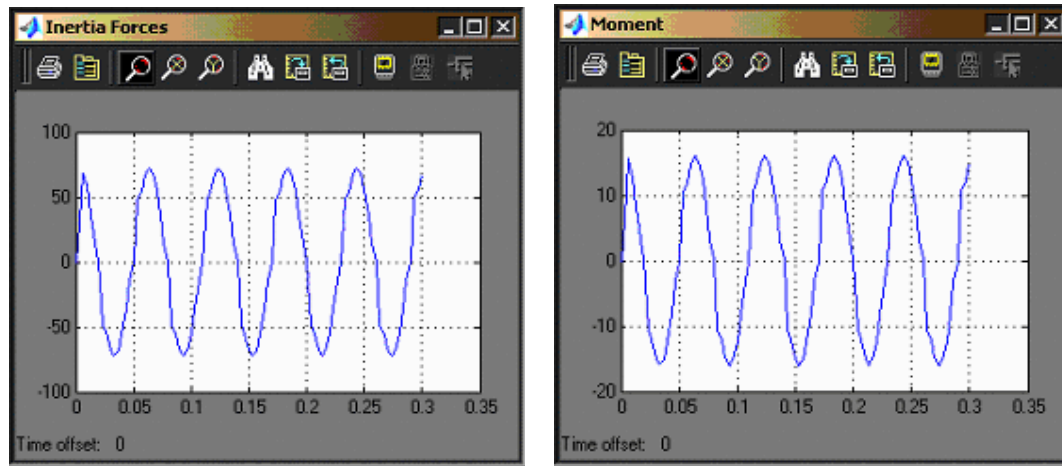


**Moment created by middle piston
assembly acted at Bearing #2**



**Moment created by rear piston assembly
acted at Bearing #2**

Figure 7.29: Moments created by the pistons assembly



Total Unbalance Force

Unbalance Moment

Figure 7.30: Total unbalance forces and moments

7.3.4 Discussion

i. Piston displacement, speed and acceleration

- a. Based on Figure 7.26, it is observed that the speed of the piston fluctuates within -2.5 m/s to 2.5 m/s (negative symbols shows opposite direction).
- b. Based on Figure 7.27, the acceleration of the piston fluctuates within -250 m/s^2 to 250 m/s^2 .
- c. The maximum speed and acceleration of the pistons is 2.5 m/s and 250 m/s^2 respectively.

ii. Inertia Forces

- a. Figure 7.28 shows the calculated inertia force of front piston assembly, middle piston assembly and rear piston assembly respectively.
- b. The maximum calculated inertia forces of front piston assembly is 70 kgm/s^2
- c. The maximum calculated inertia forces of middle piston assembly is 72 kgm/s^2
- d. The maximum calculated inertia forces of front piston assembly is 70 kgm/s^2

iii. Moment

- a. Figure 7.29 shows the calculated moment for front piston assembly, middle piston assembly and rear piston assembly created at bearing #2.
- b. It was shown that maximum moment created by each piston assembly :-
 - i. Front piston assembly : $9.5 \text{ kgm}^2/\text{s}^2$
 - ii. Middle piston assembly : $3.2 \text{ kgm}^2/\text{s}^2$
 - iii. Rear piston assembly : $3.0 \text{ kgm}^2/\text{s}^2$

iv. Maximum Unbalance Force and Moment

The maximum unbalance force,

$$\begin{aligned}
 &= \text{Maximum inertia force of front piston assembly} + \text{Maximum inertia force of middle piston assembly} + \text{Maximum inertia force of rear piston assembly} \\
 &= F_{\text{front}} + F_{\text{middle}} + F_{\text{rear}} \\
 &= (-70) + (-72) + (70) = -72 \text{ kgm/s}^2 \text{ for } 0 \text{ to } \pi, \\
 &= (70) + (72) + (-72) = 72 \text{ kgm/s}^2 \text{ for } \pi \text{ to } 2\pi,
 \end{aligned}$$

The calculated total unbalance force is shown in Figure 7.30. The direction of forces is shown in Figure 7.31 and 7.32.

For 0 to π , the maximum inertia forces:

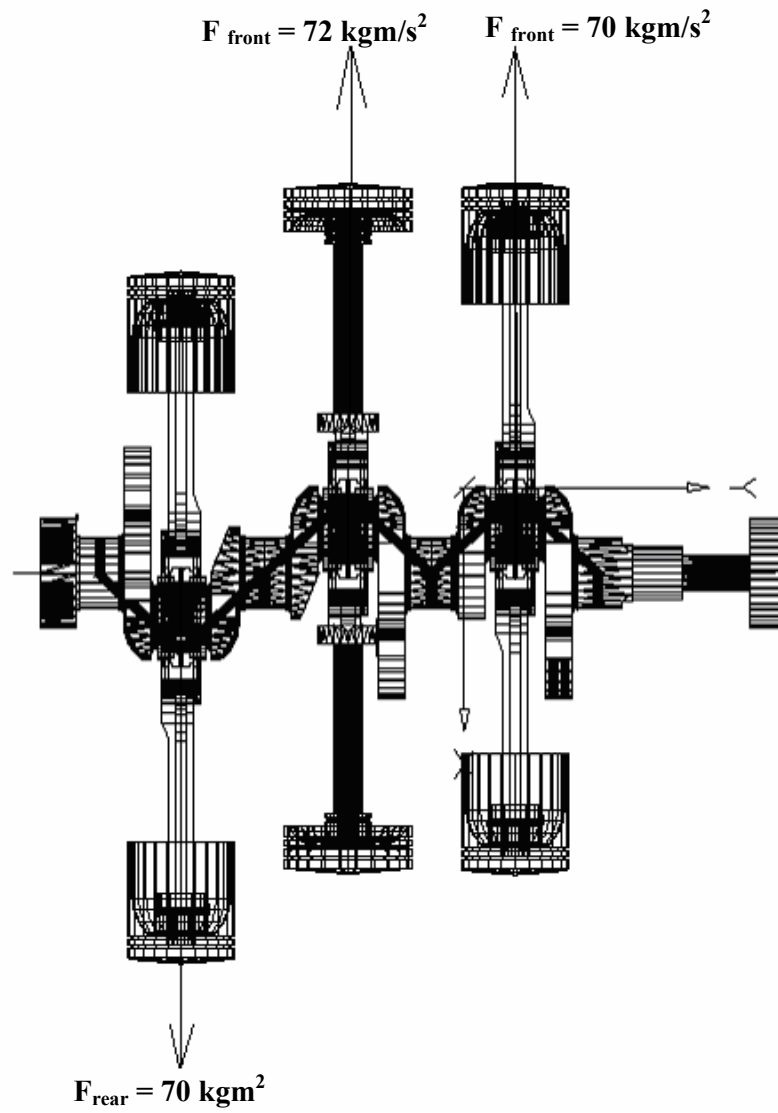


Figure 7.31: Magnitude and direction of maximum inertia forces

For π to 2π , the maximum inertia forces:

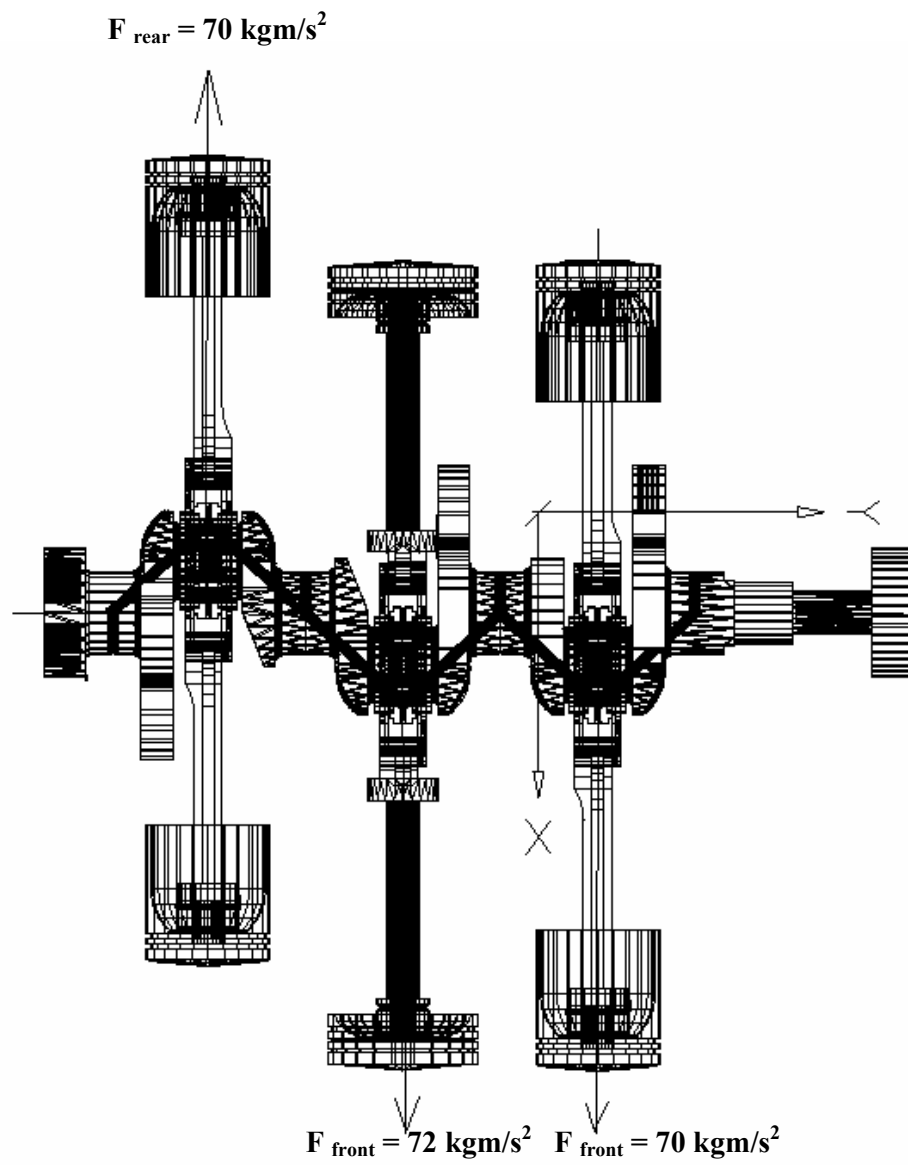


Figure 7.32: Magnitude and direction of maximum inertia forces

v. Maximum Moment

The maximum moment =

= Maximum moment front piston assembly + Maximum moment of middle piston assembly + Maximum moment of rear piston assembly

$$= M_{\text{front}} + M_{\text{middle}} + M_{\text{rear}}$$

$$= (9.5) + (3.2) + (3.0) = 15.7 \text{ kgm}^2/\text{s}^2 \text{ for } 0 \text{ to } \pi$$

$$= (-9.5) + (-3.2) + (-3.0) = -15.7 \text{ kgm}^2/\text{s}^2 \text{ for } \pi \text{ to } 2\pi$$

The calculated total unbalance force is shown in Figure 7.30 with the magnitude and direction of forces shown in Figure 7.33 and 7.34.

For 0 to π , the maximum moment:

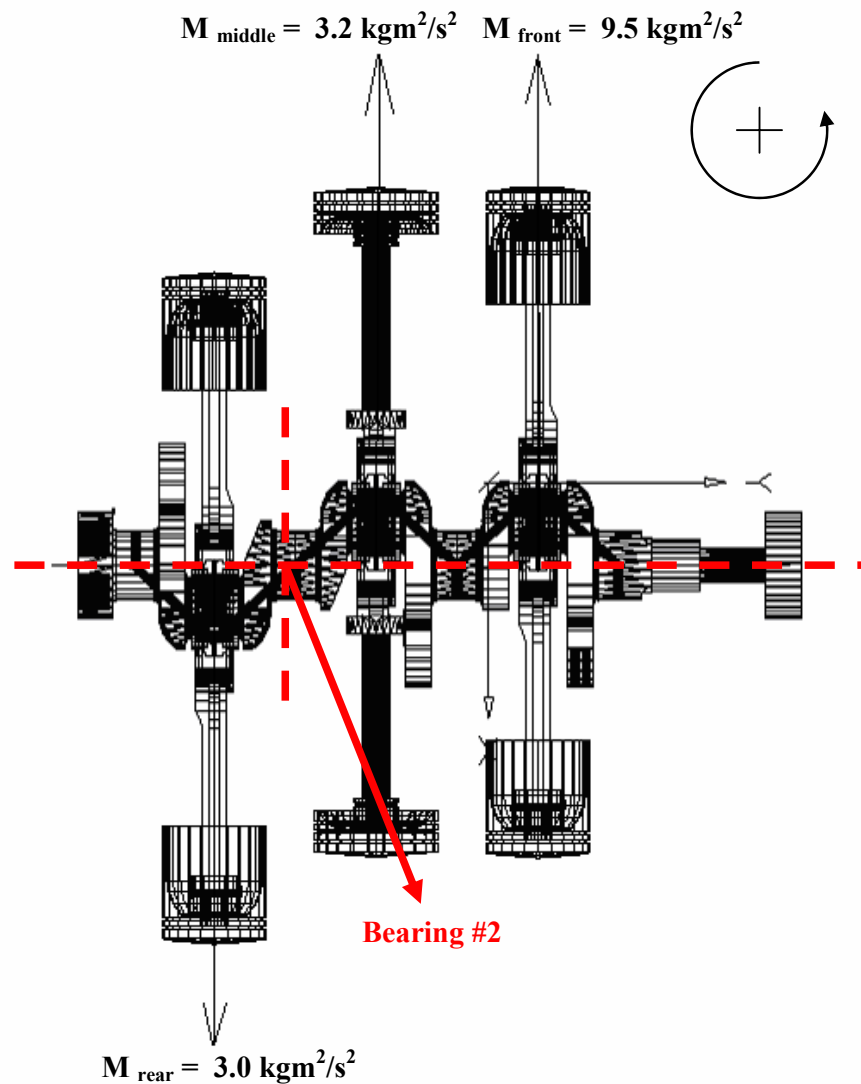


Figure 7.33: Unbalance moment on crankshaft

For π to 2π , the maximum moment:

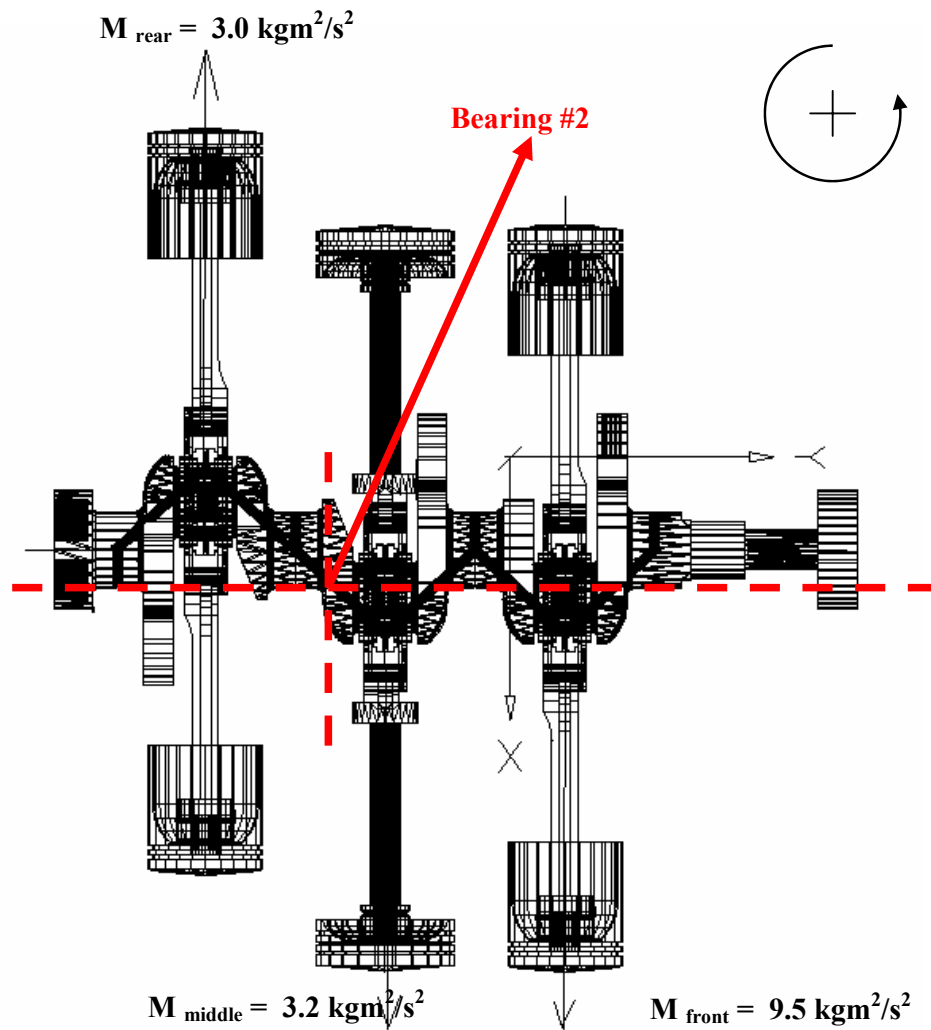


Figure 7.34: Unbalance moment on crankshaft

7.3.5 Conclusion

At this stage, the unbalance inertia forces and moment have been identified. The maximum inertia force and moment varies with crankshaft speed. For 1000 RPM the maximum inertia forces is $72 \text{ kgm}/\text{s}^2$ and maximum moment is $15.7 \text{ kgm}^2/\text{s}^2$. After this stage, it is proposed to proceed with the design of balance shaft by the engine designer.

When this is completed, the mechanism simulation has to be done for the second time to evaluate the percentage of the balancing achieved utilizing the balance shaft.

CHAPTER VIII

BACK PRESSURE, CATALYTIC CONVERTER, MATERIALS AND HEAT LOSSES

This chapter reports on the determination of back pressure of the exhaust system, identifying suitable catalytic converter, identifying existing and new materials for the engine components and calculating the heat losses from the fins.

8.1 Back Pressure

Back pressure is the resistance of airflow in a vehicle's exhaust system. Exhaust parts such as mufflers, resonators and catalytic converters all contribute to back pressure. Back pressure is a trade off between reducing engine noise/pollution and good engine performance. An exhaust pipe with many bends or kinks will have increased pressure compared to smooth, flowing pipes. Too much back pressure such as a plugged or severely restricted muffler, catalytic converter or pipe can reduce engine performance because it reduces the engine's ability to "breathe".

8.1.1 Back Pressure Test

This test will require a back-pressure gauge. An inexpensive back-pressure gauge can be made from a small pressure gauge that reads from 0 to 30 psi, a piece of vacuum tubing and a small 3 mm O.D. piece of copper tubing with a 3 mm I.D. viton O-ring. This O-ring will help to seal the hole that the copper tube is inserted into, or a back-

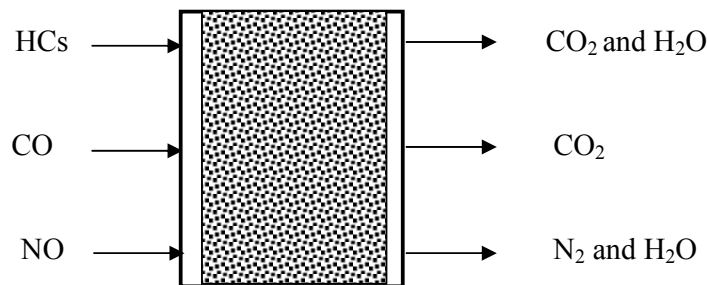
pressure gauge may be purchased from numerous sources pre-made. The exhaust pipe at the front of each converter. With the engine running, check the back pressure. The back pressure should be no more than 4 to 5 psi. This reading is with the throttle partly open at 2500 rpm. When checking exhaust back pressure, be sure to check at the inlet and outlet of each converter or exhaust component tested.

Three types of back pressure gauge were suggested and the information is attached in Appendix 8A. The backpressure test was not carried out on the muffler as the simulation results on the muffler are reliable enough to ensure acceptable magnitude of back pressure.

8.2 Catalytic Converter

i. Functions

- a) Clean the exhaust emissions by converting the harmful gases, such as hydrocarbon, carbon monoxide and nitric oxide to CO_2 , H_2O and N_2 .



- b) Reduced smoke produced by the two stroke engine operation.
- c) Reduced noise levels to acceptable standards

ii. Type of Catalytic Converter for 2-Stroke Engines.

a) Metallic Catalytic Converter

▪ Base metal catalysts

The base metal catalysts, such as vanadium pentoxide and titanium dioxide, operate in the intermediate temperature range (310°C - 400°C), but at high temperature they promote oxidation of SO_2 to SO_3 .

▪ Noble metal catalysts

The noble metal catalysts, such as platinum (Pt), palladium (Pd) and rhodium (Rh), operate in a low temperature (240°C - 270°C), but are inhibited by the presence of SO_2 . This type of metallic catalysts converter is commonly use for 2-stroke engine, which usually are mechanically and thermally stressful, and the atmosphere over the catalyst remain constantly rich of stoichiometric (i.e. lacking of oxygen).

b) Non-Metallic Catalytic Converter

▪ Zeolite catalysts

The zeolite can withstand temperature up to 600°C and it has an even wider range of operating temperatures when impregnated with a base metal.

iii. Selection of catalysts converter

a) Back pressure

The increasing of exhaust back power pressure may cause high exhaust temperature, loss of the power and even stalling. The pressure will drop while gas flow through the catalytic converter. The change of the pressure duct follow very fast and pressure drop in catalyst is cause by laminar and turbulent flow. How much the total pressure drop depends on the flow area and the length of the catalyst.

b) Emission

Two-stroke engines have CO emission similar to four-stroke engines, but much higher hydrocarbon (HC). The high hydrocarbon emission of two-stroke engines is mainly due to the fraction of air-fuel mixture which escapes from the combustion process during the scavenging phase. In unfavorable operating conditions (high load and low speed) the exhaust hydrocarbon consistency is similar to fuel composition. NO_x emissions are very low in all operating conditions due to rich mixtures and the combustion instability. Total CO and HC emissions from two-stroke engines have to be measured in order to work best with the catalysts to reduce emissions.

c) Temperature

Catalytic converter does not work until the exhaust is hot enough. It works optimally at an elevated catalyst temperature, generally at or above 300°C. The time period between when the exhaust emission begins until the time when the substrate heat up to a light-off temperature. Light-off temperature (LOT) is defined as the catalyst temperature at which 50% of the emissions from the engine are being converted as they pass through the catalysts.

d) Location of converter

Catalytic converter placed at the end of exhaust pipe will increase the engine power and specific fuel consumption at low and middle range speed. Catalytic converter placed in diffuser of exhaust pipe increase move maximum engine power to middle range speed and increase bsfc at lower and higher speeds.

e) Two stroke lubrication oil

Two-stroke engines need to burn a fuel and lubrication oil mixture for proper lubrication. Some of it will not be burned during combustion and will settle on the converter surfaces. A wrong oil will make the converter to loose activation within 500 km. With the proper lubrication oil, it could help the converter to maintain activation to 6000 km. Correct lubrication oil could help to lengthen the converter life and Japanese Automotive Standards Organization (JASO) FC grade oil is recommended.

iv. Conclusion

The selection of catalysts converter is governed by the back pressure, emission, exhaust temperature, location of converter in the exhaust system and correct lubrication oil. It was decided by the project team of not to install the catalytic converter until the performance of the engine and muffler is stable. The main problem is that the catalytic converter has to be installed either at the exhaust manifold or inside the muffler which requires additional compartment. This requires changes to be made on the exhaust outlet which will delay in the performance testing of the engine. Additionally, special lubrication oil has to be used to avoid settlement of unburnt fuel on the catalytic converter which is very expensive.

8.3 Materials For Two-Stroke Engine

Figure 8.1 shows the diagram of the various components of an engine and the commonly used and new materials for these components are listed in Table 8.1. The specifications of some of the materials are attached in Appendix 8B.

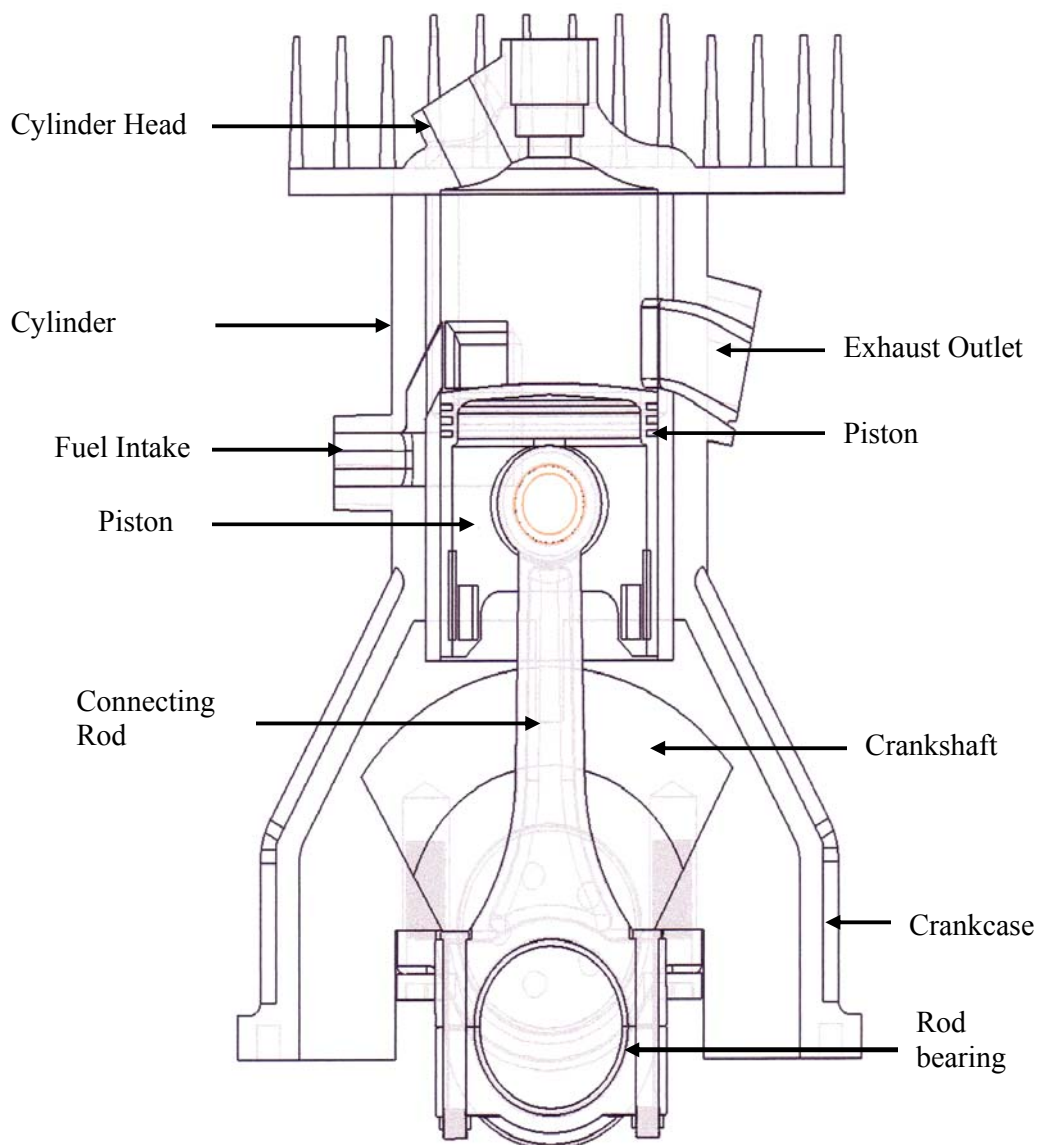


Figure 8.1: Various components of 2-stroke engine

Table 8.1: Common and new materials for engine components

Part	Common Material	New Material
Cylinder head	<ul style="list-style-type: none"> • Cast gray iron (SAE J431) • Iron alloy • Aluminium alloy 	<ul style="list-style-type: none"> • Compacted Graphite Iron (CGI): reduce engine weight and withstand higher cylinder pressure. However, it's difficult to machine, need advance machine and machine tools. • Magnesium Alloy: not only lighter, they have other benefits such as high shock and dent resistance, and a greater ability than aluminium to dampen noise and vibration, but there are many difficulties associated with handling molten magnesium and to stop it from burning, and more expensive than aluminium alloys.
Cylinder block	<ul style="list-style-type: none"> • Aluminium, with cast iron liner: since aluminium surface is not resistant to wear, it may create high friction against the movement of piston. Traditional solution is cover the cylinder bore surface with a cast iron liner of several mm thickness. 	<ul style="list-style-type: none"> • Aluminium, with Nikasil treatment: advanced solution is coating a thin (just several micrometer thick) layer of Nickel-silicon carbide by electrolytic deposition. The layer is even more frictionless than cast iron, thus benefit power output and fuel consumption. Moreover, the weight and size of cylinder block can be reduced.

	<ul style="list-style-type: none"> • Grey cast iron (SAE J431) 	<ul style="list-style-type: none"> • Compacted Graphite Iron • Magnesium Alloy
Piston	<ul style="list-style-type: none"> • Aluminium • Grey Cast Iron (SAE J431) 	<ul style="list-style-type: none"> • Alloy: Using alloy pistons are not very costly, what prevent most mass production all-alloy engines from using them is the friction generated between pistons and cylinder walls. It is commonly known that the contact between two aluminium surfaces results in high friction - much higher than between cast-iron and aluminium. Therefore many engines with aluminium block have to employ cast iron pistons
Connecting rod	<ul style="list-style-type: none"> • Forged steel • Alloy steel, forged steel (AISI 4340) 	<ul style="list-style-type: none"> • Titanium: Titanium has very high rigidity / weight ratio. However it's very expensive and hard to machine.
Crankshaft	<ul style="list-style-type: none"> • Billet steel • Steel forgings (AISI4340) • Cast steel • Malleable steel • Cast iron (Grade 80-55-06) 	
Crankcase	<ul style="list-style-type: none"> • Aluminium • Gray cast iron (SAE J431) 	<ul style="list-style-type: none"> • Magnesium Alloy

Intake manifolds	<ul style="list-style-type: none"> • Cast-iron • Aluminium alloy 	<ul style="list-style-type: none"> • Plastic: Nylon 66 and other reinforced plastic are commonly used in constructing intake manifold. They are light weight and most important, cheap to produce. However it produces more noise than metal. • Magnesium: A metal which is even lighter than aluminum. Expensive.
Piston ring	<ul style="list-style-type: none"> • Grey cast iron (SAE J431) • Ductile iron • Al Alloys 	<ul style="list-style-type: none"> • Steel: Not compatible with cast iron cylinder walls, so it must be coated with either chrome or Molybdenum or gas nitrided (a heat treatment process that impregnates the surface of the metal with nitrogen to case hardens the metal). Expensive than cast iron manufactured in smaller quantity.
Exhaust manifolds	<ul style="list-style-type: none"> • Cast iron • Nodular iron • Stainless steel 	
Rod bearing	<ul style="list-style-type: none"> • Bronze • Aluminium • Babbitt 	

8.3.1 Conclusion

The project team has decided to use the commonly used materials at the first stage of the fabrication of new engine. The use of new materials results in manufacturing and fabrication problems as new materials for the cutting and machines tools have to be identified and used.

8.4 Heat Transfer Analysis On Engine Fins

This section presents the heat transfer analysis of fins at engine block and cylinder head of the single cylinder compound piston engine. The mode of heat transfer in the analysis are :-

- a) conduction and
- b) free convection

The expected results from the analysis are :-

- a) temperature distribution over the fins surface, and
- b) total heat dissipation from the fins

8.4.1 Objective

- a. To estimate the temperature distribution within fins, and
- b. To estimate the total heat dissipation through fins of a single cylinder engine based on steady state heat transfer analysis.

8.4.2 Scope of Work

Finite Element Analysis consists of

- a) Simplifying fin geometry into simple plate model,
- b) Geometry modeling, meshing and load setting, and
- c) Heat transfer analysis to quantify total heat dissipation based on finite element method.

8.4.3 Problems And Solutions

- a. The single cylinder compound piston engine is an air-cooled type. It utilizes fins to dissipate the heat generated by the combustion process transmitted from cylinder wall to all over the engine body. Thus, it is necessary to estimate the total heat dissipation through the fins.
- b. A steady state heat transfer analysis was carried out using Finite Element ascertain if both the specification and the numbers of fins designed are sufficient to dissipate the heat generated by the engine.
- c. The analysis was limited to the heat transfer through conduction (from cylinder wall to fins edge) and free convection (over fins surface)
- d. The boundary conditions in the analysis are:
 - i. The wall temperature was assumed to be $300\text{ }^{\circ}\text{C}$ and ambient temperature was $30\text{ }^{\circ}\text{C}$
 - ii. Heat transfer coefficient was assumed to be $10\text{ W/m}^2\text{ }^{\circ}\text{C}$
 - iii. Heat flux at the fin's edge is 0.

8.4.4 Fins Geometry

- a. The physical model of cylinder head fins is shown in Figure 8.2.
- b. The physical model of engine block fins is shown in Figure 8.3.
- c. The simplified model of the cylinder head fin is shown in Figure 8.4.
- d. The simplified model of the engine block fin is shown in Figure 8.5.

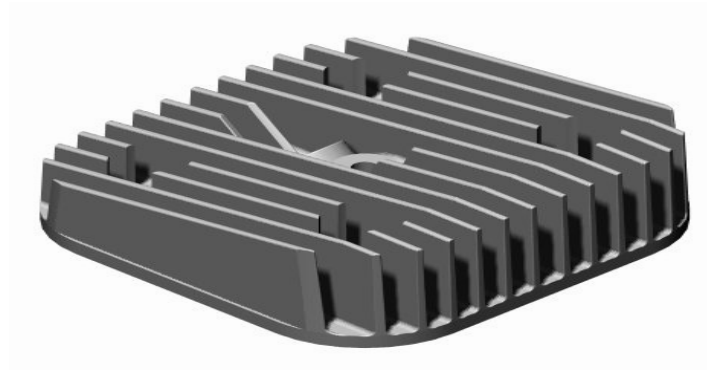


Figure 8.2: Cylinder head fins

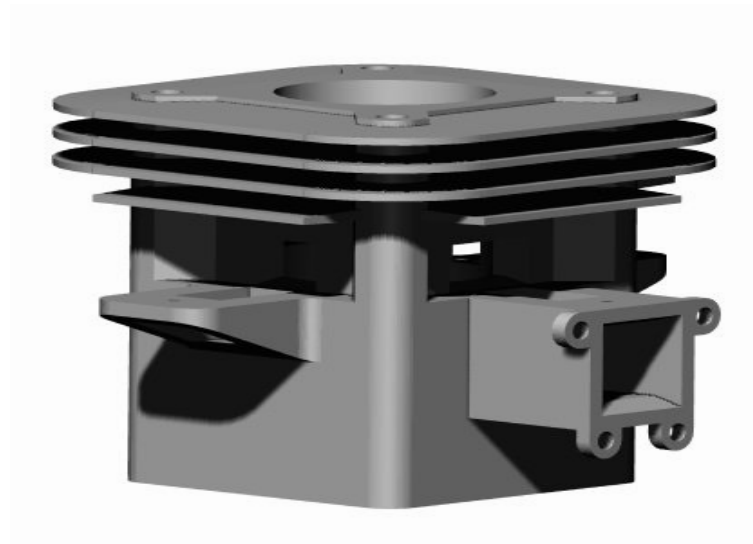


Figure 8.3: Engine Block Fins

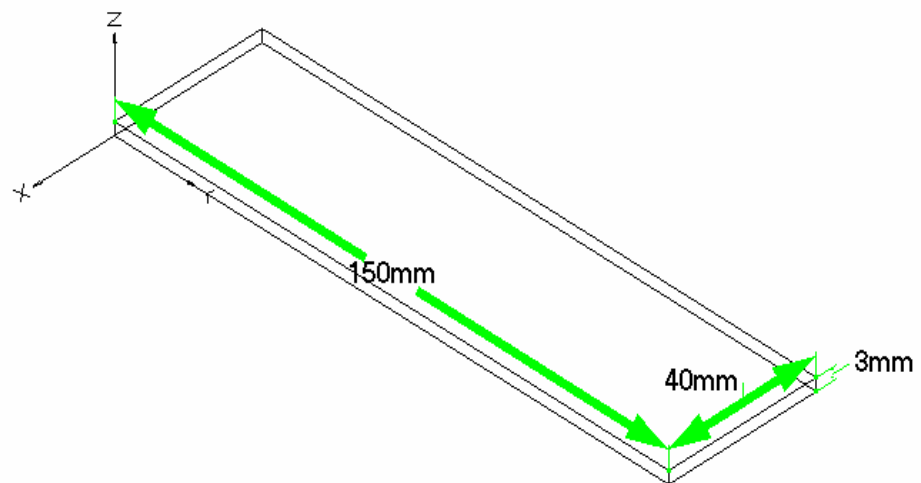


Figure 8.4: Dimension of Simplified Model of Cylinder Head Fin

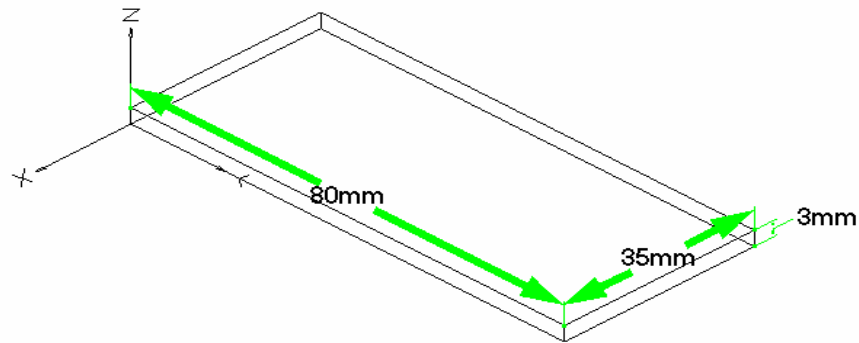


Figure 8.5: Dimension of Simplified Model of Engine Block Fin

8.4.5 Finite Element Model

- The finite element model for the fins is utilizing the triangular and plate elements.
- The model created using triangular element is shown in Figure 8.6 and 8.7. While for the model created using plate element is shown in Figure 8.7 and figure 8.8.
- The material of the fin is Aluminum alloy. Figure 8.9 specifies the properties of the material.
- The load set for the analysis is named Conduction and Convection. For conduction the wall temperature is set to 300°C, while for the Convection the heat transfer coefficient is assumed to be 10 W/m²K and the ambient temperature is set to 30°C.

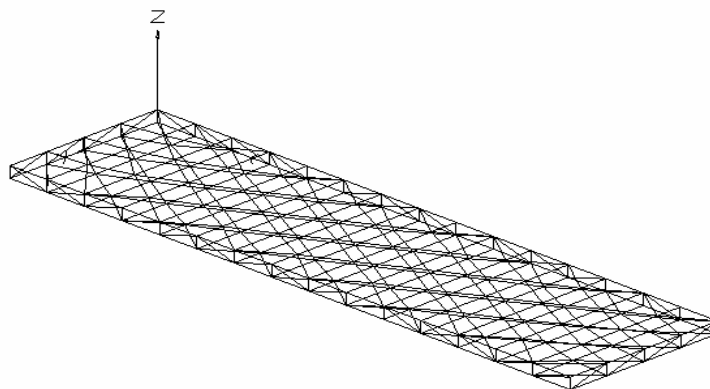


Figure 8.5: FE Model of cylinder head fin (triangular element)

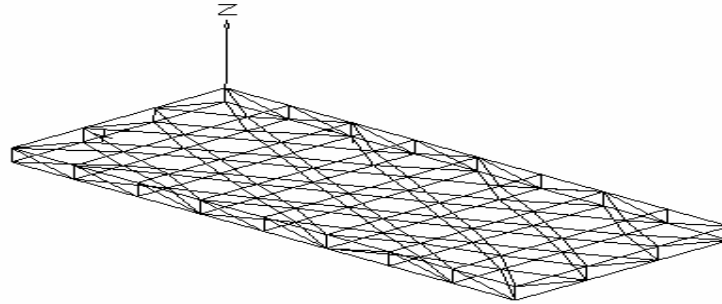


Figure 8.6: FE Model of engine block fin (triangular element)

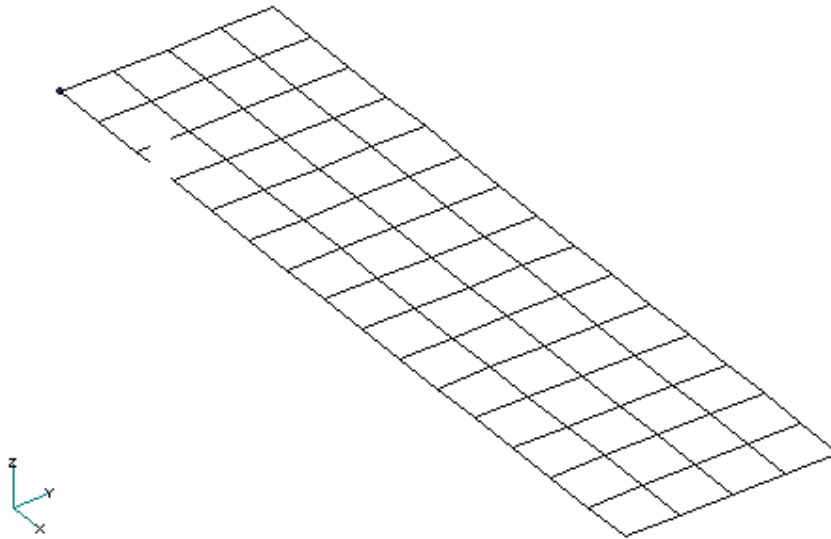


Figure 8.7: FE model of cylinder head fin (plate element)

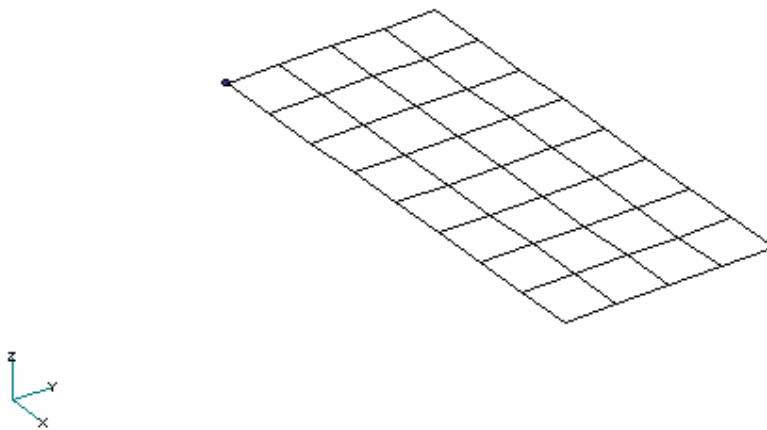


Figure 8.8: FE model of engine block fin (plate element)

Material Selector

Material: Aluminum 2024-T3

Mass Density	2.77e-6	kg/mm ³
Elastic Modulus	7.31e+10	Pa
Poisson's Ratio	0.33	
Yield Stress	3.45e+8	Pa
Ultimate Tensile Stress	4.83e+8	Pa
Specific Heat	962	J / kg K
Thermal Conductivity	0.19	W / mm K
Thermal Coeff. of Expansion	2.25e-5	mm / mm K

Buttons: Visit the DataMart, OK, Cancel

Figure 8.9 Aluminum Alloy Material Properties

8.4.6 Results

(a) Temperature Distribution (Triangular Element)

- i. Figure 8.10 shows the plot of the temperature distribution of cylinder head fin
- ii. Figure 8.11 shows the plot of the temperature distribution of engine block fin

(b) Temperature Distribution (Plate Element)

- i. Figure 8.12 shows the plot of the temperature distribution of cylinder head fin
- ii. Figure 8.13 shows the plot of the temperature distribution of engine block fin

(c) Total Heat Dissipation

- i. Table 8.2 contains tabulated results showing heat dissipation calculated for cylinder head fins and engine block fins.

Number of fins at cylinder head : 14

Number of fins at engine block : 14

(d) Total heat loss

$$\begin{aligned}
 &\text{Heat dissipation at cylinder head fins} + \text{Heat dissipation at engine block fins} \\
 &= 14(31.854 \text{ W}) + 14(14.910 \text{ W}) \\
 &= 445.956 \text{ W} + 208.74 \text{ W} \\
 &= \mathbf{654.696 \text{ W} \approx 655 \text{ W}}
 \end{aligned}$$

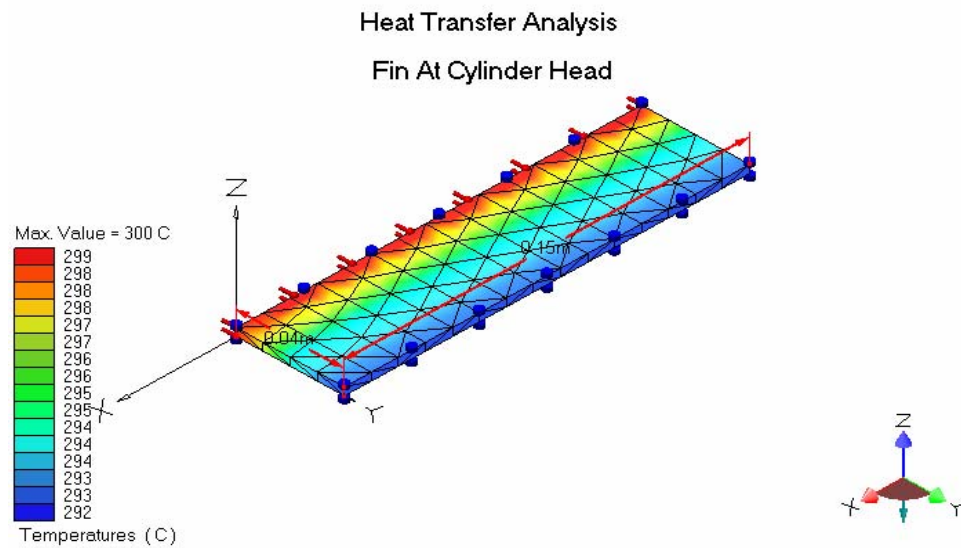


Figure 8.10: Temperature distributions at cylinder head fin (Triangular element)

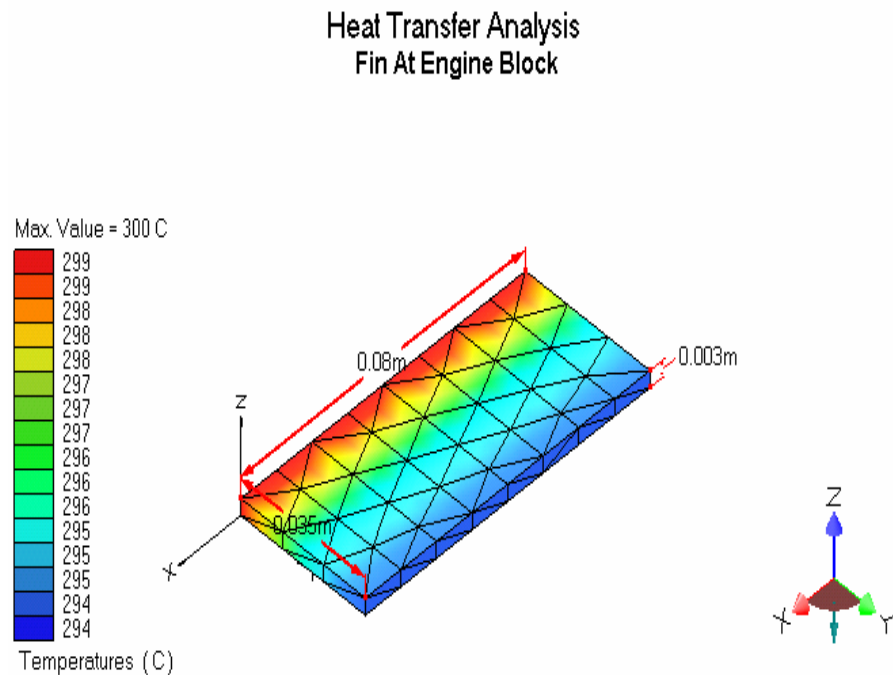


Figure 8.11: Temperature distribution at engine block fin (Triangular element)

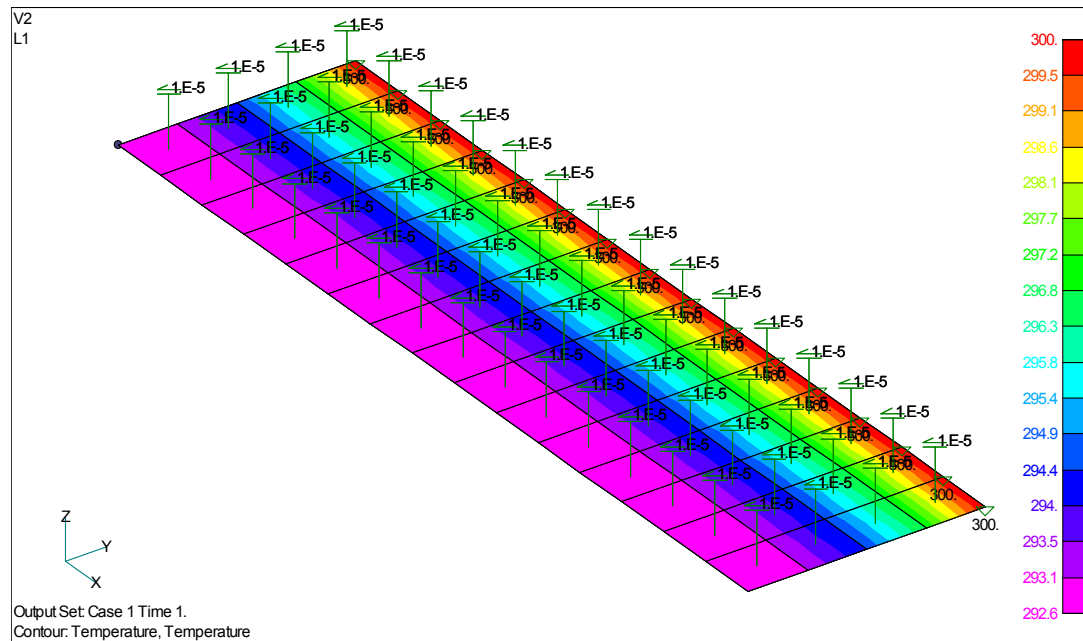


Figure 8.12 Temperature distributions at cylinder head fin (Plate element)

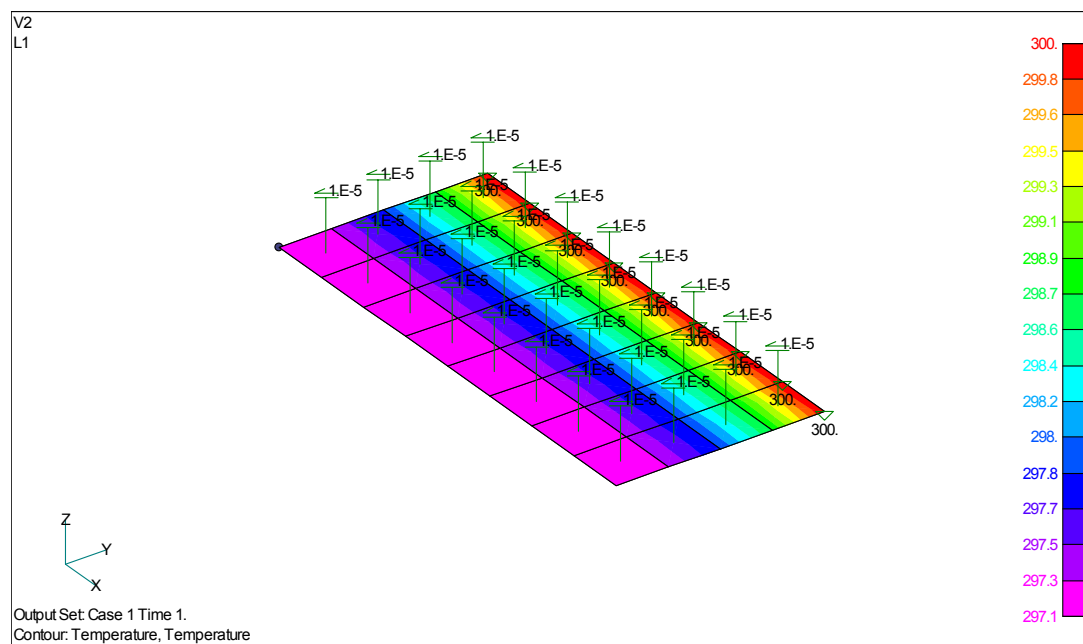


Figure 8.13 Temperature distributions at cylinder block fin (Plate element)

Table 8.2a: Estimated Heat Dissipation from 1 Fin at Cylinder Head

Average Temperature (° C)	Surface Area (m ²)	Heat Dissipation (W)
299	1.2×10^{-3}	3.228
297	0.6×10^{-3}	1.602
296	1.2×10^{-3}	3.192
294	1.5×10^{-3}	3.960
293	1.5×10^{-3}	3.945
Total heat dissipation for 1 fin through both surfaces		2(15.927)=31.854W

Table 8.2b: Estimated Heat Dissipation From 1 Fin at Engine Block

Average Temperature (° C)	Surface Area (m ²)	Heat Dissipation (W)
299	0.56×10^{-3}	1.506
298	0.28×10^{-3}	0.751
297	0.56×10^{-3}	1.495
295	0.70×10^{-3}	1.855
294	0.70×10^{-3}	1.848
Total heat dissipation for 1 fin through both surfaces		2(7.455)=14.910W

Note:

1. Ambient temperature = 30°C

(e) Heat Loss Percentage Calculation

Heat Generated By the Engine,

$$= \text{Fuel mass flow rate} \times \text{Gasoline calorific value} \times \text{Combustion Efficiency}$$

Efficiency

$$= (0.00008) \text{ kg/s} \times (44.4 \times 10^6) \text{ J/kg} \times 0.03$$

$$= 1066 \text{ J/s}$$

Heat Dissipate By Fins = 655 J/s

$$\text{Percentage of Heat Loss} = 655/1066 \times 100\%$$

$$= 61.44 \%$$

8.4.7 Conclusion

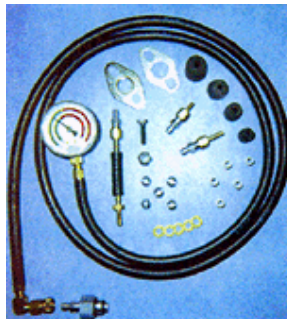
- The estimated total heat dissipation from all fins is equal to 655 Watt.
- The calculated heat generated by the engine is 1066 J/s
- The percentage of heat loss is 61.44 % through the fins

APPENDIX 8A

Exhaust Back Pressure Kit 3 Way



No. STR 0024 - Exhaust Back Pressure Tester Kit



No. STR 0024 Includes Plastic Storage Case

Three Way Exhaust Back Pressure Kit

- This **THREE** way tester allows quicker and more accurate testing of exhaust blockages in catalytic converters, mufflers, etc.
- Can test in **THREE DIFFERENT PLACES** - Oxygen Sensor, Exhaust Pipes, and Air Injection System. **The only tool like it on the Market today!**

1. Oxygen Sensor adapter includes M12 & M18 thread. Flange and gasket also included for cars with flange-type oxygen sensors.

2. Exhaust Pipes testing, includes threaded inserts, an installing tool, sealing screws & washers are included. Testing can be done on either side of catalytic converter and muffler to pinpoint blockage.

3. Air Injection System testing, includes four rubber adapters and quick coupler plugs to use at the air injection pipe inlet fitting.

Network Tool Warehouse

800.939.8665 - U.S. CALL FREE

888.866.5329 - U.S. FAX FREE

International: 330.659.3032 Phone - 330.659.3454 Fax

Catalyst Back Pressure Test Kit



BPT01

Quickly identify clogged catalytic converters!

- * Universal O2 Port adapter,
- * No drilling and filling!
- * 0-15 PSI gauge, 2-1/2" dial face
- * Protective rubber boot
- * Limited lifetime warranty.
- * Durable storage case.



Back Pressure Tester TU24APB			TU24APB
This three way tester allows quicker and more accurate testing of exhaust blockages in catalytic converters, mufflers, etc			
MSRP	Etoolcart Price	Qty	
\$105.95	\$85.95	1	

Detailed Description

3 WAY BACK PRESSURE KIT This three way tester allows quicker and more accurate testing of exhaust blockages in catalytic converters, mufflers, etc.

Test in three different places:

1. Oxygen Sensor adapter includes M12 and M18 thread. Flange and gasket also included for cars with flange-type oxygen sensors.
2. To test thru the Exhaust Pipes, threaded inserts, and installing tool, sealing screws and washers are included. Testing can be done on either side of catalytic converter and muffler to pinpoint blockage.
3. For testing through the Air Injection System four rubber adapters and quick coupler plugs are included to use at the air injection pipe inlet fitting.

- Special gauge has two multi-colored bands-idle and 2500 RPM, with pressures shown in PSI and bar.
- Hose is 6 feet, enough length for you to test from the drivers seat.

APPENDIX 8B- Specification of Materials

SAE J431 automotive gray cast iron, SAE grade G3000

Subcategory: Gray Cast Iron; Metal

Key Words: UNS F10006, ferritic, pearlitic, soft iron castings

Component Wt. %

C	3.1 - 3.4
Fe	94
Mn	0.6 - 0.9
P	0.1
S	0.15
Si	1.9 - 2.3

Material Notes:

If Carbon or Silicon is on the high % range end, the other should be on the low % end. Properties determined from as-cast test bar 30.5 mm diameter. Pearlitic microstructure. Applications include **automobile and diesel cylinder blocks, cylinder heads, flywheels, differential carrier castings, pistons, medium duty brake drums and clutch plates**. 1000 kg minimum transverse load, 5.1 mm minimum deflection.

Physical Properties	Metric	English	Comments
Density	7.15 g/cc	0.258 lb/in ³	Typical for Gray Cast Iron

Mechanical Properties

Hardness, Brinell	187 - 241	187 - 241	
Hardness, Knoop	238	238	Converted from Brinell hardness.
Hardness, Rockwell C	14.1	14.1	Approximated. Converted from Brinell hardness. Value below normal HRC range, for comparison purposes only.
Hardness, Vickers	225	225	Approximated. Converted from Brinell hardness.
Tensile Strength, Ultimate	Min 207 MPa	Min 30000 psi	

Ductile Iron grade 80-55-06

Subcategory: Ductile Iron; Metal

Key Words: UNS F33800, ASTM A536, ferritic, pearlitic, crankshafts, gears, rollers

Component	Wt. %	Component	Wt. %	Component	Wt. %
C	3.6 - 3.8	Fe	90.738 - 94.175	Ni	0.05 - 0.2
Ce	0.005 - 0.2	Mg	0.03 - 0.06	P	Max 0.03
Cr	0.03 - 0.07	Mn	0.15 - 1	S	Max 0.002
Cu	0.15 - 1	Mo	0.01 - 0.1	Si	1.8 - 2.8

Material Notes:

Carbon represents the total carbon in the above composition. Cerium is an optional constituent in ductile iron. Most ductile irons are specified based on mechanical properties and have loosely defined compositions. For example, 80-55-06 ductile iron is specified to have a minimum tensile strength of 80 ksi (552 MPa), a yield strength of 55 ksi (379 MPa) and an elongation of 6%. Ferritic/pearlitic, as cast. Applications include **crankshafts, gears and rollers**. Hardness and machinability data provided by manufacturer/supplier, Siltin Industries, Inc.

Mechanical Properties	Metric	English	Comments
Hardness, Brinell	187 - 269	187 - 269	for 80-55-06 T-4 ductile iron.
Hardness, Knoop	254	254	Converted from Brinell hardness.
Hardness, Rockwell C	16.7	16.7	Approximated. Converted from Brinell hardness.
Hardness, Vickers	240	240	Converted from Brinell hardness.
Tensile Strength, Ultimate	Min 552 MPa	Min 80100 psi	
Tensile Strength, Yield	Min 379 MPa	Min 55000 psi	
Elongation at Break	6 %	6 %	In 50 mm.
Machinability	0 %	0 %	Good machinability. No numerical rating available.

Aluminum Alloys, General

Subcategory: Aluminum Alloy; Metal; Nonferrous Metal

Key Words: Aluminium Alloys, General; Al Alloys

Component **Wt. %**

Al 87 - 100

Material Notes:

These properties are typical of commercial aluminum alloys. Some properties, such as strength and hardness, vary too much for a reasonable generalization. See entries for individual alloys for more specific information. Aluminum 1199 is the highest purity (99.99% Al min.) in the database.

Physical Properties	Metric	English	Comments
---------------------	--------	---------	----------

Density	2.7 g/cc	0.0975 lb/in ³	
---------	--------------------------	---------------------------	--

Mechanical Properties

Modulus of Elasticity	70 GPa	10200 ksi
Poisson's Ratio	0.33	0.33
Shear Modulus	26 GPa	3770 ksi

Electrical Properties

Electrical Resistivity	5e-006 ohm-cm	5e-006 ohm-cm
------------------------	-------------------------------	---------------

Thermal Properties

Heat of Fusion	390 J/g	168 BTU/lb	
CTE, linear 20°C	24 µm/m-°C	13.3 µin/in-°F	from 0-100°C (32-212°F)
CTE, linear 250°C	25 µm/m-°C	13.9 µin/in-°F	
Heat Capacity	0.88 J/g-°C	0.21 BTU/lb-°F	
Thermal Conductivity	190 W/m-K	1320 BTU-in/hr-ft ² -°F	
Melting Point	620 - 650 °C	1150 - 1200 °F	
Solidus	620 °C	1150 °F	
Liquidus	650 °C	1200 °F	

CHAPTER IX

DESIGN OF EXHAUST SYSTEM

9.1 Single Cylinder Exhaust System

9.1.1 Introduction

A new two stroke stratified charge lean burn gasoline engine was developed by the engine design group. The engine has a step piston with 125 cc swept volume and is air cooled. The engine is quite unique as its piston is of compound type producing the step. Step piston means that there are physically two pistons in the cylinder of the engine. Its scavenging technique was further improved producing maximum output power of 9.1 KW at 8700 rpm. Gas and noise from an internal combustion engine must be released to the atmosphere through the exhaust system. Thus an exhaust system is required to complete the system of engine.

Exhaust system is important to the engine because it is required to suppress the noise from the engine and filter dangerous gas. Additionally, the exhaust system can improve the power and torque of the engine and decrease the pollution of air and noise.

9.1.2 Literature Review

The noise radiated from the tail pipe of the engine plays an important role in the total noise emitted for a small two stroke mopeds. As the noise emission regulations in most areas of the world are getting more and more stringent, the noise reduction

technique becomes very important. In order to reduce the noise emission, while keeping the engine performance unaltered, the exhaust pipe and muffler design are the critical parts in the engine design and development process.

Mikiya et.al (1) developed the exhaust manifold muffler without the deterioration of engine performance by allocating the volume at the junction of the exhaust manifold branch pipes. Acoustic characteristics of “Exhaust Manifold Muffler” have been analyzed using FEM and experimental methods. It was concluded that greater silencer volume could increase noise attenuation and reduce back pressure. Allocating the volume at the junction of exhaust manifold branch pipe gave high muffling efficiency and prevented it from amplifying the exhaust noise and the exhaust manifold muffler could improve volumetric efficiency, and hence increases the engine performance.

Selamet and Radavich (2) investigated the effect of the length on the acoustic attenuation performance of concentric expansion chambers. Three approaches were employed to determine the transmission loss. The first approach is the two dimensional axisymmetric analytical solution, second is the three-dimensional computational solution base on the boundary element method and third is an experiment on an extended impedance tube setup with nine expansion chambers fabricated with fixed inlet and outlet ducts, fixed chamber diameters and varying chamber length to diameter ratio from $l/d = 0.2$ to 3.53. An experimentally verified expression was obtained to relate the number of repeating transmission loss domes to the l/d ratio of the chamber.

Single cylinder two stroke engine was developed by Huai Lu and Feng Yang (3) to determine the noise emitted from the exhaust pipe. Seven different configurations of exhaust pipes were studied, including three straight pipes, two diverging-converging pipes, one with expansion chamber and a real exhaust pipe. The test engine was run in both motoring and firing conditions. Pressure variations in the exhaust pipe and the total sound level and the one third octave frequency distributions outside the exhaust pipe were recorded. The conclusion was, for the simple geometry pipe at motoring conditions, the calculated results of the pressure variations inside the exhaust pipe and the noise level outside the exhaust pipe agreed quite well with the measured data. However, for the complex geometry pipe at the firing conditions, the calculated results were consistent with the experimental data at low engine speeds only.

Cheng and Wu (4) discussed the use of a component based computer simulation tool for design and analysis of exhaust mufflers. A comprehensive computer program base on the direct Mixed Body Boundary Element Method was developed to predict the transmission loss characteristic of muffler systems. The transmission loss was calculated by an improve four-pole method that does not require solving the boundary element matrix twice at each frequency, and hence, it is a significantly faster approach when compared to the conventional four-pole method. The BEM prediction showed very good comparison with the measured results.

Blanco and Andrew (5) describe the methodologies developed to reduce the noise radiated from silencers while keeping or improving the engine performance; i.e. whilst minimizing the pressure loss through the silencer. The methodology was developed using the boundary element method (BEM). This method is able to calculate the acoustic variables in the interior and exterior fluid of the silencer. The conclusions from this paper are that it is possible to effectively predict the acoustic performance of a silencer using the boundary element method and it is acceptable to ignore small feature, perforate sheets and heat isolation material for low frequency noise prediction.

Torregrosa et.al (6) described a methodology base on experimental and theoretical studies for the modeling of typical exhaust systems used in two stroke small engines. The steady and dynamic behaviors of these systems have been measured in a flow test rig and in an impulse test rig, respectively. A complete 50 cc engine was modeled and comparisons between predicted and measured instantaneous pressure at the exhaust port show a fair agreement, the results of the hybrid approach being more accurate. The main conclusions are a new methodology based on flow and impulse test rig experiments for exhaust system modeling has been established.

The subject of noise emission from an internal combustion engine, and its reduction, is a specialized topic. Many text book and technical paper have been written on this subject. Instead, it is intended to orient the noise emission pertaining to two stroke engines and to the problems of silencer design for this particular type of power unit.

9.1.3 Theory of Silencer Design

The exhaust system for two stroke engine consists of two parts, the expansion chamber and the silencer. Expansion chamber plays major part in tuning the performance of the engine while silencer plays the part in suppressing the exhaust noise.

There are three basic type of silencer; diffusing silencer, side resonant silencer and absorption silencer. Each and every silencer has their noise reduction characteristics and often described by insertion loss or transmission loss value. Insertion loss is defined as the difference in sound pressure level at a specified point beyond the silencer with and without silencer while transmission loss (also known as sound power transmission coefficient) is defined as the ratio of the power incident on the silencer to the power transmitted through the silencer (7). The value of the insertion loss depends on the properties of the source, termination and surrounding environment as well as the silencer (8), transmission loss however depends solely on the silencer element itself (9). Because of that, transmission loss is said to be the most important characteristic of the silencer and most calculated results concerning the noise reducing properties of silencer elements are in term of transmission loss. Due to this reason, silencer characteristics in this report will be described in term of transmission loss.

There are three most common type of silencer; the diffusing silencer, the side-resonant silencer and the absorption silencer (8). For most basic silencer, the diffusing silencer, transmission loss is basically a function of two parameters, the expansion ratio (ratio between expansion chambers to the pipe diameter) and the relationship between the wave lengths of the sound to the length of the expansion chamber.

From Fukuda (8), the transmission loss of the diffusing silencer is given by:

$$TL = 10 \text{ Log}_{10} (A_{r2} F(k, L))^2 \text{ dB} \quad (9.1)$$

$$\text{where} \quad F(k, L) = \frac{\sin(kL_b) \times \sin(kL_t)}{\cos(kL_1) \times \cos(kL_2)} \quad (9.2)$$

$$A_{r2} = \frac{A_b}{A_2} \quad k = \frac{2\pi f}{a_o} \quad a_o = \sqrt{\gamma R T_o}$$

and

TL= transmission loss

a_o = acoustic velocity

γ = ratio of specific heat

R= gas constant (J/kgK)

T_o = exhaust gas temperature (K)

A_b = box area

A_2 = area of pipe 2

A_{r2} = expansion ratio

L_b = length of box

L_t = length of pipe 2

L_1 = re-entrant length of pipe 1

L_2 = re-entrant length of pipe 2

f = frequency (Hz)

Figure 9.1 shows the significant dimension of a diffusing silencer element.

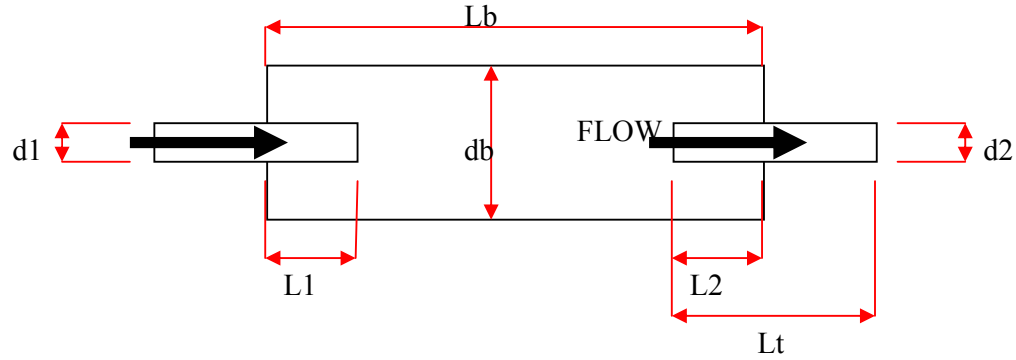


Figure 9.1: Significant dimension of a diffusing silencer element

For side-resonant silencer, the transmission loss depends on the natural frequency of the side-resonant system, the conductivity of the holes and the volume of the resonant cavity. Transmission loss for this type of silencer is given by Davis (8) as:

$$TL = 10 \log_{10} (1 + Z^2) \text{ dB} \quad (9.3)$$

where

$$Z = \frac{\frac{\sqrt{K_h V_b}}{2A_3}}{\frac{f}{f_{sr}} - \frac{f_{sr}}{f}} \quad K_h = \frac{N_h A_h}{x_t + 0.8A_h}$$

$$f_{sr} = \frac{a_o}{2\pi} \sqrt{\frac{K_h}{V_b}} \quad V_b = A_b L_b - \frac{\pi L_b (d_3 + 2x_t)^2}{4}$$

and

TL= transmission loss	a_o = acoustic velocity
A_b = box area	K_h = conductivity of the holes
A_3 = pipe area	L_b = length of box
f_{sr} = frequency of side resonant system	
V_b = box volume	L_2 = re-entrant length of pipe 2
x_t = pipe thickness	A_h = area of holes
N_h = number of holes	d_3 = inner diameter of pipe

Figure 9.2 shows the significant dimension of a side-resonant silencer element.

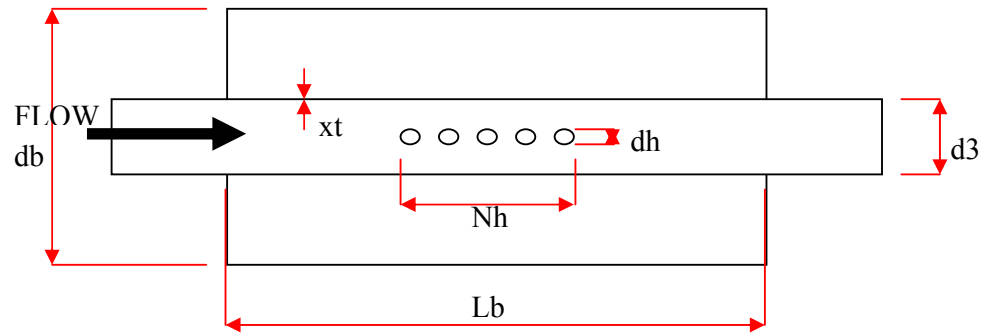


Figure 9.2 Significant dimension of a side resonant silencer element

The last type of silencer element, the absorption silencer, is similar to the side-resonant silencer (geometrically) except that the total cross sectional area occupied by the holes is more than five times the pipe area whereas in side-resonant silencer the total cross sectional area compared to the pipe area is less than unity (8). Absorption silencer is packed with sound absorbing material, usually a glass-reinforced fiber material or mineral wool. The transmission loss of the silencer depends on the absorption coefficient, which depends on the frequency, angle of incident, material porosity, density and thickness (7).

Transmission loss of the absorption silencer as given by Sabine (8) is:

$$TL = 12.6 \frac{P}{A_d} \alpha^{1.4} \text{ dB/ft} \quad (9.4)$$

where P = perimeter (in)

A_d = cross-sectional area (in^2)

α = absorption coefficient

Figure 9.3 shows the significant dimension of an absorption silencer element.

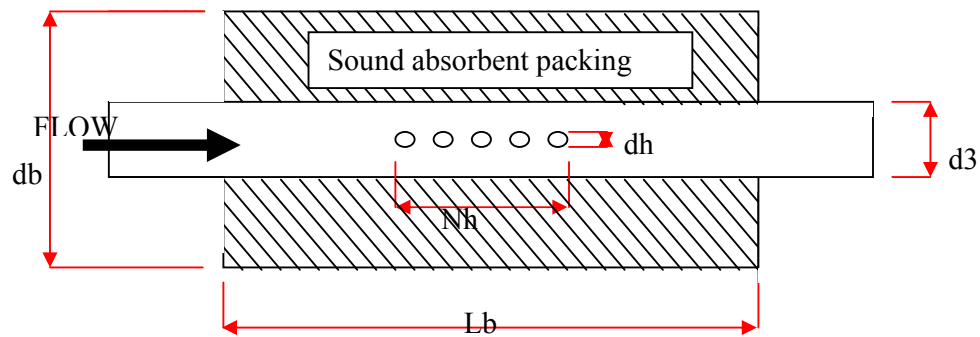


Figure 9.3 Significant dimension of an absorption silencer element

On real life case, one silencer system is made of combination of several chambers consist of these three basic silencer elements to obtain better noise suppression characteristic.

9.1.4 Study on the Existing Silencer (Suzuki TXR Gamma 150cc)

A two-stroke exhaust system consists of four main parts; header pipe, expansion chamber, silencer and stinger. The layout of the exhaust system and the function of each part are shown in Figure 9.4 and Table 9.1.

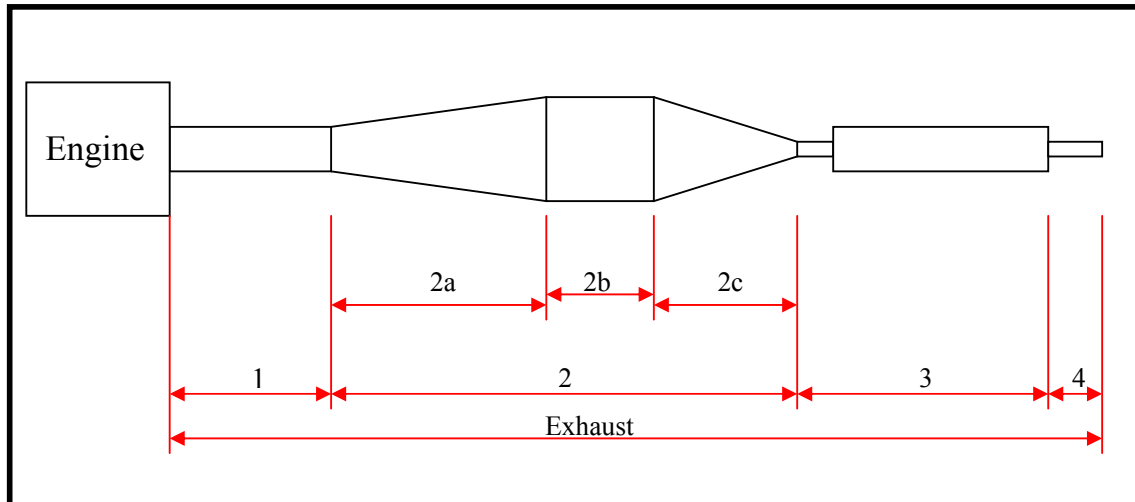


Figure 9.4: Layout of the exhaust system

Table 9.1: Function of each component of exhaust system

No.	Part name	Function
1	Header pipe	Tuned power at desired rpm
2	Expansion chamber	Tune the engine performance
	(a) Divergent cone	Produce negative wave that help sucks the exhaust gas out of the cylinder and place fresh mixture into the combustion chamber
	(b) Convergent cone	Produce positive wave that will stuff the charge (fresh mixture) that was suck into exhaust pipe back to the cylinder
	(c) Neutral chamber	Timing the action between convergent cone and divergent cone
3	Silencer	Suppress exhaust noise, tune engine performance
4	Stinger	Control the amount of back pressure, tune peak power

In this study, the expansion chamber was not considered as the tuning of the engine is done by the fuel injection of the new engine. Silencer itself consists of several chambers to enhance its noise suppression characteristic. Figure 9.5 is the cross sectional view of the silencer.

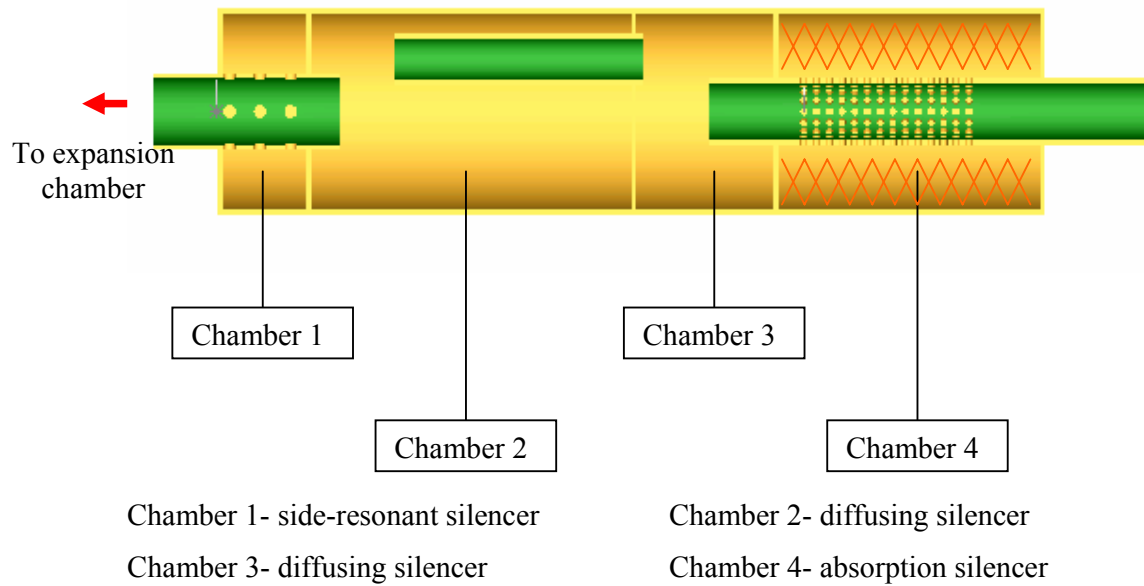


Figure 9.5: The cross sectional view of the silencer.

9.1.4 Transmission loss behavior of silencers

a. Side resonant silencer

The fundamental behavior of this type of silencer is to absorb a relatively narrow band of sound frequency by the resonance of side cavity at its natural frequency (8). Equation (9.1) was used to determine and plotted the transmission loss for the side resonant silencer as illustrated in Figure 9.6. The parameters input to the equation are as follow:

γ = ratio of specific heat

R = gas constant (J/kgK)

T_o = exhaust gas temperature (K)

A_b = box area

A_2 = area of pipe 2

A_{r2} = expansion ratio

L_b = length of box

L_t = length of pipe 2

L_1 = re-entrant length of pipe 1

L_2 = re-entrant length of pipe 2

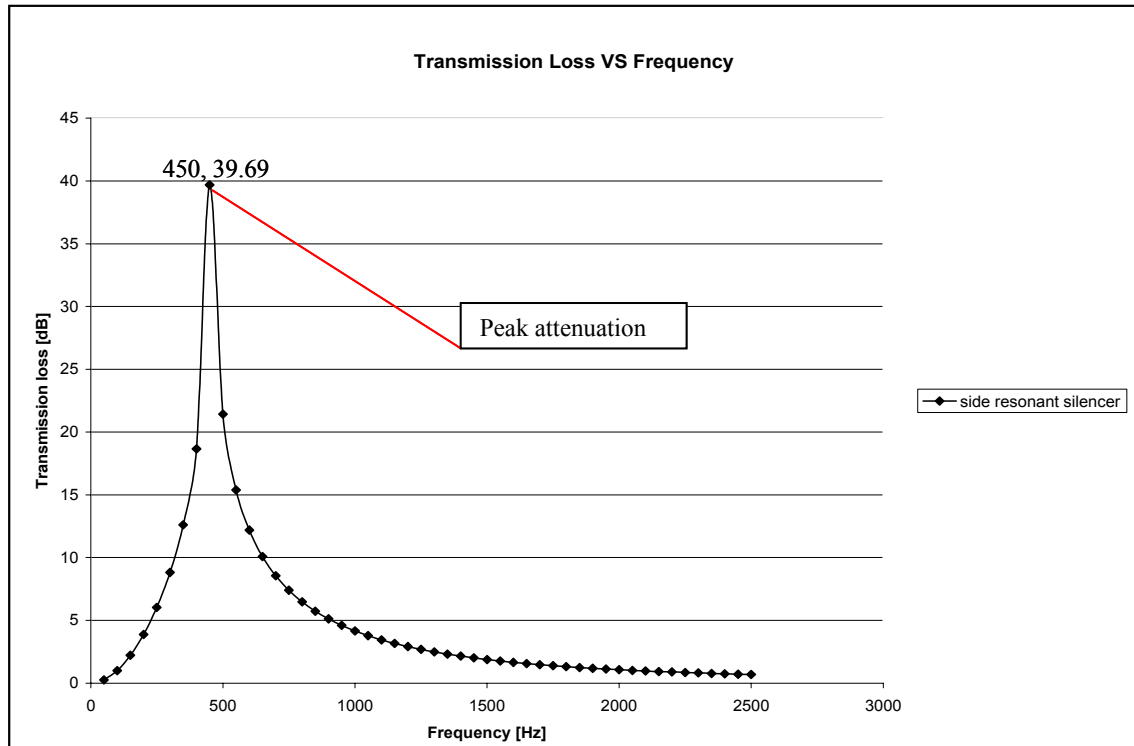


Figure 9.6: Transmission loss versus frequency for side resonant silencer.

It is observed that high transmission loss occurred at discrete frequency of about 450Hz. Such discrete frequency can be varied by varying the physical dimension of the silencer.

b. Diffusing silencer

This type of silencer absorbs fundamental frequency except at the resonant frequencies of the box (6). These frequencies are known as “pass band” frequencies and the transmission loss at these frequencies are zero as shown in Figure 9.7.

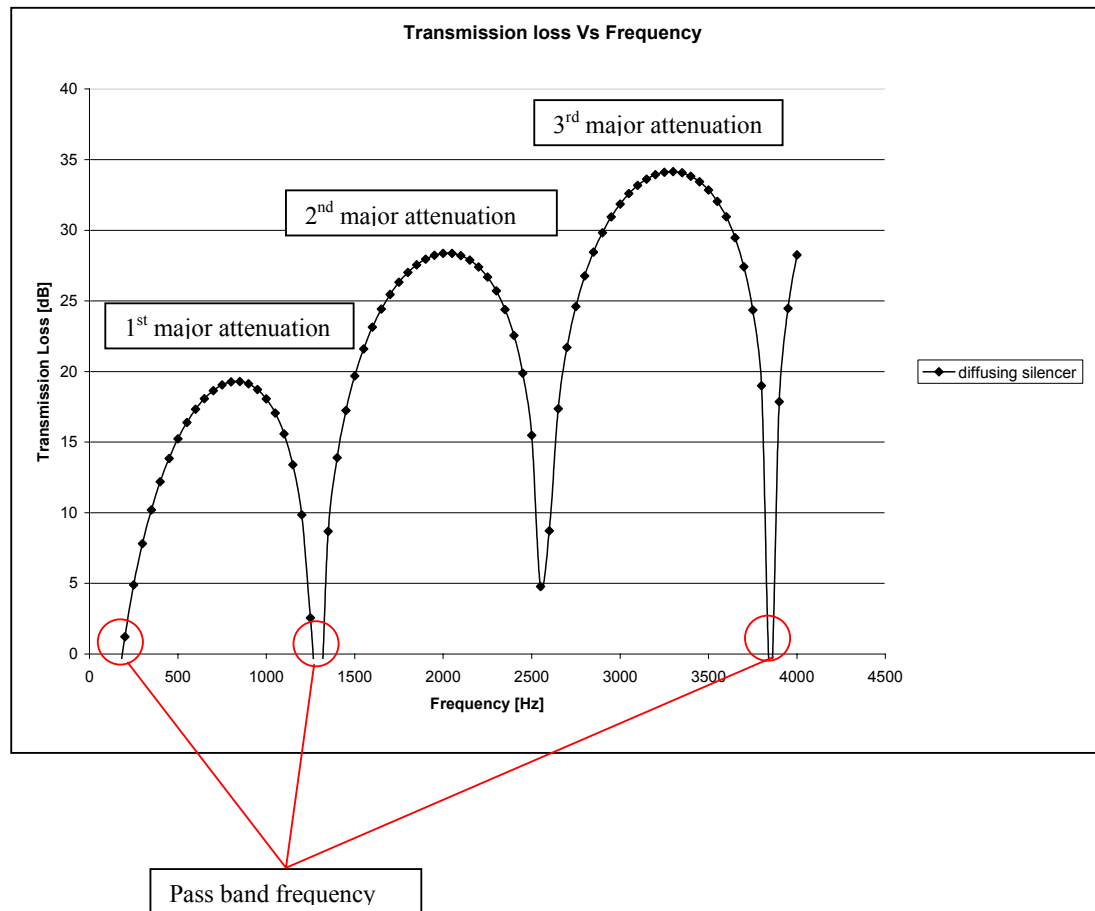


Figure 9.7: Transmission loss versus frequency for diffusing silencer.

c. Absorption silencer

This type of silencer absorbs noise at all frequency range, most effectively at high frequency (5) as illustrated in Figure 9.8

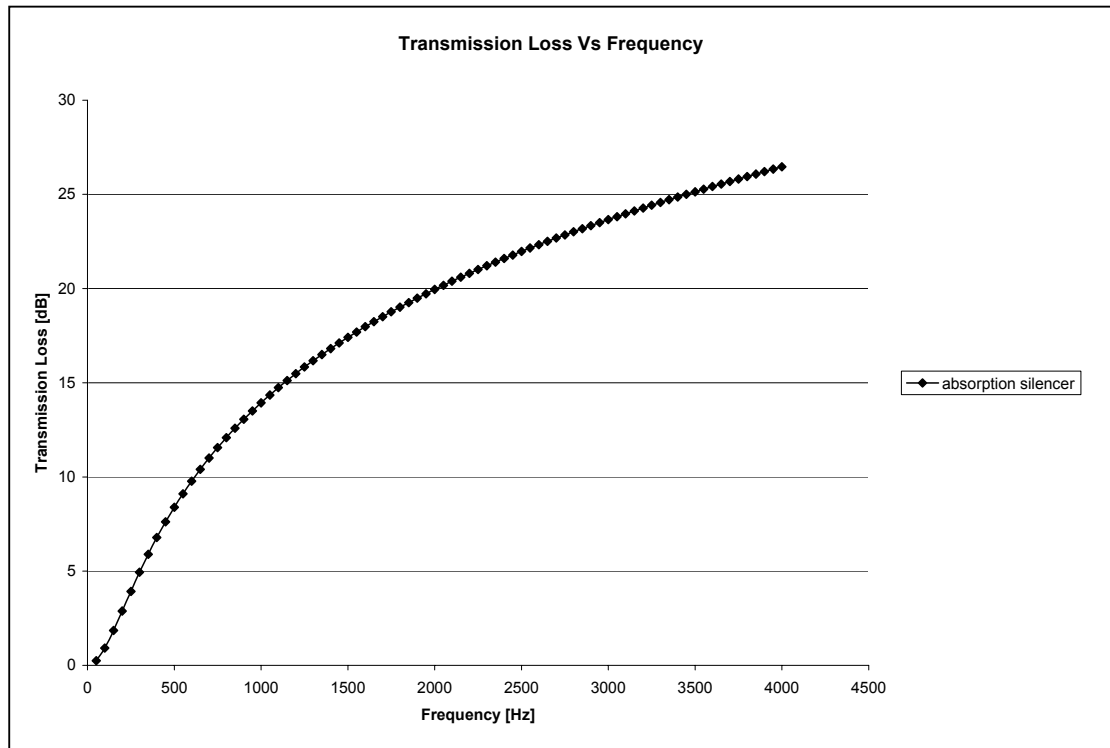


Figure 9.8: Transmission loss versus frequency for absorption silencer.

d. Multiple chambers silencer element and transmission loss

As described above, each silencer element has their disadvantages. To improve the silencing effect, the basic silencer element need to be combined together to produce a system that can silence any desired range of noise. Below is an example of a silencer system consists of three basic silencer elements and their noise attenuation (transmission loss) characteristics.

The first chamber is designed so that it will suppress noise at the desired frequency range, usually the first fundamental noise from the engine. The other range of noise can be reduced by using diffusing silencer (as a second chamber) because of its broadband attenuation characteristic, except at its pass band frequency. The pass band frequency has to be covered with another silencer element to suppress the noise. In this case, the pass band noise is suppressed by fitting another side-resonant silencer (side-resonant #2) which had peak attenuation in the region of the pass band frequency of the second silencer element. Then, the fourth silencer element is added to absorb the remaining noise.

The result of the simulation is shown in Figure 9.10. The exhaust gas that passes through the expansion chamber brings along noise from the combustion, from flow itself and from collision with the wall (expansion chamber, pipe etc). As the noise passes through the side-resonant silencer #1, low frequency noise will be suppressed, then the noise is further suppressed when it enters the second chamber (diffusing silencer), but since the pass band frequency occurs at 2450-2700 Hz, the noise at these frequencies will be transmitted to the third chamber. Due to this reason the third chamber is designed exactly to suppress the pass band noise from second chamber (i.e.; the combination between physical properties of the silencer is arranged so that the resonance of side cavity occurs at the pass band frequency of the second chamber element). Lastly, the fourth chamber (absorption silencer) will absorb the remaining noise before the exhaust gas passes through to the atmosphere. Figure 9.9 shows the layout of multiple chambers silencer element and Figure 9.10 shows the transmission loss of multiple chambers silencer element.

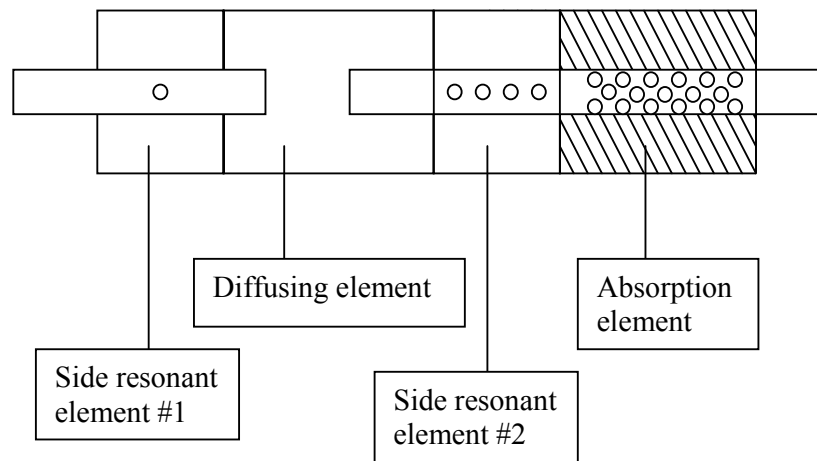


Figure 9.9: The layout of multiple chambers silencer element.

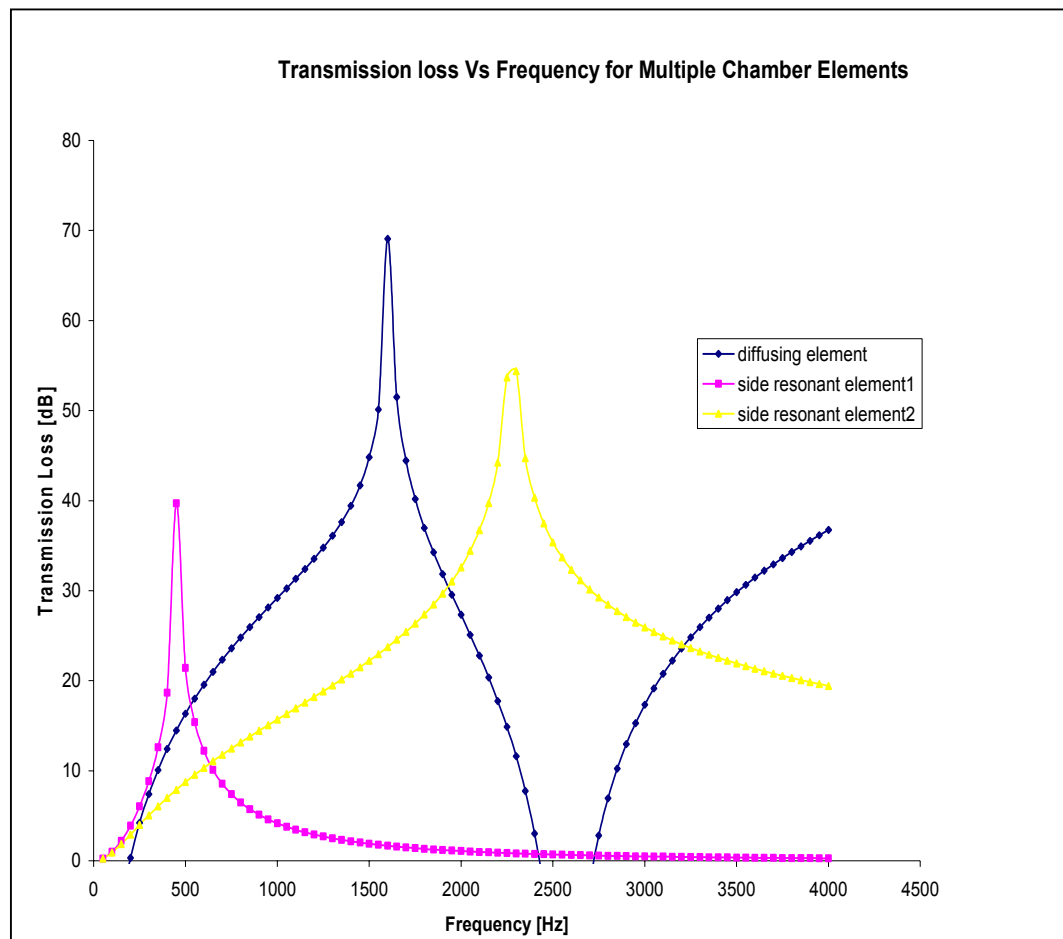


Figure 9.10: Transmission loss versus frequency for multiple chambers silencer element.

e. Simulation Process

The simulation process in designing the muffler used GT Power software from GT-Suite Version 5.2. Figure 9.11 shows the process of simulation.

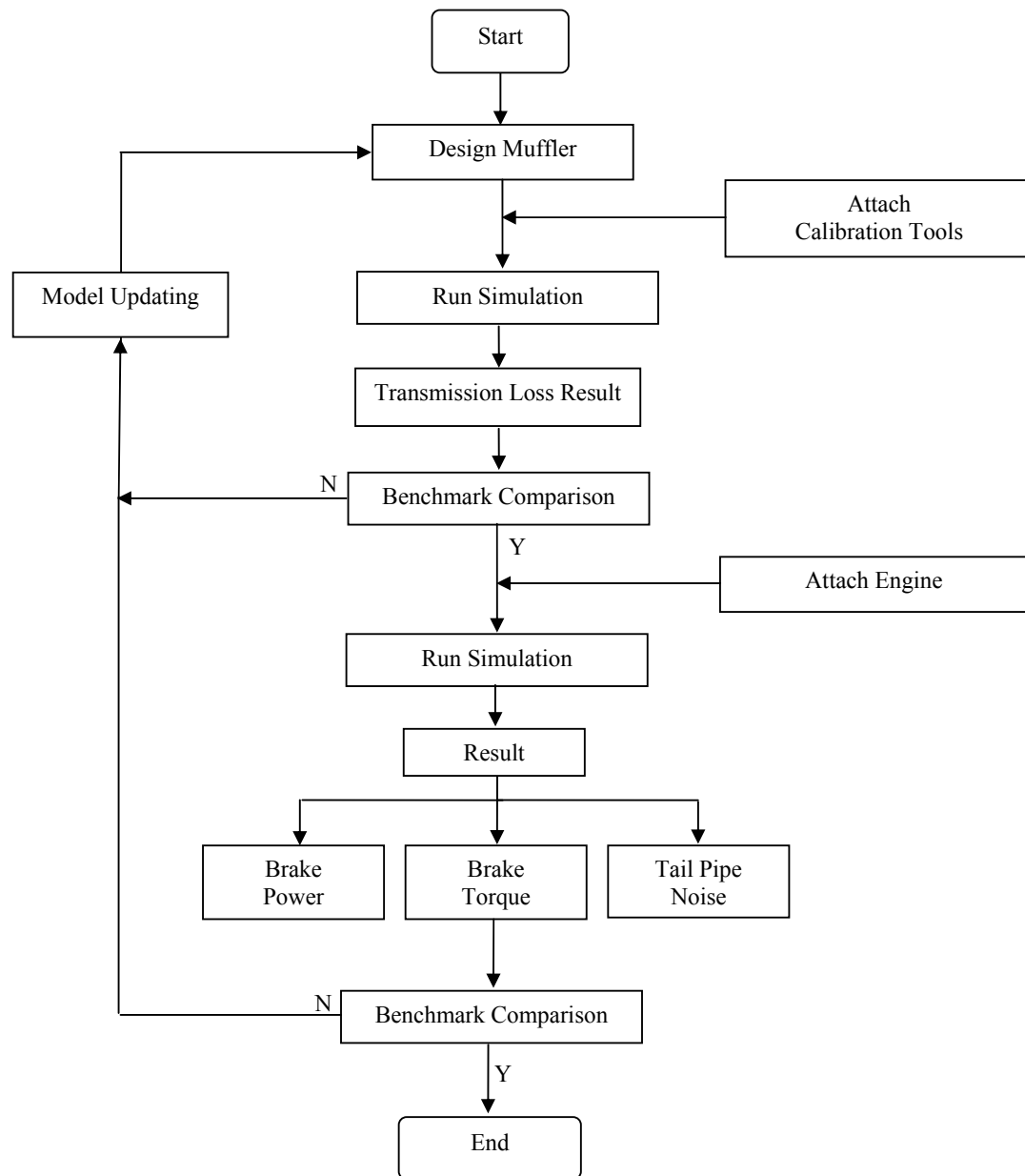


Figure 9.11: Motion of Simulation Process flowcharts.

9.1.5 New Muffler Design

The following is the procedure used to design a new muffler for the engine. Single cylinder exhaust consist of two part, first; exhaust pipe for tuning and second; muffler for noise suppression. Several mufflers were fitted onto the engine and were analyzed using GT Power software. Three parameter that are engine power, engine torque and noise reduction level was used to measure the muffler performance. Tuning part was neglected since the engine uses injector which performs the tuning process on the engine.

The Suzuki Gamma's performances were used as a benchmark. The muffler was coupled with the test engine and then the parameter such as the effect of the muffler to transmission loss, power curve, torque curve and noise at tail pipe was taken into consideration to select the best design. Figure 9.12 below shows the configuration of the benchmark muffler.

The configuration and specification of the engine were input to the GT Power software and then the muffler design configuration in then connected to the engine. Thus the muffler design is customized to the actual design having required power and torque.

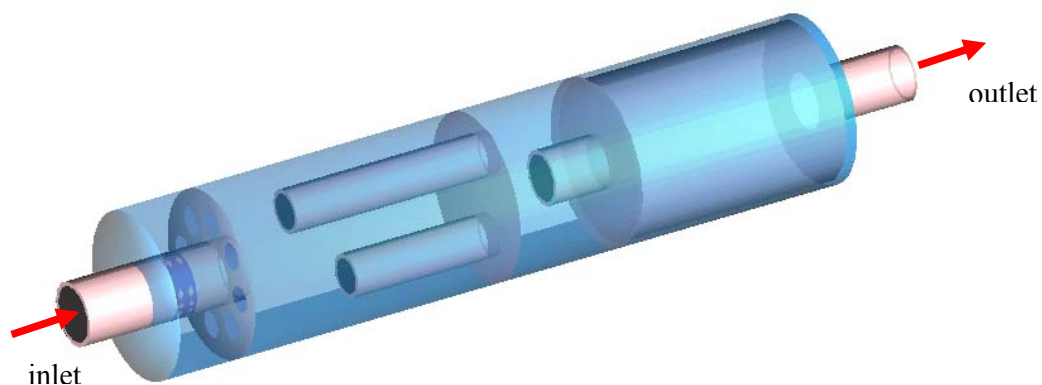


Figure 9.12: Benchmark muffler.

This silencer is cylinder in shape and thus the length is long compare to the engine size. Due to this reason, a shorter silencer must be designed to replace this silencer to suit to the architecture of the engine. So a shorter silencer is designed where the length is 200mm and the diameter is 100mm. The muffler consists of four chambers, which are the combination of diffusing, side resonant and absorption silencer element. The proposed new silencer named Muffler 1 is shown in Figure 9.13.

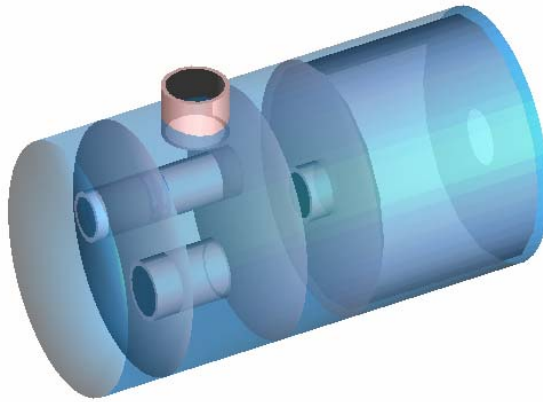


Figure 9.13: Muffler 1

The initial design for the new muffler with volume 10 times to the engine swept volume (almost the same as Gamma's volume) was proposed. This muffler has inlet pipe at the side of the muffler to suit to the engine arrangement. The position of the muffler to the engine is shown in Figure 9.14.

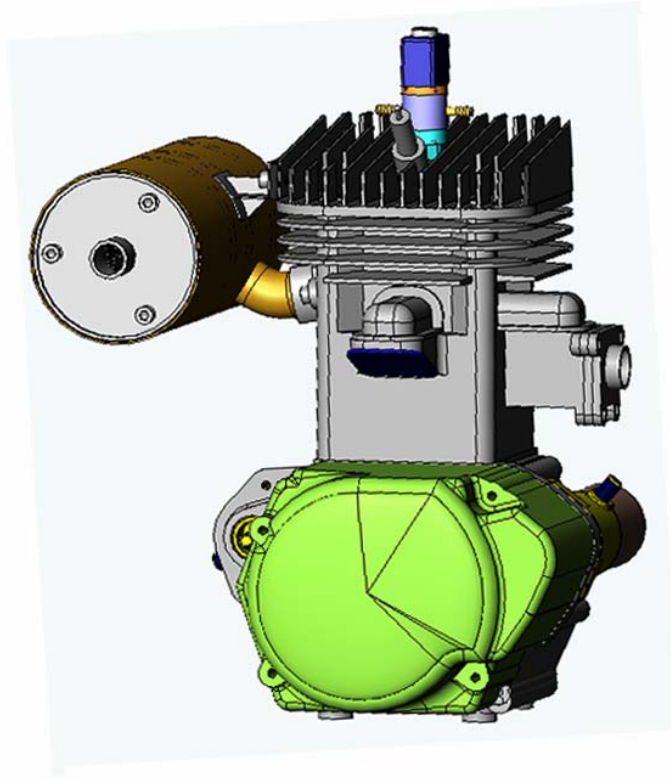
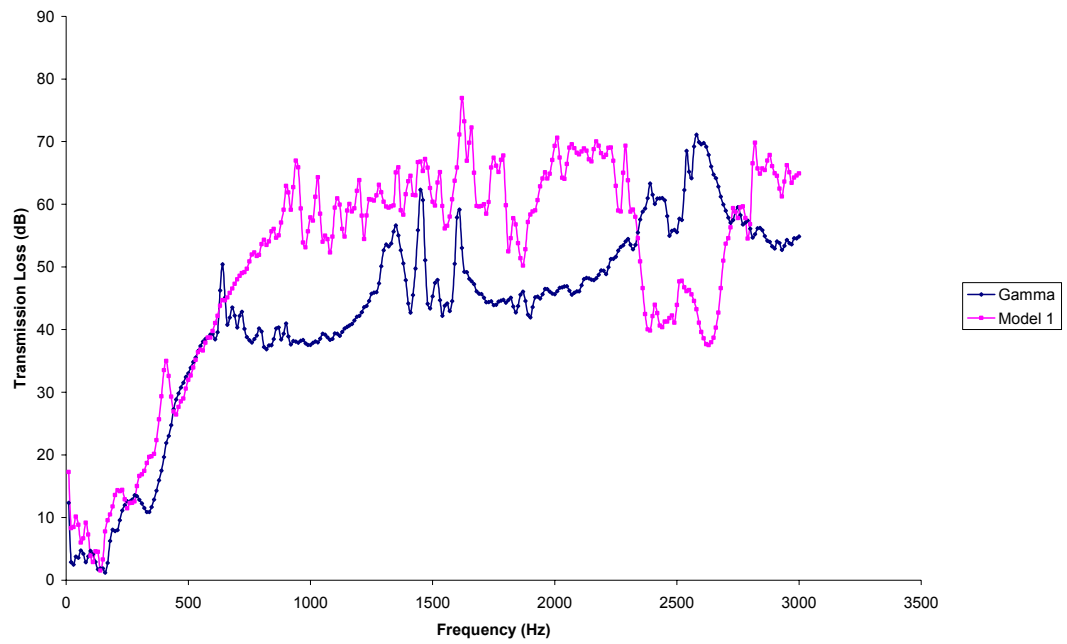


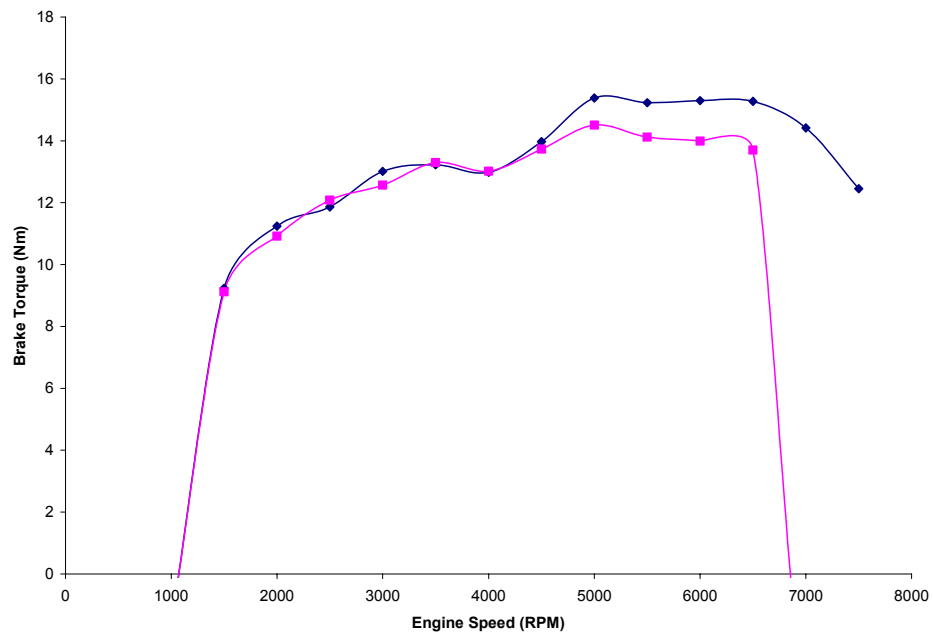
Figure 9.14: Position of the muffler to the engine.

Simulation result of the transmission loss, brake torque, brake power and tail pipe noise for muffler 1 compared to gamma muffler is shown in Figure 9.15. It indicates maximum transmission loss increase of about 30 dB for the new muffler which is large. Overall, there is a big improvement in the new design as compared to the existing Gamma muffler. This is expected as the new design is based on the new engine. With the improvement of transmission loss, the brake torque and brake power and tail pipe noise are almost the same until 6000Hz.

(a) Transmission Loss vs Frequency



(b) Brake Torque vs Engine Speed



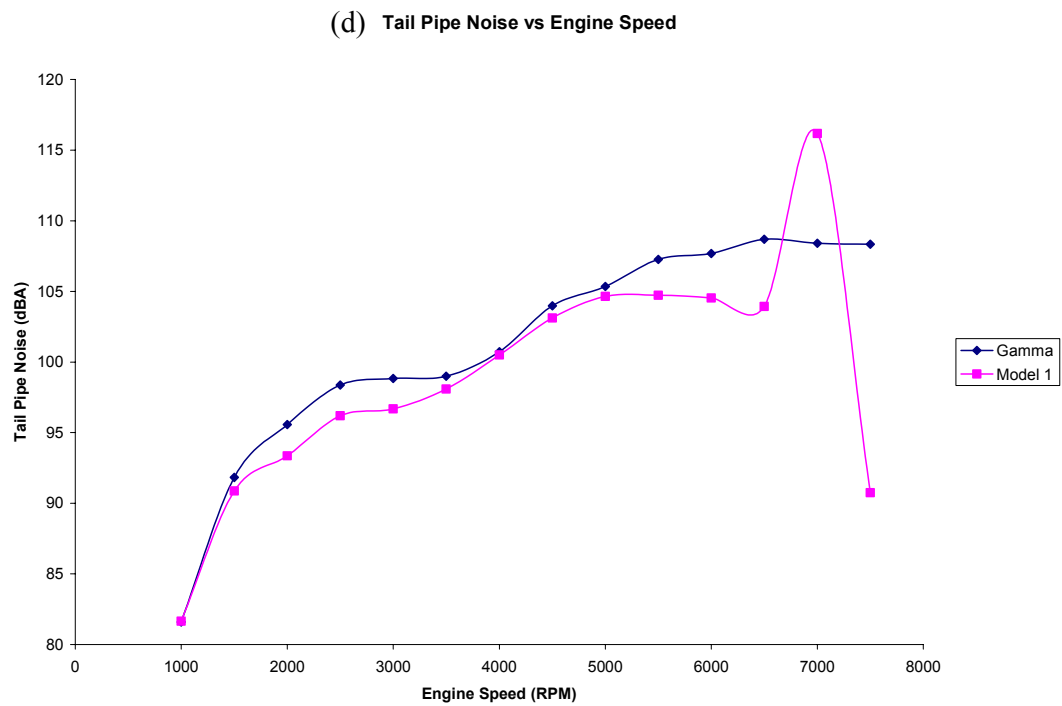
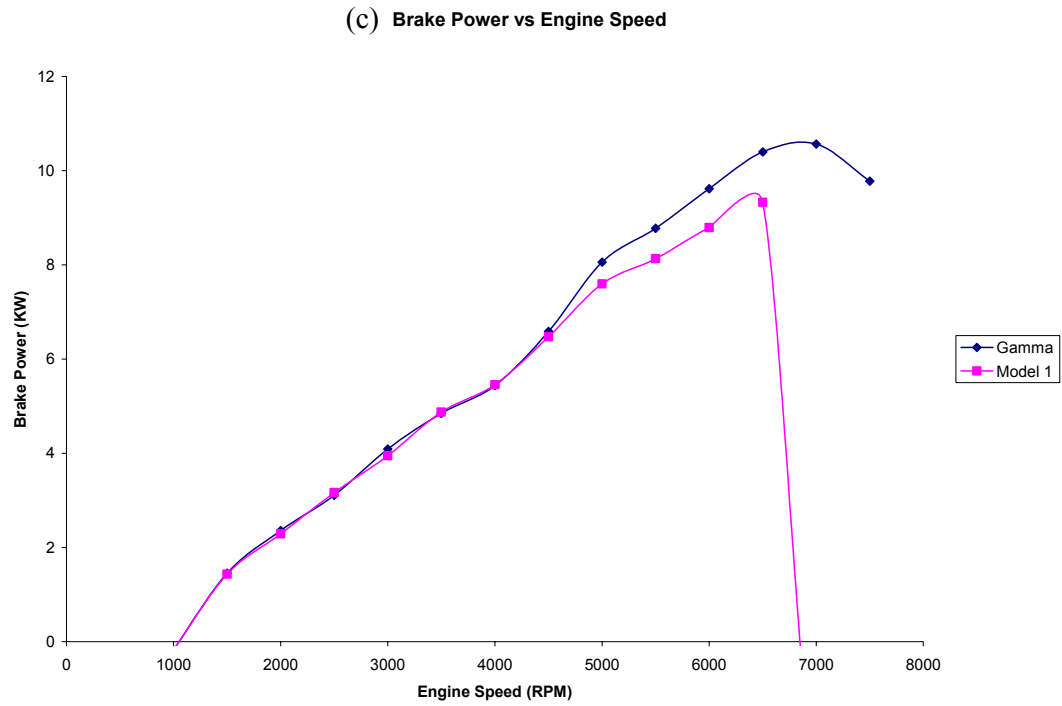


Figure 9.15: Result between Muffler 1 and Gamma muffler.

Several modifications have been done to the Muffler 1 to increase the brake power and brake torque and to obtain better noise reduction. The description on each modification of each model is described in Table 9.2. Description is done by referring to the Muffler 1 layout in Figure 9.16.

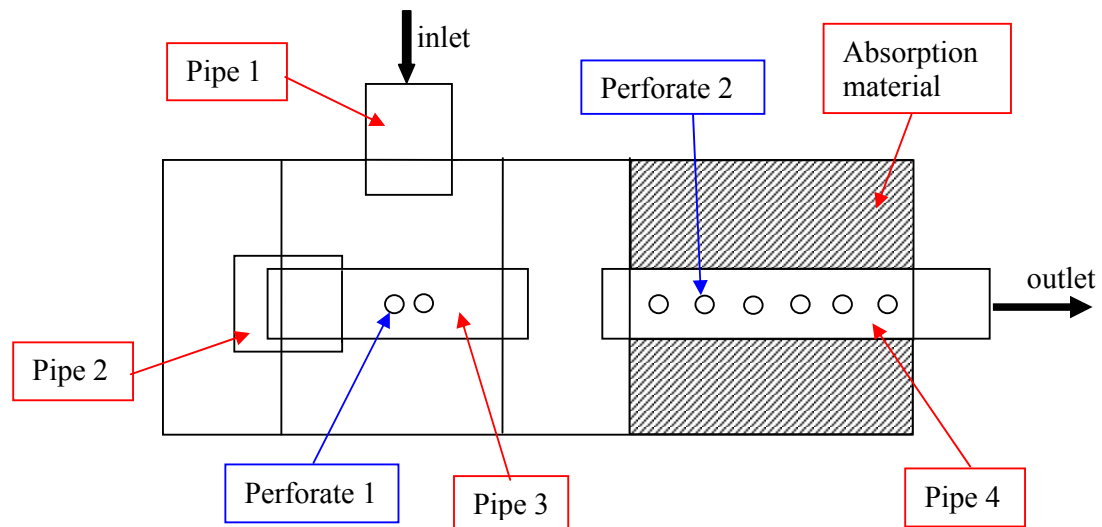


Figure 9.16: Muffler 1 layout

Specification :

Pipe 1: diameter = 25mm, length = 20mm

Pipe 2: diameter = 20mm, length = 35mm

Pipe 3: diameter = 16mm, length = 70mm

Pipe 4: diameter = 18mm, length = 100mm

Perforate 1: diameter = 3mm, quantity = 10 holes

Perforate 2: diameter = 3mm, quantity = 200 holes

Table 9.2: Description on the modification of muffler 1

Model	Description (compared to muffler 1)
Model A	Pipe 1 are longer (25mm) Pipe 4 are longer (110mm) Numbers of perforate 1 are increased to 30 holes.
Model B	Pipe 1 are longer (30mm) Numbers of perforate 1 are increased to 30 holes.
Model C	Diameter of pipe 2 are smaller (18mm) Pipe 4 are longer (120mm)
Model D	Pipe 4 are longer (110mm) Numbers of perforate 1 are increased to 30 holes.
Model E	Diameter of pipe 2 are smaller (16mm) Numbers of perforate 1 are increased to 30 holes. Pipe 4 are longer (120mm)
Model F	Pipe 3 are longer (80mm) Diameter of perforate 1 is 2mm and the numbers are same.
Model G	Diameter of pipe 2 are larger (25mm) Diameter of perforate 1 is 2mm and the numbers are same.
Model H	Diameter of pipe 2 are smaller (16mm) Diameter of perforate 1 is 2mm and the numbers are same.
Model I	Pipe 1 are longer (30mm) Diameter of pipe 2 are smaller (16mm)

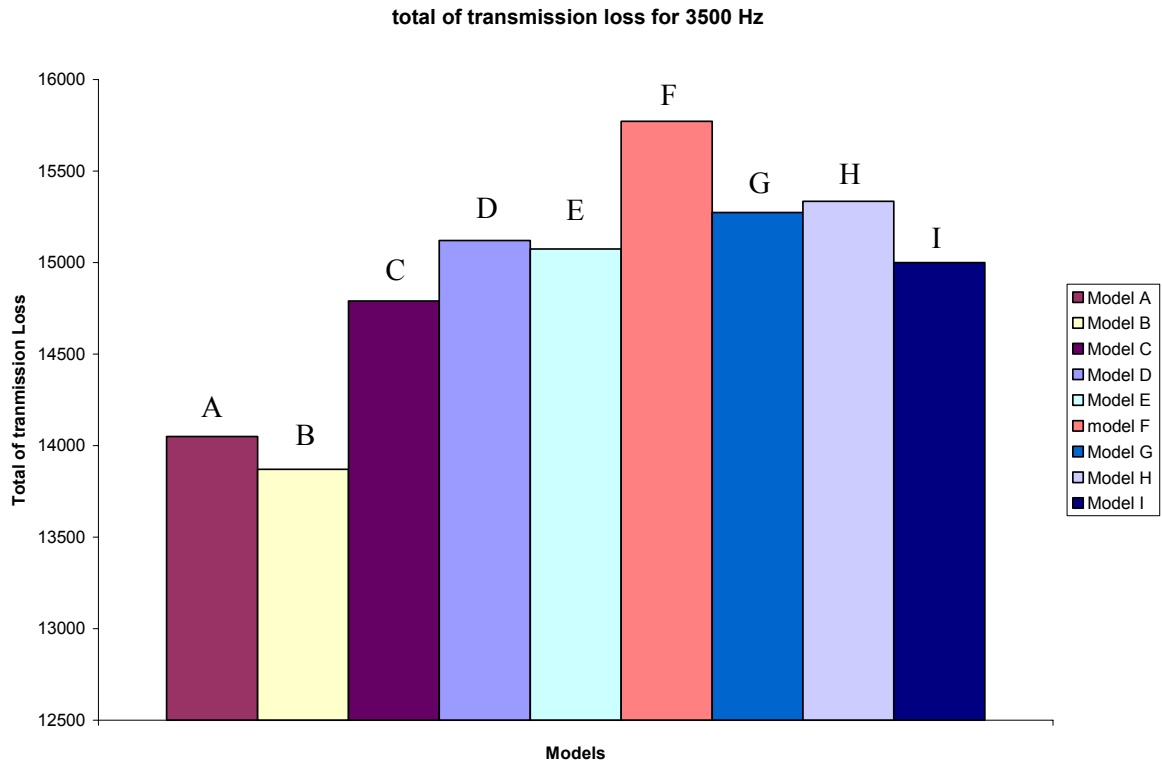


Figure 9.17: Total of transmission loss (Pa Hz) for frequency of 0 to 3500 Hz.

Figure 9.17 shows the total transmission loss coverage from 0 Hz to 3500 Hz for all the models. From this chart, several models have low total transmission loss and others are higher compare to the benchmark muffler. Lower transmission loss can cause the tail pipe noise to increase but higher transmission loss will affect the brake torque and brake power. Thus, only four models are selected for the next step. The models are model E, F, G, and H. These models were coupled to the engine to obtain the power and torque curves as shown in Figure 9.18 and 9.19.

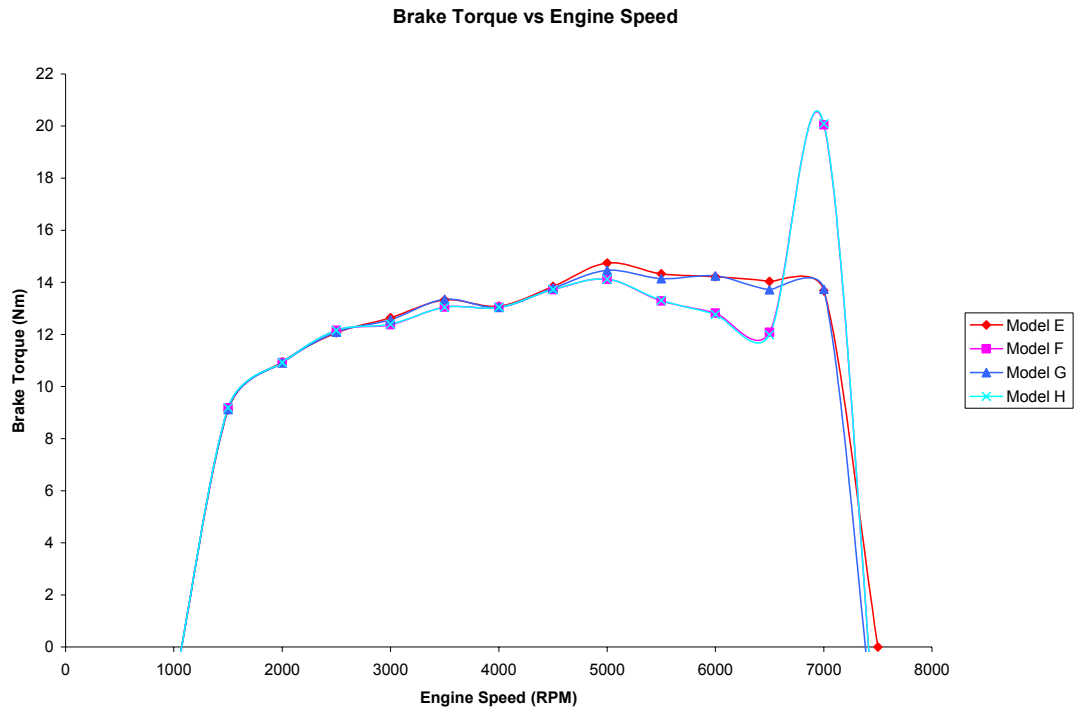


Figure 9.18: Comparison of torque curve for model E, F, G and H.

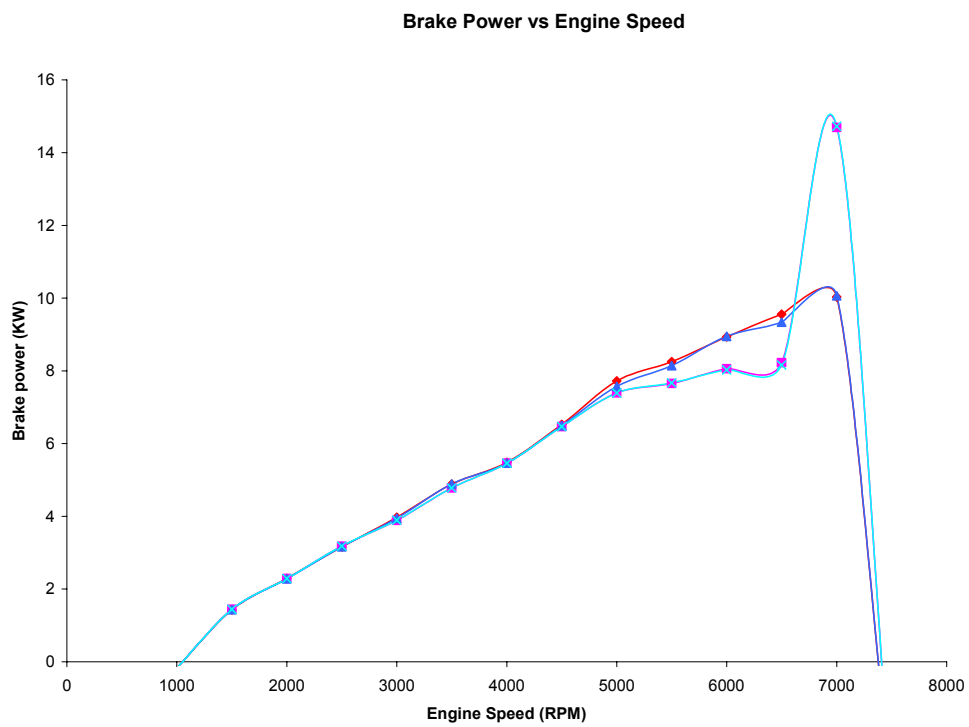


Figure 9.19: Comparison of power curve for model E, F, G and H.

From these four models, only two models are selected and these are model E and G which produced almost the same torque and power curves. The torque and power for model F and model H drop at around 6000 RPM. The final two models are compared to the Gamma muffler as illustrated in Figure 9.20 to 9.22. Comparison was made based on three parameters that are power, torque and tail pipe noise.

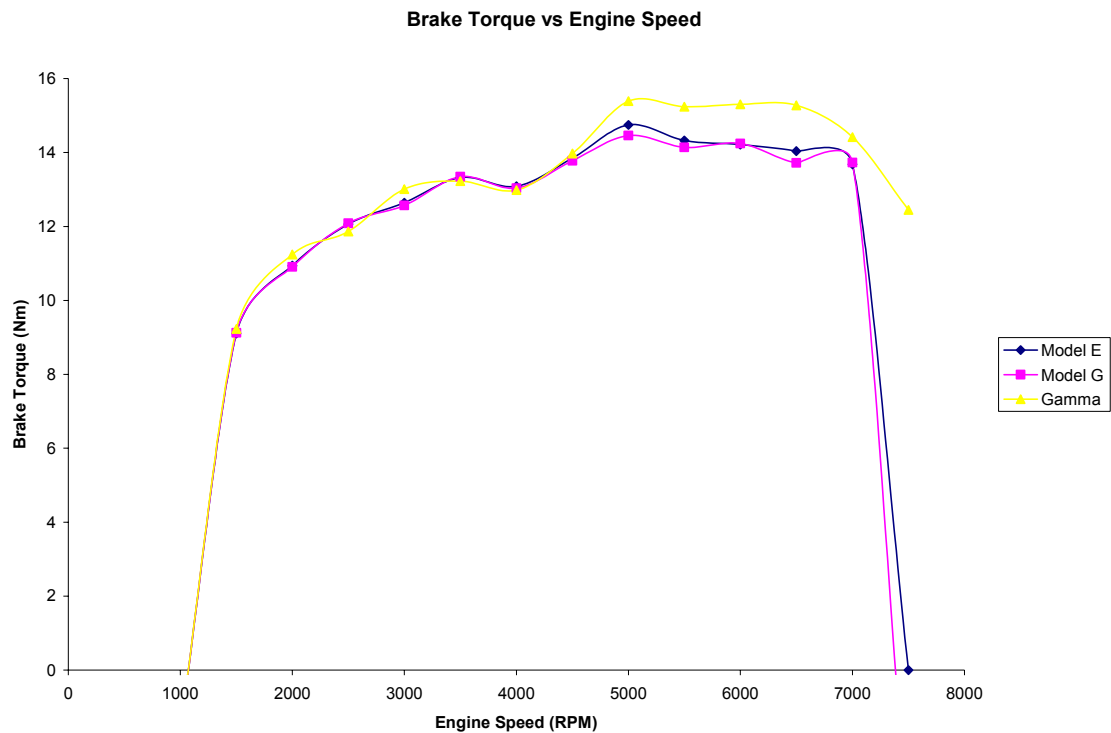


Figure 9.20: Comparison of torque curve for Gamma's muffler, model E and G.

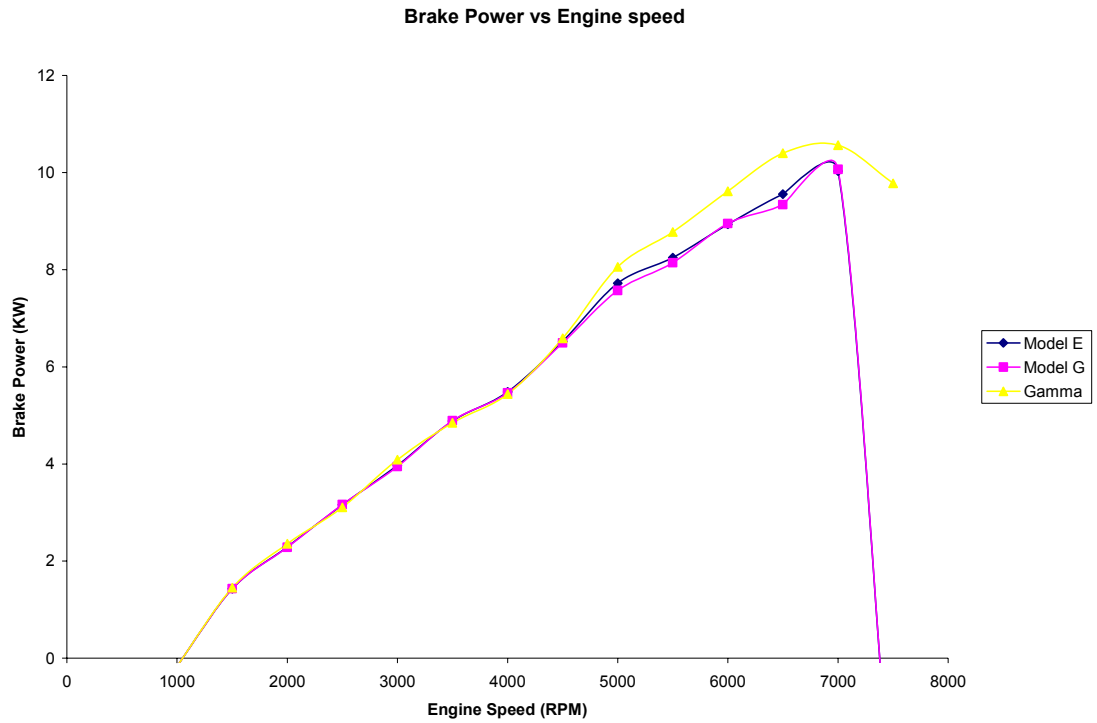


Figure 9.21: Comparison of power curve for Gamma's muffler, model E, and G.

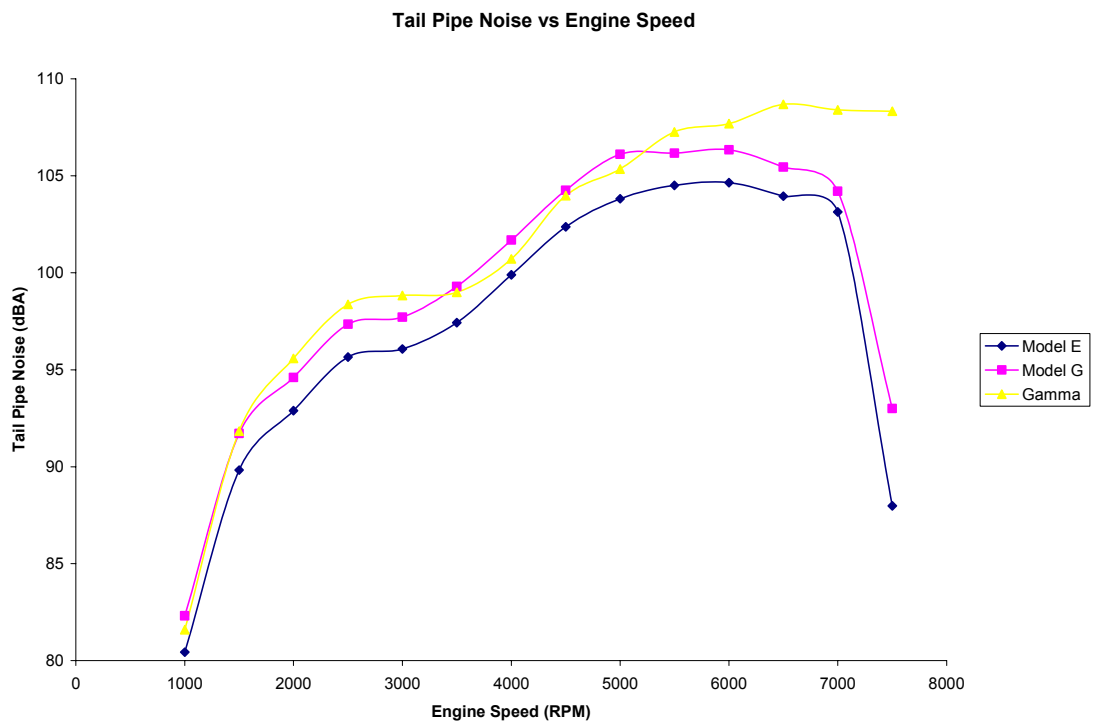


Figure 9.22: Comparison of tail pipe noise for Gamma's muffler, model E, and G.

Based on Figure 9.20 to 9.22, it is observed that the power and torque curve for the Model E and G are almost the same but lower than the Gamma's muffler. For the tail pipe noise, a big difference was noticed. Model E has better (lower) tail pipe noise than model G and gamma's muffler. Due to that, model E was chosen as a final muffler design. The maximum brake torque is 14.7 Nm at 5500 RPM and brake power is 9.5 KW at 6500 RPM. The selected muffler design is shown in Figure 8.12. Dimension for this muffler is shown in the Appendix.

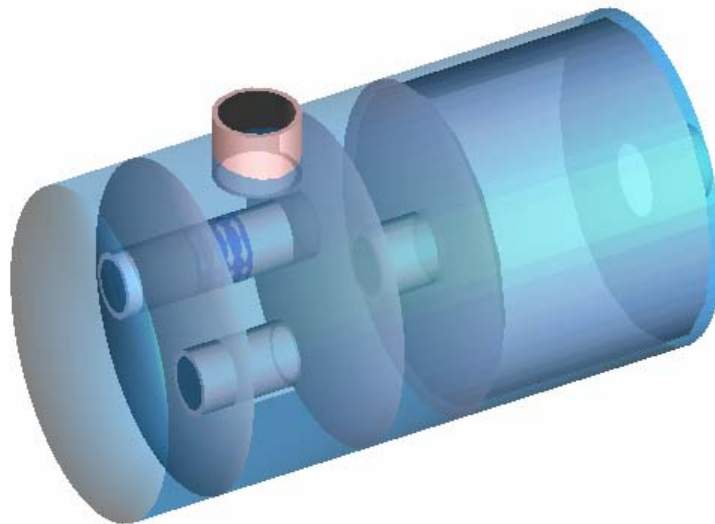


Figure 9.23: The selected muffler.

9.1.6 Flow Analysis

Flow analysis was carried out on Muffler E by using common computational fluid dynamics programs, the COSMOSFloWorks. An engine speeds was simulated to obtain the gas flow through the muffler. The results for this simulation is shown in Figure 9.24 to 9.27.

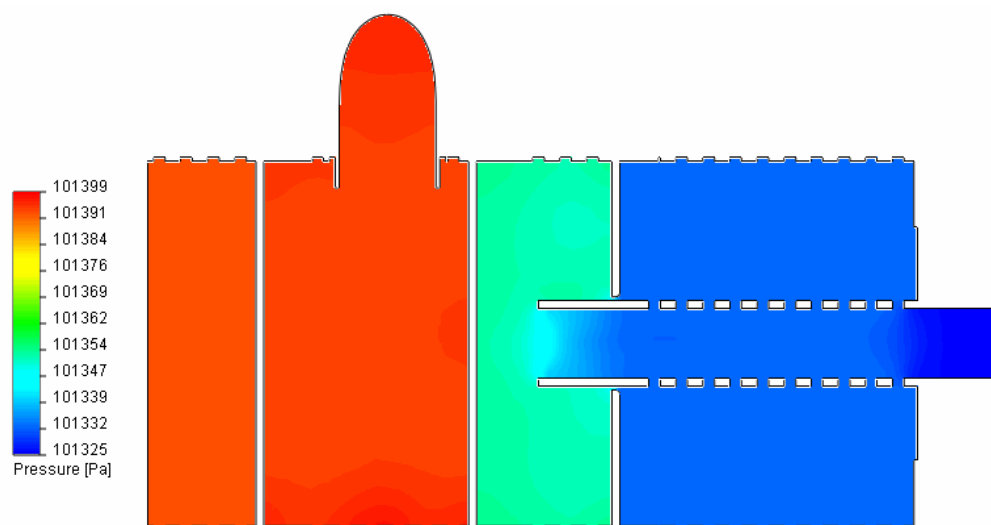


Figure 9.24: Pressure through the muffler at 1000 RPM from top view.

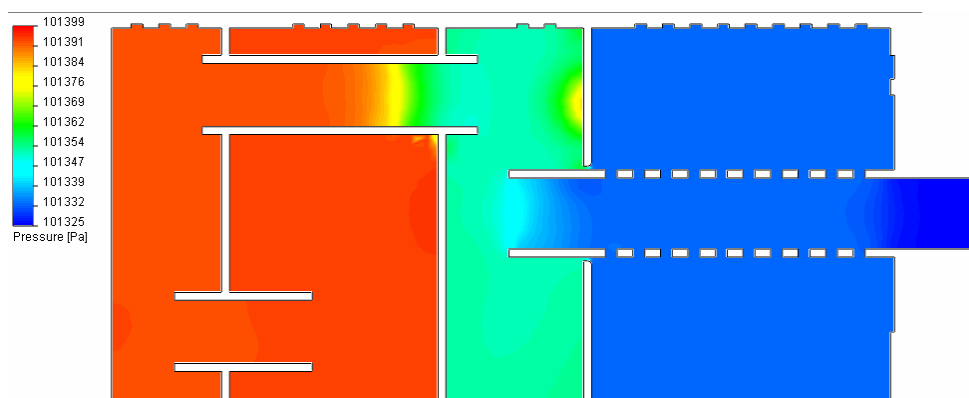


Figure 9.25: Pressure through the muffler at 1000 RPM from side view.

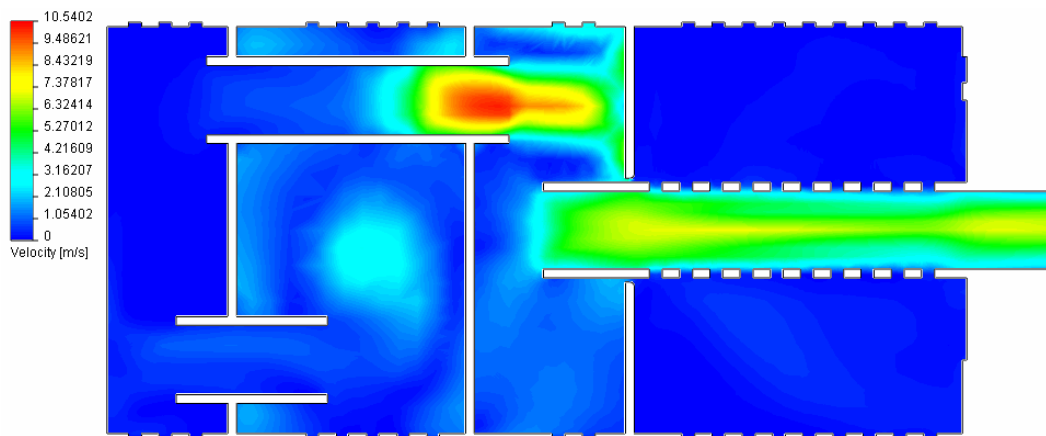


Figure 9.26: Velocity through the muffler at 1000 RPM from side view.

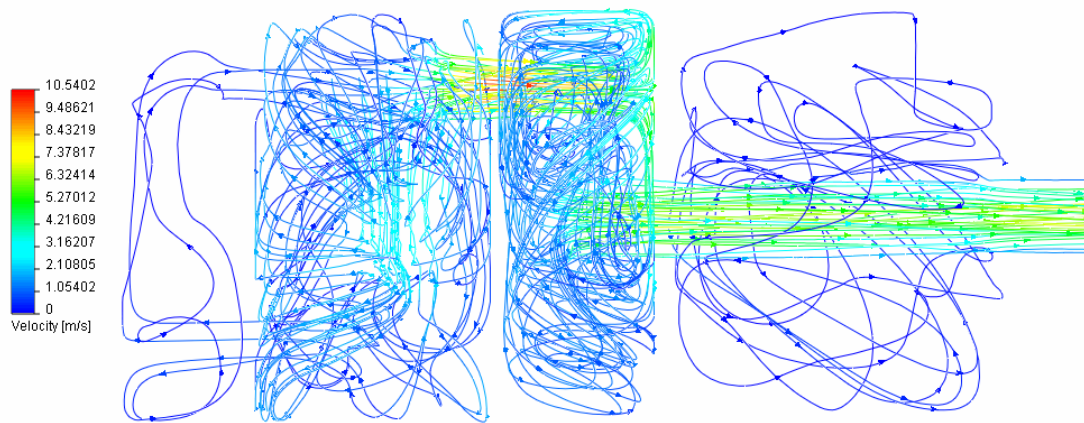


Figure 9.27: Stream line Velocity through the muffler at 1000 RPM from side view.

From this simulation study, the pressure and velocity of the muffler was observed to be stable. There was a smooth flow of gas and no back pressure is observed. Thus, this muffler design was found to be satisfactory and it was decided to fabricate and install to the new engine.

9.1.8 Conclusion

A customized new muffler design was successfully developed for the new two-stroke engine. The size of the muffler was controlled to suit to the architecture of the engine without lacking on the engine power, torque and transmission loss.

9.1.9 References

1. Mikiya Hosomi, Sumio Ogawao, Toshiyuki Imagawa, Yuichi Hokazono, *Development of Exhaust Manifold Muffler*, Toyota Motor Corp. et.al, SAE 930625.
2. A. Selamet and P.M. Radavich, *The effect of Length on the Acoustic Attenuation performance of Concentric Expansion Chambers: An Analytical, Computational, and Experimental Investigation*. The University of Michigan, SAE 950544.
3. Jau Huai Lu and Hsiu-Feng Yang, *Measurements and Analysis of the Exhaust Noise of Single Cylinder Two Stroke Engines*, National Chung-Hsing University, SAE 960369.
4. C.Y.R. Cheng and T.W. Wu, *Exhaust Muffler Design and Analysis Using A Boundary Element Method Based Computer Program*, Nelson Industries, Inc. SAE 1999-01-1661.
5. Jesus Blanco and Andrew Earnshaw, *Study of the Noise Characteristics of Motorcycle Silencers*, Advanced Analysis Ltd. and Triumph Designs Ltd, SAE 2001-01-1209.
6. A.J. Torregrosa, J. Galindo, R. Payri and Hcliment, *Modeling the Exhaust System in Two Stroke Small Engine*, CMT. Universidad politecnica de Valencia, SAE 2001-01-3317.
7. Larry J. Eriksson, *Noise Control in Internal Combustion Engines*, John Wiley & Sons, USA, 1982, Chap 5 (silencer)

8. Gordon P.Blair, *Design and Simulation of Two Stroke Engines*, Society of Automotive Engineers Inc, Warrandale, 1996, Chap.8 (reduction of noise emission from two stroke engine)
9. R. Singh and T. Katra, Journal of Sound and Vibration (1978) 56(2), *Development of an Impulse Technique for Measurement of Muffler Characteristic.*

9.2 Multi Cylinder Exhaust System

The objective of this study is to achieve high performance, low noise and low emission for a multi cylinder 2-stroke gasoline engine. Full study on this type of exhaust system has been carried out by Mohd Hafizi in his first degree project thesis (1).

9.2.1 Background of the engine

This study uses a newly developed two-stroke, four cylinder, V engine. This engine uses direct injection system and unique piston called compound piston which make it difference from the existing two-stroke engine. The system mention above assures better air-fuel ratio and scavenging process to improve combustion characteristic, hence increase power output and reduce the exhaust emission compared to the existing one. The engine is required to be equipped with exhaust system to gather more power out of it and further reduced the noise radiated. This engine must be equipped with a complete exhaust system (piping system, catalytic converter and muffler) and properly tuned to achieve the stated objective.

9.2.2 Design characteristics

Several restrictions were identified in this design, which are:

- a. compact exhaust
- b. appropriate tuning technique
- c. catalytic converter selection
- d. adequate silencing

a. Suggested exhaust system

Due to the restriction on the exhaust length, exhaust pipe will be made as short as possible without deteriorating the engine performance. Figure 9.28 shows the suggested exhaust system for the multi cylinder engine, which use a 4-2-1 piping system. Exhaust port from cylinder 1 are connected to port 2 while port 3 to port 4 using a single pipe and both of these pipes are jointed together before entering the catalytic converter and then to the muffler.

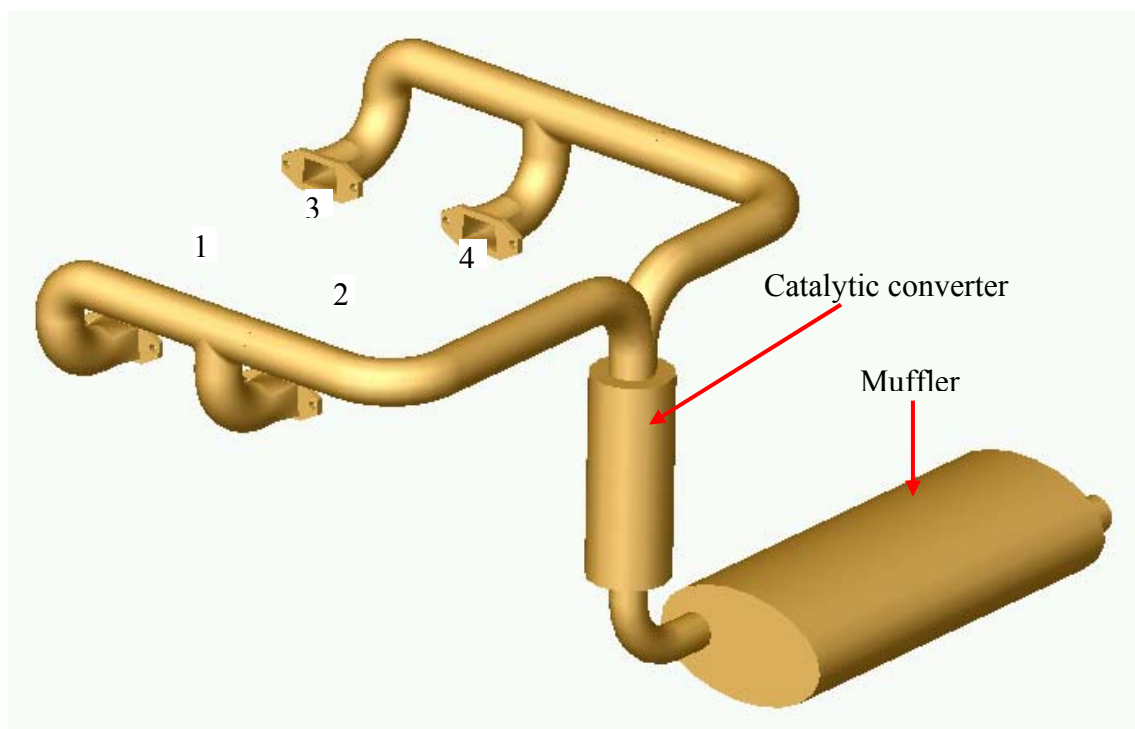


Figure 9.28 Multi cylinder exhaust system

b. Tuning technique

Cross stuffing technique was suggested for the tuning purpose. This technique is independent of speed, thus it can produce good power and fuel economy at a wider speed range whereas tuning using expansion chamber only give power and fuel economy at narrower speed range. Moreover, it can save space (more compact) and reduce the overall weight. Using this technique, pressure pulse from cylinder 1 and 2 can help stuffing fresh charge on each other and so do the cylinder 3 and 4.

c. Catalytic converter

Selection of the catalytic converter was suggested to be done after the prototype is ready since it required back pressure and emission data as the design parameter. Also special lubrication oil is required to avoid blocking of the catalytic converter due to dirt attachment.

d. Muffler

The muffler proposed is aimed to suppress all range of noise. This 2.7 liter muffler consist of several chamber, each chamber is assigned to suppress certain range of frequency. Figure 9.29 shows each segment of the muffler and the predicted transmission loss is shown in Figure 9.30.

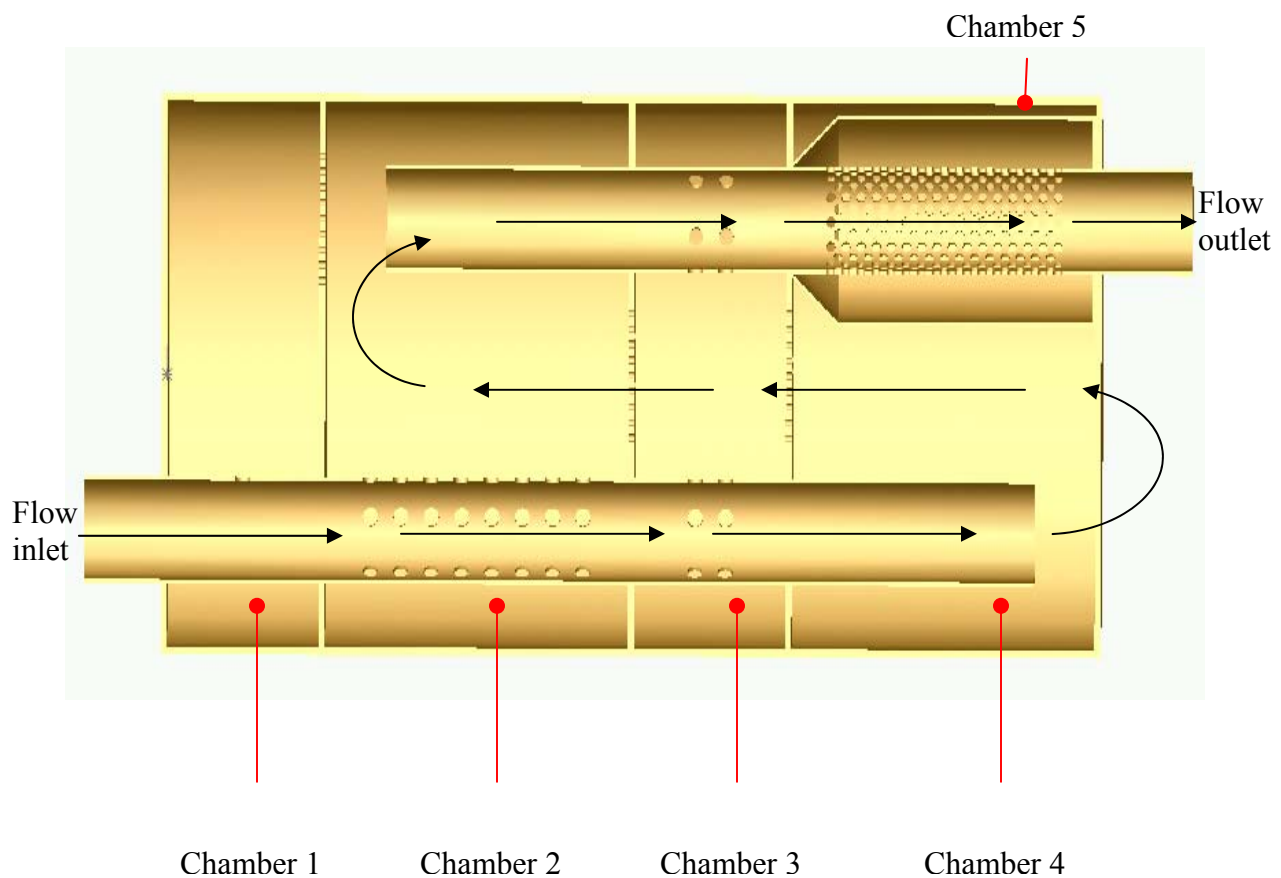


Figure 9.29 Section view of muffler

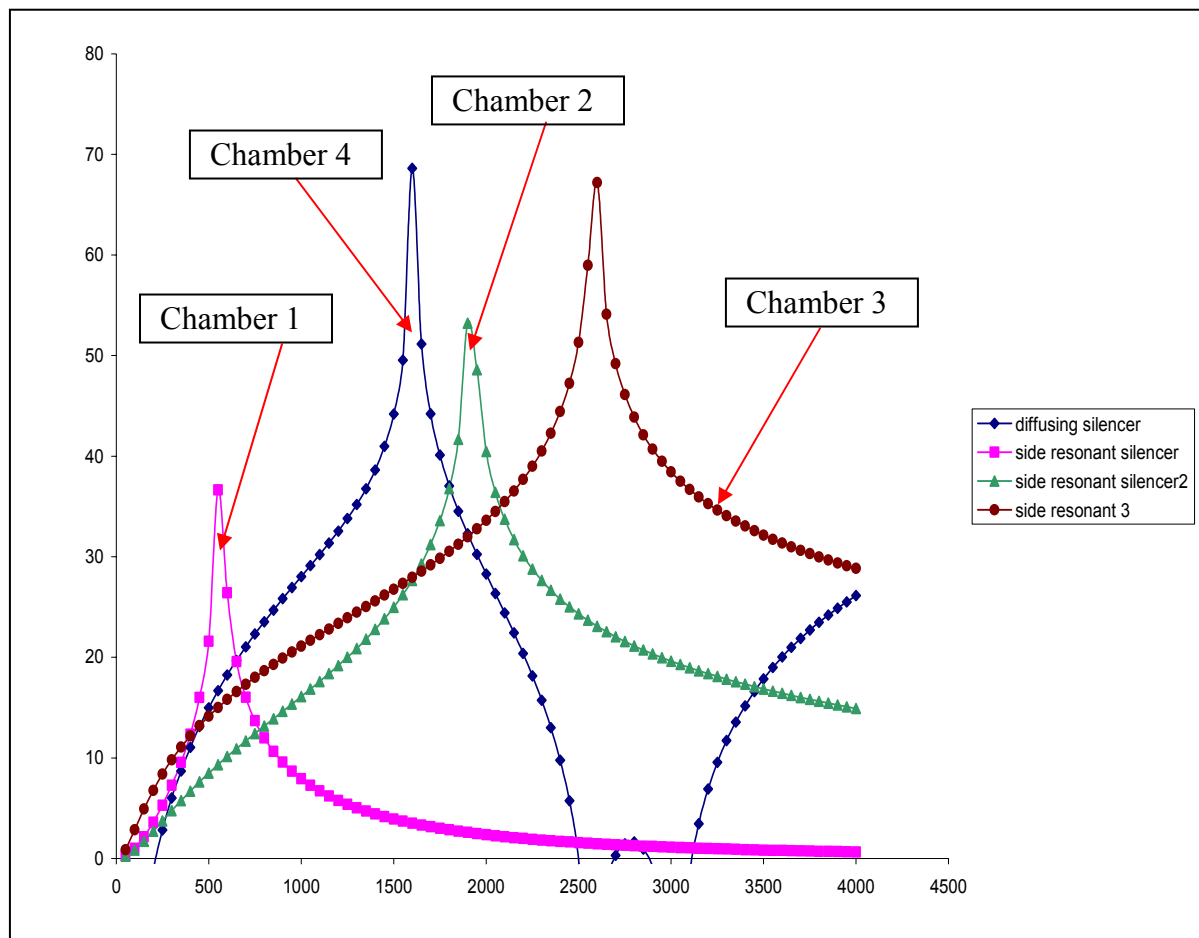


Figure 9.30 Transmission loss of each chamber

Chamber 1, 2 and 3 are side resonant silencer element, each and every of them is aimed to suppressed specific range of frequency which is to assist the frequency range that cannot be covered by the diffusing silencer element (chamber 4), such as the pass band frequency. Chamber 5 (absorption silencer element) is then added to suppress the remaining high frequency noise from the exhaust pulse itself and from turbulent eddies generated when the flow passes through sharp edge of the pipes.

9.2.3 Materials

Table 9.3 shows the proposed material for the exhaust system

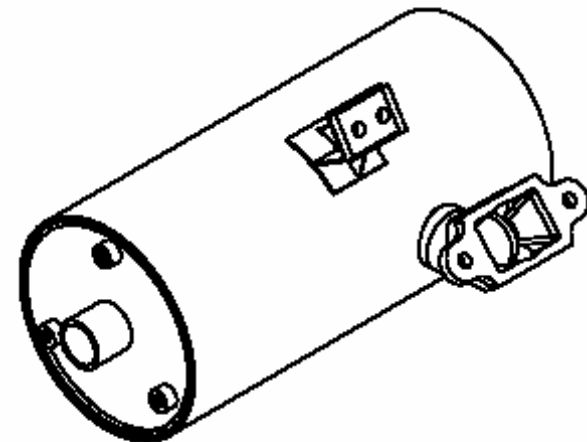
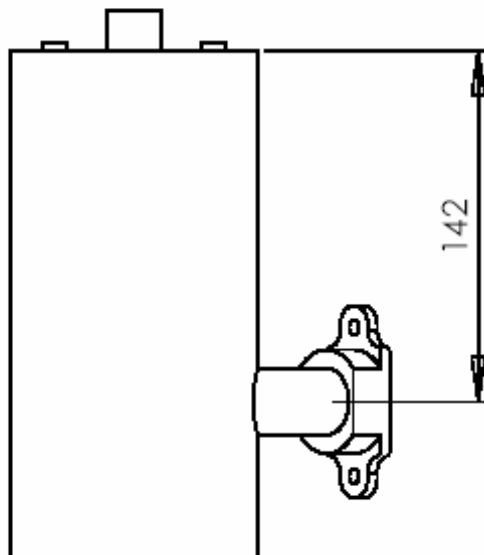
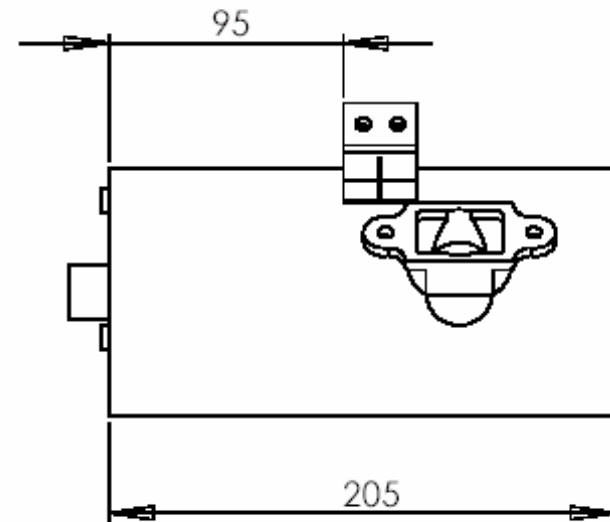
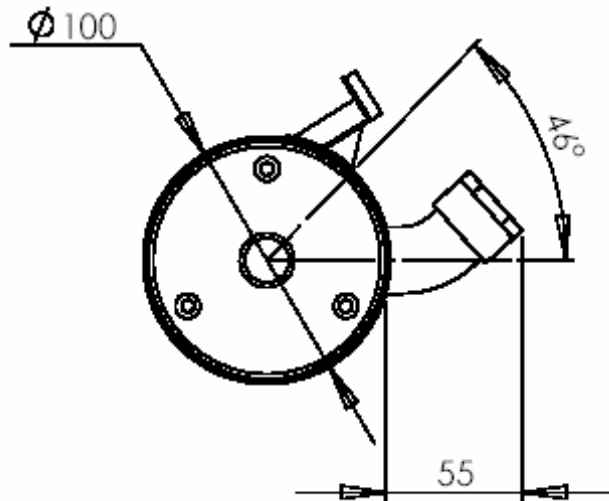
Table 9.3: Material for exhaust part

Part	Material
Exhaust manifold	Cast iron
Exhaust pipe	Mild steel
Muffler	Mild steel/409 stainless steel/aluminize stainless steel

9.2.4 References

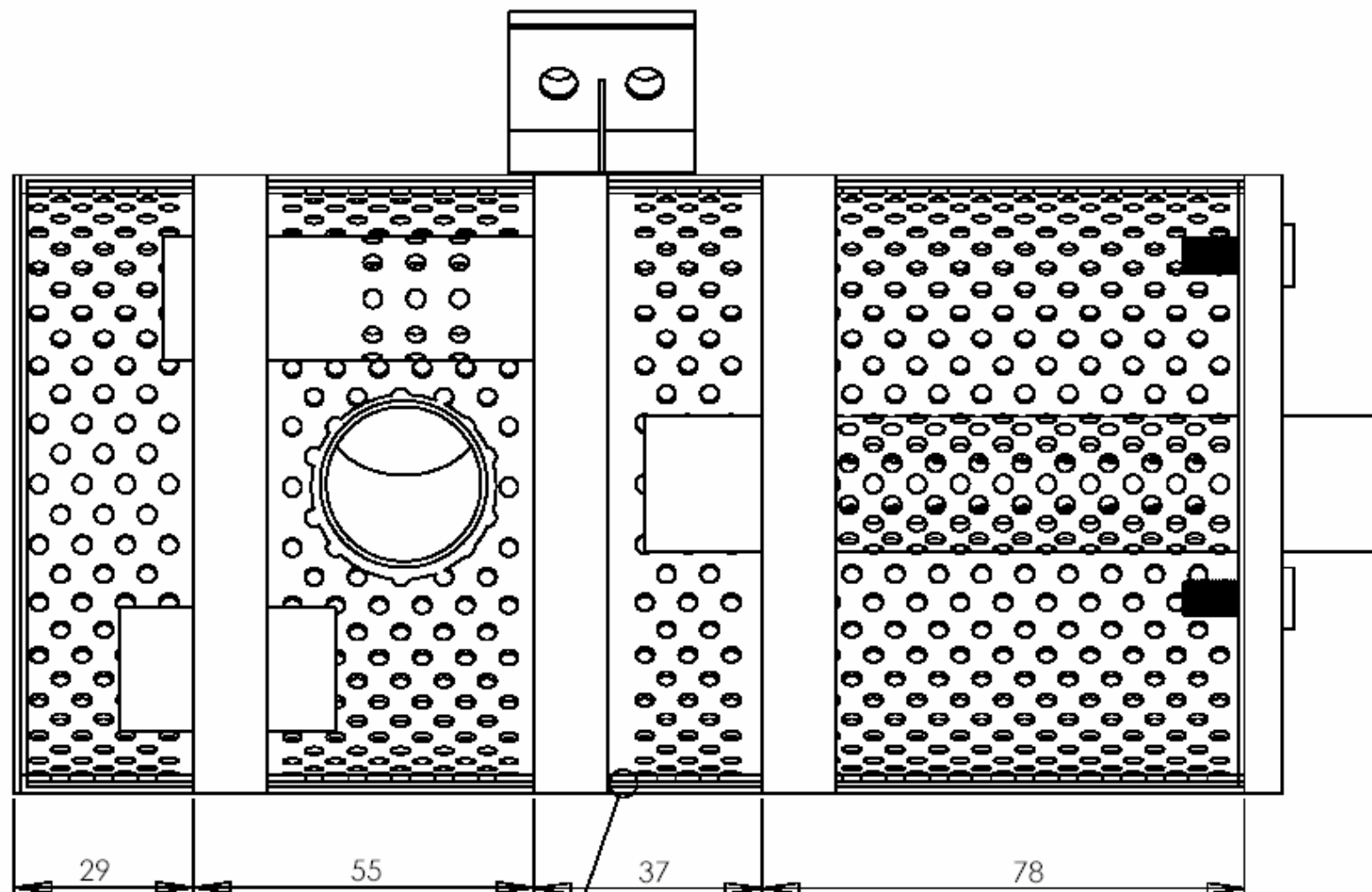
1. Mohd Hafizi b Md. Zin, “ Exhaust System Design for Two-Stroke Multi-Cylinder Engine”, B.Eng. Thesis,UTM. 2004.

APPENDIX 9a

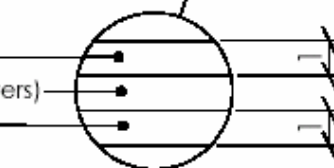


surface treatment: chrome

	NAME	DATE	AUTOMOTIF DEVELOPMENT CENTRE (ADC), UTM		
DRAWN	RUMAIZI BIN SAUIM	23/04/04	TITLE : MUFFLER		
CHECKED	ASSOC. PROF. DR ROSLAN B. ABD RAHMAN		MATERIAL : MILD STEEL		
ENG APPR.					
DIMENSIONS IN MILLIMETERS			SCALE: 1:3	WEIGHT:	DWG. NO. 2 SHEET 1 OF 1



perforate sheet (thickness = 1mm)
 wire mesh/net (1mm x 1mm x 2 layers)
 casing (thickness = 1mm)



casing section view

NAME		DATE	AUTOMOTIF DEVELOPMENT CENTER (ADC), UTM	
DRAWN	RUMADI BIN SALIM	23/06/04	TITLE : MUFFLER (SECTION VIEW)	
CHECKED	ASSOC. PROF. DR ROSLAN S. ABD RAHMAN		MATERIAL : MILD STEEL	
ENG APPR.			SCALE:1:1	
DIMENSIONS IN MILLIMETERS			WEIGHT:	DWG. NO. 4
				SHEET 1 OF 1

CHAPTER X

PARAMETRIC STUDY ON NOISE ATTENUATION OF MUFFLER

This chapter looks into the relationship between silencer dimension and sound attenuation as the parameters of the muffler are varied. Scope of this study is to focus on diffusing silencer and side-resonant silencer element only. A detail study has been carried out by Abdull Rahim in his B.Eng project thesis (1).

10.1 Diffusing Silencer Element

From Fukuda (2), the transmission loss of the diffusing silencer is given by Equation (9.1) in Chapter IX as,

$$TL = 10 \log_{10} (A_{r2} F(k, L))^2 \text{ dB}$$

Figure 10.1 shows the significant dimension of a diffusing silencer element with,

L_b = length of box

L_t = length of pipe 2

L_1 = re-entrant length of pipe 1

L_2 = re-entrant length of pipe 2

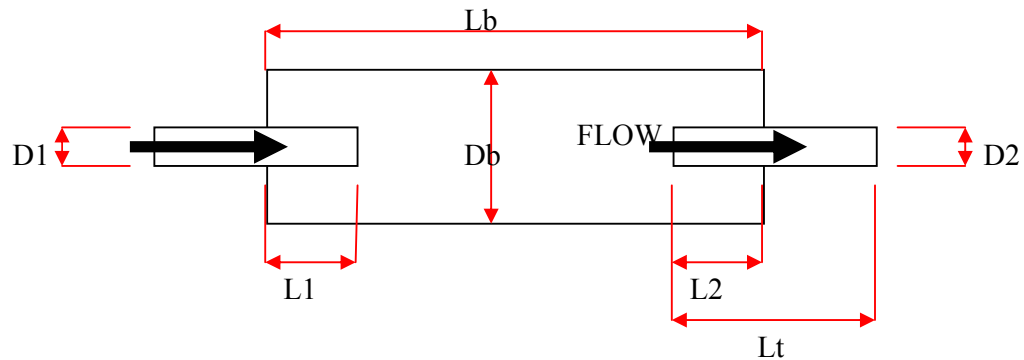


Figure 10.1: Significant dimension of a diffusing silencer element

Assuming inlet pipe and outlet pipe are of the same diameter, the effect of each physical dimension on sound attenuation was taken into consideration.

a. Effect of expansion ratio (D_b/D_2) on sound attenuation of a diffusing silencer

Figure 10.2 shows results of expansion ratios variation on transmission loss which indicates that the frequency span of high transmission loss becomes wider as the expansion ratio increases. At the same time the pass band frequency decreases.

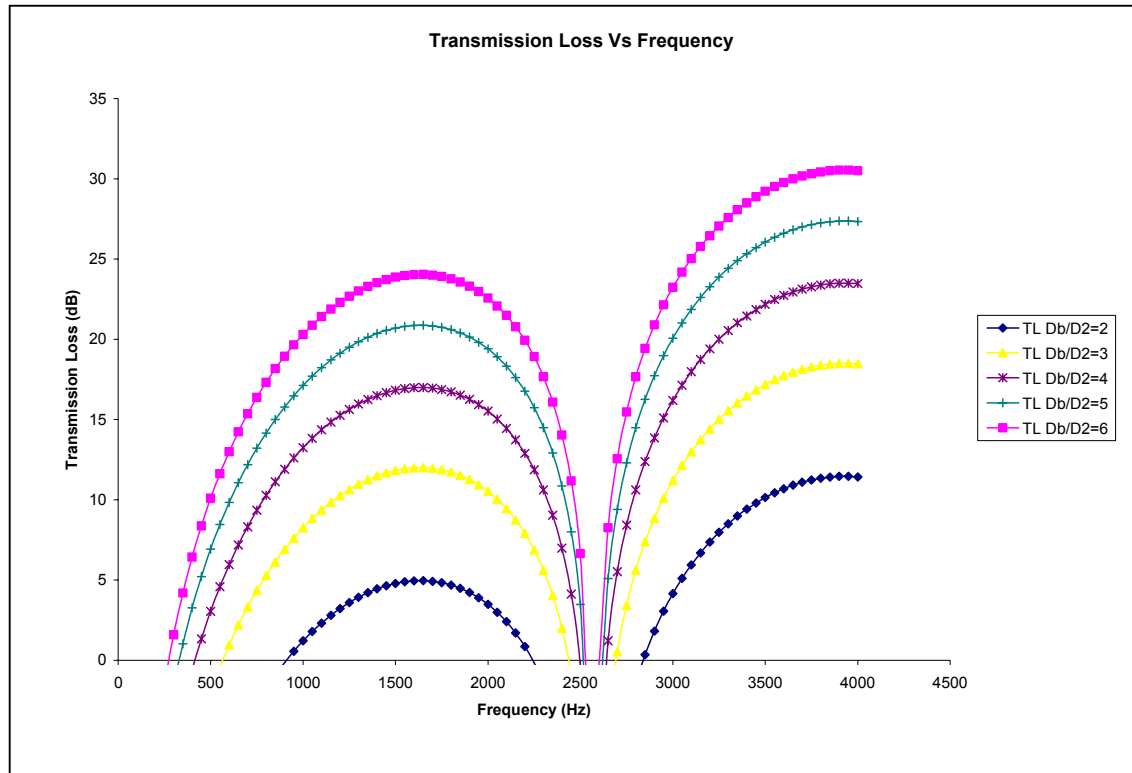
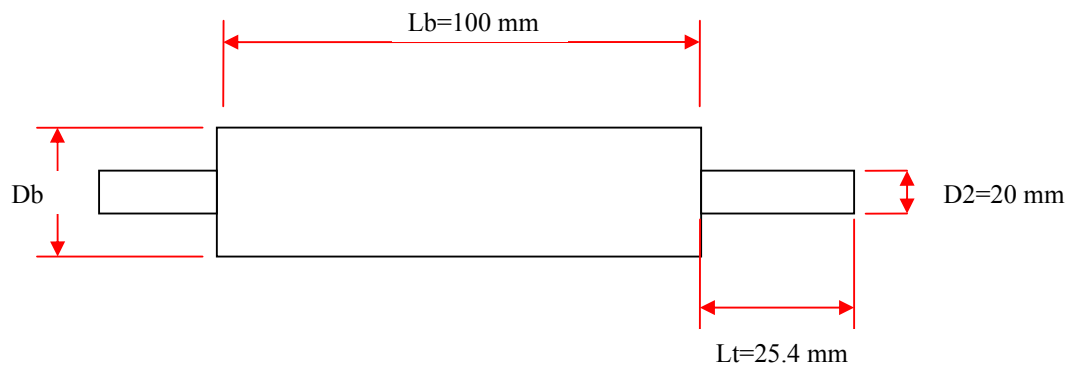


Figure 10.2: Transmission loss of diffusing silencer with different expansion ratio

b. Effect of length over diameter ratio (L_b/D_b) on sound attenuation of a diffusing silencer element

Figure 10.3 shows results in the variation in length over diameter ratio on transmission loss of the muffler. The frequency span for high transmission loss increases as the diameter ratio decreased.

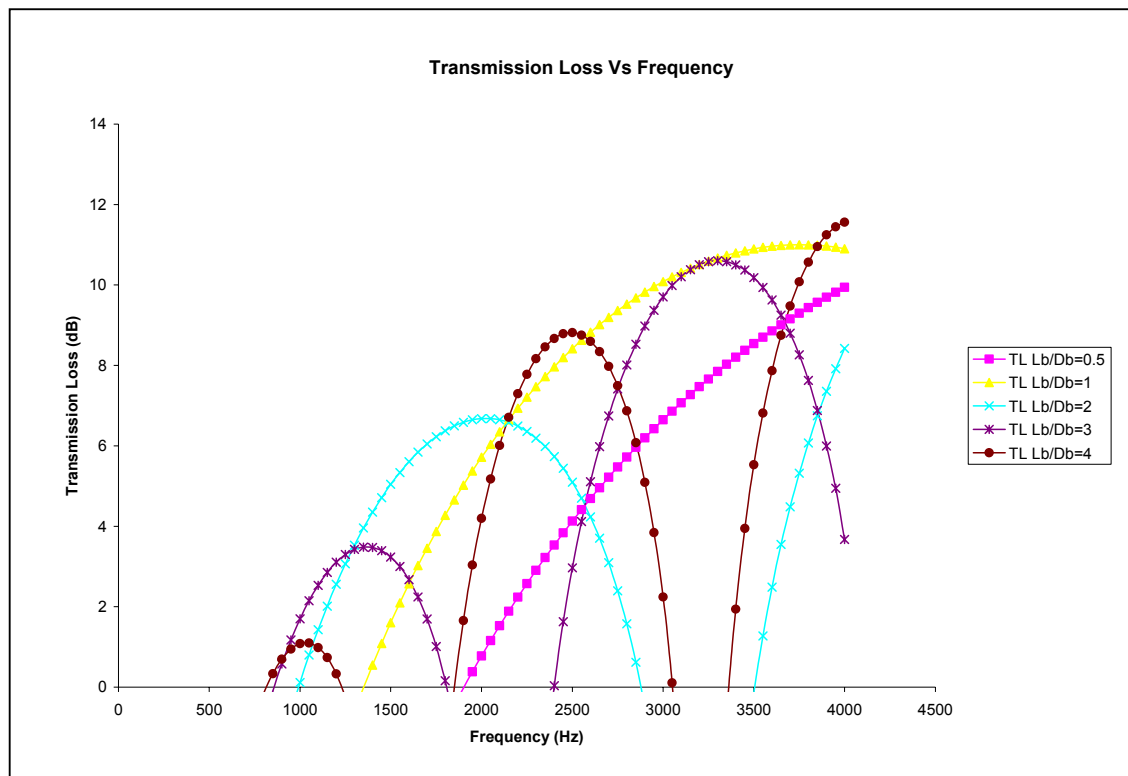
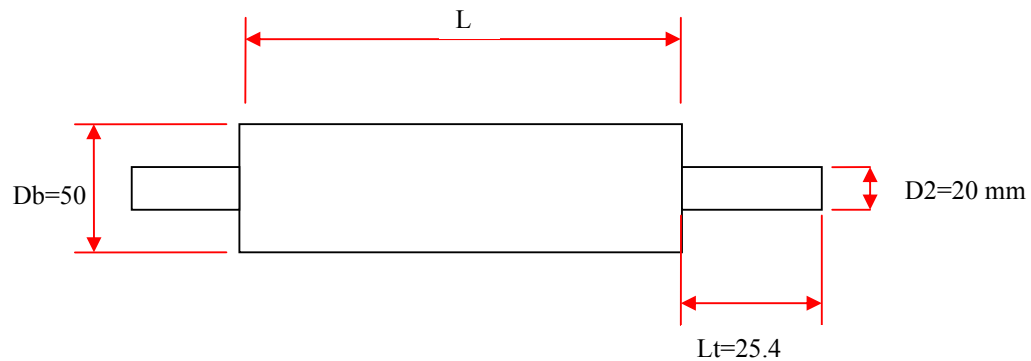


Figure 10.3: Transmission loss of diffusing silencer element with different length/diameter ratio

c. Effect of re-entrance inlet pipe (L1) on sound attenuation of a diffusing silencer

Figure 10.4 shows high transmission loss at discrete frequency start to occurred at inlet pipe length is 70 % of the box length L_b .

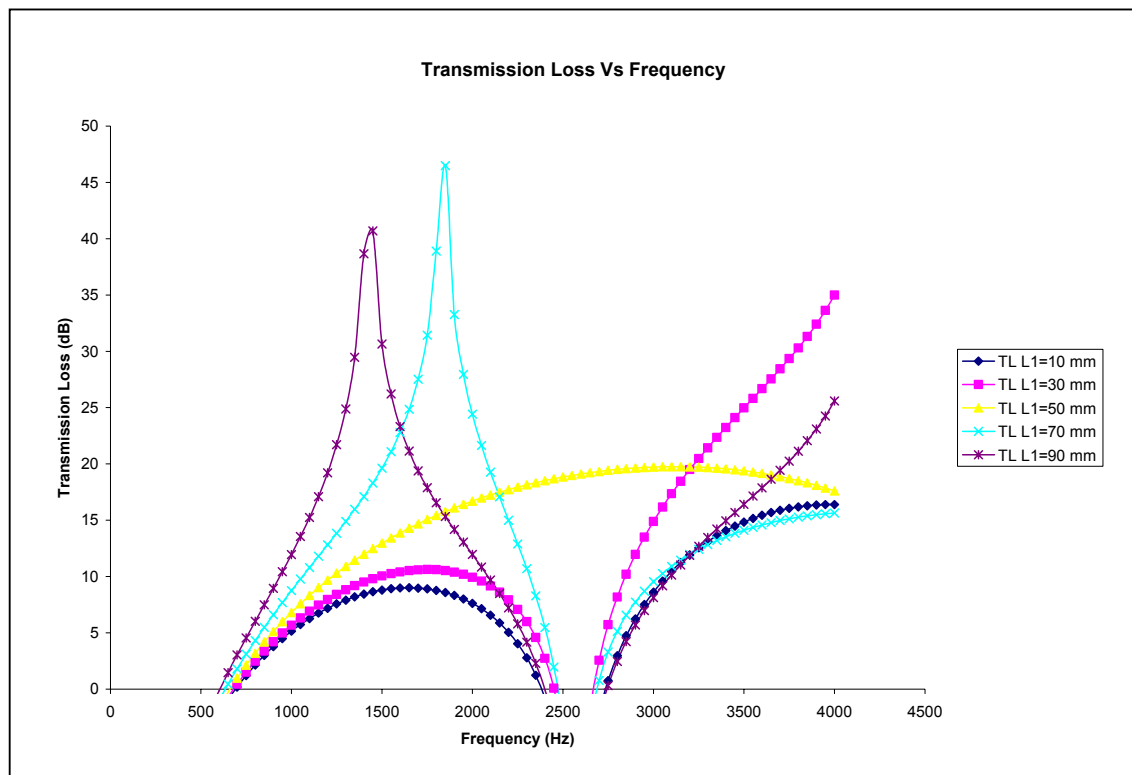
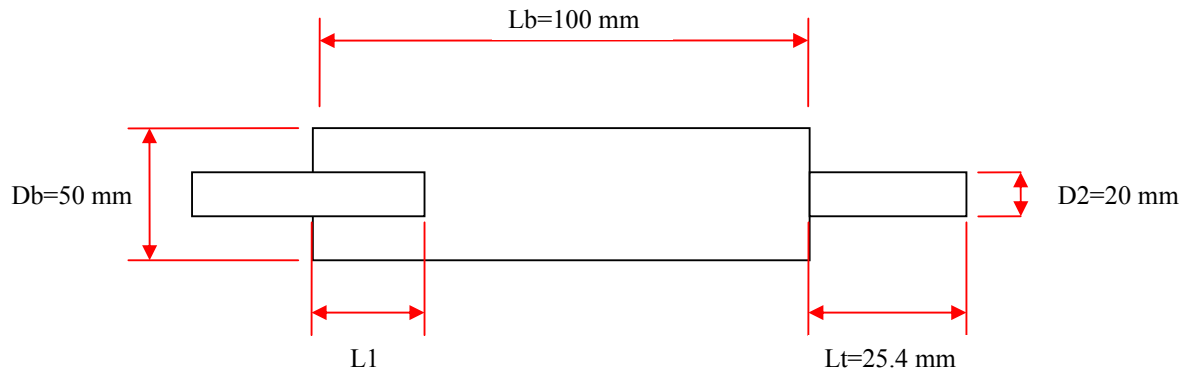


Figure 10.4: Transmission loss of diffusing silencer element with different re-entrance inlet pipe (L1) length

d. Effect of re-entrance outlet pipe (L2) on sound attenuation of a diffusing silencer

The transmission loss achieved maximum value at discrete frequency as shown in Figure 10.5 when the outlet pipe is also 70 % of box length, Lb.

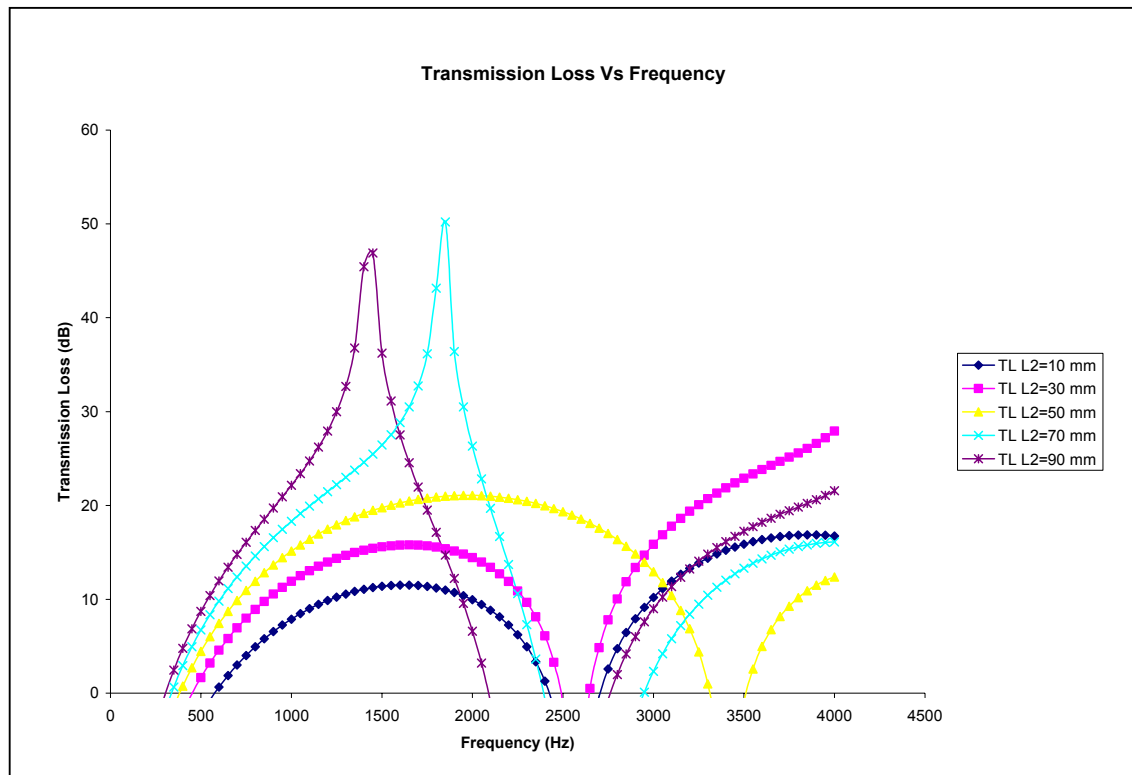
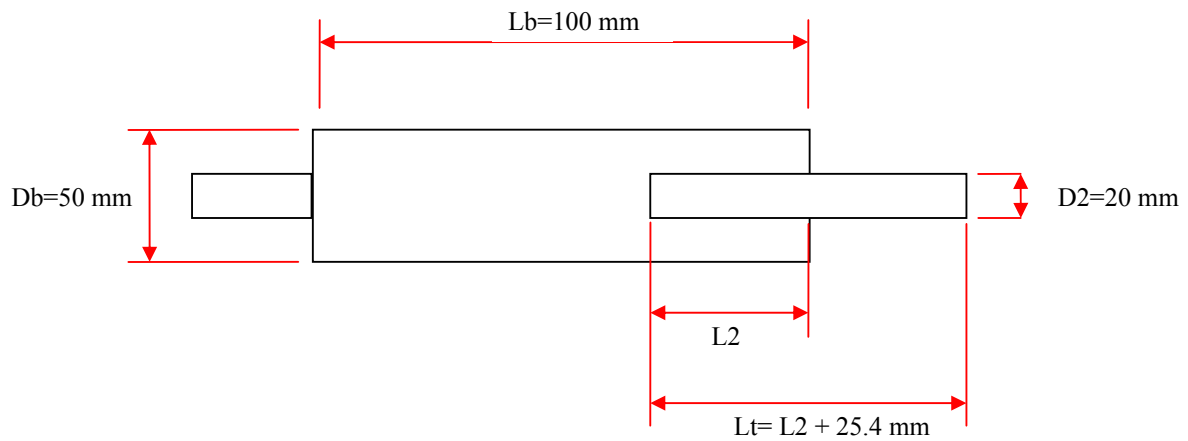


Figure 10.5: Transmission loss of diffusing silencer element with different reentrance outlet pipe (L_2) length

e. Effect of tail pipe length (L_t) on sound attenuation of a diffusing silencer

The results of transmission loss in Figure 10.6 shows that the magnitude of the transmission loss and frequency coverage increased as the tail pipe length increased.

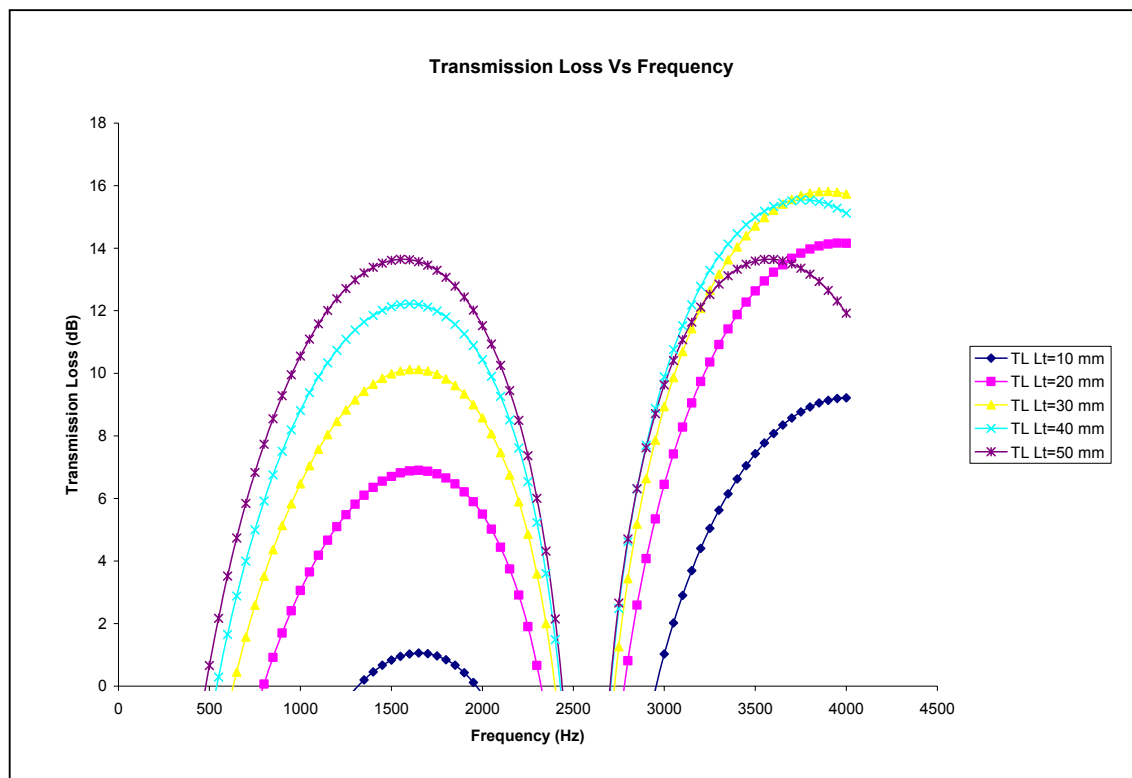
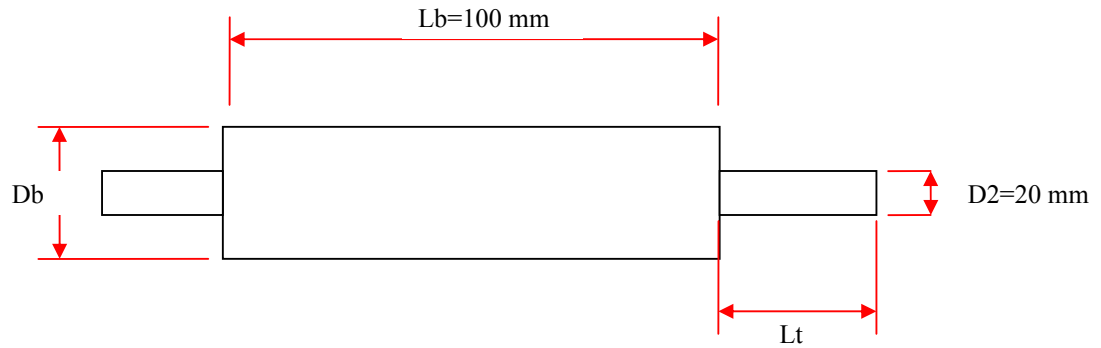


Figure 10.6: Transmission loss of diffusing silencer element with different tail pipe (L_t) length

The results parameter study on the diffusing silencer indicates that to have high transmission loss covering a wider frequency span, the choice of parameters are as follows:

D_b/D_2 ratio should be high

L_b/D_b ratio should be less than 1 but the shape becomes boxy

$L_1/L_b = \frac{1}{2}$ to cover wide frequency range but much less transmission loss

$L_2/L_b = \frac{1}{2}$ to cover wide frequency range but much less transmission loss

L_t/L_b should be high to give high transmission loss over a wide frequency range.

10.2 Side-Resonant Silencer Element

Transmission loss for this type of silencer is given by Equation 9.3 in Chapter IX as,

$$TL = 10 \log_{10} (1 + Z^2) \text{ dB}$$

Figure 10.7 shows the significant dimension of a side-resonant silencer element.

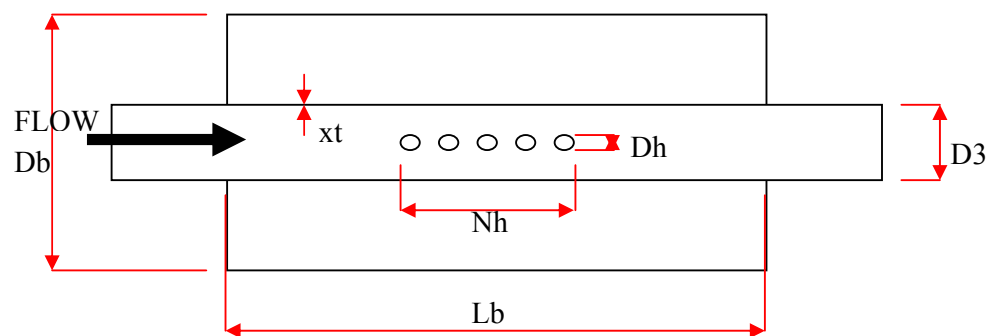


Figure 10.7: Significant dimension of a side resonant silencer element

a. Effect of expansion ratio (D_b/D_3) on sound attenuation of a side-resonant silencer

The result of Transmission loss shown in Figure 10.8 indicates that the maximum transmission loss occurring at discrete frequency shifted towards higher frequency the expansion ratio is reduced. Thus identification of troubling frequency for the engine is required so that the muffler design is customized at that frequency.

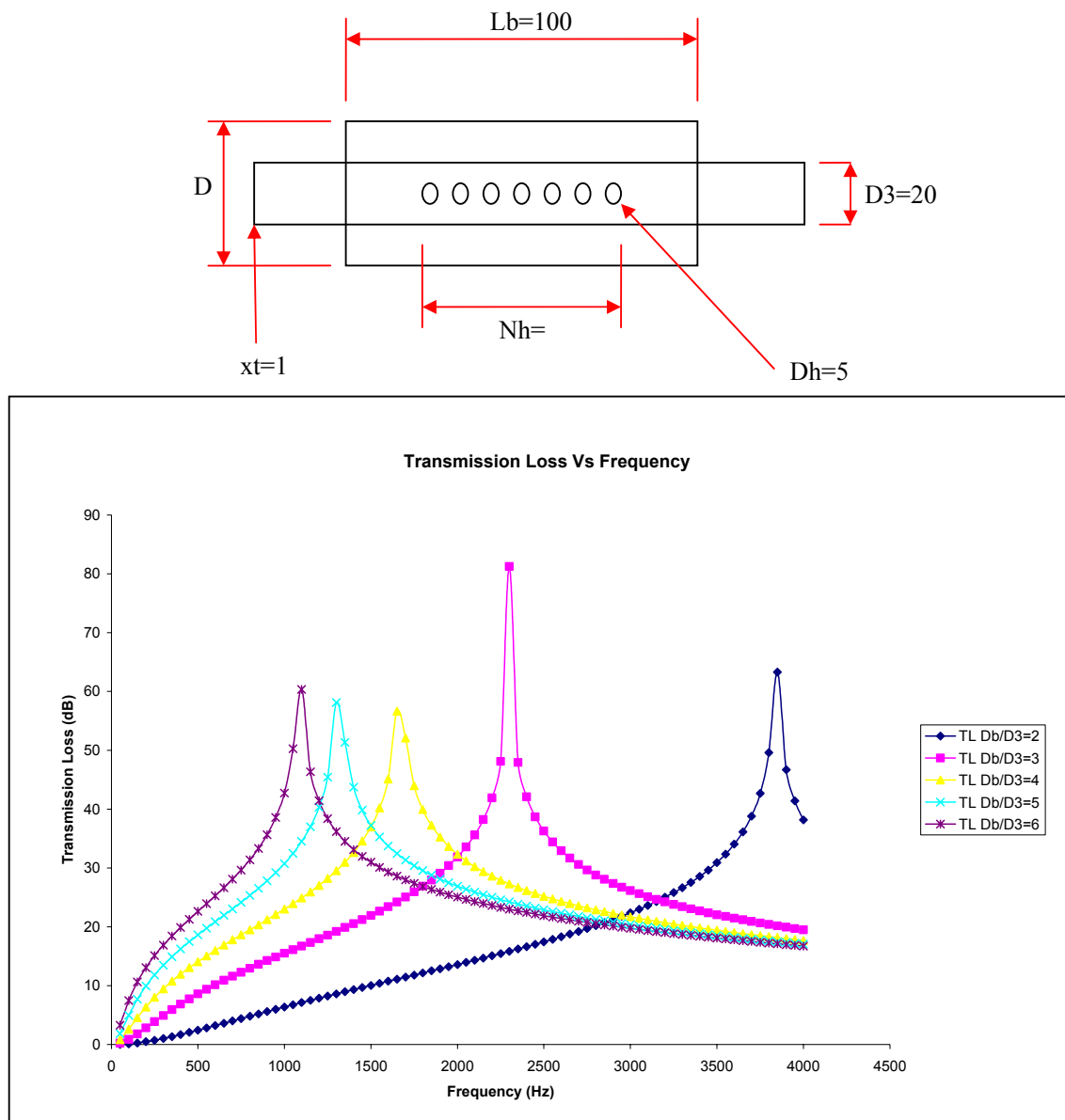


Figure 10.8: Transmission loss of side-resonant silencer element with different expansion ratio (D_b/D_3)

b. Effect of length over diameter ratio (L_b/D_b) on sound attenuation of a side-resonant silencer

The maximum transmission loss occurred at discrete frequency and is shifted towards higher frequency as the length to diameter ratio is reduced as depicted in Figure 10.9.

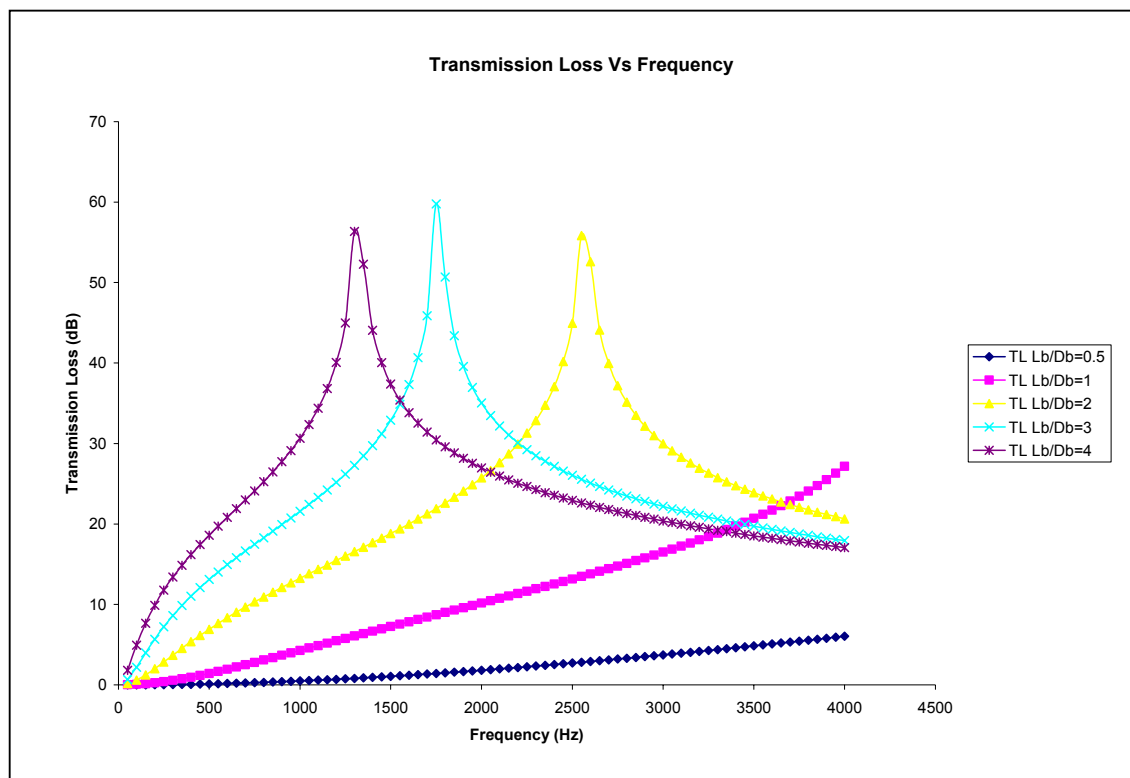
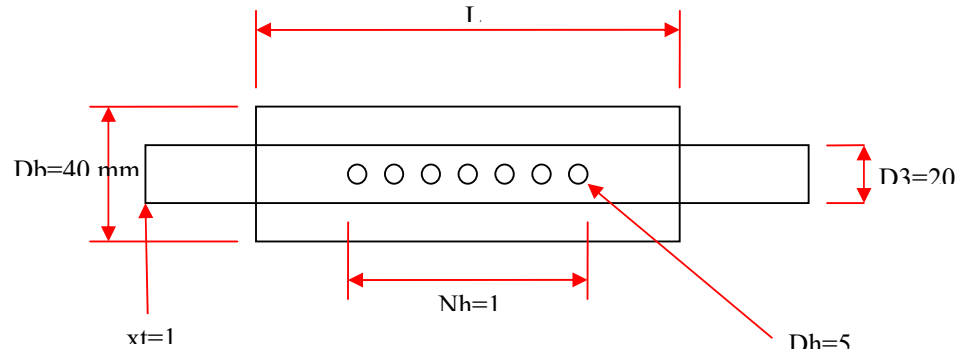


Figure 10.9: Transmission loss of side-resonant silencer element with different length/diameter (D_b/D_3) ratio

c. Effect of hole number (N_h) on sound attenuation of a side-resonant silencer

Figure 10.10 also indicates that the discrete frequency at which maximum transmission loss occurred, shifted towards higher frequency as the number of holes are increased.

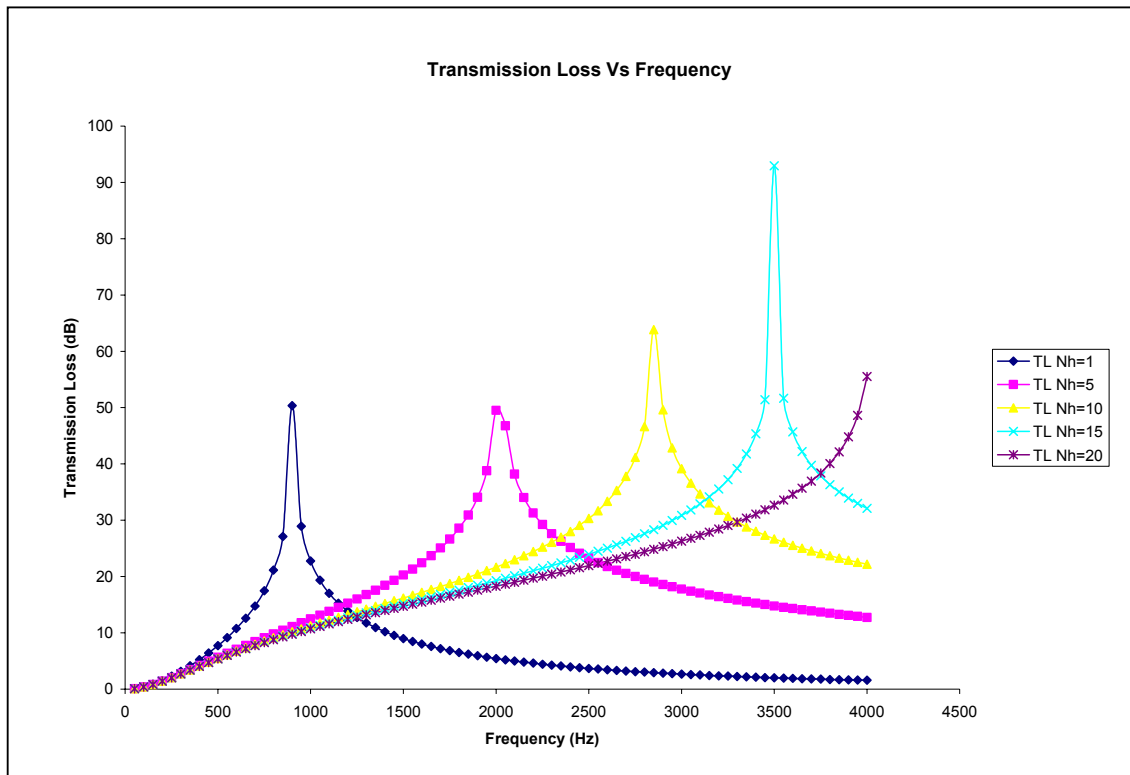
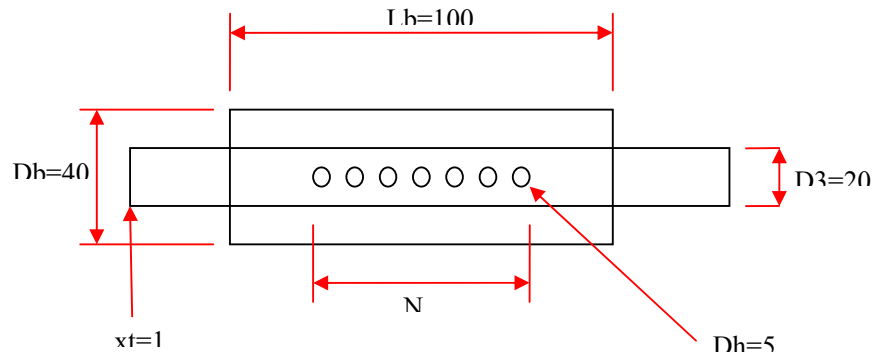


Figure 10.10: Transmission loss of side-resonant silencer element with different hole number (N_h)

d. Effect of hole size (D_h) on sound attenuation of a side-resonant silencer

Figure 10.11 shows that the maximum transmission loss approaches towards lower frequency as the holes size are reduced.

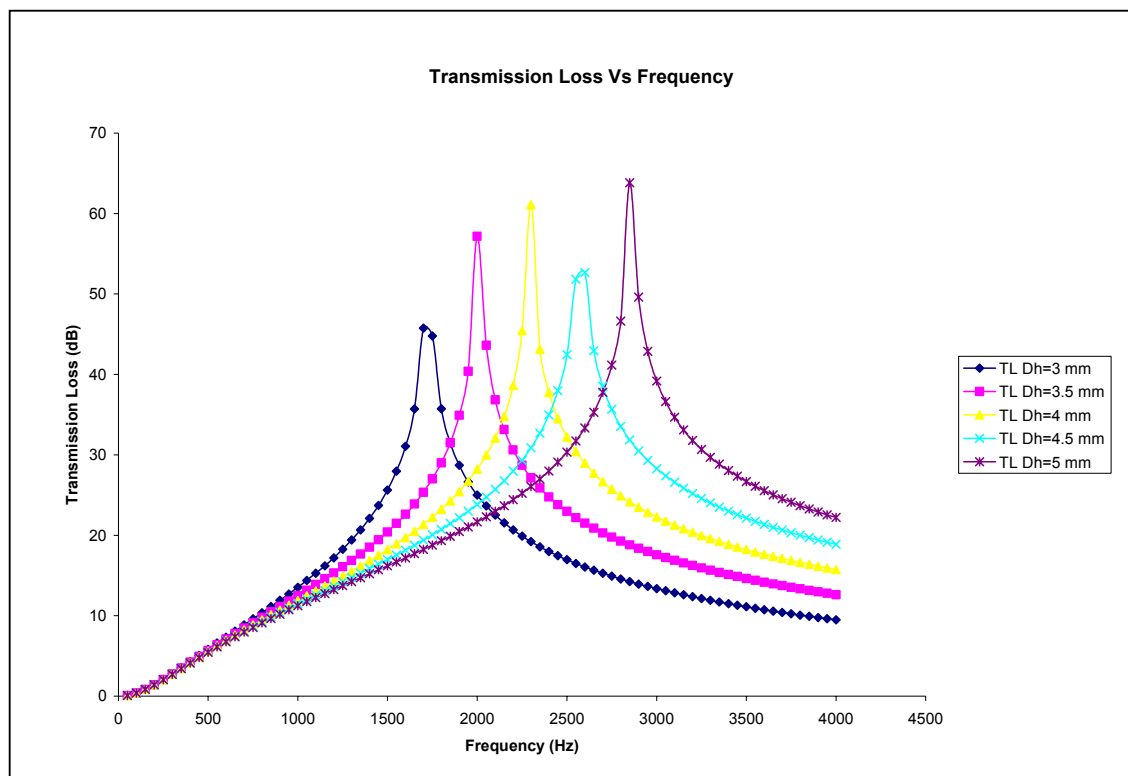
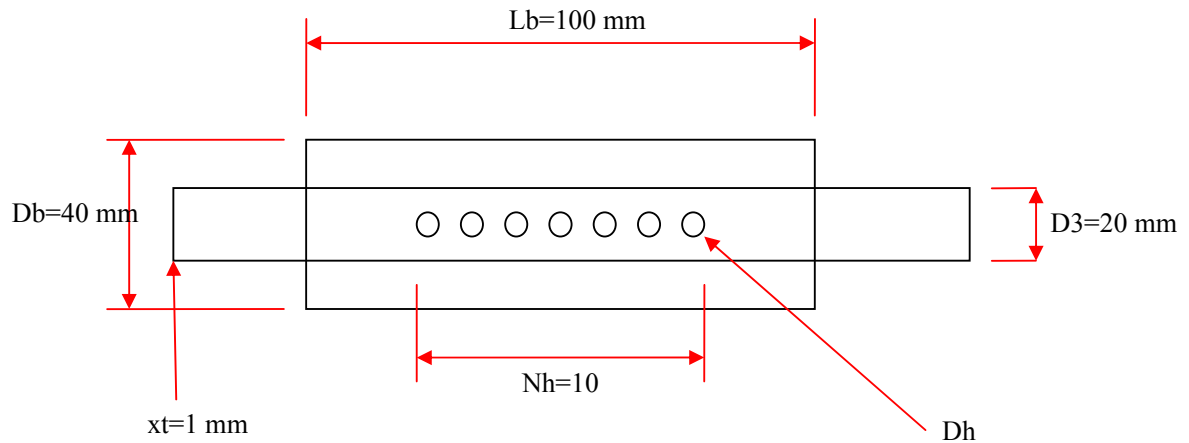


Figure 10.11: Transmission loss of side-resonant silencer element with different hole size (D_h)

e. Effect of pipe thickness (x_t) on sound attenuation of a side-resonant silencer

Increasing the pipe thickness results in the shifting of maximum transmission loss towards lower frequency as shown in Figure 10.12.

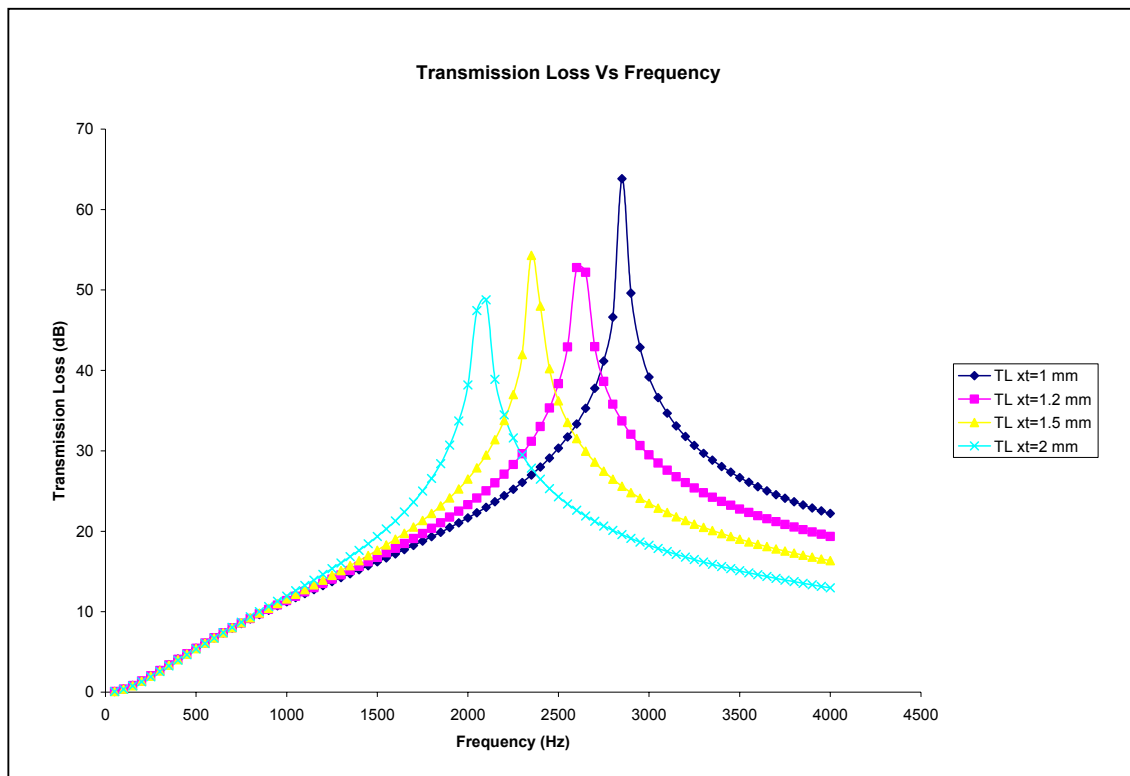
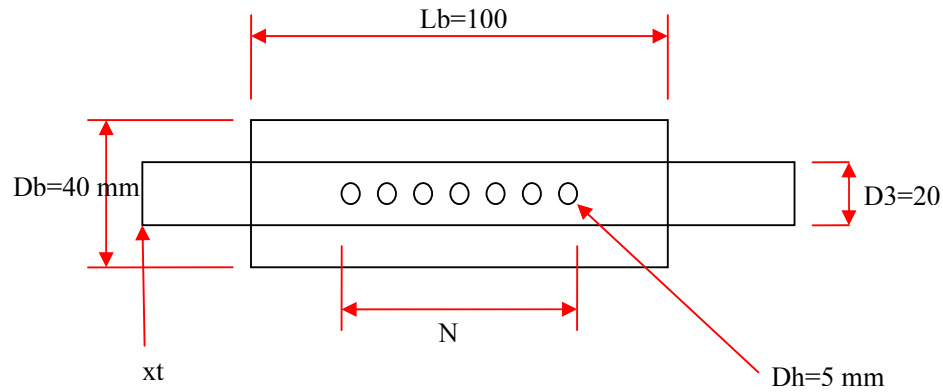


Figure 10.12: Transmission loss of side-resonant silencer element with different pipe thickness (x_t)

In summary, for a side resonant silencer element, to achieve better transmission loss, the following parameter variation has to be taken into account:

Expansion ratio (D_b/D_3)	higher for maximum TL to occur at low frequency
Length to Diameter ratio (L_b/D_b)	higher for maximum TL to occur at low frequency
Number of holes	high for maximum TL to occur at high frequency
Hole size	high for maximum TL to occur at high frequency
Pipe thickness	thicker pipe gave maximum TL at lower frequency

10.3 References

1. Abdull Rahim b Abu Bakar, “Parameter Study on the Performance of a Muffler”, B.Eng. Thesis UTM, 2005.
2. Gordon P. Blair, *Design and Simulation of Two Stroke Engines*, Society of Automotive Engineers Inc, Warrendale, 1996, Chap.8 (reduction of noise emission from two stroke engine)

CHAPTER XI

DESIGN OF 2-STROKE INTAKE SYSTEM

11.1 Introduction

The engine give the power and at the same time, noise emanating from the engine. The obvious sources of noise are the intake and exhaust systems, due the presence of gas pressure waves. The common belief is that the exhaust is the noisier of the two, and in general this is true. However, the most rudimentary of exhaust silencers will almost inevitably leave the intake system as the noisier of these two sources, so it requires silencing to the same level and extend. Intake system is important to the engine because it is needed to suppress the noise from the induction pressure pulses and filter the dust from the outside. Beside this, the intake system can improve the power and torque of the engine and the other function is to keep the air clean and care the performance of the engine. Due to that, the objective is to design the best intake system for the new UTM two-stroke gasoline engine. The study will only concentrate on a single cylinder engine with a capacity of 125 cc swept volume.

11.2 Literature Review

Compared to an automobile, it is more difficult to reduce intake noises in a motorcycle because the air cleaner in a motorcycle is usually compact and not as well-isolated as the one in automobile. Also, in most application, as the improvement of the engine performance and the reduction of intake noises are two contradicting matters, it requires much time and effort to find specification that satisfies both requirements. It is

important, during the development, to estimate the sound pressure level of the intake and determine the most appropriate specifications that other limiting factors permit.

Jianwen et.al (1) developed a frequency analysis technique which is based on one dimensional wave action equations to study the pressure frequency spectrum of intake and exhaust manifolds for engines. The frequency spectra of gas pressure pulsation in the manifolds with different cylinder number, different manifold layouts and different manifold parameters are calculated and the effects of various parameters on the spectrum characteristics are studied. The conclusion from this paper is the primary pipe parameters have a stronger impact on the second natural frequency of intake manifold, while the secondary pipe parameters have a stronger impact on the first frequency.

New engines, other than observing the future legislative limits of noise emissions, will also be necessary to improve the acoustic behavior of plastic air intake manifolds. An investigation was done by Pricken (2) to evaluate alternative and common manufacturing methods. Extensive investigations of different plastic and non plastic materials have provided some materials database. In the following step FEM/BEM calculations with a model of a simplified intake manifolds have been done. The investigations have shown new opportunities in the selection of manufacturing methods. The acoustical performance for plastic and non plastic materials greatly influences the material chosen for a specific application and serves as a benchmark for new, alternate materials. The optimization of the design stresses the advantages of plastic for intake manifolds.

Modeling the sound source of an intake and predicting the intake sound pressure level for a motorcycle was developed by Hideki and Hiroyuki (3). It is difficult to estimate the source of the intake only by calculation, due to the aforementioned reasons, actual measurements were carried out to define the sound source. The method is such that the sound source is modeled by acoustic impedance and volume velocity in the engine, and the acoustic impedance and volume velocity in the engine, and the acoustic impedance is measured using an impedance tube. Then the volume velocity is calculated backwards using the results of measurement and the intake system unit model. This method allows defining the sound source by experiments. The conclusion can be drawn

are it has been confirmed that the vibro-acoustic coupling analysis improves modeling accuracy of an intake system unit. Second conclusion is defining of sound source of an intake has become possible by using measured acoustic impedance of the engine and sound pressures at the intake opening. Third conclusion is combination of those results enables accurate estimate of sound pressure level at the intake opening when the air cleaner is modified.

11.3 Theory of Intake Silencer

The design of an engine intake system involves many design considerations. Two very important areas of design are the intake manifold's volume and geometry (4). In considering these variables there are several difference possible intake configurations. Such configurations will include single and dual plenum designs, as well as volume transitions.

Probably the simplest and most effective form of intake silencer is of the type in Figure 11.1. The geometry illustrated is for a single-cylinder engine but the same arrangement can also apply to a multi-cylinder design.

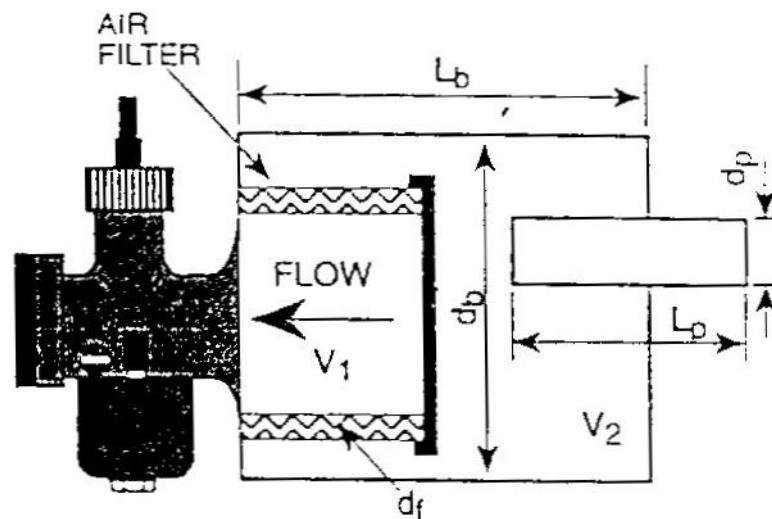


Figure 11.1: Form of intake silencer.

This intake supplies the basic mechanism of induction silencing, being a volume connected to the induction system. On the atmospheric side of this box is a pipe of length, L_b and area, A_b or with diameter, d_b , if it circular crosses section. The air cleaner is placed within the box, helping to act as an absorption silencer of the various high frequency components emanating from the edges of throttles or carburetor slides. Assuming that is reasonably transparent to the air flow, this has no real effect on the silencing behavior of the box volume, V_b .

The design of the silencer is accomplished by setting the natural frequency of the silencer, f_i , correspond to natural frequency of the induction pulse from the engine, f_e . The natural frequency, f_i

$$f_i = \frac{a_0}{2\pi} \sqrt{\frac{A_p}{L_{eff} V_b}}$$

Where,

a_0 = acoustic velocity, and

V_b = box volume.

L_{eff} = effective length of the intake pipe

The engine forcing frequency of direct design interest, f_e is that corresponding to the engine speed of rotation and the number of cylinder. The engine forcing frequency, f_e ,

$$f_e = \frac{\text{number of cylinders} \times \text{rpm}}{60}$$

The effective length of the intake pipe, L_{eff} , is related to the actual length, L_p , and the diameter, d_p as follows,

$$L_{eff} = L_p + \frac{\pi d_p}{4}$$

There are several other criteria to be satisfied as well in this design process, such as ensuring that the total box volume and the intake pipe area are sufficiently large so as not to choke the engine induction process and reduce the delivery ratio. Such a calculation is normally accomplished using unsteady gas-dynamic engine model, extend to include the intake and exhaust silencers. However, an approximate guide to such parameters is given by the following relationship.

Box volume, V_b ,	$10 \times V_{sv} \sqrt{N_{cy}} < V_b < 20 \times V_{sv} \sqrt{N_{cy}}$
Intake pipe diameter, d_p ,	$0.6d_2 < d_p < 0.8d_2$
where,	V_{sv} = swept volume of any one cylinder
	N_{cy} = number of cylinder
	d_2 = diameter of intake duct

11.3.1 Transmission loss and its relationship with intake silencer (Physical properties)

The silencer has the noise reduction characteristic and often described by insertion loss or transmission loss value. Insertion loss is defined as the difference in sound pressure level at a specified point beyond the silencer with and without silencer while transmission loss (also known as sound power transmission coefficient) is defined as the ratio of the power incident on the silencer to the power transmitted through the silencer (5). The value of the insertion loss depends on the properties of the source, termination and surrounding environment as well as the silencer (6), transmission loss however depends solely on the silencer element itself (7).

Because of that, transmission loss is said to be the most important characteristic of the silencer and most calculated results concerning the noise reduction properties of silencer elements are in term of transmission loss (5,6). Due to this reason, silencer characteristic in this chapter will be described in term of transmission loss.

Diffusing silencer is the most basic silencer where the transmission loss is basically a function of two parameters. The parameters are the expansion ratio (ratio between expansion chambers to the pipe diameter) and the relationship between the wave lengths of the sound to the length of the expansion chamber. From Fukuda (6), the transmission loss of the diffusing silencer is given by Eqn. 9.1 as:

$$TL = 10 \text{ Log}_{10} (A_{r2} F(k, L))^2 \text{ dB}$$

The significant dimension of a diffusing silencer element is as already shown in Figure 9.1.

11.3.2 Simulation Process

The simulation process to design the intake system is by using GT power software from GT-Suite Version 5.2. Figure 11.2 shows the process of simulation.

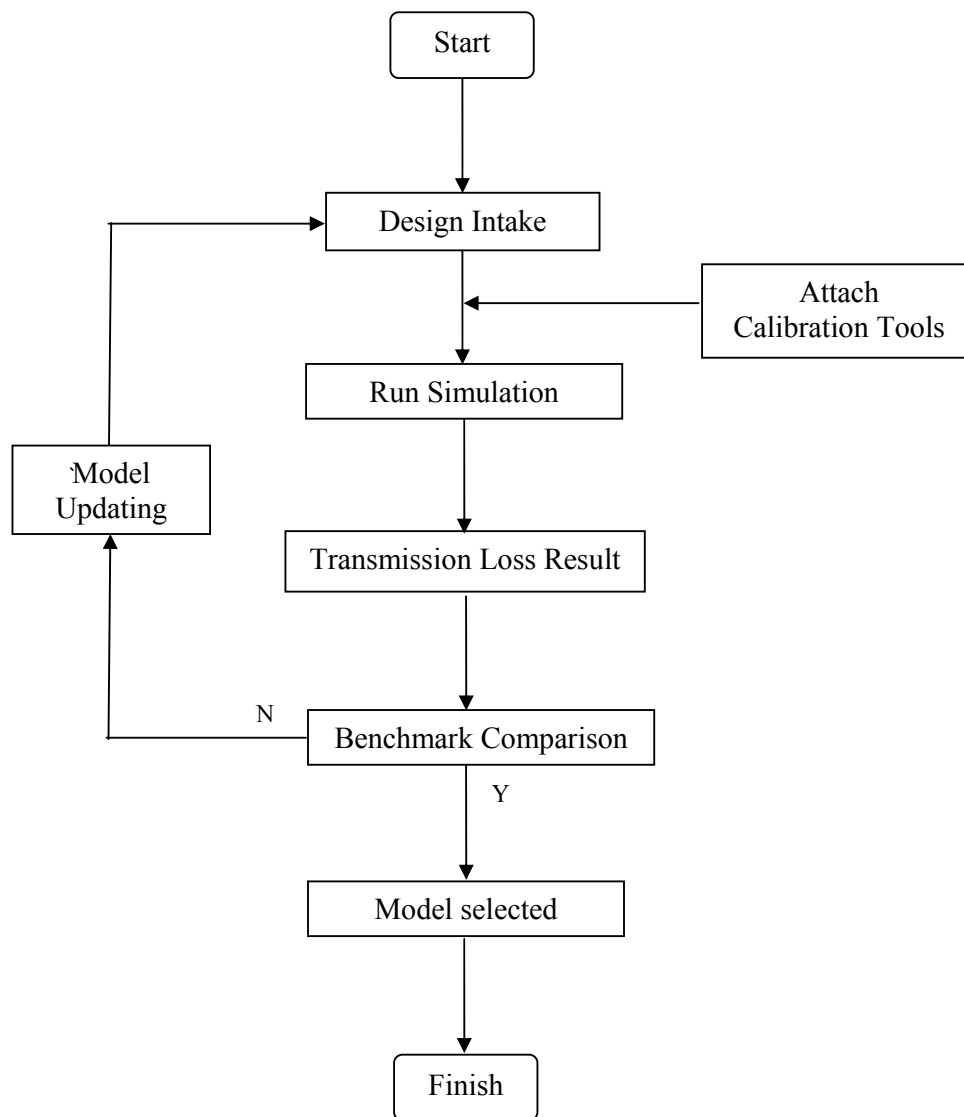


Figure 11.2: Motion of Simulation Process flowcharts.

11.3.3. Development of Intake System

This two stroke engine still uses the carburetor for the fuel injection system. So, the intake system must be designed to match it with the carburetor. Several intakes silencer were calculated using Fukada formula. The transmission loss was used to measure the intake performance. Figure 11.3 below shows the initial design for the intake silencer.

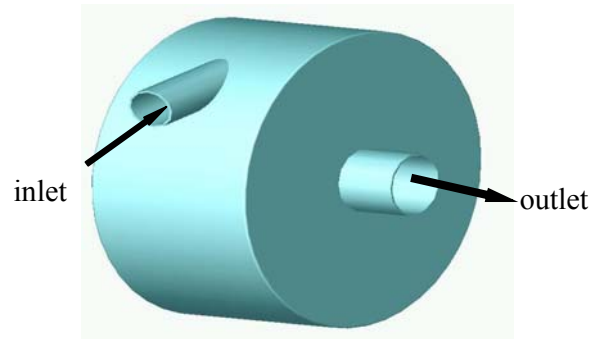


Figure 11.3: Model 1 intake silencer.

This intake silencer design is cylindrical in shape and the diameter of the outlet pipe is set to 30mm as the diameter of the intake duct for the carburetor is 30mm. The design for the intake silencer with volume 10 times to the engine swept volume was proposed. The position of the intake silencer to the engine is shown in Figure 11.4.

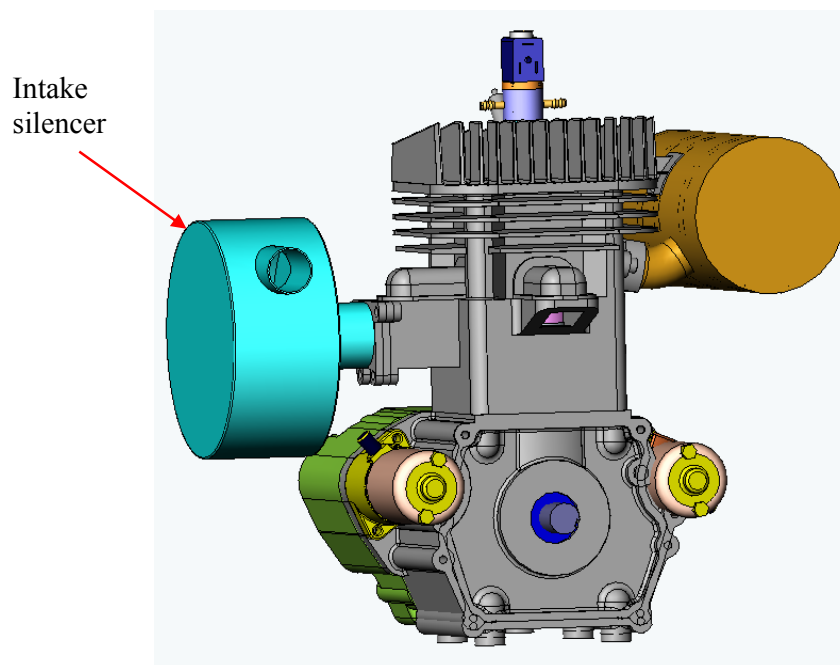


Figure 11.4: Position of the intake silencer to the engine.

The result of the transmission loss for Model 1 intake silencer is shown in Figure 11.5. The pass band frequency where the intake silencer is ineffective is quite wide, from 2400 Hz to 2600 Hz (200 Hz band). The transmission loss is most effective in the region of 1500 Hz at the lower frequency end.

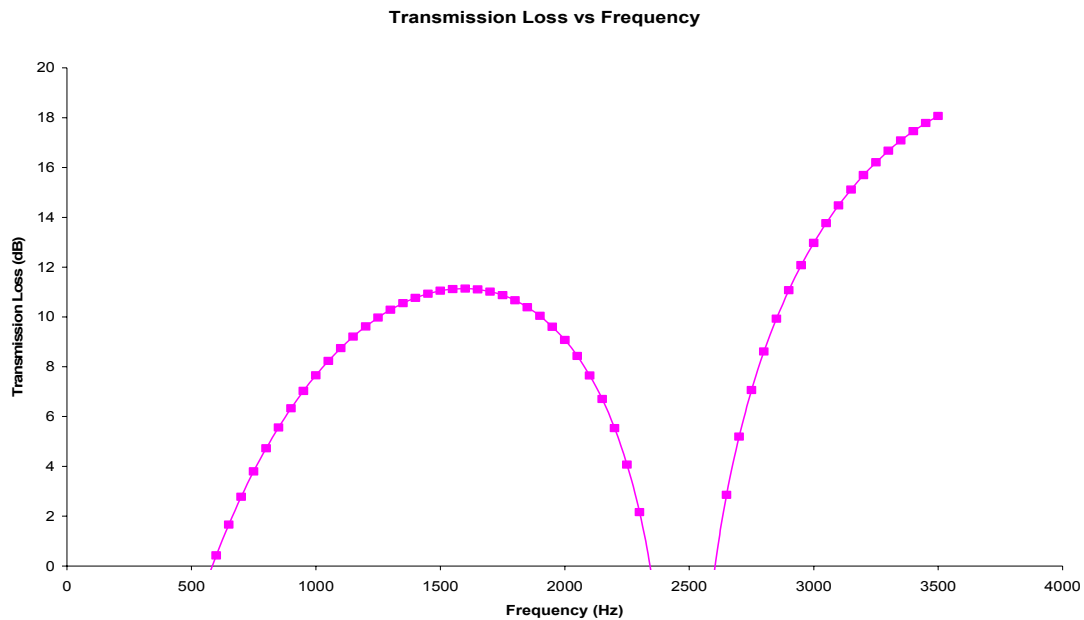


Figure 11.5: Transmission loss for Model 1 intake silencer

Several modifications have been done to Model 1 to increase the transmission loss and obtain better noise reduction. The description on each modification of each model is described in Table 11.1. Description is done by referring to the Muffler 1 layout in Figure 11.6. The dimension of the elements in the intake system are as follows :

$$D_b = 0.15 \text{ m}$$

$$L_b = 0.07 \text{ m}$$

$$L_t = 0.01 \text{ m}$$

$$L_1 = 0.0 \text{ m}$$

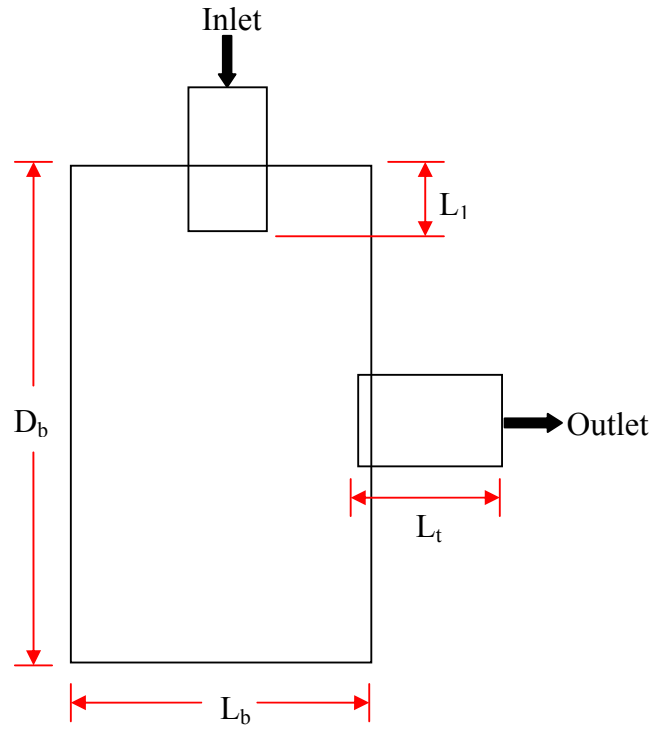


Figure 11.6: Model 1 layout.

Table 11.1: Description on the modification of model 1

Model	Description (compared to muffler 1)	
Model A	$D_b = 0.15 \text{ m}$	$L_t = 0.01 \text{ m}$
	$L_b = 0.07 \text{ m}$	$L_1 = 0.01 \text{ m}$
Model B	$D_b = 0.15 \text{ m}$	$L_t = 0.01 \text{ m}$
	$L_b = 0.07 \text{ m}$	$L_1 = 0.02 \text{ m}$
Model C	$D_b = 0.15 \text{ m}$	$L_t = 0.02 \text{ m}$
	$L_b = 0.07 \text{ m}$	$L_1 = 0.0 \text{ m}$
Model D	$D_b = 0.15 \text{ m}$	$L_t = 0.02 \text{ m}$
	$L_b = 0.07 \text{ m}$	$L_1 = 0.01 \text{ m}$
Model E	$D_b = 0.15 \text{ m}$	$L_t = 0.02 \text{ m}$
	$L_b = 0.07 \text{ m}$	$L_1 = 0.02 \text{ m}$
Model F	$D_b = 0.15 \text{ m}$	$L_t = 0.03 \text{ m}$
	$L_b = 0.07 \text{ m}$	$L_1 = 0.0 \text{ m}$
Model G	$D_b = 0.15 \text{ m}$	$L_t = 0.03 \text{ m}$
	$L_b = 0.07 \text{ m}$	$L_1 = 0.01 \text{ m}$

Model H	$D_b = 0.15 \text{ m}$ $L_b = 0.07 \text{ m}$	$L_t = 0.03 \text{ m}$ $L_l = 0.02 \text{ m}$
Model I	$D_b = 0.15 \text{ m}$ $L_b = 0.07 \text{ m}$	$L_t = 0.04 \text{ m}$ $L_l = 0.0 \text{ m}$
Model J	$D_b = 0.15 \text{ m}$ $L_b = 0.07 \text{ m}$	$L_t = 0.04 \text{ m}$ $L_l = 0.01 \text{ m}$
Model K	$D_b = 0.15 \text{ m}$ $L_b = 0.07 \text{ m}$	$L_t = 0.04 \text{ m}$ $L_l = 0.02 \text{ m}$

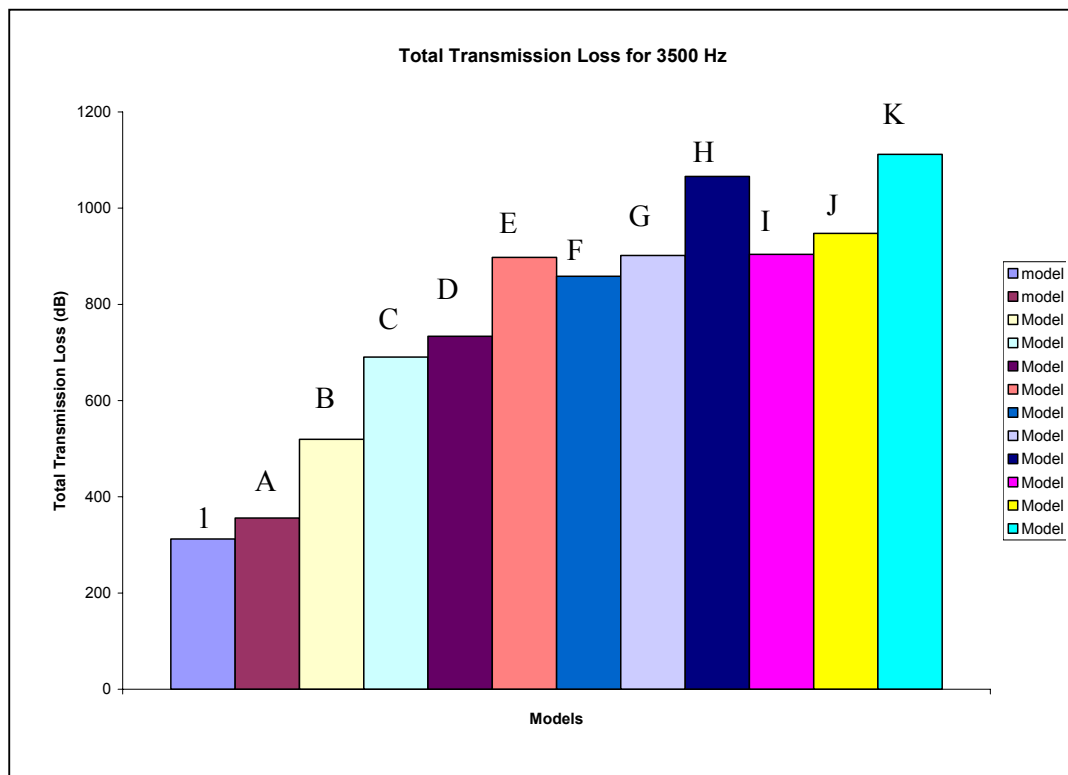


Figure 11.7: Total transmission loss (dB Hz) coverage up to 3500 Hz frequency.

Figure 11.7 shows the total of transmission loss in dB Hz which covers the frequency until 3500 Hz frequency for all models. From this chart, several models have low total transmission loss coverage and others are high compare to the benchmark muffler. Lower transmission loss can cause the noise to increase but higher transmission loss can affect the brake torque and brake power. So, only three models are selected for the next selection. The models are model H, J and K. The transmission loss of these models is compared, and the results are shown in Figure 11.8.

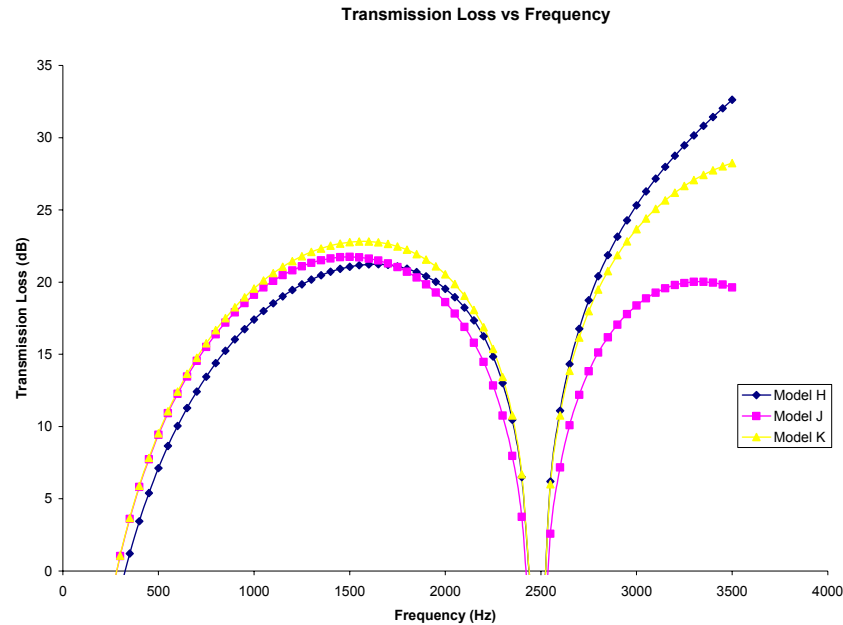


Figure 11.8: Transmission loss for the three models.

From this graph, model K has the better transmission loss compare to the other model. Model K was thus selected for the intake system and the engineering drawing for this muffler is shown in Appendix 11.

11.4 Conclusion

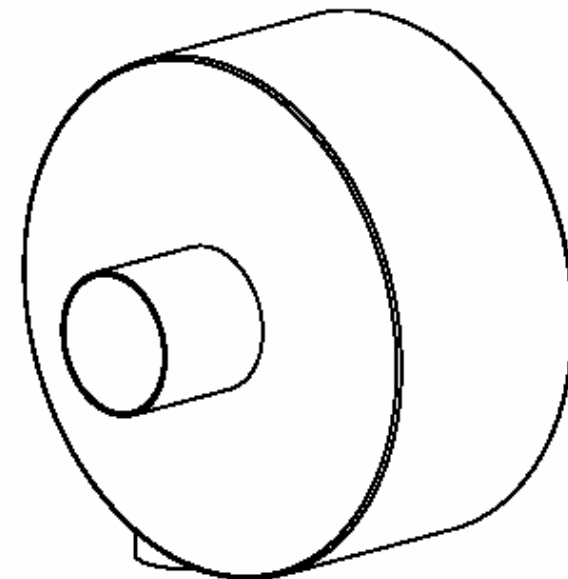
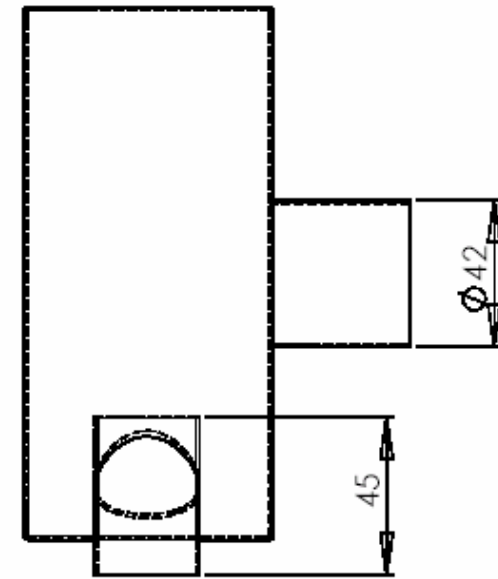
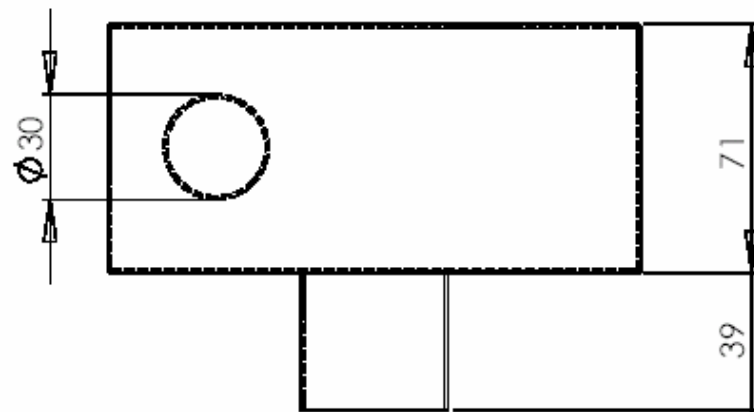
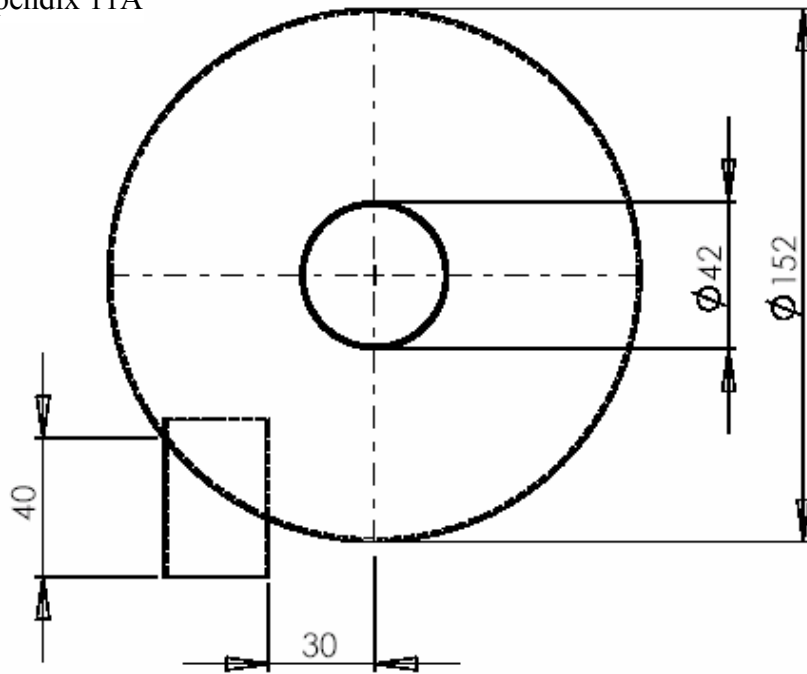
The size of the intake box was 10 to 15 times the swept volume of the engine in order to achieve reduction in noise level. Silencer with the smooth mass flow has lower noise level. There are several suggested methods to reduce the intake noise, among them are:

- a. To select adequate diameter and length of intake pipe with the right balance of silencing effect and engine performance.
- b. To increase body rigidity.
- c. To improve the silencing effect using a two-chamber expansion type of the inside structure instead of a single expansion room.
- d. To decrease the specific low frequency by using a resonator.
- e. To enlarge the volume of the air-cleaner as much as possible, this becomes a silencer.

11.5 References

1. Jianwen Li, Bao Zhou, Deming Jiang and Keyu Pan, *Frequency Analysis Technique for Intake and Exhaust Manifold Design*, Xi'an Jiaotong University, SAE 952070.
2. Franc Pricken, Top acoustic of plastic air intake manifolds, Filetrwerk Mann+Hummel GMBH, SAE 1999-01-0319.
3. Hideki Kido and Hiroyuki Kuwahara, *Modeling the sound source of an intake and predicting the intake sound pressure level for a motorcycle*, Honda R&D Co., Ltd. SAE 2003-32-0058.
4. Badih Jawad et.al., *Intake design for maximum performance*, Society of Automotive Engineers Inc., Warrendale 2003.
5. Larry J. Eriksson, *Noise control in internal combustion engines*, John Wiley & Sons, USA 1982. Chapt. 5.
6. Gordon P. Blair, *Design and simulation of two-stroke engines*, SAE, Warrendale, 1996. Chapt. 8.
7. R. Singh and T. Karta, *Development of an impulse technique for measurement of muffler characteristics*, Journal of Sound and Vibration, 1978, 56 (2).

Appendix 11A



sheet thickness = 1mm

	NAME	DATE	AUTOMOTIF DEVELOPMENT CENTER (ADC), UTM		
DRAWN	RURAUZI BIN SALIM	24/08/04	TITLE : INTAKE SILENCER		
CHECKED	ASSOC. PROF. DR ROSLAN B. ABD RAHMAN		MATERIAL : ZINC		
ENG APPR.			SCALE:1:2		
DIMENSIONS IN MILLIMETERS			WEIGHT:	DWG. NO.1	SHEET 1 OF 1

CHAPTER XII

SOUND INTENSITY MEASUREMENT

12.1 Introduction

Any piece of machinery that vibrates radiates acoustical energy. A sound source radiates power and this results in a sound pressure. But simple sound pressure measurement does not produce any information about sound power. Sound power is the cause and sound pressure is the effect. Sound power is the rate at which energy is radiated (energy per unit time). A method of sound identification using sound intensity measurements and the noise source's contribution can be determined by using sound intensity. Sound intensity is a time-averaged, directional quantity that measures the rate of energy flowing through a specified unit area. Standard sound intensity measurements are in Watts per square meter, or simply, decibels relative to one piconWatt per square meter.

Sound intensity also gives a measure of direction as there will be energy flow in some directions but not in others. In some cases energy may be traveling back and forth and this will not be measured. If there is no net energy flow, there will be no net intensity. Therefore sound intensity is a vector quantity and is usually measured in a direction normal (at 90°) to a specified unit area through which the sound energy is flowing.

Sound intensity can be measured in any sound field. No assumptions need to be made. This property allows all the measurements to be done directly in situ. Measurements on individual machines or individual components can be made even when all the others are radiating noise. This is because steady background noise makes

no contribution to the sound power determined when measuring intensity. Since sound intensity gives a measure of direction as well as magnitude, it is also very useful when locating sources of sound and thus radiation pattern of machinery can be studied.

Thus the objective of this study is to identify the noise sources from the engine system by using sound intensity technique and means of reducing these sources.

12.2 Background Theory

Sound intensity is the product of particle velocity and pressure. It is equivalent to the power per unit area,

$$\begin{aligned}
 \text{Intensity} &= \text{Pressure} \times \text{Particle Velocity} \\
 &= \text{Force/Area} \times \text{Distance/Time} \\
 &= \text{Energy} / (\text{Area} \times \text{Time}) \\
 &= \text{Power} / \text{Area}
 \end{aligned}$$

Thus, the intensity of a sound wave is the amount of power in the wave per unit area and has units of W/m^2 . The intensity of a sound wave depends on how far we are from a source. If we label that distance as R , then the sound intensity is

$$\text{Sound Intensity} = \text{Sound Power} / (4 \pi R^2)$$

The sound intensity level in logarithmic scale is defined as,

$$\text{Sound Intensity level} = L_I = 10 \log (I / I_0)$$

With the reference intensity defined as $I_0 = 10^{-12} \text{ W/m}^2$.

A single microphone can measure pressure, but measuring particle velocity is not as simple. The particle velocity can be related to the pressure gradient (the rate at which the instantaneous pressure changes with distance) with the linearized Euler equation. With this equation, it is possible to measure this pressure gradient and relate it to particle velocity. It is the pressure gradient that accelerates a fluid of density ρ . With knowledge of the pressure gradient and the density of the fluid, the particle acceleration can be calculated. Integrating the acceleration signal then gives the particle velocity.

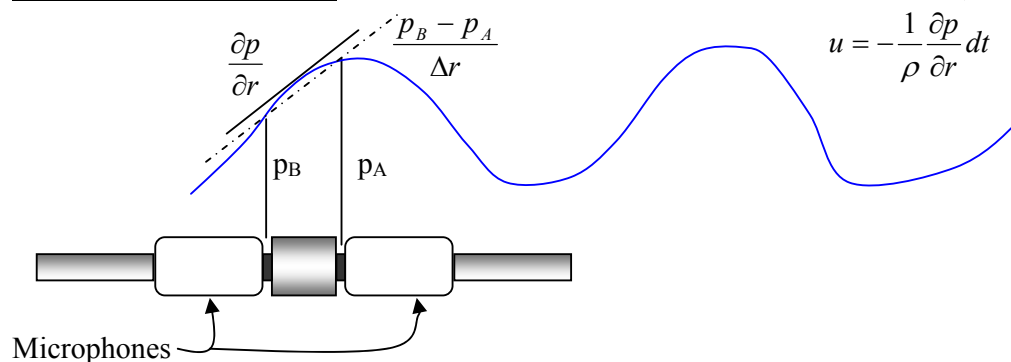
$$a = -\frac{1}{\rho} \text{grad}(p)$$

$$\frac{\partial u}{\partial t} = -\frac{1}{\rho} \frac{\partial p}{\partial r}$$

$$u = -\int \frac{1}{\rho} \frac{\partial p}{\partial r} dt$$

The pressure gradient is a continuous function. With two closely spaced microphones, it is possible to obtain a straight line approximation to the pressure gradient by taking the difference in pressure and dividing by the distance between them. This is called a finite difference approximation.

Time Domain Formulation



The Finite Difference Approximation

$$u = -\frac{1}{\rho} \int \frac{p_B - p_A}{\Delta r} dt$$

The pressure gradient signal must now be integrated to give the particle velocity. The estimate of particle velocity is made at a position in the acoustic centre of the probe, between the two microphones. The pressure and particle velocity signals are then multiplied together and time averaging gives the intensity.

$$p = \frac{p_B + p_A}{2}$$

Average Pressure

$$I = \bar{p} \bar{u}$$

$$I = -\frac{p_A + p_B}{2\rho\Delta r} \int (p_B - p_A) dt$$

A sound intensity analyzing system consists of a probe and an analyzer. The probe simply measures the pressure at the two microphones. The analyzer does the integration and calculations necessary to find the sound intensity. An FFT analyzer relates the intensity to the imaginary part of the cross spectrum of two microphone signals to give sound intensity.

Frequency Domain Formulation for FFT Analyzers

By using Fourier transform, sound intensity can also be expressed as

$$I = -\frac{1}{\rho\omega\Delta r} \text{Im}(G_{AB})$$

where ω is the angular frequency, $\text{Im}G_{AB}$ is the imaginary part of a one-sided cross-power spectrum density function between microphone channels A and B, ρ is the density of air, and r is the separation distance between the two microphones.

12.3 Sound Intensity Mapping

Every noise control problem is first of all a problem of the sound field generated by a source. Contour and 3-D plots give a more detailed picture of the sound field generated by a source. Several sources and/or sinks can then be identified with accuracy. A grid is set up to define a surface. Sound intensity measurements normal to the surface are made from a number of equally spaced points on the surface. There is now a matrix of intensity levels- one value for each point. Lines of equal intensity can be drawn by interpolating and joining up points of equal intensity. These lines can be drawn either at single frequencies or for an overall level. The same data can be used to generate 3-D plots which provide easy visualization of the sound field generated by a source.

12.4 Sound Intensity Equipment Testing

There are three components in a sound intensity analyzing system : the probe, the analyzer and post-processing equipment. Below are the type and brand of instrumentation used on measuring the sound intensity of the 2-stroke engine and is shown in figure12.1 to figure12.4.

1. PAK MKII Muller BBM Analyzer
2. A pair of Intensity microphone (GRAS)
3. 1/4" Preamplifiers set (GRAS)
4. 1 lot sound intensity measurement equipments (GRAS)
5. Laptop with Muller BBM version 5.5 software
6. Power Module (GRAS)



Figure 12.1 PAK MKII Muller BBM Analyzer



Figure 12.2 Sound intensity measurement equipments



Figure 12.3 A pair of Intensity microphone (GRAS)



Figure12.4 Intensity microphone with Preamplifiers set (GRAS)

12.5 Test Set-up and Procedure

- i. In order to study the noise produced by a source, one or more imaginary surfaces near the source must be identified, and then define a grid on each surface. The vector sound intensity is then measured at each grid element. The normal component of the sound intensity on five (5) surfaces surrounding the source was measured. These surfaces and grids are defined by string which is placed over a wooden rectangular frame as shown in Figure 12.5. Measurements will be made at the center of each rectangle. The grid spacing was set to 7cm/grid.



Figure 12.5 Wooden frame with string forming the grid placing on top of the engine

- ii. Assemble the Intensity Probe with ½-inch microphones with 12-mm spacing
- iii. Plug the Intensity Probe into the intensity probe input of the PAK Muller Analyzer. This input uses both channels, one for each microphone.
- iv. Power up the frequency analyzer.
- v. Set up the analyzer for taking intensity measurements.
- vi. The measurements were carried out on the front, rear, left side, right side and top side of the engine. The engine was running at about 2000 rpm at no load and external fan was used to cool the engine during the measurement. Figure 12.6 shows the position of the probe on the grid.



Figure 12.6 Picture showing the location of measuring probe, grid-frame and engine

- vii. The intensity probe is held so that the axis on which the microphones lie is perpendicular to the grid rectangle for each measurement location. Hold the probe so that the spacing between microphones is at the center of each rectangle. Microphones were positioned about 0.5 m from the engine faces due to the small size of the engine.
- viii. Due to the unavailability of an anechoic room, the engine is installed at the open space of a workshop with all machinery being switch off. The test was not carried out with the dynamometer as the location of the dynamometer is in the closed room which will affect the sound intensity measurement. The reflection of noise from the wall will cancelled out the noise radiated thus giving incorrect measurements results.

12.6 Test Results

The test results of the sound intensity measurement on the 2-stroke gasoline engines are shown in figure 12.7(a) to figure 12.7(e). The figures show the map out of the normal component of the vector sound intensity. From the five maps of intensity shown, it is observed that the rear engine measurement result shows high intensity of 0.34 W/m^2 compared to other side of engine measurements. This was probably due to the external fan noise radiation facing the measuring probe during the measurement.

The fan was used to cool down the engine as some components of the engine particularly at joints and gaskets shows sign of smoke. Some discrepancy in sound mapping occurred for the left-side of the engine as shown in Figure 12.7 (d) which showed negative sound intensity radiation which probably due also to the fan sound pressure.

The front side shows relatively high sound radiation around the intake and exhaust with magnitude of around 0.07 W/m^2 . High intensity was also observed at the exhaust on the rear and right side of the engine. The top side of the engine shows source of noise radiation mainly from the exhaust of magnitude 0.034 W/m^2 and less magnitude from the fin of the cylinder head around 0.028 W/m^2 .

12.7 Conclusion

From these results it can be concluded that the noise radiation from the cylinder block and crank case are minimum. The noise radiation from the cylinder fin can be reduced by fitting several rubber blocks between the fins to reduce the reverberation of the fins. The main contribution to noise radiation is from the exhaust and intake. However, the magnitude of the noise is low compared to other exhaust and intake system fitted to the same engine. The noise radiation in the exhaust system can be further reduced by placing more volume of fiber-glass wool in the absorption component of the exhaust muffler.

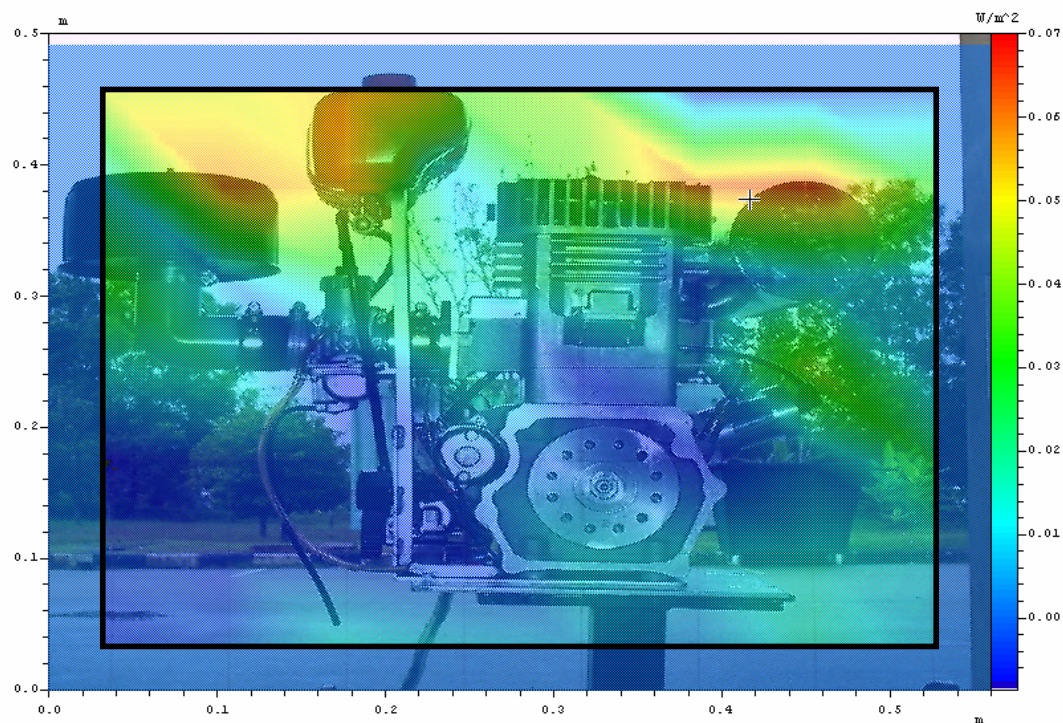


Figure 12.7(a) Sound Intensity mapping for front side of engine.

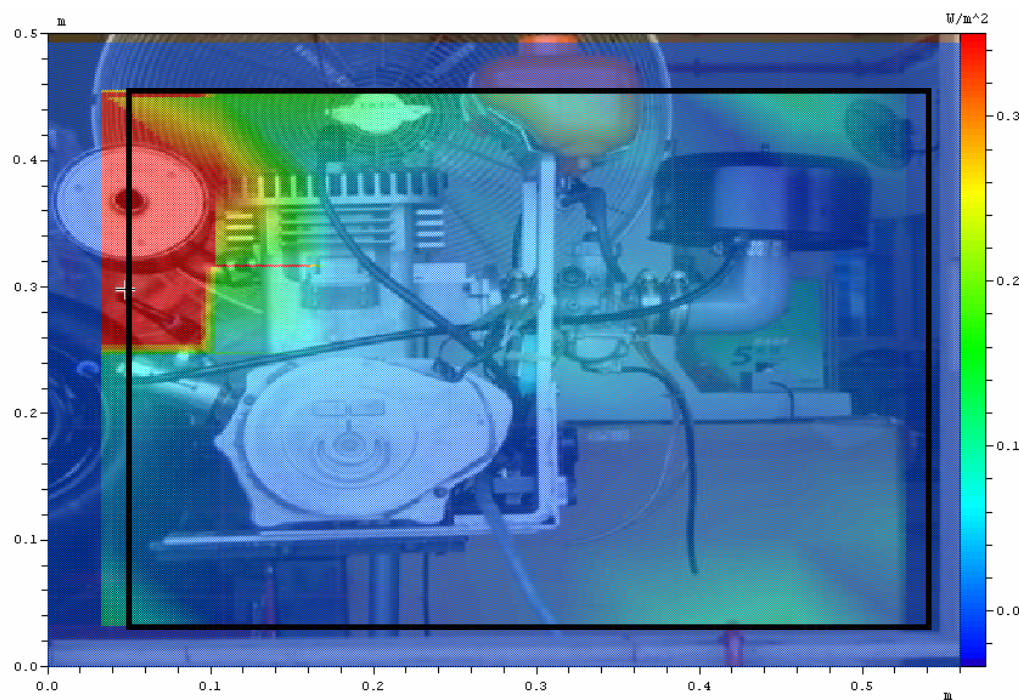


Figure 12.7 (b) Sound Intensity mapping for rear side of engine.

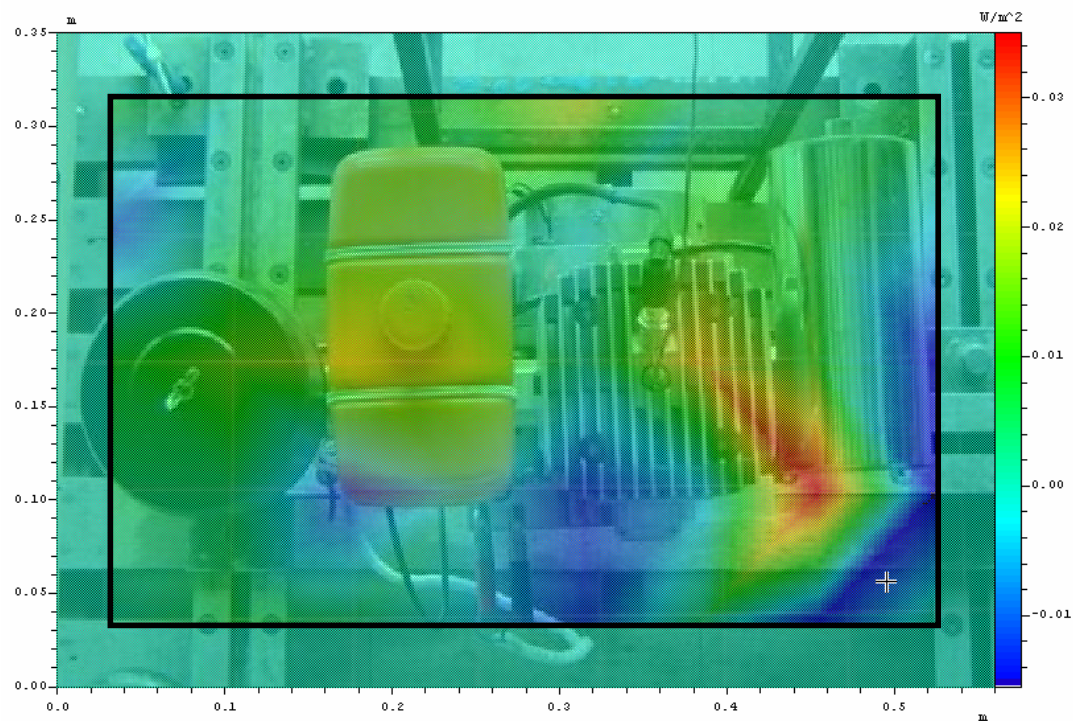


Figure 12.7(c) Sound Intensity mapping for top side of engine.

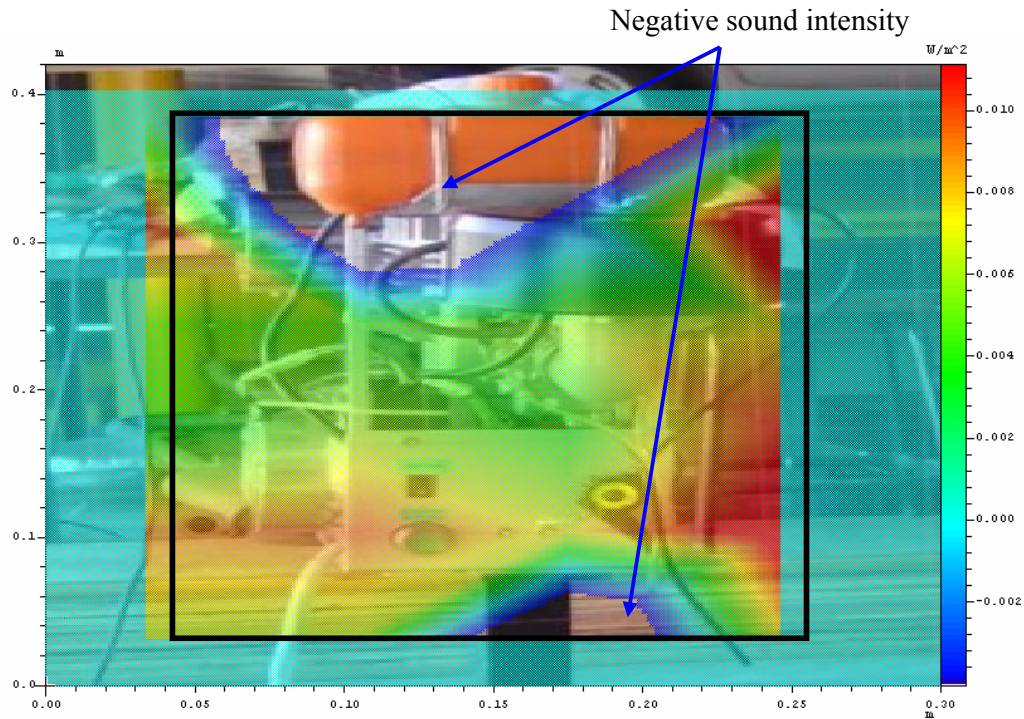


Figure 12.7(d) Sound Intensity mapping for left side of engine.

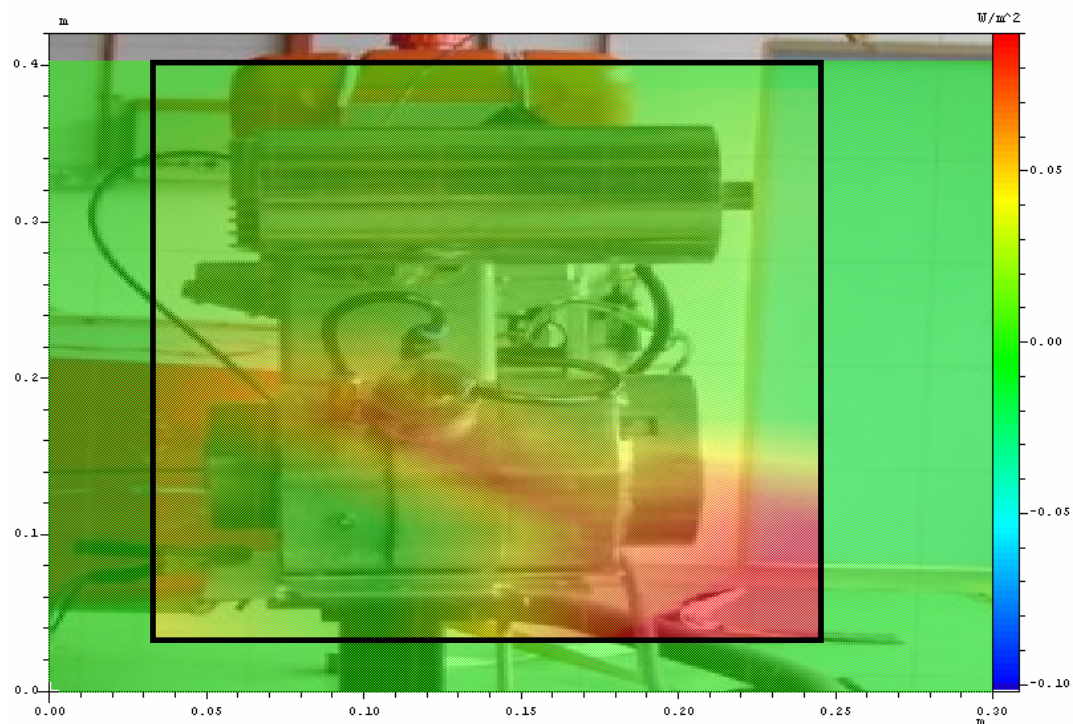


Figure 12.7(e) Sound Intensity mapping for right side of engine.

CHAPTER XIII

OVERALL VIBRATION AND NOISE MEASUREMENTS OF NEW 2-STROKE SINGLE CYLINDER GASOLINE ENGINE

The objective of this chapter is to highlight the results of overall vibration and noise measurements on the newly developed 2-stroke single cylinder engine and to identify the dominant frequency range for the running engine.

13.1 Engine Specification

Overall vibration test was carried out on two-stroke gasoline engine at Automotive Development Center Universiti Teknologi Malaysia. The test undertaken intends to gather vibration data and identifying the dominating frequency range for this engine . Table 13.1 shows the specification of engine.

Table 13.1: Engine Specifications

Item	Description
Capacity	125 cc (Step Piston)
Stroke	Two-stroke
Cylinder	Single cylinder
Cooler	Air-cooled
Fuel system	Carburetor

These engines were installed on a test bed mounted on the floor and isolated with rubber mounting pad to reduce the transfer of vibration force to the test bed. Figure 13.1 shows the test bed used on the engine.



Fig.13.1: Two-Stroke Gasoline Engine.

13.2 Test Instrumentation, Set-Up and Procedure

The instruments used consist of a multi analyzer and accelerometers. Overall vibration data were capture within PAK Muller-BBM analyzer. Table 13.2 shows the specifications of the instruments used for the test. The instrumentation set-up is illustrated in Figure 13.2a and 13.2b. Accelerometers were attached at measurement points (glued with cement stud) at cylinder head (2 points), engine block (2 points), crankcase and magneto covers.

Table 13.2: Instrumentation

Instruments	Type
Multi Analyzer Unit	PAK Muller Portable Multi-Channel Signal Analyzer
Computer Laptop	Compaq Evo N610c Installed with PAK Mueller-BBM VibroAkustik Systeme version 5.2 Software
Accelerometer	Kistler Top End Accelerometer Type 8774A50

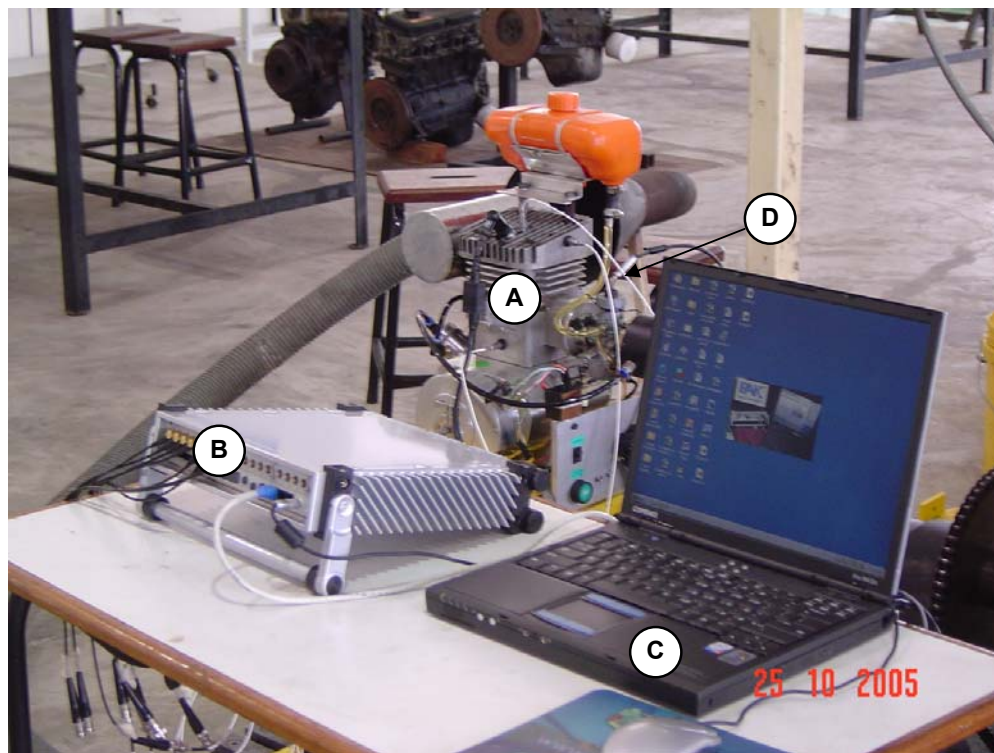


Figure 13.2a: The instrumentation set-up.

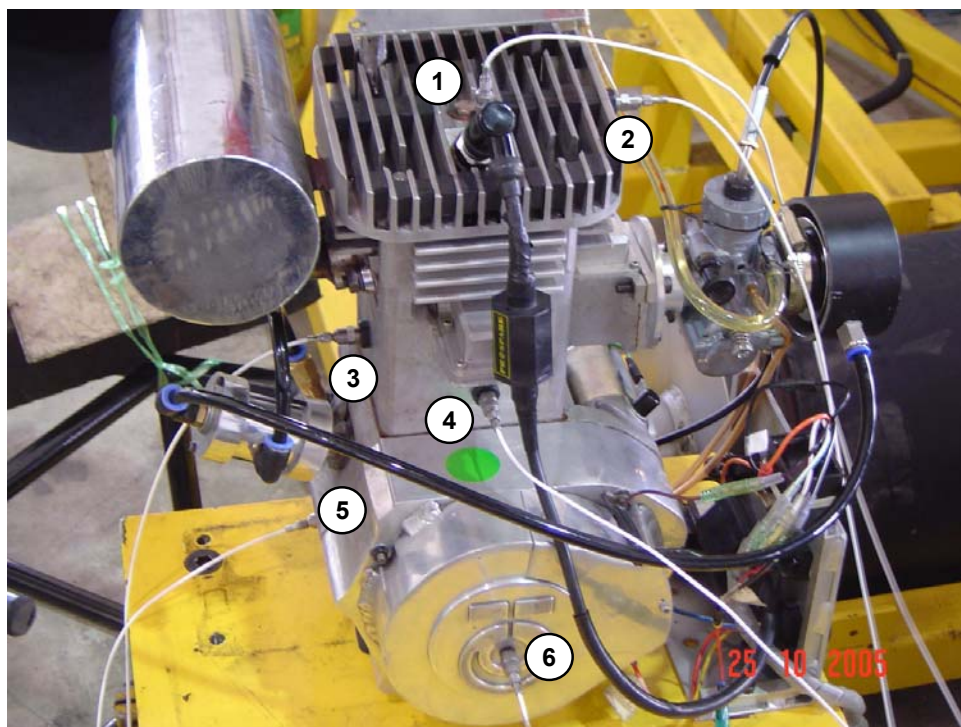


Figure 13.2b: The instrumentation set-up

Equipments Description

A	Two-Stroke Gasoline Engine
B	PAK Muller Portable Multi-Channel Signal Analyzer
C	Laptop with PAK Mueller-BBM VibroAkustik Software
D	BNC connecting cable between accelerometers and analyzer
1,2,3,4,5 & 6	Kistler accelerometer

The engines were ran at idling speed under no load condition and vibration spectrums at several points on the engines were then recorded. The procedures were repeated at several constant engine speeds. The engine speeds were measured by using a tachometer.

13.4 Experimental Results

Below are the results from Overall Vibration test on the engine between 1500 rpm to 4500 rpm.

i. 1500 rpm

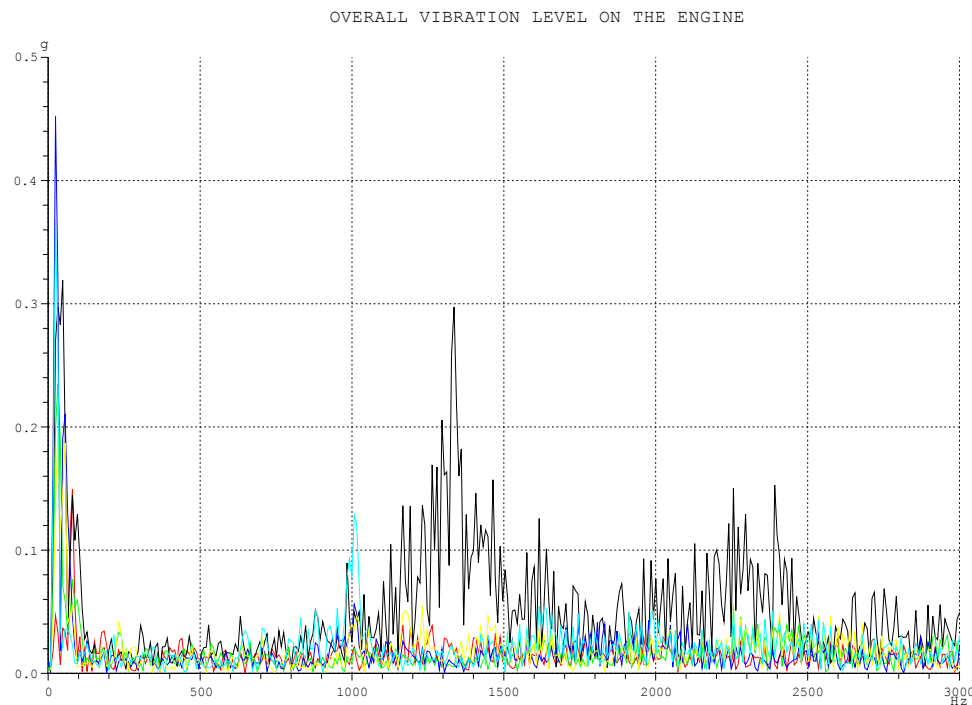


Figure 13.3: Superimpose of Overall Vibration Spectras on the engine at 1500 rpm for all measurement points

ii. 2200 rpm

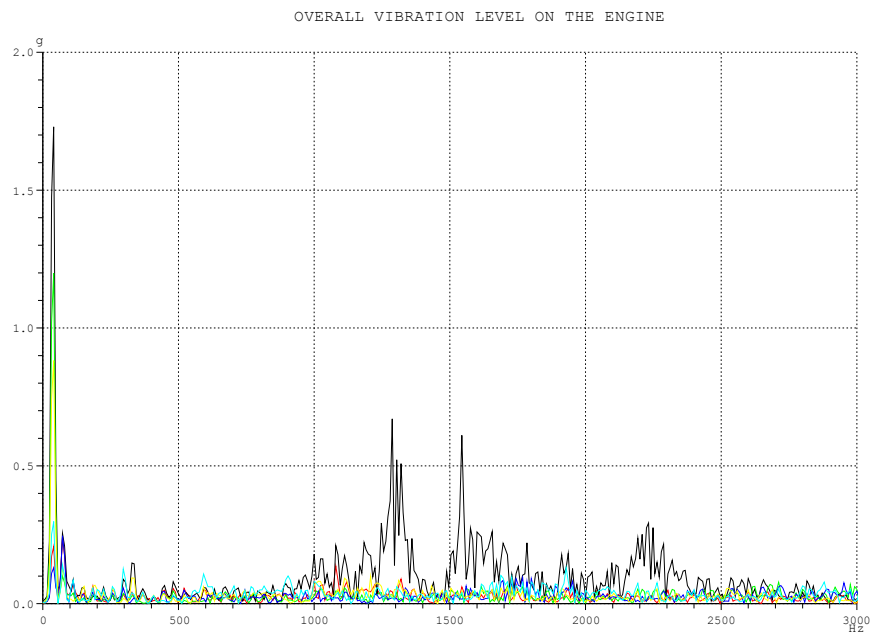


Figure 13.4: Superimpose of Overall Vibration Spectras on the engine at 2200 rpm for all measurement points.

iii. 2500 rpm

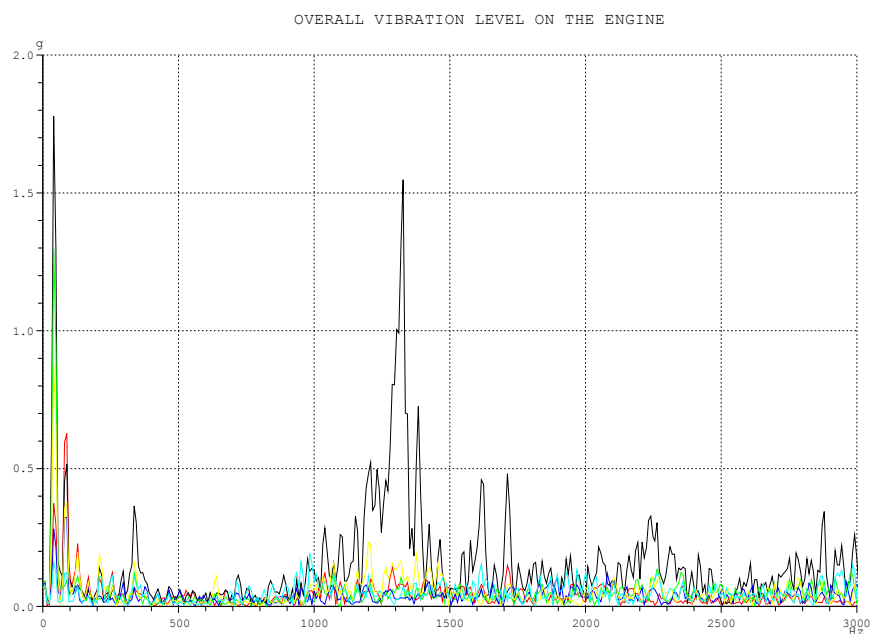


Figure 13.5: Superimpose of Overall Vibration Spectras on the engine at 2500 rpm for all measurement points.

iv. 2800 rpm

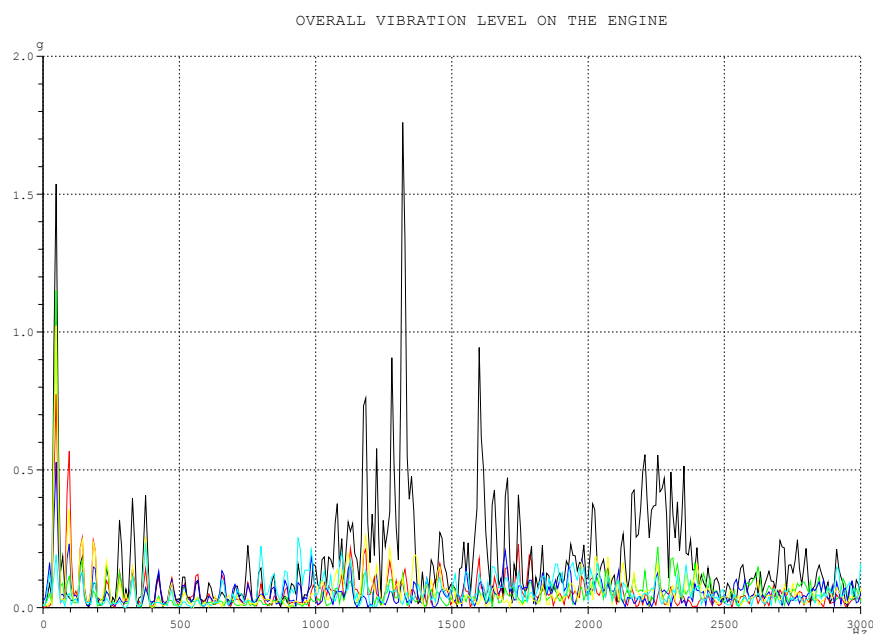


Figure 13.6: Superimpose of Overall Vibration Spectras on the engine at 2800 rpm for all measurement points.

v. 3000 rpm

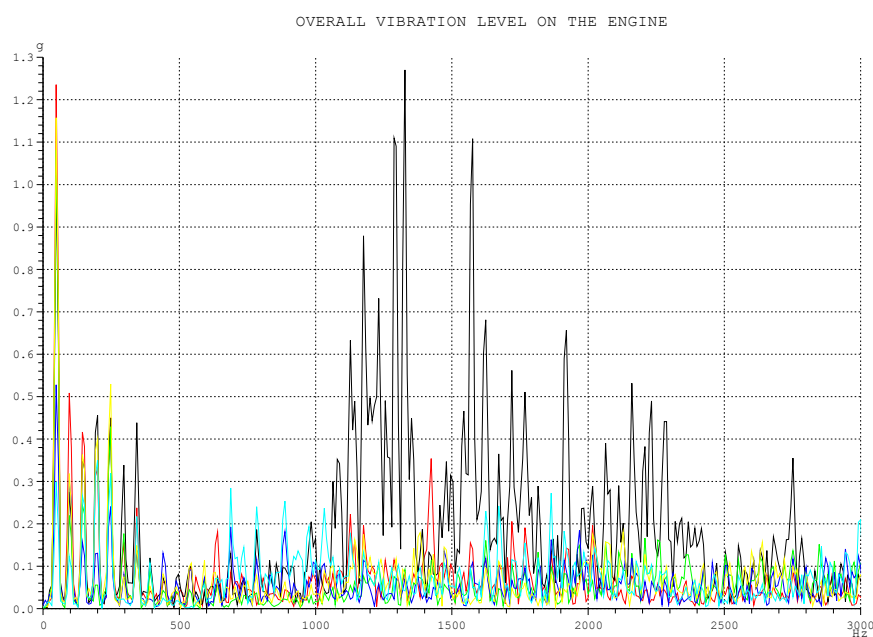


Figure 13.7: Superimpose of Overall Vibration Spectras on the engine at 3000 rpm for all measurement points.

v. 3500 rpm

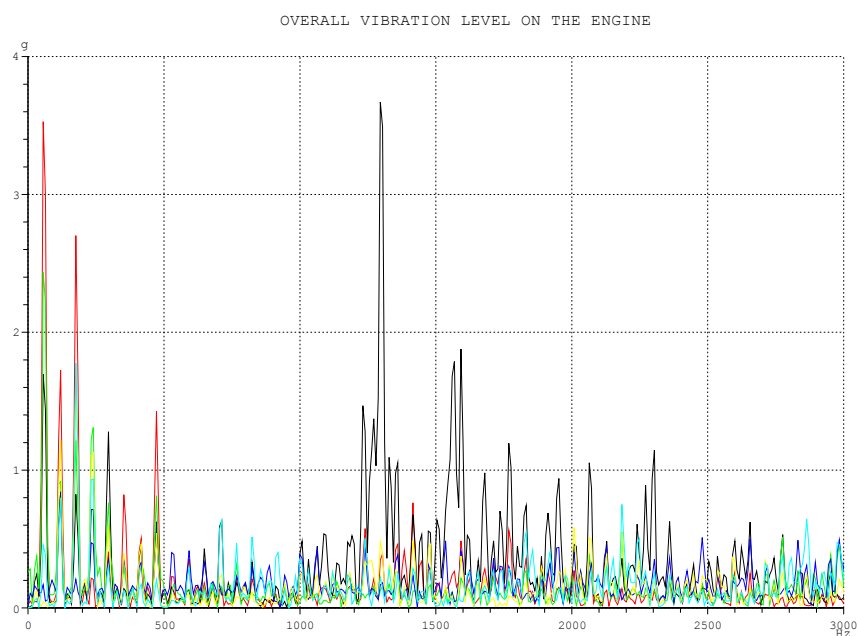


Figure 13.7: Superimpose of Overall Vibration Spectras on the engine at 3500 rpm for all measurement points.

v. 4300 rpm

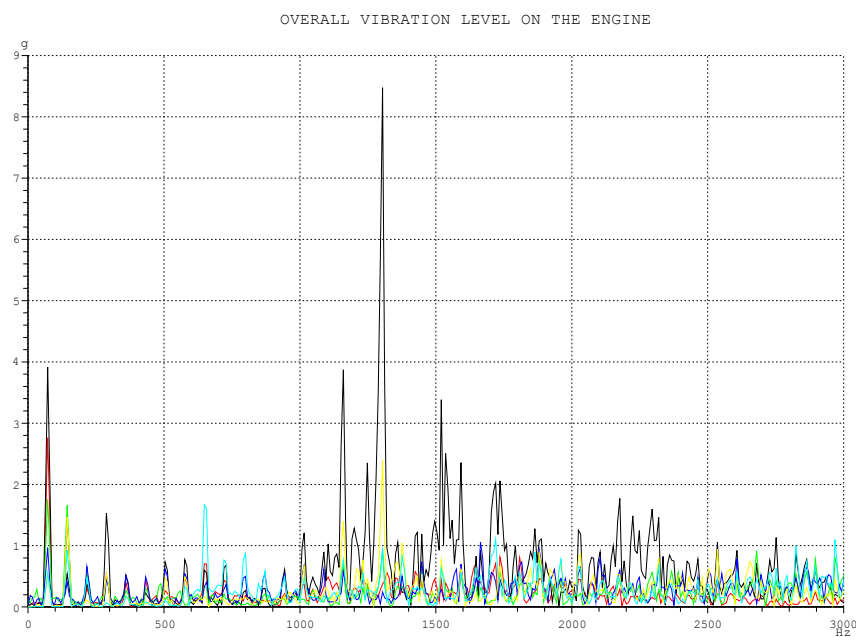


Figure 3.7: Superimpose of Overall Vibration Spectras on the engine at 4300 rpm for all measurement points.

v. 4500 rpm

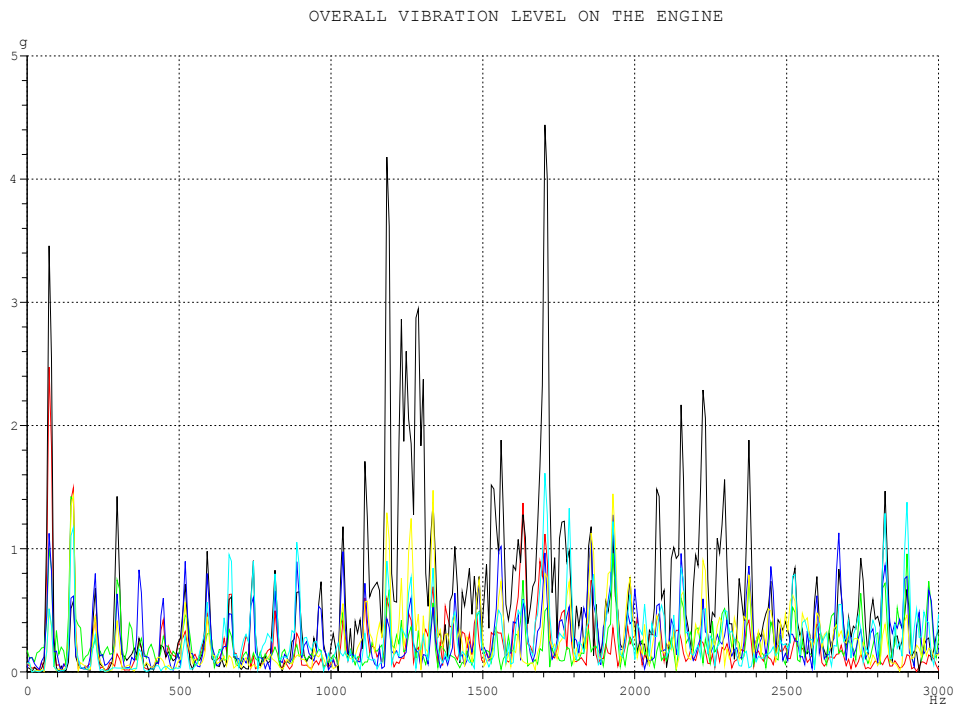


Figure 3.7: Superimpose of Overall Vibration Spectras on the engine at 4500 rpm for all measurement points.

13.5 Discussion

Overall vibration level for the engine showed that the vibration occurred between 0-2500 Hz. The engine peak frequencies above 1g level begin to emerge when the engine speed is above 2000 rpm. High acceleration occurred at all running speed of the engine and the level increased as the speed increased. There is a pattern of high peak acceleration at around 1350 rpm particularly and 1550 rpm which occurred at all engine speeds. All these peaks only emerged for measurement point 2 which is at the side of cylinder head fin. The maximum amplitude, 8.04g occurred at 4300 rpm at frequency around 1300 Hz. While at other measurement points such as crankcase, cylinder block and magneto cover, vibration levels were quite low.

Below are detail discussions on vibration at various points on engine.

a). Cylinder Head Overall Vibrations Response Level

Measurement points on cylinder head were set at 2 locations; fin at right side and at top cylinder head beside spark plug (Figure 13.8). It is observed that the high vibration amplitude occurred at the right fin. The highest amplitude is 8.04g at 1300 rpm. Table 13.3 shows the vibration amplitude of the engine at various engine speed.

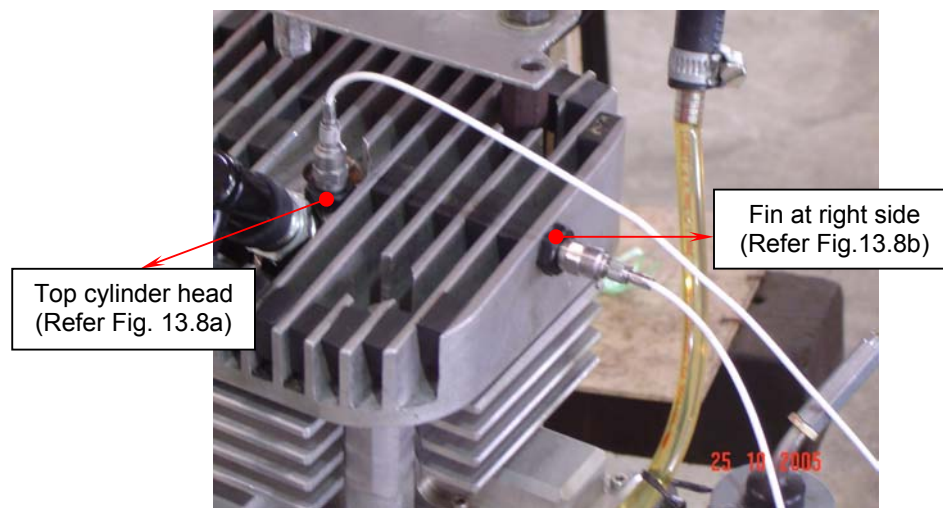


Fig. 13.8: Measurement points at Cylinder head

Table 13.3 Vibration amplitude of the engine due to engine speed.

Engine Speed (rpm)	Vibration at Top Head, (g)	Vibration at Right Fin, (g)
	72 Hz	1304 Hz
1500	0.05	0.26
2200	0.26	0.32
2500	0.57	0.39
2800	0.75	0.89
3000	1.24	0.5
3500	3.31	1.58
4300	2.48	8.48
4500	2.27	2.92

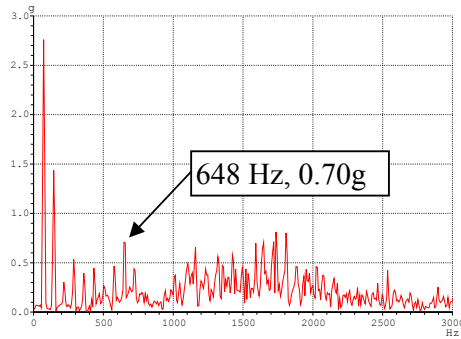


Figure 13.8 (a)

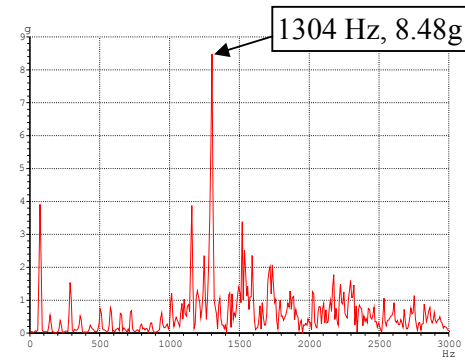


Figure 13.8 (b)

Highest vibration occurred at this fin

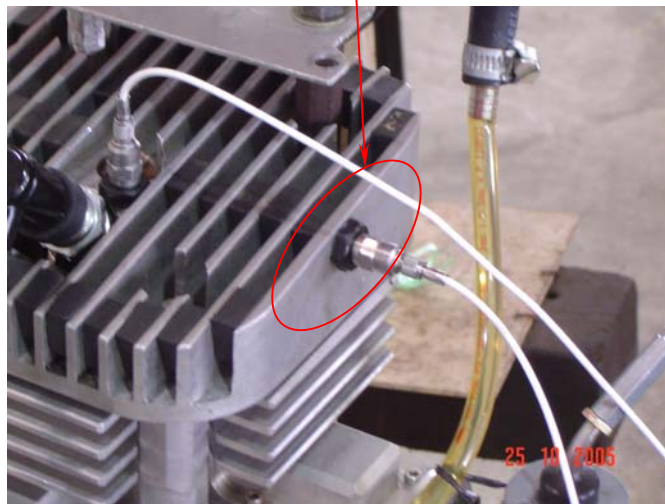


Fig. 13.9: Highest vibration position.

The highest vibration occurred on this side of the fin as it was not rigid enough and possibly due to its vertically highest position of the engine. Thus it has the highest displacement motion in the engine.

(b). Engine Block Overall Vibrations Response Level

Measurement points on engine block were set at 2 locations, two of them are shown in Figure 13.10. Figure 3.11 (a) and (b) shows the vibration spectrums at these points. The results indicate that the amplitude of vibration is below 1g except at the running speed of the engine.

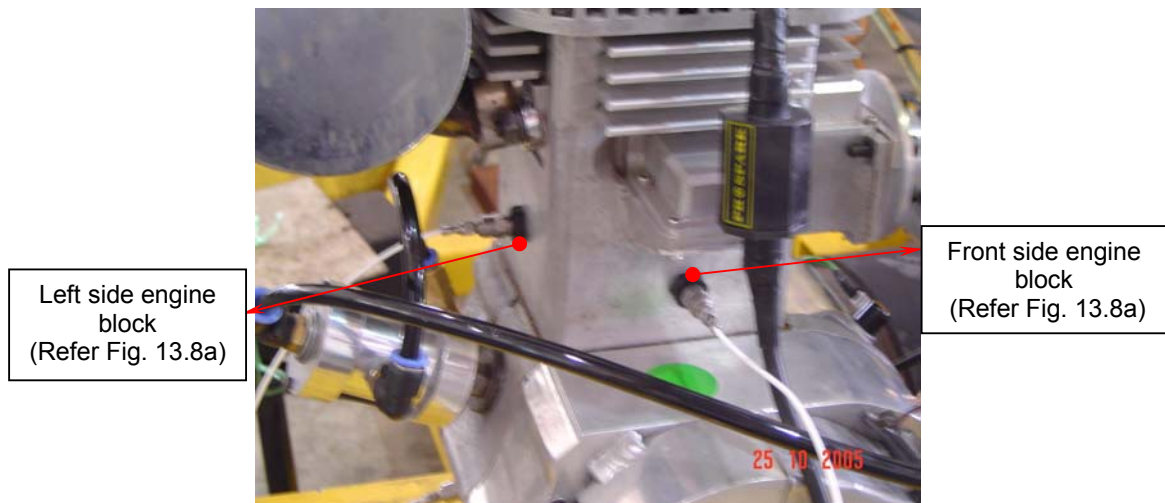


Figure 13.10: Measurement points at Engine Block.

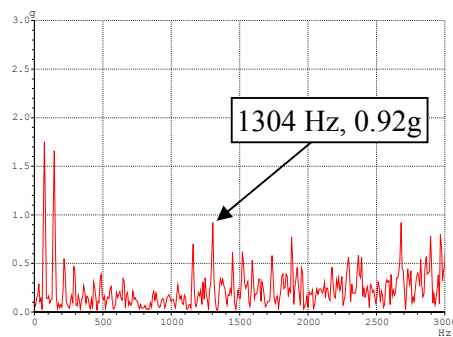


Figure 13.11a

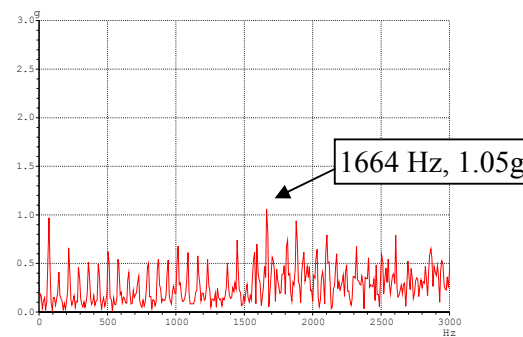


Figure 13.11b

(c). Crankcase Overall Vibrations Response Level

Measurement points on crankcase were set at 1 location as shown in Fig. 13.12. The measured vibration spectra for the crankcase is shown in Fig.13.12(a). The amplitude is below 0.2g and no high peak was observed in the plots.

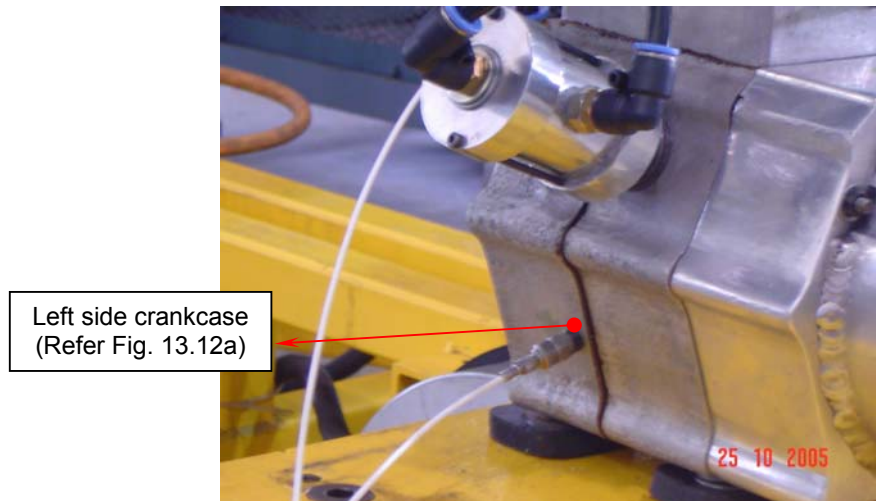


Fig.13.12: Measurement points at Crankcase.

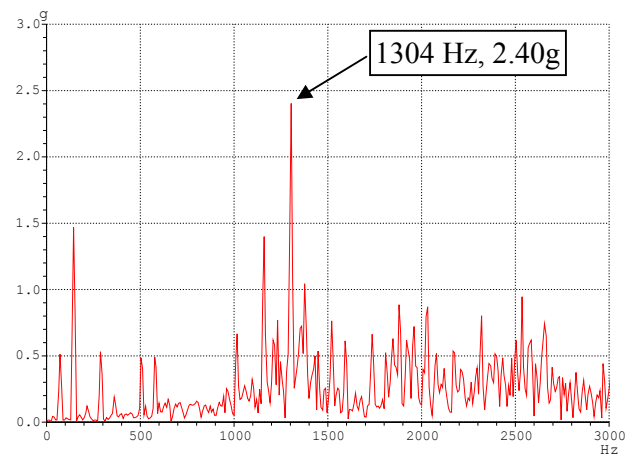


Figure 13.12(a)

(d) Magneto Cover

Figure 13.13 shows the location of the measurement point on the magneto cover, with the measured vibration spectrum shown in Figure 13.13a. The amplitude is also below 0.2 G and no peak was found in the plots. This is due to the stiffening of the magneto cover.

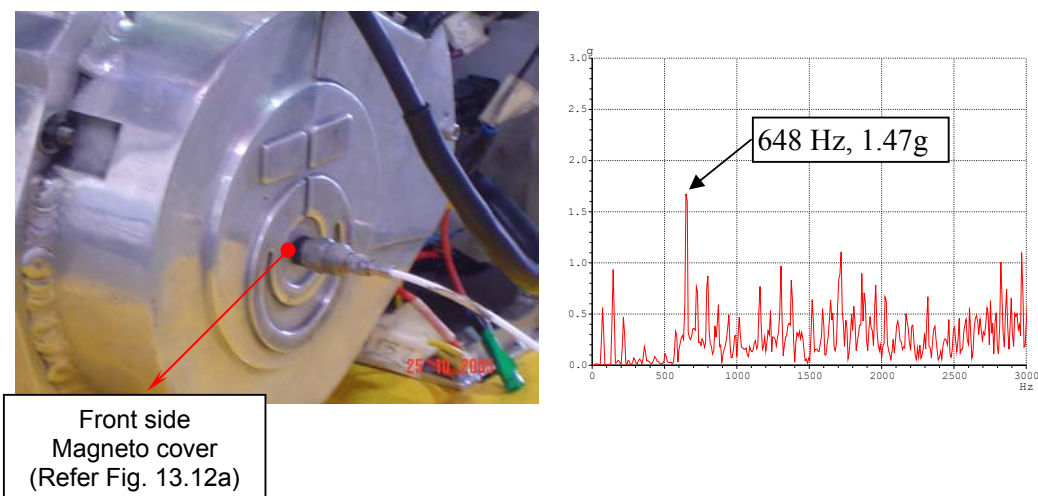


Fig.13.13: Measurement Point on Clutch Cover

Figure 13.13a

The overall vibration frequency for all the engines tested is summarized in Table 13.4 with respect to various components of the engine. The engine shows dominant frequency range from 500 Hz to 2000 Hz.

Table 13.4: Summary of Overall Vibration for the engine operating at 4300 RPM
(highest vibration amplitude)

Part	Direction	Point	Peak Frequency				
			0-500 Hz	500- 1000Hz	1000- 1500 Hz	1500- 2000 Hz	2000- 2500 Hz
Cylinder Head	Vertical Up	Top		X			
	Horizontal	Fin			X		
Cylinder Block	Horizontal	Left side			X		
		Front side				X	
Crankcase	Horizontal	Left side			X		
Magneto Cover	Horizontal	Front side		X			

13.6 Overall Noise Measurement

Overall noise measurement on the engine was also carried out at various engine speeds. A precision sound level meter of type Bruel & Kjaer shown in Figure 13.14 was used.



Figure 13.14 Precision sound level meter

The environmental noise during the test was recorded as 56.9 dBA and 61 dBA when the fan for cooling the tested engine was operating. Such level does not affect the actual noise measurement on the engine as the engine noise it is far above 10 dB then the environment noise. Table 13.5 shows the level of noise emitted from the engine at various speeds and is plotted in Figure 13.15.

Table 13.5 Noise emitted from running engine

Engine Speed (RPM)	Noise (dBA)
1500	80.2
2200	80.3
2400	80.3
2500	80.3
2700	82.5
3000	85.7
3500	93.5
4200	94
4300	94.6

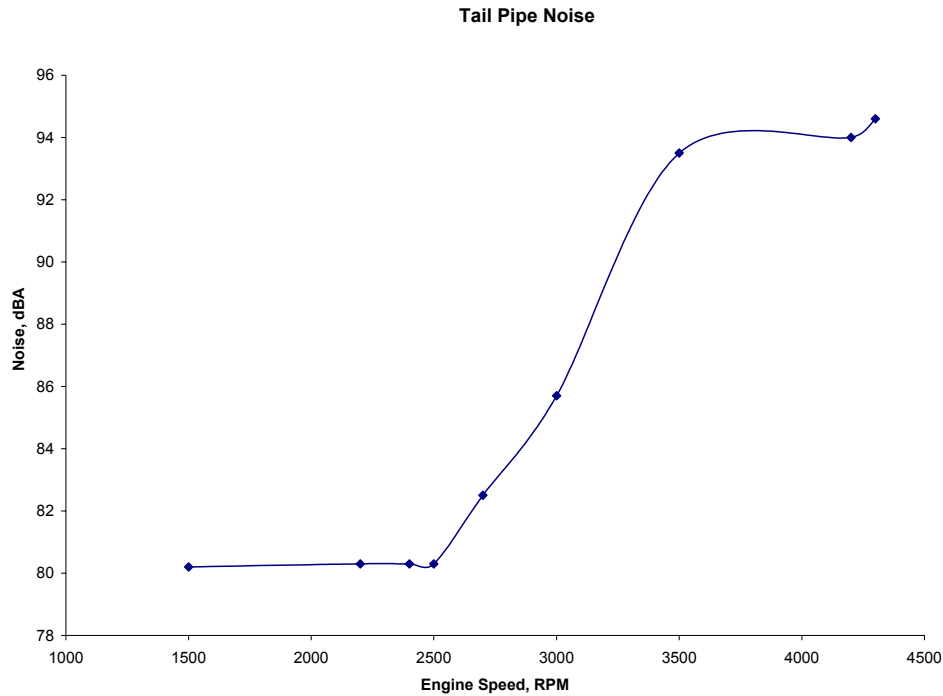


Figure 13.15 Noise emitted at 1 m from the tail pipe of muffler

The results indicate that at idling and low speed the noise level are almost constant and begin to increased sharply at around 2500 rpm. The highest level recorded is around 4500 rpm at 94 dB emitted mainly from the fabricated muffler.

13.7 Conclusion

The overall vibration test on the engine at several constant speeds and at no load condition indicates that the dominant frequency lies in the range 500 Hz to 2.0 kHz. The highest peaks acceleration occurred at the side fin which is the same as tested for the existing engines reported in Chapter 3. Thus to reduce the amplitude of vibration the fin needs to be further stiffened and damped using hard rubber. The noise level recorded shows acceptable level of noise emitted mainly from the designed muffler.

CHAPTER XIV

DISCUSSION, CONCLUSION AND RECOMMENDATION

14.1 Introduction

This chapter describes the overall discussion and conclusion for the project and recommendation that can be implemented to ensure that the engine produced is quite and running smooth as far as noise, vibration and harshness are concern.

14.2 Overall Discussion

The utilization of various noise reduction techniques to attenuate noise and vibration of the new engine have been successfully employed. Comprehensive literature review has enabled to identify the noise suppression techniques commonly used by researchers on engines development. The main sources of noise are from the exhaust and intake systems. Sources from combustion are in the lower frequency region while major source from mechanical noise lies in the higher frequency region.

Initial test on existing engines have assisted the project in identifying acceptable techniques to use in reducing the noise and vibration of the engines and verifying the results of other researchers on the frequency range. Overall vibration test results showed that the dominant frequency ranges is in the region of 400 Hz to 1.5 kHz. Thus finite element method is the most suitable simulation technique within such frequency range.

Simulation studies using finite element methods on the new engine have suggested several modifications to be made on several components of the new engine, with the objective of obtaining a rigid and low engine weight. These engine characteristics were claimed by researchers as the typical characteristic for low noise engine. The modifications suggested were submitted to the engine design group but not all modifications were implemented due to manufacturing constraint.

Noise radiation software was purchased to predict the noise radiation of the engine. A force spectrum of vibration is first required to be determined and is then used as source of input to the engine boundary element model. Results showed most noise

radiation were predicted to be on the top and side of the engine. It should be pointed out that the engine model does not include the intake and exhaust systems.

Balancing of three types of engines was also carried out. These engines are the single cylinder, V-4 and Scotch Yoke engines. A Nastran software was used to identify the unbalanced forces created due to the rotation of then crankshaft. The single cylinder engine has acceptable unbalance force, V-4 engine has unbalance moment which can be reduced by changing the sequence of crank throw phase angles. The Scotch Yoke engine showed unbalance inertia forces and moments which need to be balanced.

Beside looking on the noise and vibration aspects of the new engine, the research also include looking on the possible effect of back pressure on the exhaust system, the use of catalytic converter, the use of new materials for the engines and the determination of possible heat loss on the engine surface particularly at the fin. It was accepted that simulation work is reliable enough to ensure acceptable magnitude of back- pressure. The function of the catalytic converter is to ensure clean exhaust emissions and reduced noise level to acceptable standards. However, it was found that the use of the catalytic converter on a 2-stroke engine requires special lubrication oil to avoid settlement of unburnt fuel commonly occurred in such type of engine.

Several new materials have been identified suitable for some component of the engines. However, for the production of the new engine, it was decided by the engine designer group to use the commonly use materials. This is to avoid problems associated with manufacturing and fabrication which may delay the engine production. Heat transfer analysis on the engine fins showed a 61.44 % of heat loss through the fins which was considered acceptable.

A detail study on the design of exhaust system for the new engine was assisted by the purchased of the customized engine software, GT-Power. Several design of mufflers were suggested and the performance of the mufflers were assessed based on the transmission loss, the torque and brake power produced by the engines and the noise at the tail pipe of the exhaust system. The chosen muffler design was then tested for back-pressure aspect using the computational fluid dynamics method. The muffler was then fabricated and fastened to the single cylinder engine. The result of the test on the running engine showed acceptable noise from the exhaust when compared to noise level of other existing mufflers. A parameter study on the effect of varying the muffler components configuration was also carried out and the results were assessed based on the transmission loss of the muffler.

To complete the engine system, an intake system was designed and fabricated for the single cylinder engine. Parameter studies were also carried out to obtain the best configuration of the intake system that gave high transmission loss which covers wider frequency range. A chosen design was then identified and purchased. It was installed to the engine and was found to produce an acceptable level of noise level of about 70-80 dB without load.

Once the engine has been completely produced, a sound intensity test was carried out to look into the distribution of noise from the engines and to identify dominant sources of noise radiation. Test results showed that the dominant sources were from the exhaust and intake system. However, the level of noise radiation from these sources was considered acceptable.

Overall noise and vibration measurements were carried out on the new engine. The vibration level was found to be high at the side fin of the cylinder head which is similar to the existing engines tested. It was recommended that this section need to be further stiffened and damped. The noise level emitted from the tail pipe of the fabricated muffler showed acceptable level of noise.

14.3 Problem

The suggested modification on the new engine based on simulation results was not carried out as most of the prototype engine components were fabricated by using machining process. However, such suggested modification will be considered for the next prototype.

Sound intensity test should be carried out in an anechoic chamber to isolate other unnecessary sources of noise. However, since such chamber was not available here, the test was then carried out in the open air to avoid reflection of sound from walls. Thus this was the main reason the test was not carried out on half and full load required by most engine manufacturers.

Vibration test on the new engine connected to the dynamometer was not carried out as the test system has lots of electrical leakage that disturb the data acquisition system. No vibration at half load and full load tests were carried out as the engine is not yet capable to run at such load.

14.4 Conclusion

The project has successfully achieved its objective in utilizing several noise reduction techniques to produce a low noise engine. The usage of new materials shall be considered once the cutting and machining process of such materials has been sorted out.

14.5 Recommendation

The simulation work of noise and vibration on the new engines should be carried out during the early design stage through vibration simulation. AVL Austria, a popular engine manufacturer, has proposed key steps and methods in the development of Low Noise Engines [1]. Taking this approach ensures that first generation engine hardware is already structurally optimized for noise. However, such approach was not followed due to lack of coordination among the groups involving with the production of the new engines.

The new engine need to be further tuned and tested for noise and vibration. Such testing should be done at no load, half-load and full load on the dynamometer test bed to ensure that the engine produced has better noise, vibration and harshness characteristics and to ensure durability of the engine as well.

References

1. Cristian V. Beidl, Alfred Rust and Michael Rasser, “ Key steps and methods in the development of low noise engines”, Sound and Vibration, April 2001.